



**HAL**  
open science

# Nouveaux Procédés de Synthèse d'Uréthanes et de Polyuréthanes

Ikechukwu Ogbu

► **To cite this version:**

Ikechukwu Ogbu. Nouveaux Procédés de Synthèse d'Uréthanes et de Polyuréthanes. Autre. Université de Bordeaux, 2022. Français. NNT : 2022BORD0107 . tel-04521191

**HAL Id: tel-04521191**

**<https://theses.hal.science/tel-04521191>**

Submitted on 26 Mar 2024

**HAL** is a multi-disciplinary open access archive for the deposit and dissemination of scientific research documents, whether they are published or not. The documents may come from teaching and research institutions in France or abroad, or from public or private research centers.

L'archive ouverte pluridisciplinaire **HAL**, est destinée au dépôt et à la diffusion de documents scientifiques de niveau recherche, publiés ou non, émanant des établissements d'enseignement et de recherche français ou étrangers, des laboratoires publics ou privés.

THÈSE PRÉSENTÉE  
POUR OBTENIR LE GRADE DE  
**DOCTEUR DE**  
**L'UNIVERSITÉ DE BORDEAUX**

ÉCOLE DOCTORALE DES SCIENCES CHIMIQUES  
SPÉCIALITÉ : CHIMIE ORGANIQUE

Par **IKECHUKWU MARTIN OGBU**

**New Processes for the Synthesis of Urethanes and Polyurethanes**

Sous la direction de : Prof. Yannick LANDAIS

Co-directeur : Dr. Frédéric ROBERT

Soutenance le 23 mars 2022

Membres du jury:

Prof. Jacques LALEVÉE	Université de Haute Alsace	Rapporteur
Dr. Laurence GRIMAUD	Université Paris Sciences & Lettres	Rapporteur
Prof. Corinne GOSMINI	École Polytechnique	Examineur
Prof. Daniel TATON	Université de Bordeaux	Examineur
Prof. Yannick LANDAIS	Université de Bordeaux	Directeur de thèse
Dr. Frédéric ROBERT	Université de Bordeaux	Co-encadrant
Prof. Henri CRAMAIL	Université de Bordeaux	Invité



## Acknowledgments

I wish to express my profound gratitude to the jury members: Prof. Jacques Lalevée, Dr. Laurence Grimaud, Prof. Corinne Gosmini, Prof. Daniel Taton and Prof. Henri Cramail for accepting to evaluate my work.

I am very grateful to my supervisor, Prof. Yannick Landais, thank you for your guidance, assistance and encouragement that have contributed immensely to this work. I appreciate your availability; you are always there for discussion of my reactions, proffering solutions and useful ideas. I did not only learn some organic chemistry from your group, but also hard work and commitment. For those early days you used to give me exercises from organic chemistry textbook, thank you so much for your time. I equally thank my co-supervisor, Dr. Frédéric Robert, your assistance and support during this project are wonderful. For your contributions in the analysis of some of my challenging reactions and results, I am very grateful to you.

To Prof. Henri Cramail, I appreciate your great assistance in the polymer aspect of this work. Thank you for giving me the opportunity to work in your laboratory (LCPO) during the polymer preparation and characterization. Also, your wonderful ideas during our regular meetings with your group greatly contributed to the success of this work. I equally appreciate the assistance of Dr. Thomas Vidil and Dr. Etienne Grau.

I thank Dr. Dario M. Bassani of NEO group for assisting me in the photocatalytic aspect of this work. I appreciate CESAMO group for their assistance in spectroscopic analysis of my compounds. I thank Dr. Philip Peixoto for his encouragement. I appreciate Engr. Amélie Vax-Wéber and Sylvain Bourasseau of LCPO for their assistance during the SEC analysis. I equally thank Dr. Anderson Medeiros, Dr. Thaissa Chaparro and Péroline Helbling for their assistance during part of my work in LCPO.

To my friends, colleagues, and members of our group: Dr. Iman, Dr. Claire, Dr. Govind, Marion, Dr. Suman, Shuai, Dickson, Dr. Gülbin, Camille, Dr. Laura, Morgan, Dr. Nivesh, Damien and Jonathan, thank you so much for your kind support.

I am highly indebted to my wife, Dr. Patience for her encouragement and, for tolerating my long absence from home during this programme. To my Children: Kamsi, Dominion and David, thank you so much for your best wishes. Also, I appreciate my parents and siblings for their emotional support.

Lastly, I am very grateful to Alex Ekwueme Federal University Ndufu Alike for their financial assistance. And to the Almighty, thank.



## Table of Contents

Résumé en Français .....	5
List of Abbreviations, Acronyms, and Symbols .....	11
General Introduction .....	15
Chapter 1 : .....	19
Urethanes and Polyurethanes .....	19
1. Introduction.....	19
2. Urethanes .....	19
2.1. Classical route to urethanes and its limitations .....	20
3. Mechanism of isocyanate reaction with alcohols.....	21
3.1. Electronic effects in the reactivity of isocyanate with alcohols and other nucleophiles .....	22
4. Limitations of classical route to urethanes and polyurethanes .....	23
5. Greener routes to urethanes and polyurethanes .....	24
5.1. Carbonate/amine route .....	24
5.2. Transurethanization .....	25
5.3. Ring-opening polymerization (ROP) of cyclic carbamates.....	25
5.4. Urethanes based on <i>in-situ</i> generation of Isocyanates.....	26
6. Polyurethanes .....	27
6.1. Classical thermoplastic polyurethane synthesis, composition and properties .....	28
6.2. Polyurethanes foams (PUs-foam) .....	29
Conclusion.....	30
Chapter 2.....	31
Oxamic acids as precursors of carbamoyl radicals and urethanes .....	31
1. Introduction.....	31
2. Oxamic acid as carbamoyl radical precursor.....	32
3. Decarboxylative coupling reactions using oxamic acids.....	34
3.1. Csp <sup>2</sup> -Csp <sup>2</sup> bond formation.....	34
3.2. Photocatalyzed Minisci reaction using oxamic acids for Csp <sup>2</sup> -Csp <sup>2</sup> bond formation.....	38
4. Csp <sup>2</sup> -Csp bond formation .....	40
4.1. Photocatalyzed decarboxylation of oxamic acids for Csp <sup>2</sup> -Csp bond formation .....	41
5. Decarboxylative cyclization of oxamic acids for heterocycles synthesis .....	42
6. Decarboxylative intermolecular addition-cyclization of oxamic acids for heterocycles synthesis.....	44
7. Photocatalyzed decarboxylative cyclization reaction for heterocycles formation.....	48
8. Oxamic acids as a precursor for isocyanate and urethane.....	49
9. Conclusion.....	50
Chapter 3.....	51
Urethane and PUs synthesis by visible light-mediated decarboxylation of oxamic acids .....	51
<i>PART 1: Basic concepts of visible-light photoredox catalysis .....</i>	<i>51</i>
1. Introduction.....	51
2. Common photocatalysts for visible-light photoredox catalysis.....	51
3. Jablonski Diagram .....	53
4. Mechanism of visible-light photoredox catalysis.....	53
4.1. Electron transfer .....	53
4.2. Energy transfer .....	56
4.3. Hydrogen atom transfer .....	56
5. Conclusion.....	57
<i>PART 2: Urethanes and PUs synthesis by visible light-mediated decarboxylation of oxamic acids..</i>	<i>58</i>
1. Introduction.....	58
2. The objective of this Project.....	60
3. Further process optimization using PIDA as oxidant.....	60
4. Bis-oxamic acids used for the photocatalyzed polyurethane synthesis .....	63
5. Design of a new photocatalyzed procedure for PU synthesis from bis-oxamic acids.....	63

5.1. Characterization of the synthesized PUs .....	65
5.2. Optimization of photocatalyzed PU synthesis .....	68
6. Photocatalyzed PU synthesis from bis-oxamic acids using 1,4-butanediol .....	71
7. Photocatalyzed PU synthesis from bis-oxamic acids using 1,6-hexanediol .....	73
8. Conclusion.....	74
<b>Chapter 4 .....</b>	<b>75</b>
<b>Near-infrared light photocatalysis. Application to the oxidative decarboxylation of oxamic acids .</b>	<b>75</b>
1. Introduction .....	75
2. Triplet–triplet annihilation upconversion (TTA-UC).....	77
3. TTA-UC from red/NIR light to blue light.....	78
4. Direct red/NIR light photocatalysis .....	82
4.1. Metalloporphyrins as direct NIR photocatalyst.....	82
4.2. Indocyanine dye as NIR photocatalyst.....	83
5. Urethanes synthesis by NIR-mediated decarboxylation of oxamic acids.....	84
5.1 Urethane synthesis from oxamic acids by direct red/NIR light photocatalysis.....	85
5.1.1. Urethane synthesis from oxamic acids using ZnTPP as a photocatalyst.....	85
5.2.2. Urethane synthesis from oxamic acids using aza-BODIPY as a photocatalyst.....	85
5.2.3. Urethane synthesis from oxamic acids using indocyanine dye as a photocatalyst.....	86
5.2. Towards triplet-triplet annihilation up-conversion (TTA-UC) .....	86
5.2.1. Towards urethane synthesis from oxamic acids by TTA-UC using methylene blue as sensitizer and tetracene as annihilator .....	87
5.2.2. Towards urethane synthesis from oxamic acids by TTA-UC using BODIPY as sensitizer and ICBPEA as an annihilator .....	88
5.2.3. Towards urethane synthesis from oxamic acids by TTA-UC using Os(btpy) <sub>2</sub> (PF <sub>6</sub> ) <sub>2</sub> as sensitizer and TTBP as an annihilator.....	89
6. Comparing the penetration depth of the NIR light and blue LED light .....	96
7. Towards polyurethane synthesis from bis-oxamic acids using bulk polymerization method using 660 nm LED light. ....	98
8. Towards Reaction Mechanism .....	98
8.1 Intermediate trapping and identification experiments.....	98
8.2. Proposed mechanism .....	100
9. Conclusion.....	101
<b>Chapter 5 .....</b>	<b>103</b>
<b>Urethanes and polyurethanes synthesis through PIDA-mediated decarboxylation of oxamic acids under thermal conditions .....</b>	<b>103</b>
Introduction .....	103
<b>PART 1: Thermoplastic polyurethane synthesis from bis-oxamic acids using the PIDA-mediated decarboxylation .....</b>	<b>104</b>
1. Process optimization .....	104
2. Thermoplastic polyurethane synthesis using PIDA-mediated decarboxylation of bis-oxamic acids .....	105
3. Optimization of the PIDA-mediated synthesis of thermoplastic PU from bis-oxamic acids.....	107
4. Kinetics studies .....	109
4.1. Kinetic studies on the oxamic acid conversion/urethane linkage formation as a function of time .....	109
4.2. Molecular weight evolution during the kinetic studies.....	111
5. Investigation of thermal behavior of the bis-oxamic acid derived PUs.....	113
6. Thermoplastic PUs from different bis-oxamic acids.....	115
7. Thermoplastic PUs from bis-oxamic acid using different polyols/diols .....	121
8. Conclusion.....	126
<b>PART 2: PIDA-mediated Synthesis of Thermoset PUs by decarboxylation of oxamic acids .....</b>	<b>127</b>
1. Introduction .....	127
2. Swelling test .....	129

3. Characterization of PU foam from bis-oxamic acid .....	129
4. Towards Reaction Mechanism of the PIDA-mediated urethane synthesis from oxamic acids....	131
4.1. Proposed mechanism .....	132
5. Conclusion.....	134
Chapter 6.....	135
Urethane synthesis from Oxamic acids Under Electrochemical Conditions.....	135
PART 1: Basic concepts on Organic electrochemistry .....	135
1. Introduction.....	135
2. Setup for organic electrochemistry.....	136
3. Organic reactions at the electrodes .....	137
3.1. Working electrode and counter electrode .....	138
3.2. Reference electrodes .....	138
4. Controlling organic reactions at the electrode .....	139
5. Cyclic voltammetry .....	140
6. Solvents for organic electrochemistry .....	141
7. Supporting electrolytes for organic electrochemistry .....	142
8. Electrode materials for organic electrochemistry .....	142
9. Kolbe reaction .....	142
10. Hofer-Moest Reaction.....	144
Conclusion.....	146
PART 2: Design of a new non-phosgene route to urethane by electrochemical oxidation of oxamic acids.....	147
1. Introduction.....	147
2. Reaction procedure and optimization .....	147
3. Substrate scope .....	149
4. Mechanistic studies .....	154
5. Limitation of the electrochemical process.....	157
Conclusion.....	160
General conclusion .....	161
Experimental Part.....	165
1. General Information:.....	165
1.1. Instruments and Methods .....	165
2. General procedure for preparation of oxamic acids.....	166
Experimental Part: Chapter 3 .....	169
3. Experimental setup visible-light photocatalyzed reactions .....	169
3.1. Synthesis of 1,2,3,5-tetrakis(carbazol-9-yl)-4,6-dicyanobenzene (4-CzIPN): .....	170
3.2. 1-Hydroxy-1,2-benziodoxol-3(1H)-one .....	171
3.3. B. Preparation of 1-Acetoxy-1,2-benziodoxol-3-(1H)-one.....	172
3.4. Procedure for photocatalyzed polymerization .....	172
3.5. Procedure for synthesis of polyurethane from commercial diisocyanate.....	173
4. Experimental Part: Chapter 4 .....	173
4.1. Synthesis of Os(btpy) <sub>2</sub> (PF <sub>6</sub> ) <sub>2</sub> .....	173
4.2. Synthesis of 2,5,8,11-Tetra( <i>tert</i> -butyl)perylene (TTBP) .....	174
4.3. Synthesis of aza-BODIPY .....	175
4.4. Synthesis of BODIPY B-7 .....	176
4.5. General procedures for the photocatalyzed urethane synthesis using NIR light.....	178
4.6. General procedures for carbamoyl radical addition to heteroarenes under NIR light.....	178
4.7. Urethanes from NIR light photocatalysis .....	179
4.8. Amides from NIR photocatalysis .....	184
5. Experimental Part: Chapter 5 .....	186
5.1. Standard procedure for polyurethane synthesis from bis-oxamic acid using PIDA-mediated thermal process .....	186
5.2. Standard procedure for kinetic investigation .....	186

5.3. Standard procedure for PU foam synthesis from bis-oxamic acid.....	192
6. Experimental Part: Chapter 6.....	193
6.1. General Procedure for Electrochemical Synthesis of Urethane .....	193
6.2. $^1\text{H}$ and $^{13}\text{C}$ NMR data of urethanes in the electrochemical process .....	194
6.3. Alcohol Recovery after Electrochemical Reaction.....	206
6.4. Cyclic voltammetry studies .....	207

## Résumé en Français

Les uréthanes, également connus sous le nom de carbamates, sont des composés organiques importants, qui sont très appréciés pour leurs nombreuses applications. Les uréthanes sont largement utilisés dans l'industrie des polymères (polyuréthanes, PU), l'agrochimie (insecticides, herbicides et fongicides) et l'industrie pharmaceutique où ils constituent des motifs structuraux-clés dans de nombreux médicaments approuvés par la "Food and Drug Administration" (FDA). Les polyuréthanes constituent une classe importante de polymères dont la demande sur le marché augmente en raison de leurs propriétés polyvalentes, notamment leur légèreté, leur capacité d'absorption d'énergie, leur excellent rapport résistance/poids et leurs caractéristiques de confort. La production annuelle moyenne de PU était de 28 millions de tonnes selon une enquête de 2018 avec une valeur sur les marchés de plus de 60 milliards USD.

Cependant, la synthèse des uréthanes et des polyuréthanes repose essentiellement sur la chimie des isocyanates et de leur précurseur, le phosgène. Les isocyanates sont potentiellement cancérigènes, irritants et peuvent provoquer de l'asthme ou de la dyspnée. De plus, l'isocyanate est conventionnellement préparé à partir du phosgène, un produit chimique très dangereux. Le phosgène est un composé hautement volatil et inodore, ce qui le rend très dangereux à manipuler. Par conséquent, la préparation, la purification et le stockage du phosgène et de l'isocyanate cancérigène restent un grand défi sanitaire et environnemental pour les industries des PU. La recherche sur les uréthanes au cours des dernières années s'est donc concentrée sur le développement de voies alternatives durables pour les uréthanes, en particulier des stratégies qui évitent complètement l'utilisation de phosgène et d'isocyanate toxiques ou leur génération *in-situ* à partir d'un matériau de départ plus sûr.

Des travaux de recherche fondamentale de Minisci a révélé que les acides oxamiques pouvaient servir de précurseur de l'isocyanate. Ils ont montré que l'oxydation par voie radicalaire de cet acide organique en utilisant un persulfate  $S_2O_8^{2-}$  comme oxydant en présence de  $AgNO_3$  et  $Cu(OAc)_2$  comme catalyseurs, fournissait des isocyanates avec un rendement modéré à bon. Bien que cette méthode utilise un produit de départ plus sûr (l'acide oxamique) au lieu du phosgène pour générer l'isocyanate, elle ne convient pas pour un accès direct aux uréthanes en raison de la présence de l'eau comme solvant, ce qui requière l'isolement et la purification de l'isocyanate avant sa transformation en uréthane. Une hydrolyse partielle de l'isocyanate ainsi généré en amine a également été observée, ce qui a un effet délétère sur le rendement en produit.

Sur la base des travaux de Minisci, notre groupe a récemment développé une approche photocatalysée sans métal pour un accès direct aux uréthanes et aux urées à partir d'acides oxamiques via la génération *in-situ* d'isocyanates (Schéma 1). Ce procédé efficace et doux utilise une source de lumière visible, un photocatalyseur organique et un réactif à base d'iode hypervalent dans un solvant organique, permettant de déclencher l'oxydation de l'acide oxamique en isocyanate, lequel, en présence d'alcool, fournit l'uréthane avec un excellent rendement dans un procédé en un seul pot. Le protocole évite totalement l'isolement, la purification et le stockage de l'isocyanate cancérigène tout

en s'appuyant sur un précurseur plus respectueux de l'environnement. La méthode convient également à la préparation d'urées à partir d'acides oxamiques et d'amines.

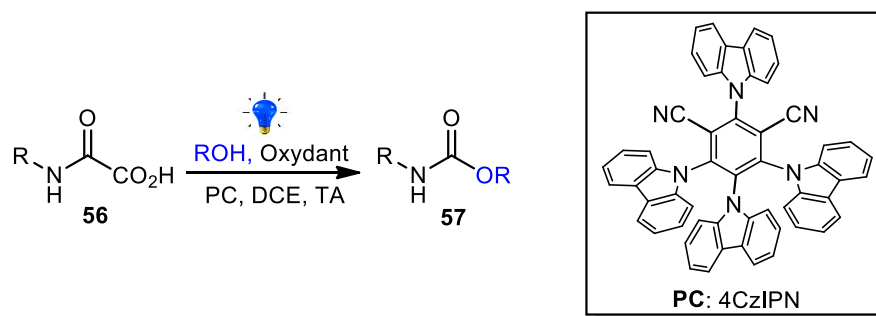


**Schéma 1:** Décarboxylation d'acides oxamiques médiée par la lumière visible pour la synthèse d'uréthanes.

Les acides oxamiques sont des composés peu toxiques et stables qui peuvent facilement être préparés par couplage direct entre des amines et des dérivés de l'acide oxalique. Ce protocole simple donne accès à des acides oxamiques d'une grande diversité structurale en utilisant diverses amines et ne nécessite pas de processus de purification fastidieux telle que la chromatographie.

L'objectif principal de ce projet était de développer une voie durable vers les polyuréthanes basée sur la génération *in-situ* d'isocyanates. Nous avons imaginé qu'avec des acides oxamiques bifonctionnels ou polyfonctionnels, des diisocyanates ou des polyisocyanates pourraient être ainsi générés *in-situ*, et qu'en présence de diols ou de polyols, ils permettraient d'obtenir des PUs par un procédé en un seul pot, sans isolement ni purification de l'isocyanate généré (Schéma 2).

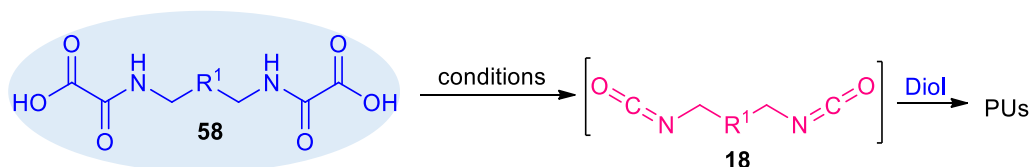


**Schéma 2:** Nouveau procédé photocatalysé pour la synthèse de PUs à partir d'acides oxamiques

Ce projet présente un certain nombre d'avantages, parmi lesquels :

- L'utilisation d'acides oxamiques comme matière première non toxique pour générer des isocyanates *in-situ* qui non seulement évitera la manipulation directe d'isocyanates cancérigènes, mais aussi l'utilisation de phosgène toxique comme précurseur d'isocyanate.
- Deuxièmement, le CO<sub>2</sub> libéré pendant le processus pourrait servir d'agent de moussage pour la préparation de mousses de PUs.
- Enfin, ce procédé peut servir de passerelle pour la synthèse de PU bio-sourcés, les acides oxamiques pouvant être dérivés de précurseurs d'amines bio-sourcés, puis transformés en polyuréthanes (Schéma 3).

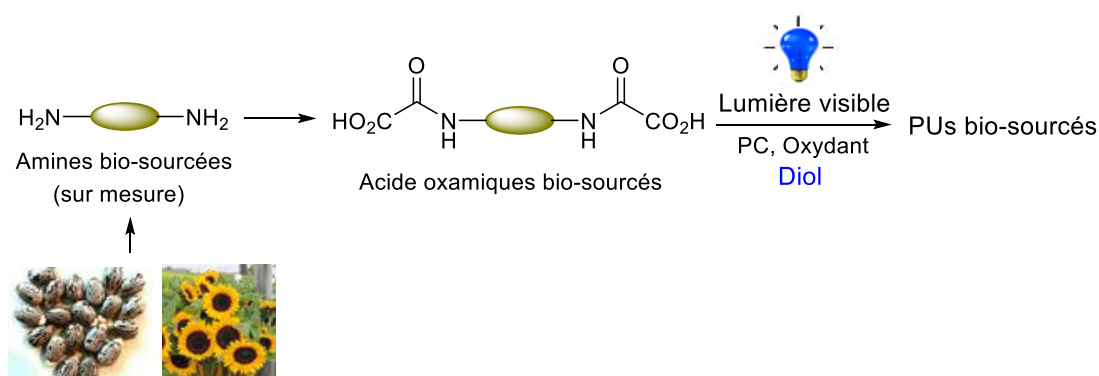


**Schéma 3:** Voie potentielle vers des PU bio-sourcés à base d'acides oxamiques bio-sourcés

Dans le cadre de ce projet, nous avons débuté par la synthèse d'acides bis-oxamiques synthétisés à partir de diamines disponibles dans le commerce. Dans notre première étape vers les polyuréthanes à partir d'acides oxamiques, nous avons soumis l'acide bis-oxamique **58** dans nos conditions optimisées de photocatalyse en utilisant le PEG-1500 **62** comme polyol (Schéma 4). Les polymères obtenus ont été analysés par RMN, FT-IR, SEC, TGA et DSC. Heureusement, il a été démontré que les PU issus de cette procédure photocatalysée possèdent des propriétés structurales similaires à celles des PU préparés par la voie traditionnelle au diisocyanate. Cependant, après plusieurs optimisations du processus, la masse molaire des PUs issus du protocole photocatalysé était généralement faible ou modeste, comparé à celui dérivé de la voie commerciale au diisocyanate.

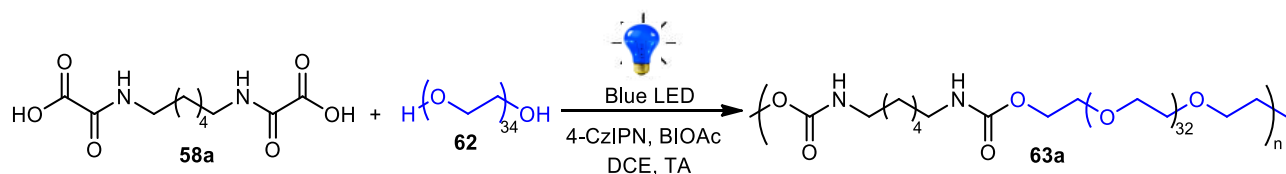


**Schéma 4:** Nouvelle approche photocatalysée à la synthèse de polyuréthanes à partir d'acides bis-oxamiques

Nous avons imaginé que le développement d'un système utilisant une lumière dans le proche infra-rouge pourrait améliorer la nouvelle voie non phosgène vers les polyuréthanes en profitant de la profondeur de pénétration plus importante de ce type d'irradiation. Cela pourrait également faciliter la mise en œuvre de la photopolymérisation en utilisant une approche sans solvant, une stratégie prometteuse pour améliorer la masse molaire et la préparation des mousses de PU. Différentes catalyses photoredox basées sur des irradiations dans le rouge ou dans le proche infra-rouge, par activation directe et par des stratégies « d'up-conversion », ont été étudiées pour leur capacité à médier la synthèse d'uréthanes à partir d'acides oxamiques. A ce jour, le photosensibilisateur  $\text{Os}(\text{bptpy})_2(\text{PF}_6)_2$  s'est avéré le plus efficace à cette fin (Schéma 5). Le fait que seule une très petite quantité de charge de catalyseur (0,3 mol%) ait été nécessaire rend cette procédure attrayante. Outre la synthèse d'uréthane, le procédé s'est également avéré efficace pour l'addition de radicaux carbamoylé sur des hétérocycles azotés pour la préparation d'amides (schéma 6).

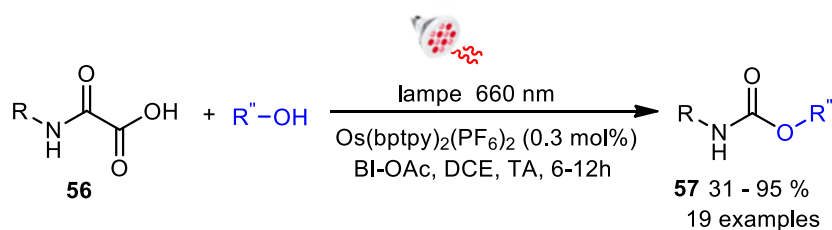


**Schéma 5:** Synthèse d'uréthanes à partir d'acides oxamiques à l'aide d'une LED 660 nm.

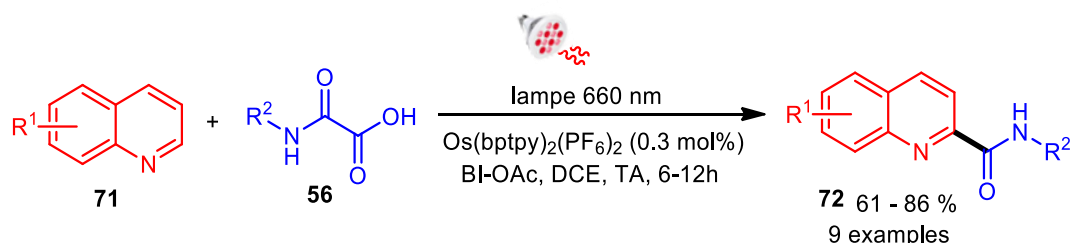


**Schéma 6:** Addition d'acides oxamiques sur des hétérocycles par photocatalyse à l'aide d'une LED 660 nm.

La profondeur de pénétration de l'irradiation dans le proche infra-rouge a été comparée à celle de la lumière bleue en utilisant différentes barrières. Notamment de la cire de paraffine de 1,5 cm, une solution d'hémoglobine, du papier blanc, de la peau d'animal, où une profondeur de pénétration supérieure du proche infra-rouge a été démontrée.

Nous avons ensuite appliqué ce système à la synthèse de PUs à partir d'acides bis-oxamiques en utilisant la méthode sans solvant. Cependant, la polymérisation a échoué en raison d'une mauvaise conversion de l'acide bis-oxamique. Ce problème pourrait être dû à la faible mobilité des monomères en réaction dans les conditions en masse.

Afin de résoudre ce problème, un nouveau protocole de décarboxylation *in situ* des acides oxamiques en isocyanates a été développé. La méthode repose sur l'utilisation de PIDA (diacétate d'iodobenzène) et un chauffage doux afin d'amorcer la décarboxylation oxydative des acides oxamiques en isocyanates. Après plusieurs optimisations, cette méthode a permis la synthèse efficace de PUs à partir d'acides bis-oxamiques et de polyols dans des conditions en masse (Schéma 7), conduisant à des polyuréthanes de masses molaires comparables à celles des diisocyanates commerciaux. Les analyses RMN, FT-IR, trace SEC, TGA et DSC indiquent une grande similarité entre les deux PU.

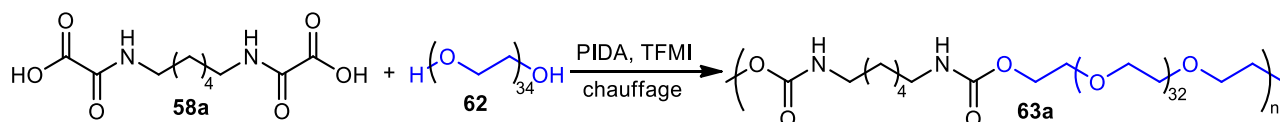


**Schéma 7:** Synthèse de PU thermoplastiques par décarboxylation d'acides bis-oxamiques à l'aide du PIDA dans des conditions thermiques

Encouragés par nos résultats sur la synthèse de PU thermoplastiques à partir d'acides bis-oxamiques, nous avons également montré que le protocole peut donner accès à des mousses de polyuréthane

(Schéma 8). Dans ce cas, le CO<sub>2</sub> libéré lors de la décarboxylation de l'acide oxamique sert d'agent de moussage.

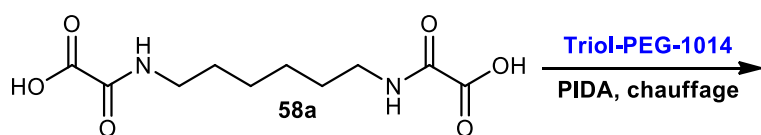


**Schéma 8:** Synthèse de mousse de PU à partir de l'acide bis-oxamique **58a** et d'un triol (Triol-PEG-1014 : éthoxylate de triméthylolpropane)

Enfin, au cours de ce projet, nous avons également développé une voie électrochimique unique pour la synthèse d'uréthanes à partir d'acides oxamiques (Schéma 9). L'objectif était de remplacer l'oxydant chimique dans notre système par une oxydation anodique. Après plusieurs optimisations du processus, la voie électrochimique s'est avérée appropriée pour la préparation de divers uréthanes à partir d'acides oxamiques, y compris chiraux sans racémisation.

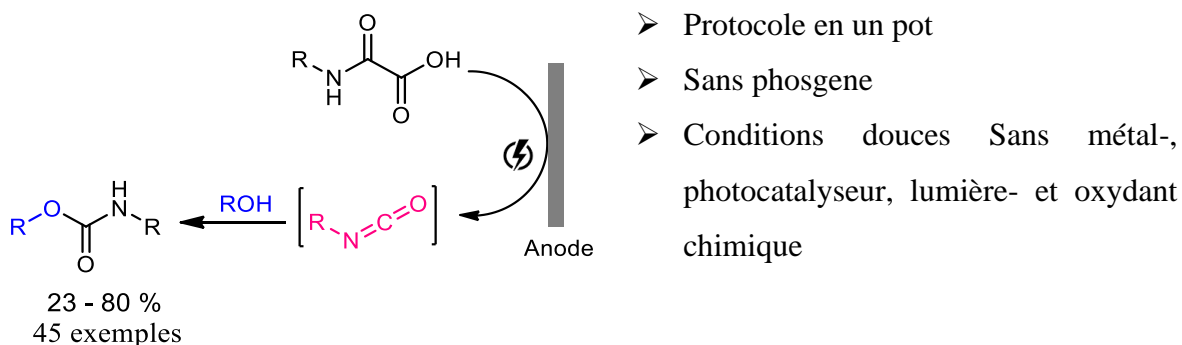


**Schéma 9:** Synthèse d'uréthanes à partir d'acides oxamiques dans des conditions électrochimiques.

Cependant, la voie électrochimique n'est pas adaptée à la synthèse des polyuréthanes car elle requière un excès d'alcool, ce qui n'est pas compatible avec la synthèse des PU, où la stœchiométrie est un point clé pour optimiser la masse molaire.

En conclusion, plusieurs nouvelles voies de synthèse « sans-phosgène » d'uréthanes et de polyuréthanes via la génération d'isocyanates *in-situ* à partir d'acides oxamiques ont été développées. Le protocole basé sur l'utilisation du PIDA dans des conditions thermiques a fourni des polyuréthanes avec des propriétés analogues aux échantillons de PU fabriqués à partir de diisocyanates standards. L'application de ce protocole à la préparation d'une mousse de PU à l'aide d'un acide bis-oxamique et d'un triol, où le CO<sub>2</sub> libéré pendant le processus de décarboxylation a servi d'agent moussant, a été démontrée avec succès. La cinétique élevée de cette réaction, associée à un matériau de départ plus écologique, la rend tout à fait attrayante comme approche alternative à la synthèse des polyuréthanes.



## List of Abbreviations, Acronyms, and Symbols

$[\alpha]_D^{25}$	specific rotation at 25°C using the sodium D line
Å	ångström ( $10^{-10}$ meter)
Abs	absorbance
Ac	acetyl group
Ac <sub>2</sub> O	acetic anhydride
AcOH	acetic acid
AIBN	azobis(isobutyronitrile)
APCI	Atmospheric Pressure Chemical Ionization
aq.	aqueous
Ar	aryl group, mono or polysubstituted
atm	atmospheric pressure
ATRA	Atom Transfer Radical Addition
BDE	Bond Dissociation Energy
BI-OAc	Acetoxybenziodoxole
BI-OH	Hydroxybenziodoxole
BF <sub>3</sub> .OEt <sub>2</sub>	boron trifluoride diethyl etherate
Bn	benzyl group
Boc	<i>tert</i> -butyloxycarbonyl group
BODIPY	Borondipyrromethene
b. p.	boiling point
brsm	based on recovered starting material
<i>i</i> -Bu	<i>iso</i> -butyl
<i>n</i> -Bu	<i>normal</i> -butyl
<i>t</i> -Bu	<i>tert</i> -butyl
<i>n</i> -BuLi	<i>normal</i> -butyllithium
<i>t</i> -BuOH	<i>tert</i> -butyl alcohol
<i>t</i> -BuOK	potassium <i>tert</i> -butoxide
<i>t</i> -BuONO	<i>tert</i> -butyl nitrite
(Bu <sub>3</sub> Sn) <sub>2</sub>	bis(tributyltin)
Bz	benzoyl group
<i>c</i>	mass concentration
°C	degree Celsius
CAS	Chemical Abstracts Service
cat.	catalytic quantity/catalyst
Cbz	carboxybenzyl group
CCDC	Cambridge Crystallographic Data Centre
CD	circular dichroism
CV	Cyclic voltammetry
CFL	Compact Fluorescent Lamp
CI	Chemical Ionization
comp. mix.	complex mixture
COSY	Correlation Spectroscopy
<i>m</i> -CPBA	<i>meta</i> -chloro perbenzoic acid
$\Delta/\delta$	delta
$\delta$	chemical shift
$\Delta$	refluxing conditions
$\Delta G$	Gibbs free energy
$\Delta H$	change in enthalpy

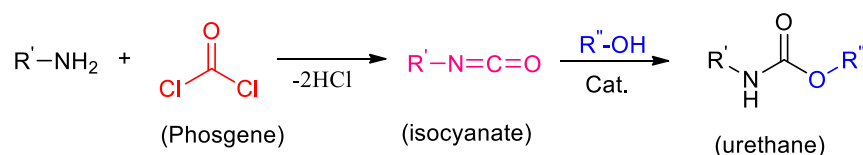
$\Phi$	diameter/quantum yield
<b>DBN</b>	1,5-diazabicyclo[4.3.0]non-5-ene
<b>DBU</b>	1,8-diazabicyclo[5.4.0]undec-7-ene
<b>DCE</b>	1,2-dichloroethane
<b>DEPT</b>	Distortionless Enhancement by Polarization Transfer
<b>DFT</b>	Density Functional Theory
<b>dia</b>	diastereomer
<b>DIBAL-H</b>	diisobutylaluminum hydride
<b>DIPA</b>	diisopropylamine
<b>DIPEA</b>	<i>N,N'</i> -diisopropylethylamine
<b>DMA</b>	dimethylacetamide
<b>DMAP</b>	4-dimethylaminopyridine
<b>DME</b>	dimethoxyethane
<b>DMF</b>	dimethylformamide
<b>DMP</b>	Dess-Martin periodinane
<b>DMPU</b>	<i>N,N'</i> -dimethylpropyleneurea
<b>DMSO</b>	dimethylsulfoxide
<b>dr</b>	diastereomeric ratio
<b>dRI</b>	differential refractive index
<b>DSC</b>	Differential Scanning Calorimetry
<b>DTBHN</b>	di- <i>tert</i> -butylhyponitrite
$\epsilon$	molar extinction coefficient
<b>E</b>	undefined electrophile
€	euro currency
$E^0$	standard reduction potential
$E_{ox}$	oxidation potential
$E_{red}$	reduction potential
<b>EDCI</b>	1-ethyl-3-(3-dimethylaminopropyl)carbodiimide hydrochloride
<b>EDG</b>	Electron Donating Group
<b>EDTA</b>	ethylenediaminetetraacetic acid
<b>ee</b>	enantiomeric excess
<b>Eq.</b>	equation
<b>eq.</b>	equivalent
<b>er</b>	enantiomeric ratio
<b>ESI</b>	ElectroSpray Ionization
<b>Et</b>	ethyl group
<b>eV</b>	electron volt
<b>EWG</b>	Electron Withdrawing Group
<b>F</b>	Faraday constant
<b><i>fac</i>-Ir</b>	<i>facial</i> -Iridium
<b>FD</b>	Field Desorption
<b>FI</b>	Field Ionization
<b>FID</b>	Flame Ionization Detector
$\gamma$	gamma
<b>GCE</b>	Glassy carbon electrode
<b>GC-MS</b>	Gas Chromatography-Mass Spectrometry
<b>[H]</b>	reduction
<b>HAT</b>	Hydrogen Atom Transfer
<b>HFIP</b>	1,1,1,3,3,3-hexafluoroisopropanol
<b>Hg-h<math>\nu</math></b>	irradiation with a mercury lamp
<b>HMPA</b>	hexamethylphosphoramide
<b>HOMO</b>	Highest Occupied Molecular Orbital

<b>HPLC</b>	High-Performance Liquid Chromatography
<b>HRMS</b>	High Resolution Mass Spectrometry
<b>HSQC</b>	Heteronuclear Single Quantum Coherence
<b>h<math>\nu</math></b>	photochemical activation
<b>Hz</b>	Hertz
<b>IBX</b>	2-iodoxybenzoic acid
<b>IR</b>	Infrared Spectroscopy
<b><i>J</i></b>	coupling constant
<b>J</b>	Joule
<b>k</b>	rate constant
<b>kcal</b>	kilocalorie
<b><math>\lambda</math></b>	lambda/wavelength
<b>LAH</b>	lithium aluminium hydride
<b>LED</b>	Light-Emitting Diode
<b>LiHMDS</b>	lithium bis(trimethylsilyl)amide
<b>LUMO</b>	Lowest Unoccupied Molecular Orbital
<b><i>m</i></b>	<i>meta</i> position
<b>M</b>	concentration (mole per liter)
<b>M</b>	undefined metal
<b>MHz</b>	megahertz
<b>mmHg</b>	millimeter of mercury
<b>mmol</b>	millimole
<b>mol</b>	mole
<b>mol %</b>	molar percentage
<b>m.p.</b>	melting point
<b>MS</b>	molecular sieves
<b>MsCl</b>	methanesulfonyl chloride
<b>Mw</b>	molecular weight
<b><math>\nu</math></b>	wavenumber
<b>n</b>	molar number
<b>nd</b>	not determined
<b>NIR</b>	Near Infrared
<b>nm</b>	nanometer (10 <sup>-9</sup> meter)
<b>NMO</b>	<i>N</i> -methylmorpholine <i>N</i> -oxide
<b>nOe</b>	Nuclear Overhauser Effect
<b>NOESY</b>	Nuclear Overhauser Effect Spectroscopy
<b>nr</b>	no reaction
<b>ns</b>	nanosecond
<b>Ns</b>	nosyl group
<b><i>o</i></b>	<i>ortho</i> position
<b>[O]</b>	oxidation
<b><i>p</i></b>	<i>para</i> position
<b>PC</b>	photocatalyst
<b>[Pd]</b>	palladium
<b>PDC</b>	pyridinium dichromate
<b>PEG</b>	Poly(ethylene glycol)
<b>PET</b>	Photoinduced Electron Transfer
<b>PG</b>	protecting group
<b>Ph</b>	phenyl group
<b>pH</b>	potential of Hydrogen
<b>PIDA</b>	phenyliodine(III) diacetate
<b>PIFA</b>	(bis(trifluoroacetoxy)iodo)benzene

<b>pKa</b>	$-\log_{10}(K_a)$ , the negative logarithm, to the base 10, of the acid dissociation constant ( $K_a$ )
<b>ppm</b>	parts per million
<b>R, R<sub>n</sub>, R'</b>	undefined alkyl group
<b>rt</b>	room temperature (20-25°C)
<b>sat.</b>	saturated
<b>SEC</b>	Size Exclusion Chromatography
<b>S<sub>N</sub>2</b>	bimolecular nucleophilic substitution
<b>SOMO</b>	Singly Occupied Molecular Orbital
<b>SPS</b>	Solvent Purification System
<b><i>t</i>/<i>tert</i></b>	<i>tertio</i>
<b>TBAF</b>	tetrabutylammonium fluoride
<b>TBDMS/TBS</b>	<i>tert</i> -butyldimethylsilyl group
<b>TBDMSCI/TBSCl</b>	<i>tert</i> -butyldimethylsilyl chloride
<b>TEMPO</b>	2,2,6,6-tetramethylpiperidine- <i>N</i> -oxy radical
<b>Tf</b>	triflate group
<b>TFA</b>	trifluoroacetic acid
<b>TFAA</b>	trifluoroacetic anhydride
<b>TFMI</b>	Bis(trifluoromethanesulfonyl)imide
<b>Tf<sub>2</sub>O</b>	triflic anhydride
<b>TGA</b>	Thermogravimetric Analysis
<b>THF</b>	tetrahydrofuran
<b>TTBP</b>	2,5,8,11-Tetra( <i>tert</i> -butyl)perylene
<b>TIPS</b>	triisopropylsilyl group
<b>TIPSCl</b>	triisopropylsilyl chloride
<b>TLC</b>	Thin Layer Chromatography
<b>TMP</b>	2,2,6,6-tetramethylpiperidine
<b>TMS</b>	trimethylsilyl group
<b>TMSCHN<sub>2</sub></b>	(trimethylsilyl)diazomethane
<b>TMSCl</b>	trimethylsilyl chloride
<b>TMSCN</b>	trimethylsilyl cyanide
<b>TOF</b>	time-of-flight
<b><i>p</i>-Tol</b>	<i>para</i> -tolyl group
<b>TPAP</b>	tetrapropylammonium perruthenate
<b>Ts</b>	tosyl group
<b>TTMS</b>	tris(trimethylsilyl)silane
<b>UV</b>	ultraviolet irradiation
<b>UV-A</b>	electromagnetic spectral range between 325 and 400 nm
<b>wt. %</b>	weight percent
<b>X</b>	undefined halogen
<b>4-CzIPN</b>	1,2,3,5-tetrakis(carbazol-9-yl)-4,6-dicyanobenzene

## General Introduction

Urethanes are important organic compounds with wide applications in pharmaceutical,<sup>1</sup> agrochemicals and polymer industries.<sup>2</sup> Their use as peptide bond surrogates in peptide chemistry and protecting group in organic synthesis are also of high value.<sup>3</sup> Otto Bayer in 1947 invented polyurethanes (PUs) through the polyaddition of polyisocyanates and polyols (Scheme 1). The specialty performance and versatile properties of PUs make them suitable for wide applications in many fields including upholstery, building insulation, automotive parts, medical, adhesives, coatings, aeronautic and textile industries.<sup>4</sup> PU foams constitutes the major global PUs production and the largest in the polymer foams market.<sup>5</sup> Recent survey revealed that the market value of PUs was about 60 billion USD in 2020 and is expected to increase to about 80 billion USD by 2026 (Figure 1), marking it a viable market.<sup>6</sup>



**Scheme 1:** Classical route to urethanes and polyurethanes

However, the most established route for accessing urethanes and PUs which has since the invention, relied on the addition of alcohols to isocyanates, suffers from the use of highly hazardous phosgene as a precursor during the preparation of isocyanate, moreover isocyanate is a known carcinogenic compound. Despite its inherent toxicity, this classical route to urethanes and PUs method has continued to thrive due to its simplicity and efficiency. Although, several promising alternative procedures for urethane and PUs have been proposed or presented over the years, they are still at developmental stages. The research in this area are mainly targeted at solving two fundamental issues with the existing isocyanate route. The first is the problem of toxicity as mentioned earlier, and the second is the question about sustainability. Current urethanes and polyurethanes production mainly depend on fossil resources<sup>7</sup> which are non-renewable and are being depleted. Hence, there is a growing interest in the use of biomass resources to design monomers for polymer synthesis.<sup>8</sup>

<sup>1</sup> R. J. Zdrahala, I. J. Zdrahala, *J. Biomater. Appl.* **1999**, *14*, 67–90.

<sup>2</sup> O. Bayer, *Angew. Chem.* **1947**, *A59*, 257–272.

<sup>3</sup> W. D. Fuller, M. Goodman, F. R. Naider, Y. F. Zhu, *Biopolymers* **1996**, *40*, 183-205.

<sup>4</sup> O. Kreye, H. Mutlu, M. A. R. Meier, *Green Chem.* **2013**, *15*, 1431-1455

<sup>5</sup> a) L. D. Mora-Murillo, F. Orozco-Gutierrez, J. Vega-Baudrit, R. J. González-Paz, *J. Renew. Mater.* **2017**, *5*, 3–4. b) K. Khemani, *Polymeric foams: An overview, in Polymeric Foams: Science and Technology*, ACS Symposium Series, American Chemical Society, Washington DC, USA (1997).

<sup>6</sup> *Market value of polyurethane worldwide from 2015 to 2020, with a forecast for 2021 to 2026*: <https://www.statista.com/statistics/720449/global-polyurethane-market-size-forecast/> (Retrieved on 19-02-2022).

<sup>7</sup> C. Liang, U.R. Gracida-Alvarez, E.T. Gallant, P. A. Gillis, Y. A. Marques, G. P. Abramo, T. R. Hawkins, J. B. Dunn, *Environ. Sci. Technol.* **2021**, *55*, 20-22.

<sup>8</sup> L. Maisonneuve, O. Lamarzelle, E. Rix, E. Grau, H. Cramail, *Chem. Rev.* **2015**, *115*, 12407–12439.

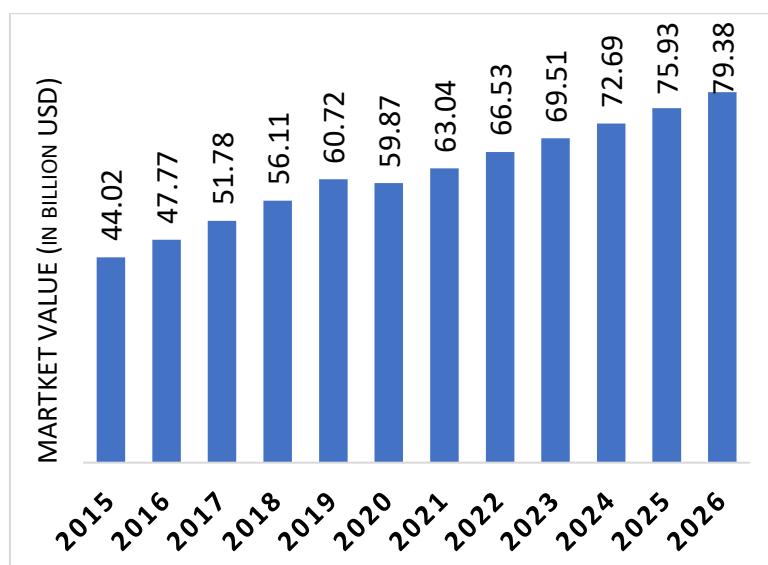
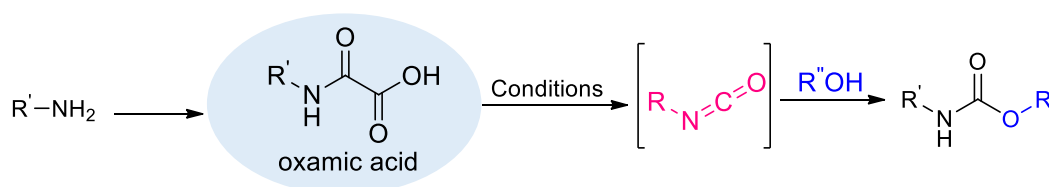


**Figure 1:** Market Value of PUs from 2015 to 2020 with forecast for 2026.<sup>6</sup>

In contribution to the ongoing efforts, this project focusses on the development of new non-phosgene routes to urethane and PUs through the *in-situ* generation of isocyanate from oxamic acids as a greener precursor (Scheme 2). Oxamic acids are relatively non-toxic compounds that can easily be accessed by coupling between amine and oxalic acid derivatives. Besides being non-toxic, oxamic acids are stable<sup>9</sup> and can easily be handled and stored compared to isocyanates and phosgene that need special handling to avoid environmental hazard and deterioration. Minisci and co-workers<sup>10</sup> originally demonstrated that oxamic acids can be oxidized into isocyanates using a persulphate as an oxidant, copper and silver salts as catalysts. Their method resulted in moderate yields of isocyanate in a biphasic medium involving water. Though Minisci method uses oxamic acids as a safer precursor, the carcinogenic isocyanate generated still had to be isolated and purified before being converted to urethanes. Also, partial hydrolysis of the generated isocyanate by the water used as solvent was detrimental to the isocyanate yield.

This project was designed to address these problems, by developing a process that could generate the isocyanate *in-situ* from oxamic acids and deliver urethanes through one pot process thereby avoiding the isolation and purification of carcinogenic isocyanate (Scheme 2).



**Scheme 2:** New non-phosgene route to urethane using oxamic acids as a safer precursor

<sup>9</sup> J.-W. Yuan, J.-L. Zhu, H.-L. Zhu, F. Peng, L.-Y. Yang, P. Mao, S.-R. Zhang, Y.-C. Lib and L.-B. Quc, *Org. Chem. Front.*, **2020**, *7*, 273-275.

<sup>10</sup> a) F. Minisci, F. Coppa, F. Fontana, *Chem. Commun.* **1994**, 679. b) F. Minisci, F. Fontana, F. Coppa, M. Y. Yan, *J. Org. Chem.* **1995**, *60*, 5430-5433.

As mentioned earlier, addition of alcohol to isocyanate according to Bayer's method is a very efficient process, however, a procedure that relies on this reactive species but generated *in-situ* using a safer precursor is quite interesting and may offer quicker solution to solving toxicity issue associated with classical urethane synthesis. Among the reported alternative procedure for urethanes preparation based on the *in-situ* generation of isocyanate are Curtius,<sup>11</sup> Hofmann,<sup>12</sup> and Lossen<sup>13</sup> rearrangements. However, toxicity issues and explosive nature of the acyl azide as a starting material for Curtius method is of great concern. Also, Hofmann and Lossen rearrangements are limited by their high susceptibility to degradation to amines by moisture,<sup>1</sup> hence Hofmann rearrangement is primarily used for conversion of amides into amines.<sup>14</sup>

The main objective of this project was to develop a sustainable route to polyurethanes based on *in-situ* generation of isocyanate from oxamic acids. We envisioned that with a bifunctional or polyfunctional oxamic acids, diisocyanates or polyisocyanates could be generated *in-situ*, and in the presence of diols or polyols would afford PUs through a one pot process, without isolation and purification of the generated isocyanate (Scheme 2). This project relies on the merit of using safer precursor to generate isocyanates *in-situ* thereby avoiding direct handling and storage of the carcinogenic compound. Also, the procedure completely avoids the use of toxic phosgene in urethane synthesis. Moreover, the CO<sub>2</sub> released during the decarboxylation process can be part of the process by serving as a blowing agent for the preparation of self-blown PU foams from oxamic acids. Ultimately, this procedure can serve as a gateway for the synthesis of bio-sourced PUs, whereby oxamic acids could be derived from bio-based amine precursors and then be transformed into bio-sourced polyurethanes.

As mentioned earlier, renewability of PU precursors is very vital for sustainable PUs synthesis. This project has the potential to deliver bio-sourced PUs, whereby oxamic acids would be derived from various bio-resources including amino-acid feedstock, fatty acids, terpenes, resinic acids, isosorbide as well as lignin derivatives or sugars.<sup>15</sup>

This thesis is divided into six chapters. Chapter 1 deals with generalities on urethanes and PUs, which offers a reasonable background information about the topic. Also, some progresses made in the past few years in the development of greener alternative procedures for urethane and PUs synthesis are highlighted in this chapter, particularly those suitable for PUs synthesis.

In chapter 2, general information on oxamic acids were presented both as precursors for carbamoyl radicals and isocyanate. Lots of work have been accomplished in the last two decades using oxamic acids as a potent carbamoyl radical source for the synthesis of amide and heterocycles. A fair review of these progress is also presented in chapter 2.

---

<sup>11</sup> a) T. Curtius, *J. Prakt. Chem.* **1894**, *50*, 275-294. b) E. F. V. Scriven, K. Turnbull, *Chem. Rev.* **1988**, *88*, 297-368.

<sup>12</sup> a) A. W. Hofmann, *Ber. Dtsch. Chem.* **1885**, *18*, 2734-2741. b) A. W. Hofmann, *Ber. Dtsch. Chem.* **1881**, *14*, 2725-2736.

<sup>13</sup> W. Lossen, *Justus Liebigs Ann. Chem.* **1872**, *161*, 347-362. b) H. L. Yale, *Chem. Rev.* **1943**, *33*, 209-256.

<sup>14</sup> a) P. Gogoi, D. Konwar, *Tetrahedron Lett.* **2007**, *48*, 531. b) W. D. Fuller, M. Goodman, M. S. J. Verlander, *J. Am. Chem. Soc.* **1985**, *107*, 5821-5822.

<sup>15</sup> V. Froidevaux, C. Negrell, S. Caillol, J.-P. Pascault, B. Boutevin, *Chem. Rev.* **2016**, *116*, 14181-14224.

Furthermore, some basic concepts of visible-light photoredox catalysis were highlighted in the first part of the chapter 3. A visible-light mediated oxidative decarboxylation of oxamic acids as a greener access to urethanes and PUs, which was developed during this project, is presented in the second part of the chapter.

There is growing interest in the use of NIR light photoredox catalysis for organic reactions and photopolymerization due to its superior penetration into media and milder nature compared to the UV/visible-light counterparts. Some basic concepts of this relatively new strategy were highlighted in the first part of chapter 4. The second part of the chapter is dedicated to the attempts made during this project towards developing more efficient photocatalytic system for PUs synthesis from oxamic acids under NIR light conditions.

PIDA-mediated decarboxylation of oxamic acids into *in-situ* generated isocyanates under thermal condition was also unveiled during this project and is presented in chapter 5. This efficient process gave access to both thermoplastic PUs, which are describe in the first part of the chapter while the thermoset PUs from oxamic acids are described in the second part of the chapter.

There is increasing interest in the use of simple electrochemical set-up in organic synthesis due to its simplicity, promising environmental benefits and ability to limit the use of stoichiometry amount of expensive reagents and waste generation. In the course of this project, urethane synthesis under electrochemical conditions was also developed. This strategy was targeted at replacing the hypervalent iodine reagent involved in our reaction with anodic oxidation. This progress is presented in chapter 6. Meanwhile, basic concepts of organic electrochemistry were discussed in the first part of chapter followed by the work accomplished during this project.

Finally, detail experimental procedures used in this project, instruments, and the data for the synthesized molecules and PUs are described in the experimental parts.

# Chapter 1

## Urethanes and Polyurethanes

### 1. Introduction

This chapter is dedicated to relevant literature on urethanes and polyurethanes, highlighting their properties, synthesis and applications. Urethane and polyurethane synthesis heavily relies on the chemistry of isocyanates and their precursor phosgene. The inherent toxicity of these chemicals has led to development of several other alternative synthetic procedures over the years. Most of these procedures are targeted at completely avoiding the toxic compounds, or their *in-situ* generation starting from safer materials. These progresses are also highlighted in this chapter, particularly, those techniques that are suitable for polyurethane synthesis. Due to its central role in classical and some greener alternative routes to urethane and polyurethanes, the reactivity of isocyanate towards alcohols including its mechanism are also emphasized in this chapter.

### 2. Urethanes

Urethanes also known as carbamates are important organic compounds, which are highly valued for their wide applications. Urethanes are extensively used in polymer industry (polyurethanes, PUs),<sup>16</sup> agroindustry (insecticides, herbicides and fungicides)<sup>17</sup> and pharmaceutical industry where they constitute key structural motifs in many FDA approved drugs.<sup>18</sup> Due to their excellent proteolytic properties, urethanes are commonly used as peptide bond surrogates.<sup>19</sup> In organic synthesis and peptide chemistry, urethanes serve as efficient protective groups for amino functions, exhibiting excellent chemical stability.<sup>20</sup> Urethanes as linkers in combinatorial chemistry has also been reported.<sup>21</sup>

The chemical behavior of urethanes is closely related to that of amides.<sup>22</sup> Just as amides, carbamates are much less nucleophilic than amines because of the lone pair on the nitrogen, which is conjugated with the carbonyl group (Figure 1.1a). This also hinders rotation about the C-N single bond, resulting in carbamate existing as *syn* and *anti* rotamers with the *anti* rotamer being the preferred conformation for secondary carbamates due to steric and electrostatic factors.<sup>23</sup>

<sup>16</sup> L. Maisonneuve, O. Lamarzelle, E. Rix, E. Grau, H. Cramail, *Chem. Rev.* **2015**, *115*, 12407–12439.

<sup>17</sup> N. Guéniche, A. Bruyere, M. Ringeval, E. Jouan, A. Huguet, L. Le Hégarat, O. Fardel, *Xenobiotica* **2020**, *50*, 1380–1392.

<sup>18</sup> A. K. Ghosh, M. Brindisi, *J. Med. Chem.* **2015**, *58*, 2895–2940.

<sup>19</sup> C. C. Y. Cho, E. J. Moran, S. R. Cherry, J. C. Stephans, S. P. Fodor, C. L. Adams, A. Sundaram, J. W. Jacobs, P. G. Shultz, *Science* **1993**, *261*, 1303–1304.

<sup>20</sup> T. W. Greene, P. G. M. Wuts, *protecting groups in organic synthesis*, J. Wiley & Sons, New York, 3rd edn, 1999, p. 503.

<sup>21</sup> D. Chaturvedi, S. Ray, *Monatshefte für Chemie*, **2006**, *137*, 127–145.

<sup>22</sup> C. Dugave, L. Demange, *Chem. Rev.* **2003**, *103*, 2475–2532.

<sup>23</sup> a) M. J. Deetz, C. C. Forbes, M. Jonas, J. P. Malerich, B. D. Smith, O. Wiest, *J. Org. Chem.* **2002**, *67*, 3949–3952. b) C. Cox, T. Lectka, *J. Org. Chem.* **1998**, *63*, 2426–2427.

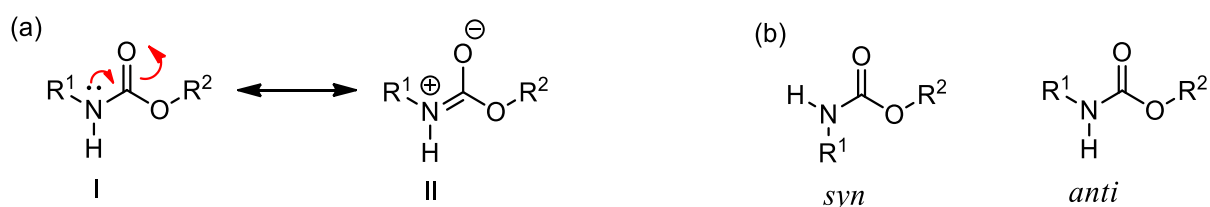
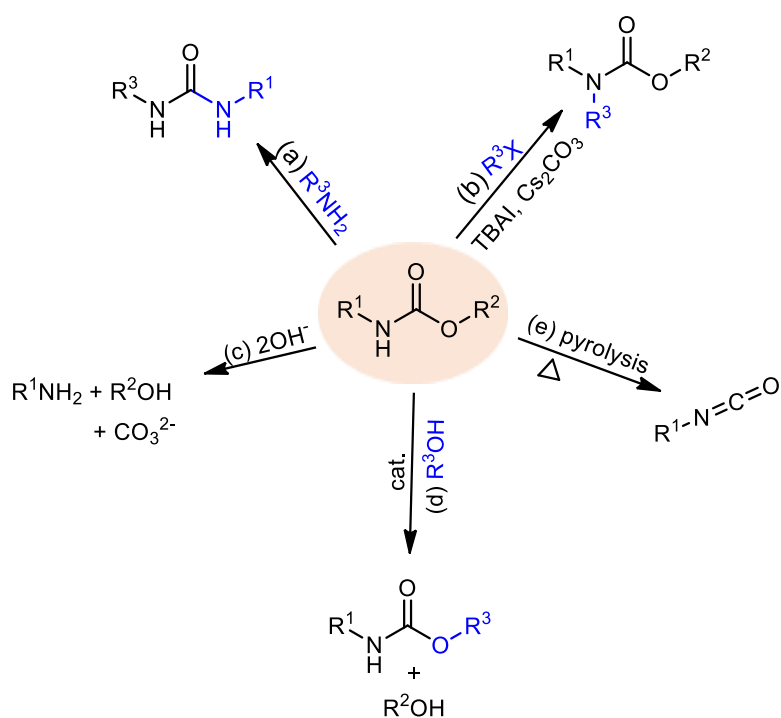


**Figure 1.1:** (a) Resonance structures in carbamate (b) carbamate rotamers

Some chemical reactivities of carbamates are summarized in Scheme 1.1. Carbamates can undergo aminolysis in the presence of amine to give urea (**a**). The hydrogen atom in the NH group of secondary carbamates is active and can be utilized to derivatize carbamate including N-alkylation and arylation using alkyl and aryl halide respectively<sup>24</sup> (**b**). It has also been shown that carbamate can undergo hydrolysis in alkaline medium resulting in alcohol, amine, and carbonate<sup>25</sup> (**c**). Urethane can equally be transurethanized in the presence of alcohol to form a new urethane<sup>26</sup> (**d**). Finally, pyrolysis of urethanes can regenerate isocyanate under thermal conditions (**e**).<sup>27</sup>



**Scheme 1.1:** Some chemical reactivities of carbamates

## 2.1. Classical route to urethanes and its limitations

Traditionally, urethane is synthesized by addition of alcohols to isocyanates **3** as developed by Otto Bayer in 1947 (Scheme 1.2).<sup>28</sup> Isocyanate is commercially prepared by the reaction between phosgene **2** and amine. Urethane synthesis with isocyanate is a very efficient reaction, and is often

<sup>24</sup> R. N. Salvatore, S. I. Shin, V. L. Flanders, K. W. Jung, *Tetrahedron Lett.* **2001**, 42, 1799-1801.

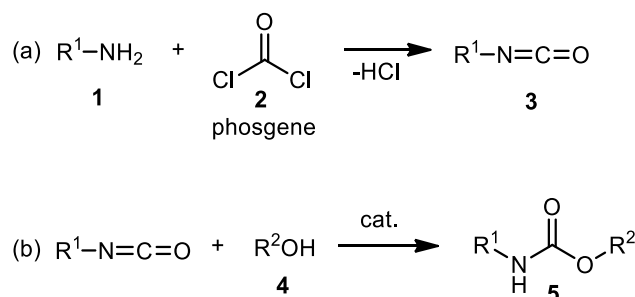
<sup>25</sup> L. W. Dittert, T. Higuchi, *J. Pharm. Sci.* **1963**, 52, 852-857.

<sup>26</sup> T. Prenveille, C. Garreau, M. Matner, D. Dijkstra, W. Oppermann, D. Johannsmann, *Polym. Chem.* **2019**, 57, 621-629.

<sup>27</sup> E. Delebecq, J. -P. Pascault, B. Boutevin, F. Ganachaud, *Chem. Rev.* **2013**, 113, 80-118.

<sup>28</sup> a) S. Ozaki, *Chem. Rev.* **1972**, 72, 457. b) O. Bayer *Angew. Chem.* **1947**, 59, 257-272.

catalyzed using organotin compounds such as dibutyltin dilaurate (DBTDL) and dibutyltin diacetate (DBTDA). However, due to the toxicity awareness of tin reagents, other alternative catalysts including 1,4-diazabicyclo[2.2.2]octane (DABCO),<sup>29</sup> N-heterocyclic carbenes,<sup>27</sup> amidines, guanidines,<sup>30</sup> organic strong or super-strong Brønsted acids catalysts<sup>31,32</sup> have been developed to accelerate this reaction.



**Scheme 1.2:** (a) Classical route to isocyanate (b) classical route to urethanes

### 3. Mechanism of isocyanate reaction with alcohols

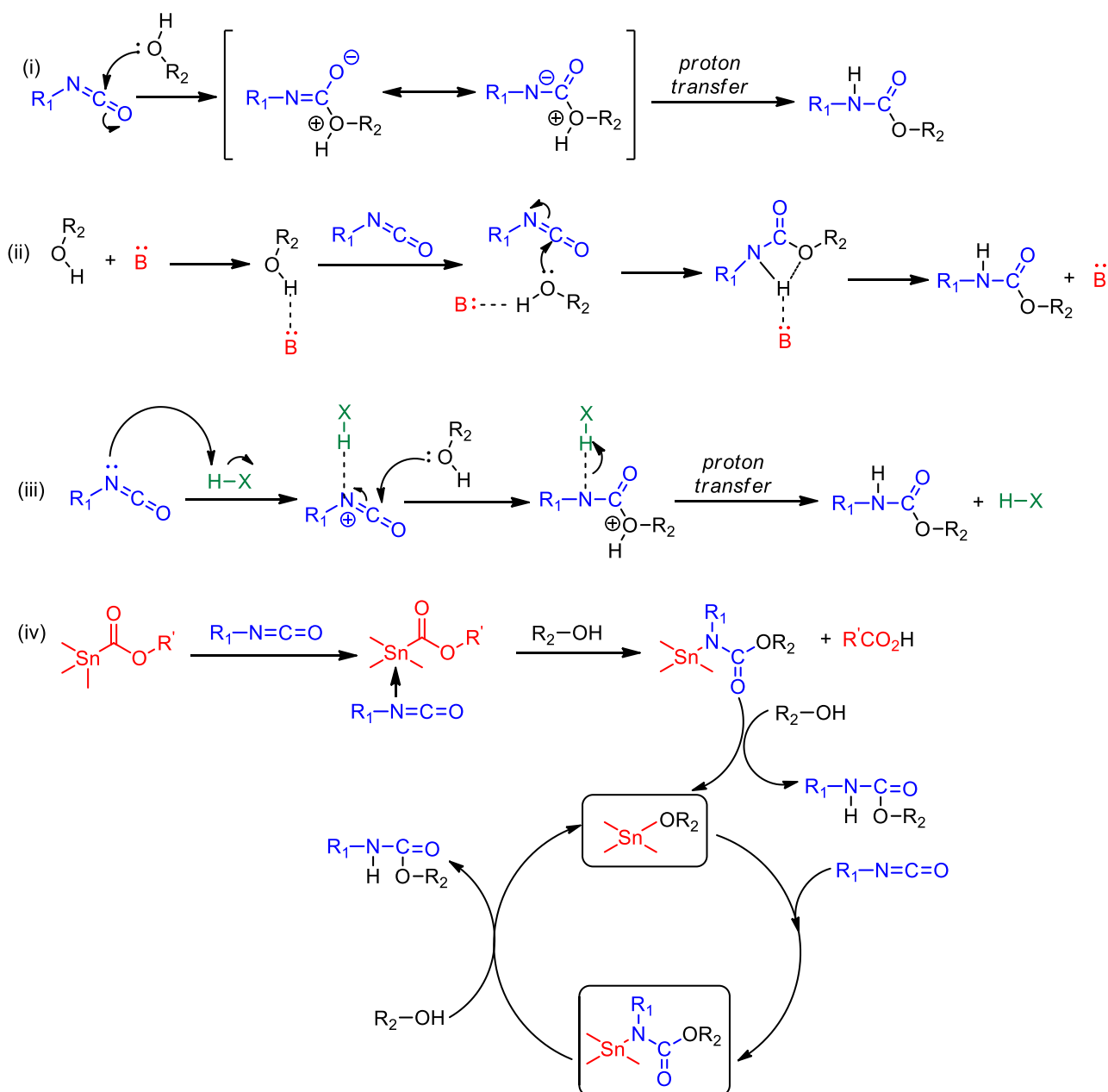
The reaction of alcohol (or similar nucleophiles) with isocyanates involves a nucleophilic attack on the electrophilic carbon of isocyanate and then deprotonation to furnish the final product (Scheme 1.3, **i**). Organobase catalysis of the reaction is based on activation of alcohol as illustrated in (**ii**), while Brønsted acid catalysis proceeds through isocyanate activation by hydrogen bonding on N atom (**iii**), though the hydrogen bonding can occur on O atom.<sup>32</sup> Furthermore, the catalytic activities of organotin in isocyanate reaction is not yet well-defined,<sup>32</sup> available information shows that it probably acts as a Lewis acid as illustrated in (**iv**), whereby N-coordination of the isocyanate with the tin alkoxide resulted from alcoholysis of the organotin catalyst, then alkoxide anion transfer onto the coordinated isocyanate would give N-stannylurethane which undergoes alcoholysis to release urethane and regenerates tin alkoxide.<sup>27,32</sup>

<sup>29</sup> A. L. Silva, J. C. Bordado, *Catal. Rev.* **2004**, *46*, 31–51.

<sup>30</sup> J. Alsarraf, Y. A. Ammar, F. Robert, E. Cloutet, H. Cramail, Y. Landais, *Macromolecules* **2012**, *45*, 2249–2256.

<sup>31</sup> H. Sardon, A. C. Engler, J. M. W. Chan, J. M. García, D. J. Coady, A. Pascual, D. Mecerreyes, G. O. Jones, J. E. Rice, H.W. Horn, J. L. Hedrick, *J. Am. Chem. Soc.* **2013**, *135*, 16235–16241.

<sup>32</sup> H. Sardon, A. Pascual, D. Mecerreyes, D. Taton, H. Cramail, J. L. Hedrick, *Macromolecules* **2015**, *48*, 3153–3165.



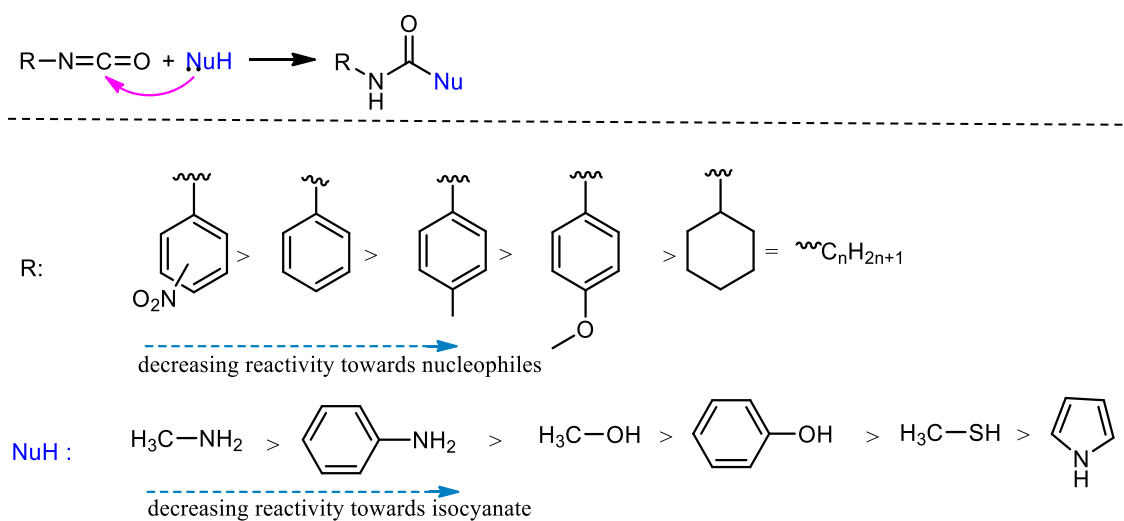
**Scheme 1.3:** Mechanism of isocyanates reaction with alcohols<sup>32</sup>

### 3.1. Electronic effects in the reactivity of isocyanate with alcohols and other nucleophiles

In the absence of other factors including steric effects, attachment of an electron-withdrawing group on  $-N=C=O$  will increase its reactivity towards nucleophilic attack through the increase of the positive charge on the carbon atom. On the other hand, electron-donating groups will reduce its reactivity towards nucleophilic attack.<sup>33</sup> This can explain why aromatic isocyanates are usually more

<sup>33</sup> R. G. Arnold, J. Nelson, J. J. Verbanc, *Chem. Rev.* **1957**, 57, 47–76.

reactive than their aliphatic counterparts. Also, the order of reactivity of common nucleophiles including amines and alcohols towards isocyanates are shown in Scheme 1.4.



**Scheme 1.4:** Electronic effects in the reactivity of isocyanate

#### 4. Limitations of classical route to urethanes and polyurethanes

Although isocyanate route to urethanes is very efficient and has remained till date the main industrial pathway to urethanes and polyurethanes, the inherent toxicity associated with process has been a big concern. Isocyanates are potentially carcinogenic, irritants and could cause allergic asthma or dyspnea.<sup>34,35</sup> Some of them including methyl isocyanate and TDI have been classified under Carcinogenic, Mutagenic and Reprotoxic (CMR) by European Reach Regulation and Global Harmonized System.<sup>34,36</sup> Moreover, isocyanate is conventionally prepared from phosgene, a very hazardous chemical.<sup>37</sup> Phosgene is highly volatile and colorless, making it a very dangerous pollutant. It was reportedly used as a chemical weapon during World War (I).<sup>38</sup> Although less volatile phosgene equivalents including diphosgene **6** (trichloromethyl chloroformate) and triphosgene **7** (bis(trichloromethyl) carbonate) (Scheme 1.5) have been developed over the years, their toxicity is still similar to that of phosgene.<sup>39</sup> Hence, preparation, purification and storage of the highly hazardous phosgene and carcinogenic isocyanate remains of great health and environmental challenge in PUs industries. Research on urethanes over the past years have therefore focused on developing sustainable alternative routes to urethanes, particularly strategies that completely avoid the use of toxic phosgene and isocyanate or their *in-situ* generation from a safer starting material.

<sup>34</sup> a) O. Kreye, H. Mutlu, M. A. R. Meier, *Green Chem.* **2013**, *15*, 1431-1455. b) R. J. Zdrahala, I. J. Zdrahala, *J. Biomater. Appl.* **1999**, *14*, 67-90.

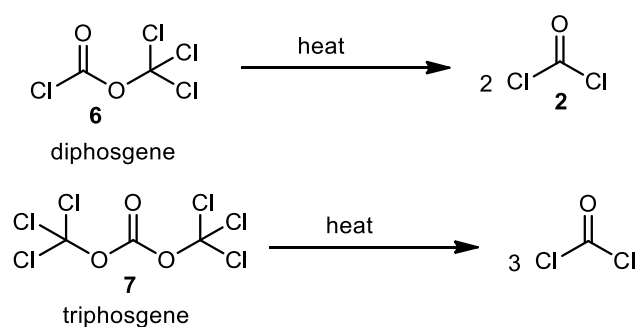
<sup>35</sup> T. Tsuda, H. Hokazono, *Chem. Res. Toxicol.* **1991**, *4*, 503-509.

<sup>36</sup> U. Romano, R. Tesel, M. M. Mauri, P. Rebora, *Ind. Eng. Chem.* **1980**, *19*, 396-403.

<sup>37</sup> a) H. Gang, D. Lee, K.-Y. Choi, H.-N. Kim, H. Ryu, D.-S. Lee, B.-G. Kim, *ACS Sustainable Chem. Eng.* **2017**, *5*, 4582-4588. b) L. S. Jr Hardison, E. Wright, A. F. Pizon, *J. Med. Toxicol.* 2014, *10*, 51-56. c) J. Borak, W. F. Diller, *J. Occup. Environ. Med.* **2001**, *43*, 110-119.

<sup>38</sup> G. J. Fitzgerald. *Am J Public Health.* **2008**, *98*, 611-625.

<sup>39</sup> S. B. Damle. "Safe handling of diphosgene, triphosgene". Chemical & Engineering News, **1993**, 71, 6. (<http://pubsapp.acs.org/cen/safety/19930208.html>, retrieved 12-03-2021).



**Scheme 1.5:** Alternatives to phosgene for isocyanate synthesis

## 5. Greener routes to urethanes and polyurethanes

In the next section, major greener alternative routes to urethane/polyurethane developed during the last few decades will be highlighted and divided under two main groups: (a) Non-phosgene and non-isocyanate route to urethanes (b) Urethanes synthesis based on *in-situ* generation of isocyanate.

### 5.1. Non-phosgene and non-isocyanate routes to Urethanes

Three major non-isocyanate routes to urethanes/polyurethanes are (i) carbonate/amine routes (ii) transurethanization (iii) ring-opening polymerization (ROP) of cyclic carbamates.

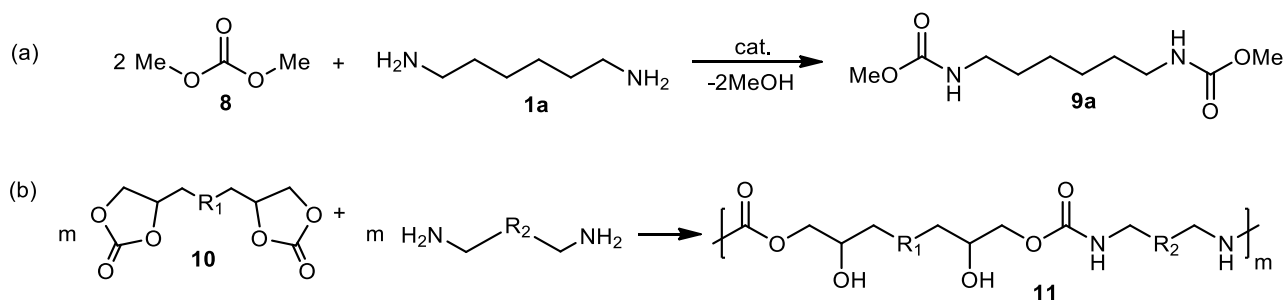
#### 5.1. Carbonate/amine route

It has been shown that bis-alkylcarbamates, and particularly methoxycarbamates **9**, can be prepared by the reaction between dimethoxycarbonate (DMC) **8** and diamines (Scheme 1.6).<sup>16</sup> Aliphatic amines show greater reactivity in this reaction as compared to aromatic amines.<sup>40</sup> Also, polyaddition between five-membered bicyclic carbonate **10** and diamine/polyamine, to give polyurethanes that contains additional hydroxyl group at the  $\beta$ -position (poly(hydroxyurethanes), PHUs **11**) has been widely studied as a non-phosgene and isocyanate-free route to polyurethanes.<sup>41,42</sup> While these procedures are promising as a greener alternative to polyurethanes, some constraints related to low kinetics, conversion and molar masses are still on the way to be addressed.<sup>16</sup> Also, PHUs have different properties than PUs due to the pendant hydroxyl group.

<sup>40</sup> T. Baba, A. Kobayashi, Y. Kawanami, K. Inazu, A. Ishikawa, T. Echizenn, K. Murai, S. Aso, M. Inomata, *Green Chem.* **2005**, *7*, 159–165.

<sup>41</sup> G. Rokicki, A. Piotrowska, *Polymer* **2002**, *43*, 2927-2935

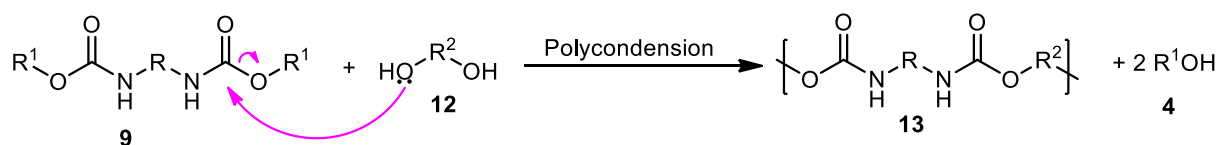
<sup>42</sup> C. Li, S. Li, J. Zhao, Z. Zhang, J. Zhang, W. Yang, *J. Polym. Res.* **2014**, *21*, 498-499.



**Scheme 1.6:** Non-phosgene route to urethanes based on addition of amines to carbonates

## 5.2. Transurethanization

Transurethanization also known as transcarbamoylation or transurethane reaction is a reaction between urethane and alcohol to form another urethane.<sup>16,27</sup> This reaction is mostly useful for synthesis of polyurethane **13** from simple urethanes using diol or polyol **12**, (Scheme 1.7). The reaction is usually performed at elevated temperature (> 150°C) in the presence of catalyst such as Ti(OBu)<sub>4</sub> or Bu<sub>2</sub>SnO. However, high temperature involved in the reaction sometimes leads to side reactions including formation of allophanates.<sup>43</sup> Besides, green access to carbamates as a starting material may be another concern.



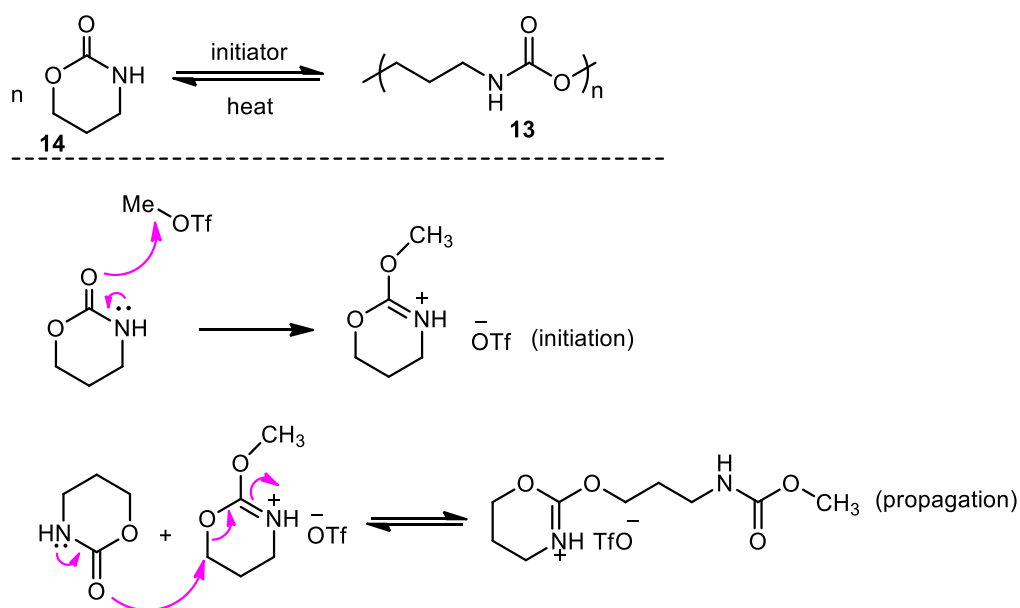
**Scheme 1.7:** Transurethanization for polyurethane synthesis

## 5.3. Ring-opening polymerization (ROP) of cyclic carbamates

Cationic ring-opening polymerization of 6- and 7-membered ring carbamates is another non-isocyanate route to PUs.<sup>32,34a</sup> The reaction is usually carried out at melt with temperature > 100°C and can be initiated using triflates and sodium hydroxide. The proposed mechanism by Höckel *et al.*<sup>44</sup> using triflates as initiator, suggests the involvement of cyclic endo iminocarbonate salt formed by the reaction between the triflate and cyclic carbamate as the active initiation species (Scheme 1.8). However, reported ring-opening polymerizations are generally limited in scope.

<sup>43</sup> T. Prenveille, C. Garreau, M. Matner, D. Dijkstra, W. Oppermann, D. Johannsmann, *J. Polym. Sci., Part A: Polym. Chem.* **2019**, *57*, 621–629.

<sup>44</sup> a) S. Neffgen, H. Keul, H. Höcker, *Macromolecules* **1997**, *30*, 5, 1289–1297. b) J. Kušan, H. Keul, H. Höcker, *Macromolecules* **2001**, *34*, 3, 389–395.



**Scheme 1.8:** Ring opening polymerization

#### 5.4. Urethanes based on *in-situ* generation of isocyanates

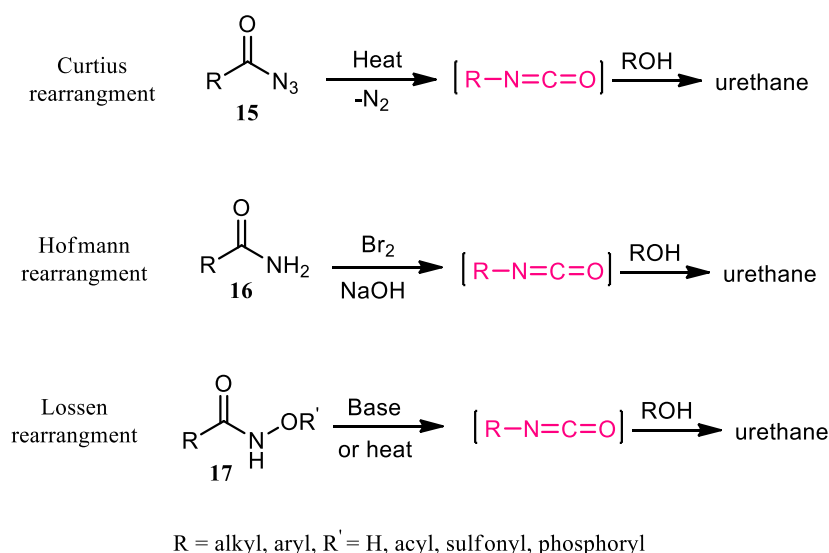
Another strategy aimed at solving the toxicity associated with classical procedure for urethane synthesis is the generation of isocyanate *in-situ* using a safer starting material. This avoids the direct handling of the carcinogenic chemical. Some methodologies developed so far in this regard for urethane synthesis have been developed based on this strategy and common among them are Curtius,<sup>45</sup> Hofmann,<sup>46</sup> and Lossen rearrangements<sup>47</sup> which use acyl azide **15**, amide **16**, and hydroxamic acid **17** respectively as precursors (Scheme 1.9). Among these methods, Curtius rearrangement has been shown to be efficient, however, high toxicity and explosive nature of the acyl azide as a starting material is of great concern. Also, Hofmann and Lossen rearrangements are limited by their high susceptibility to degradation to amines by moisture,<sup>19a</sup> resulting that Hofmann rearrangement is primarily used for conversion of amides into amines.<sup>48</sup>

<sup>45</sup> a) T. Curtius, *J. Prakt. Chem.* **1894**, 50, 275-294. b) E. F. V. Scriven, K. Turnbull, *Chem. Rev.* **1988**, 88, 297-368.

<sup>46</sup> a) A. W. Hofmann, *Ber. Dtsch. Chem.* **1885**, 18, 2734-2741. b) A. W. Hofmann, *Ber. Dtsch. Chem.* **1881**, 14, 2725-2736.

<sup>47</sup> W. Lossen, *Justus Liebigs Ann. Chem.* **1872**, 161, 347-362. b) H. L. Yale, *Chem. Rev.* **1943**, 33, 3, 209-256.

<sup>48</sup> a) P. Gogoi, D. Konwar, *Tetrahedron Lett.* **2007**, 48, 531. b) W. D. Fuller, M. Goodman, M. S. J. Verlander, *J. Am. Chem. Soc.* **1985**, 107, 5821-5822.



**Scheme 1.9:** Methods for urethane synthesis through *in-situ* generation of isocyanate

## 6. Polyurethanes

Polyurethanes (PUs), generally referred to as polymers that contain urethane linkages (-N-C(O)-O-), were invented by Otto Bayer and co-workers in 1947 through the polyaddition between diols and diisocyanates (Scheme 9).<sup>28b</sup> They are special class of polymers with increasing market demand due to their versatile properties including lightweight, energy absorbing capacity, excellent strength to weight ratio and comfort features.<sup>49</sup> PUs are well known for their wide applications in upholstery, building insulation, automotive parts, medical, adhesives, coatings, aeronautic and textile industries.<sup>16,34</sup> PUs exist in different forms and can be segmented into flexible foams (used for cushioning in furniture, mattresses, pillows...), rigid foams (insulating foams for thermal and acoustic insulations), elastomers (automobile parts), coatings, adhesives, and sealants (Figure 1.2). The average annual production of PUs was reported in 2018 to be 28 million tons with a market value of over 60 billion USD.<sup>50</sup>

<sup>49</sup> J. O. Akindoyo, M. D. H. Beg, S. Ghazali, M. R. Islam, N. Jeyaratnama, A. R. Yuvarajc, *RSC Adv.*, **2016**, *6*, 114453-114482.  
<sup>50</sup> a) N. V. Gama, F. Artur, A. Barros-Timmons, *Materials* **2018**, *11*, 1841. b) *Polyurethane Global Market Size Forecast 2021*: <https://www.statista.com/statistics/720449/global-polyurethane-market-size-forecast/> (Retrieved on 05-12-2021).

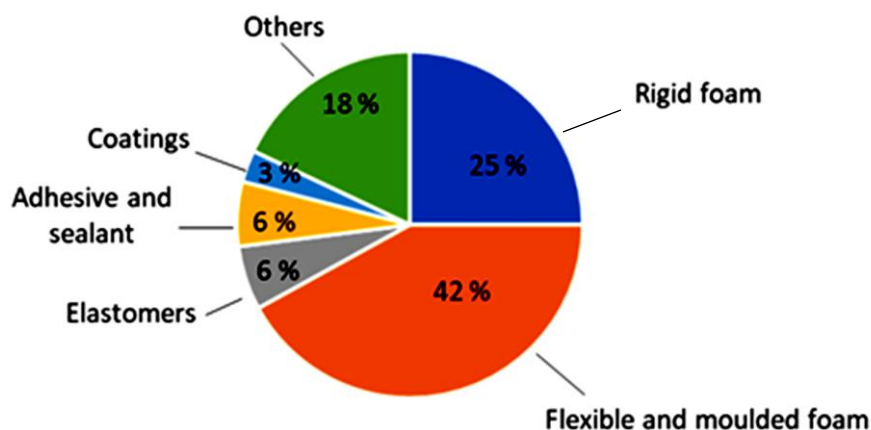
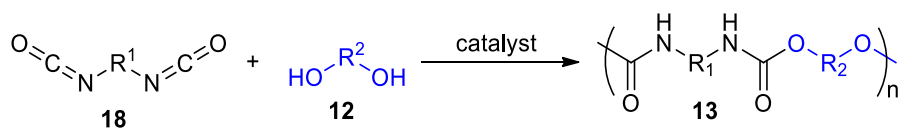


**Figure 1.2:** World polyurethane consumption in 2016.<sup>6a</sup>

### 6.1. Classical thermoplastic polyurethane synthesis, composition and properties

Classical thermoplastic PUs are often prepared by the reaction between diisocyanates **18** and flexible polyols **12** (macrodiols) (Scheme 1.10), and often, short chain diols or diamines are used as chain extenders. PUs synthesis follows step-growth polymerization, that is, monomers add to form short chains, which can also add to form a longer one. This is different from chain-growth polymerization where only monomers add to the growing chain.

Polyurethanes of diverse physico-chemical properties can be prepared by varying the nature of diisocyanates and polyols.<sup>16</sup> Polyols constitute the soft segment of PUs while diisocyanates and chain extenders make up the hard segment. Thus, PUs are characterized by microphase separation comprising soft and hard segments. Various polyols can be employed for PUs synthesis, the common ones being polyether polyols and polyesters polyols (Figure 1.3). While polyether-derived PUs have higher resistance to hydrolysis and lower glass transition temperature compared to polyester derived counterparts, the latter exhibit higher stability in lipophilic medium. Examples of polyether polyols popularly used for PUs synthesis include polyethylene glycol (PEG) and poly(tetramethylene oxide) (PTMO). PEG based thermoplastic PUs are soluble in various solvents including water and can be used in many waterborne and water-soluble PUs techniques.<sup>51</sup>



**Scheme 1.10:** Classical thermoplastic PU synthesis

Common diisocyanates used for PUs synthesis include methylene diphenyl diisocyanate (MDI), toluene diisocyanate (TDI), hexamethylene diisocyanate (HDI) and isophorone diisocyanate (IPDI) (Figure 1.3). Aromatic diisocyanates such as MDI and TDI are widely employed for industrial

<sup>51</sup> a) N. Kebir, S. Nouigues, P. Moranne, F. Burel. *J. Appl. Polym. Sci.* **2017**, *134*, 44991. b) Z. Xie, C. Lu, X. Chen, L. Chen, X. Hu, Q. Shi, X. Jing, *Eur. Polym. J.* **2007**, *43*, 2080-2087. c) M. -S. Yen, P.-Y. Tsai, P. -D. Hong, *J. Appl. Polym. Sci.* **2007**, *105*, 1391-1399. d) V. Doseva, S. Shenkov, S. Vasilev, V.Y. Baranovsky, *J. Appl. Polym. Sci.* **2004**, *91*, 3651-3658.

synthesis of PUs due to their outstanding mechanical properties, which could be attributed to their high crystallinity.<sup>52</sup> However, aromatic diisocyanate-derived PUs are more prone to degradation that may release potentially carcinogenic products.<sup>52,53</sup> As a result, the aliphatic counterparts are preferred for biomaterials and are more biodegradable. Furthermore, aromatic diisocyanate-derived PUs exhibit higher glass transition, tensile strength and modulus compared to the aliphatic counterparts but the latter have advantage of higher elongation at break and lower tensile strength.<sup>52,54</sup> and are commonly used for the synthesis of coatings, especially HDI and IPDI.<sup>6a</sup>

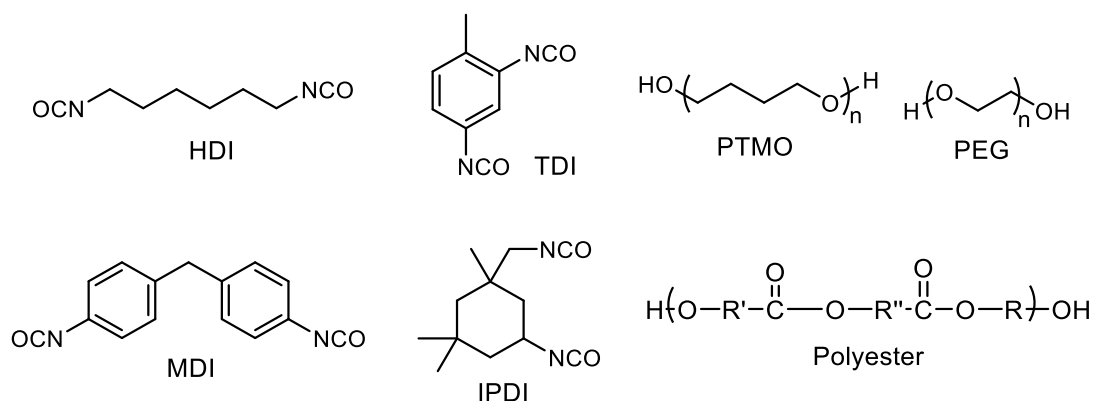


**Figure 1.3:** Common diisocyanates and polyols used for PUs synthesis

## 6.2. Polyurethanes foams (PUs-foam)

As mentioned earlier, PU foams constitutes the major global PU production (over 67%) and the largest in the polymer foams market.<sup>55</sup> Conventionally PU foams are prepared by polyaddition between diisocyanate (or polyisocyanate) and polyols to give highly cross-linked PUs which, in the presence of foaming agent and surfactant, forms a foam. In this technique, one or both monomers should contain at least three functionalities to be able to form a cross-linked PU. For the choice of polyols for PU foams, higher molecular weight polyols (>2000 gmol<sup>-1</sup>) are more favorable for preparation of flexible PU foams, while lower molecular weight polyols are better for making more rigid PU foams due to short chain length and greater density of crosslinks. Typically, flexible PU foams preparation is usually achieved using polyether triols of about 3000 to 5000 molecular weights with hydroxyl number of about 30 to 70.<sup>57</sup>

Among the classical blowing agent for PU foams are chlorofluorocarbons (CFCs), however rapidly banned due to environmental concerns. The use of water contamination to induce hydrolysis of isocyanates for *in-situ* generation of CO<sub>2</sub> as blowing agent is now commonly used.<sup>56</sup> In the mechanism (Scheme 1.11), isocyanate reacts with water to form unstable carbamic acid, which

<sup>52</sup> D. Aoki, H. Ajiro, *Macromolecules* **2017**, *50*, 6529–6538.

<sup>53</sup> R. H. Cardy, *J. Nat. Canc. Inst.* **1979**, *62*, 1107-1116.

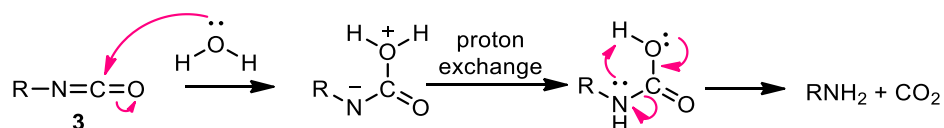
<sup>54</sup> I. Javni, W. Zhang, *J. Appl. Polym. Sci.* **2003**, *88*, 2912–2916.

<sup>55</sup> a) L. D. Mora-Murillo, F. Orozco-Gutierrez, J. Vega-Baudrit, R. J. González-Paz, *J. Renew. Mater.* **2017**, *5*, 3–4. b) K. Khemani, *Polymeric foams: An overview*, in *Polymeric Foams: Science and Technology*, ACS Symposium Series, American Chemical Society, Washington DC, USA (1997).

<sup>56</sup> F. Monie, B. Grignard, J.-M. Thomassin, R. Mereau, T. Tassaing, C. Jerome, C. Detrembleur, *Angew. Chem. Int. Ed.* **2020**, *59*, 17033-17041.

decomposes into amine with release of CO<sub>2</sub>. In this strategy, water is regarded as a chemical blowing agent because it is involved in the chemical reaction during the PU foam synthesis. However, there are other classes of blowing agent used in PU foam production such as volatile liquids (including pentane, hexane or acetone), which blow PUs by vaporization. They are not involved in any chemical reaction during the process and are known as physical blowing agents.

During PU foaming, the blowing agent forms either air bubbles or air tunnels within the matrix of the crosslinked PUs, and these are referred to as closed-cell and open-cell structures respectively.<sup>57</sup> PU foams comprising of closed-cell are usually more rigid due to pressure inbuilt by the entrapped air. In the other hand, open-cell PU foams are generally flexible.



**Scheme 1.11:** Water as a blowing agent during PUs foam synthesis

## Conclusion

Urethanes are important organic compounds extensively used in polymer, agro- and pharmaceutical industries. Particularly, polyurethanes are one of the most demanded polymers in the market due to their versatile properties. However, traditionally routes to urethanes and polyurethanes which has relied on addition of alcohol to isocyanates as developed by Otto Bayer in 1947 has huge drawbacks due to the carcinogenic nature of isocyanate and toxicity of its precursor phosgene. This has motivated diverse research leading to development of some promising alternative synthetic routes to urethanes and polyurethanes as highlighted in this chapter. However, most of them are still at developmental stages.

<sup>57</sup> A. S. Dutta, *Polyurethane Foam Chemistry* In: S. Thomas, A. V. Rane, K. Kanny, V. K. Abitha, M. G. Thomas, *Recycling of Polyurethane Foams*, Elsevier, **2018**, pp. 17-21.

## Chapter 2

### Oxamic acids as precursors of carbamoyl radicals and urethanes

#### 1. Introduction

Oxamic acid, also known to as oxalic acid monoamide, has emerged as a powerful greener precursor for generation of carbamoyl radical and its derivatives in organic synthesis. Oxamic acids can easily undergo decarboxylation through a single electron oxidation resulting in reactive carbamoyl radical, which can engage in diverse radical reactions or undergo a second single oxidation as originally unveiled by Minisci to generate isocyanate<sup>58</sup>- another potent intermediate for the synthesis of nitrogen-containing organic molecules. This makes oxamic acid a versatile precursor for construction of varieties of functionalities in organic synthesis.

Oxamic acid function can be viewed as a combination of carboxylic and secondary amide group<sup>59</sup> exhibiting special properties. Quantum-chemical studies<sup>60</sup> have suggested that oxamic acid probably exhibits amide–iminol tautomerism (Figure 2.1), with the amide tautomer **I** considered more stable, though this hypothesis has yet to be experimentally validated. Furthermore, the nature of hydrogen bonding in oxamic acids has been widely studied,<sup>61,59a</sup> and there is evidence that oxamic acid does not exist in zwitterionic form in solid state.<sup>62</sup> The simplest oxamic acid ( $\text{H}_2\text{NCOOH}$ ) was popularized due to its potential medicinal application owing to its chemical similarities (isoelectronic and isosteric) with pyruvic acid ( $\text{CH}_3\text{COOH}$ ), an important biomolecule involved in glucose metabolism).<sup>59b,63</sup>

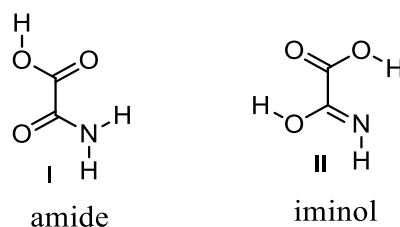


**Figure 2.1** : Hypothetical tautomerism in oxamic acid

<sup>58</sup> a) F. Minisci, F. Coppa, F. Fontana, *Chem. Commun.* **1994**, 679. b) F. Minisci, F. Fontana, F. Coppa, M. Y. Yan, *J. Org. Chem.* **1995**, *60*, 5430-5433.

<sup>59</sup> a) I. Wolfs, H. O. Desseyn, *Spectrochimica Acta Part A* **52**, **1996**, 1521-1528. b) A. J. Dugarte-Dugarte, J. van de Streek, A. M. dos Santos, L. L. Daemen, A. A. Puzetky, G. D. de Delgado, J. M. Delgado, *J. Mol. Struct.* **2019**, *1177*, 310-316.

<sup>60</sup> a) E. D. Raczynska, M. Hallmann, K. Duczmal, *Comput. Theor. Chem.* **2011**, *964*, 310-317. b) B. Bankiewicz, S. Wojtulewski, S. J. Grabowski, *J. Org. Chem.* **2010**, *75*, 1419-1426.

<sup>61</sup> a) G. N. R. Tripathi, J. E. Katon, *Acta Mol. Biomol. Spectrosc.* **1979**, *35A*, 401-407. b) F. Wallace, E. Wagner, *Spectrochim. Acta Mol. Biomol. Spectrosc.* **1978**, *34A*, 589-606.

<sup>62</sup> S. P. Perlepes, T. F. Zafiroopoulos, J. K. Kouinis, A. G. Galinos, *Inorg. Nucl. Chem. Lett.* **1980**, *6*, 475-480.

<sup>63</sup> E. D. Raczynska, M. Hallmann, K. Duczmal, *Comput. Theor. Chem.* **2011**, *964*, 310-317.

## 2. Oxamic acid as carbamoyl radical precursor

The most common synthetic application of oxamic acids is based on their oxidative decarboxylation to generate carbamoyl radical as originally unveiled by Minisci.<sup>58</sup> Carbamoyl radical (Figure 2.2) is a nucleophilic radical that can readily add to an electron deficient system via SOMO–LUMO interaction,<sup>64</sup> providing a reliable strategy for construction of a vast number of nitrogen-containing compounds. Carbamoyl radical displays a similar reactivity with other  $\alpha$ -type carbonyl radicals such as acyl and alkoxy carbonyl (Scheme 2.1). Interestingly, it is relatively long-lived compared to these other analogue radicals<sup>65,66,67</sup> which are prone to decarbonylation and decarboxylation respectively resulting in more stable alkyl radical.<sup>68</sup> Decarbonylation of carbamoyl radical is less favored (except when R = Ph), because it would lead to a higher energetic aminyl radical.

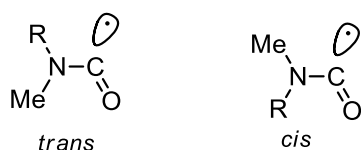
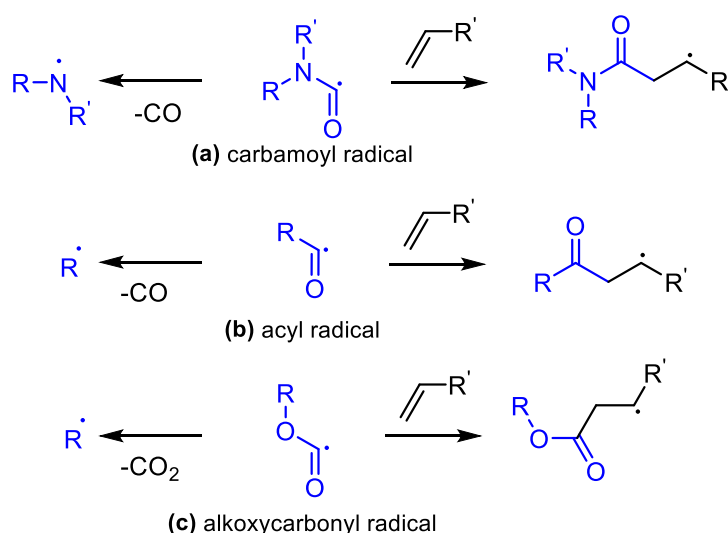


**Figure 2.2** : Carbamoyl radical structure



**Scheme 2.1** : Reactivity of carbamoyl, acyl and alkoxy carbonyl radicals

Although less attention was paid to carbamoyl radical compared to acyl radicals, recent years have witnessed a dramatic interest in the use of carbamoyl radical in synthetic organic chemistry and this among other factors, could be attributed to the rediscovery of oxamic acid as its potent precursor (Scheme 2.2). In traditional radical chemistry, carbamoyl radical is usually generated by the homolytic cleavage of  $\text{R}_2\text{NC}(\text{O})-\text{X}$  precursors using a radical initiator, heat, or UV light, where X

<sup>64</sup> D. Elad, J. Rokach, *J. Org. Chem.* **1964**, *29*, 1855-1859.

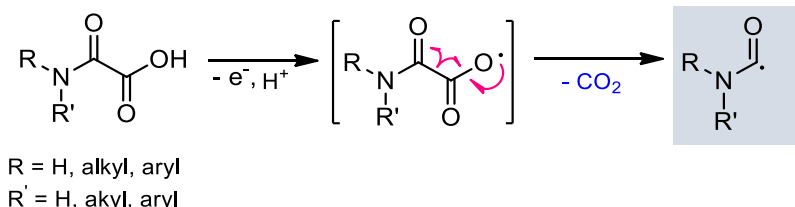
<sup>65</sup> A. H. Jatoi, G. G. Pawar, F. Robert, Y. Landais, *Chem. Commun.* **2019**, *55*, 466-469.

<sup>66</sup> C. Chatgililoglu, D. Crich, M. Komatsu, I. Ryu, *Chem. Rev.* **1999**, *99*, 1991-2065.

<sup>67</sup> W. F. Petersen, R. J. K. Taylor, J. R. Donald, *Org. Biomol. Chem.* **2017**, *15*, 5831-5845.

<sup>68</sup> a) C. M. Jensen, K. B. Lindsay, R. H. Taaning, J. Karaffa, A. M. Hansen, T. Skrydstrup, *J. Am. Chem. Soc.* **2005**, *127*, 6544-6545. b) C. Raviola, S. Protti, D. Ravelli, M. Fagnoni, *Green Chem.* **2019**, *21*, 748-764.

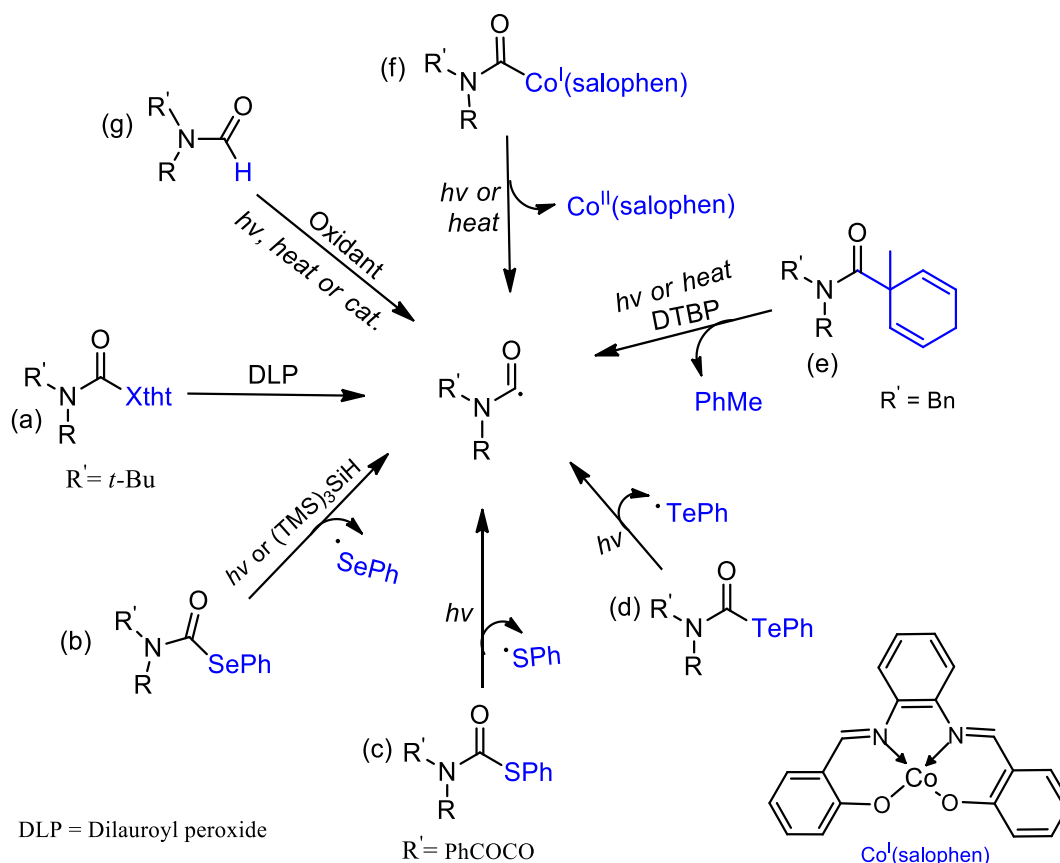
can be H,<sup>69</sup> SPh,<sup>70</sup> xanthate,<sup>71</sup> Co(salophen),<sup>72</sup> TePh,<sup>73</sup> PhMe,<sup>74</sup> or SePh<sup>75</sup> (Scheme 2.3). Other studied methods for accessing carbamoyl radical include photocatalyzed cleavage of weak S-C bond in dithiocarbamate<sup>76</sup> and reductive decarboxylation of *N*-hydroxyphthalimido oxamides.<sup>10,77</sup> These strategies sometimes are inefficient,<sup>75</sup> require the use of complex reagents,<sup>69,72</sup> leading to poor atom economy or display regioselectivity problem which could lead to mixture of products.<sup>78</sup> For example, C–H abstraction from formamides (R<sub>2</sub>N(C=O)H) can occur concurrently at CHO and α to nitrogen, resulting in a mixture of products.<sup>65,69b</sup>



**Scheme 2.2** : Oxamic acid as a potent carbamoyl radical source

The generation of carbamoyl radicals from oxamic acids has been shown to be very efficient and can circumvent the regioselectivity issues associated with these classical routes to carbamoyl radical.<sup>65</sup> Unlike the well-studied decarboxylative coupling of carboxylic acids and ketoacids, decarboxylation of oxamic acids proceeds under milder reaction conditions.<sup>58</sup> Oxamic acids are bench stable non-toxic compounds that can easily be prepared by direct coupling of amines with commercially available oxalic acid derivatives.<sup>58,79</sup> This simple procedure gives access to oxamic acids of wide structural diversity using various amines and does not require tedious purification processes such as chromatography.

- <sup>69</sup> a) V. G. Correia, J. C. Abreu, C. A. E. Barata, L. H. Andrade, *Org. Lett.* **2017**, *19*, 1060-1063. b) M. B. Zhou, R.-J. Song, X.-H. Ouyang, Y. Liu, W.-T. Wei, G.-B. Deng, J.-H. Li, *Chem. Sci.* **2013**, *4*, 2690-2694. c) X.-P. Yan, C.-K. Li, S.-F. Zhou, A. Shoberu, J.-P. Zou, *Tetrahedron* **2020**, *76*, 131342. d) L. Friedman, H. Shechter, *Tetrahedron Lett.* **1961**, *2*, 238-242. e) L. Grossi, *J. Chem. Soc. Chem. Commun.* **1989**, 1248-1248. f) W. E. Stewart, T. H. Siddal, *Chem. Rev.* **1970**, *70*, 517-551. g) Y. Zhang, K. B. Teuschera, H. Ji, *Chem. Sci.* **2016**, *7*, 2111-2118. h) F. Minisci, F. Recupero, C. Punta, C. Gambarotti, F. Antonietti, F. Fontanab, G. F. Pedullic, *Chem. Commun.* **2002**, 2496-2497. i) M. Fagnoni, D. Dondi, D. Ravelli, A. Albini, *Chem. Rev.* **2007**, *107*, 2725-2756.
- <sup>70</sup> M. Sakamoto, M. Takahashi, T. Fujita, T. Nishio, I. Iida, S. Watanabe, *J. Org. Chem.* **1995**, *60*, 4682-4683.
- <sup>71</sup> a) A. Millan-Ortiz, G. Lopez-Valdez, F. Cortez-Guzman, L. D. Miranda. *Chem. Comm.* **2015**, *51*, 8345. b) G. Lopez-Valdez, S. Olguín-Urbe, A. Millan-Ortiz, R. Gamez-Montano, L. D. Miranda, *Tetrahedron* **2011**, *67*, 2693-2701. c) M. Betou, L. Male, J. W. Steed, R. S. Grainger, *Chem. Eur. J.* **2014**, *20*, 6505-6517. d) G. Lopez-Valdez, S. Olguin-Urbe, L. D. Miranda, *Tetrahedron Lett.* **2007**, *48*, 8285-8289.
- <sup>72</sup> G. B. Gill, G. Pattenden, S. J. Reynolds, *J. Chem. Soc. Perkin Trans. 1*, **1994**, 369-378.
- <sup>73</sup> S. Fujiwara, Y. Shimizu, T. Shin-ike, N. Kambe, *Org. Lett.* **2001**, *3*, 2085-2088.
- <sup>74</sup> a) L. V. Jackson, J. C. Walton, *Chem. Commun.* **2000**, 2327-2328. b) A. F. Bella, L. V. Jackson, J. C. Walton, *Org. Biomol. Chem.* **2004**, *2*, 421-428.
- <sup>75</sup> P. H. Mazzocchi, M. Bowen, *J. Org. Chem.* **1976**, *41*, 1279-1282.
- <sup>76</sup> E. de P. Beato, D. Mazzarella, M. Balletti, P. Melchiorre, *Chem. Sci.* **2020**, *11*, 6312-6324.
- <sup>77</sup> M. Yuan, L. Chen, J. Wang, S. Chen, K. Wang, Y. Xue, G. Yao, Z. Luo, Y. Zhang, *Org. Lett.*, **2015**, *17*, 346-349.
- <sup>78</sup> a) M. Chmielewski, J. N. BeMiller, D. P. J. Cerretti, *J. Org. Chem.* **1981**, *46*, 3903-3908. b) A. Albini, M. Fagnoni *Photochemically- generated intermediates in synthesis*, John Wiley & Sons, Hoboken, **2013**, pp. 77-78.
- <sup>79</sup> G. G. Pawar, F. Robert, E. Grau, H. Cramail, Y. Landais, *Chem. Commun.* **2018**, *54*, 9337-9340.



**Scheme 2.3:** Some methods for generation of carbamoyl radical in traditional radical chemistry.

Lots of organic reactions have been developed over the years based on decarboxylative carbamoyl radical cross-coupling reactions<sup>80,81,82</sup> intramolecular cyclization<sup>77,83</sup> and intermolecular addition/cyclization with electron deficient alkenes,<sup>84,85,86</sup> using oxamic acids and some of these reactions are highlighted in this section.

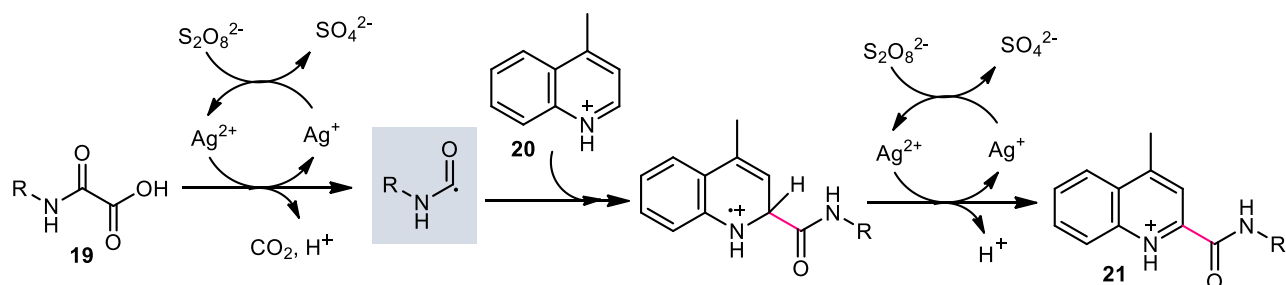
### 3. Decarboxylative coupling reactions using oxamic acids

#### 3.1. Csp<sup>2</sup>-Csp<sup>2</sup> bond formation

As mentioned earlier, Minisci and co-workers<sup>58</sup> originally showed that oxidative decarboxylation of oxamic acids **19** using stoichiometric amount of ammonium persulfate as oxidant and a silver salt as catalyst generates carbamoyl radicals, which could be trapped by a protonated heteroaromatic base **20**, to furnish amides **21** in excellent yield. According to their proposed mechanism, the silver (II) determines the oxidation of oxamic acid to carbamoyl radical (Scheme 2.4). This seminal work by

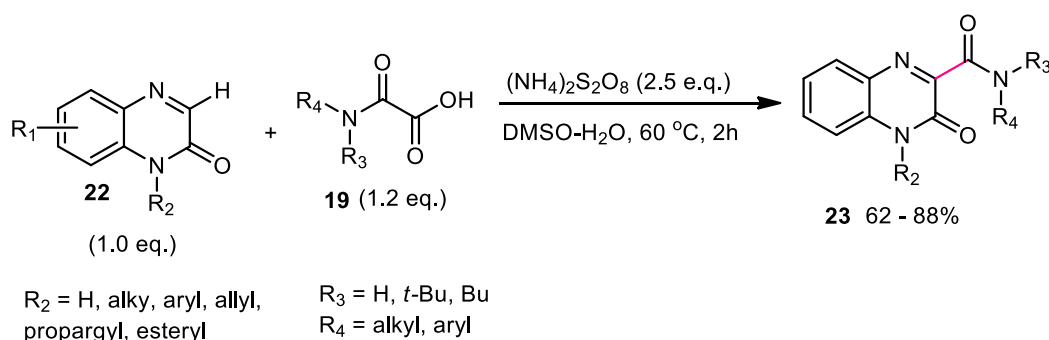
- <sup>80</sup> a) M. Li, C. Wang, P. Fang, H. Ge, *Chem. Commun.* **2011**, 47, 6587–6589. b) J. Miao, H. Ge, *Synlett* **2014**, 25, 911–919.  
<sup>81</sup> K. Jing, P.-C. Cui, G.-W. Wang, *Chem. Commun.* **2019**, 55, 12551–12554.  
<sup>82</sup> W.-M. Cheng, R. Shang, H.-Z. Yu, Y. Fu, *Chem. Eur. J.* **2015**, 21, 13191–13195.  
<sup>83</sup> H. Fan, P. Pan, Y. Zhang, W. Wang, *Org. Lett.* **2018**, 20, 7929–7932.  
<sup>84</sup> G. Chen, C. Li, J. Peng, Z. Yuan, P. Liu, X. Liu, *Org. Biomol. Chem.* **2019**, 17, 8527–8532.  
<sup>85</sup> Q.-Q. Han, Y.-Y. Sun, S.-H. Yang, J.-C. Song, Z.-L. Wang, *Chin. Chem. Lett.* **2021**, 32, 3632–3635.  
<sup>86</sup> C. Jin, J.-Y. He, Q.-F. Bai, G. Feng, *Synlett.* **2020**, 31, 1517–1522.

Minisci has continued to attract increasing attention in organic synthesis and has led to many different simple procedures for preparation of amides of biological interests using oxamic acids.<sup>87, 88</sup>



**Scheme 2.4:** Minisci reaction using oxamic acid as carbamoyl radical source.

A silver-free version of the Minisci reaction was recently reported by different groups and was also efficient for carbamoylation of varieties of heteroarenes including quinoxalin-2(1*H*)-ones,<sup>89</sup> phenanthrolines<sup>90</sup> and 2*H*-indazoles<sup>91</sup>. This procedure uses  $(\text{NH}_4)_2\text{S}_2\text{O}_8$  as oxidant, DMSO/ $\text{H}_2\text{O}$  as solvent and temperature between 50-60°C to furnish the corresponding amide in moderate to high yield without the need for silver salt catalyst or acidification. Solvent choice was very important for the procedure. The reaction was shown to work more efficiently with DMSO: $\text{H}_2\text{O}$  (600:1) as solvent, DMSO or water alone only providing inferior product yield while other organic solvents such as DCE,  $\text{CH}_3\text{CN}$ , MeOH and 1,4-dioxane were not suitable for the reaction.<sup>89</sup> A plausible mechanism proposed by Yuan and co-workers<sup>89</sup> (Scheme 2.5) suggests that the reaction proceeds first by decomposition of  $\text{S}_2\text{O}_8^{2-}$  in DMSO to give  $\text{SO}_4^{\cdot-}$ , and the latter mediates oxidative decarboxylation of oxamic acid into carbamoyl radical **I**. Then, selective addition of the carbamoyl radical to the C3 position of quinoxalin-2(1*H*)-one **22** would result in a nitrogen radical intermediate **II**, then single electron transfer (SET) from **II** mediated by  $\text{S}_2\text{O}_8^{2-}$  would give a cationic species **III** which undergoes deprotonation to afford the final product.



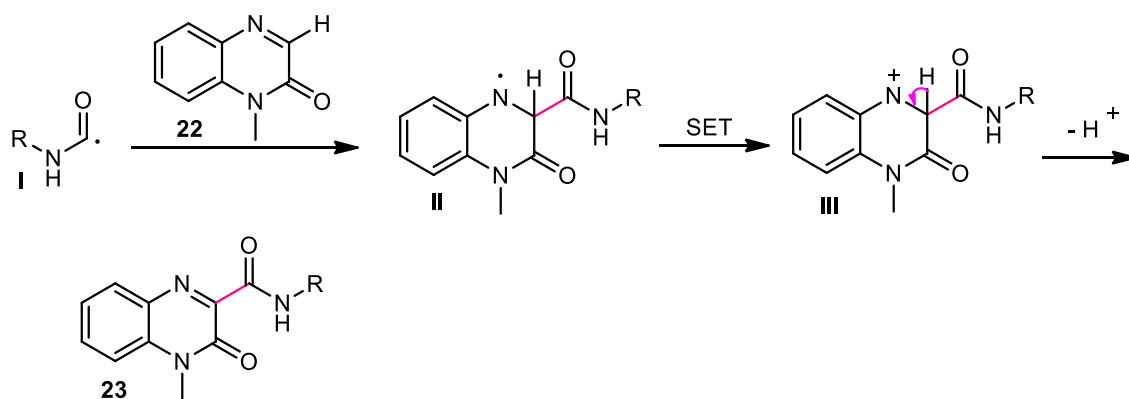
<sup>87</sup> J. Kos, C. F. Ku, I. Kapustikova, M. Oravec, H. J. Zhang, J. Jampilek, *ChemistrySelect* **2019**, *4*, 4582-4587.

<sup>88</sup> J.-W. Yuan, Q. Chen, C. Li, J.-L. Zhu, L.-R. Yang, S.-R. Zhang, P. Mao, Y.-M. Xiao, L.-B. Qu, *Org. Biomol. Chem.* **2020**, *18*, 2747-2757.

<sup>89</sup> J.-W. Yuan, J.-L. Zhu, H.-L. Zhu, F. Peng, L.-Y. Yang, P. Mao, S.-R. Zhang, Y.-C. Lib, L.-B. Qu, *Org. Chem. Front.* **2020**, *7*, 273-285.

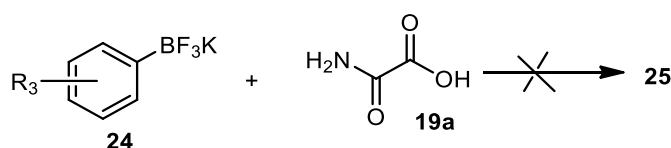
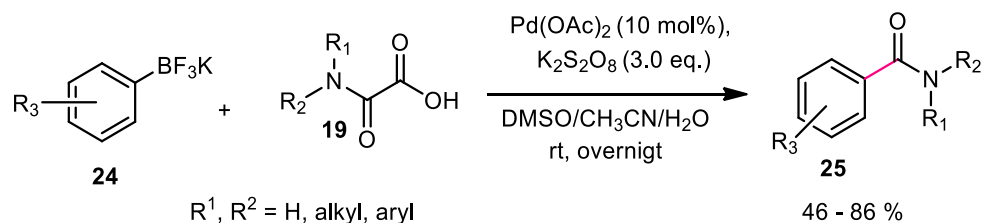
<sup>90</sup> T. Mooney, B.D.T. Donkin, N. Demirel, P.R. Moore, A.-L. Lee, *J. Org. Chem.* **2021**, *86*, 17282-17293

<sup>91</sup> V. S. Bhat, A. Lee, *Eur. J. Org. Chem.* **2021**, *23*, 3382-3385.



**Scheme 2.5:** C3 carbamoylation of quinoxalin-2(1*H*)-ones using oxamic acid

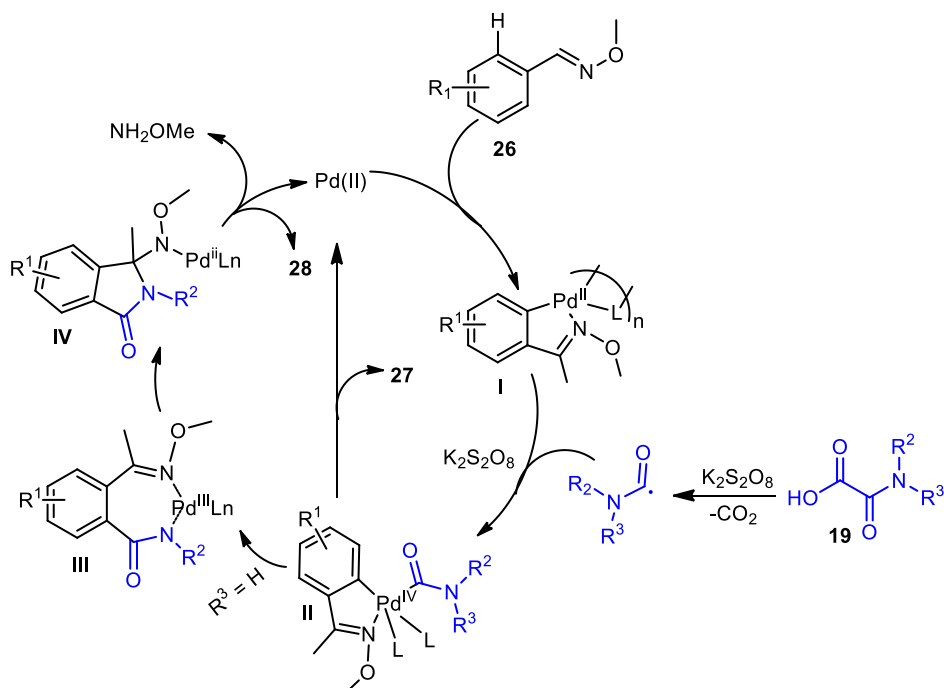
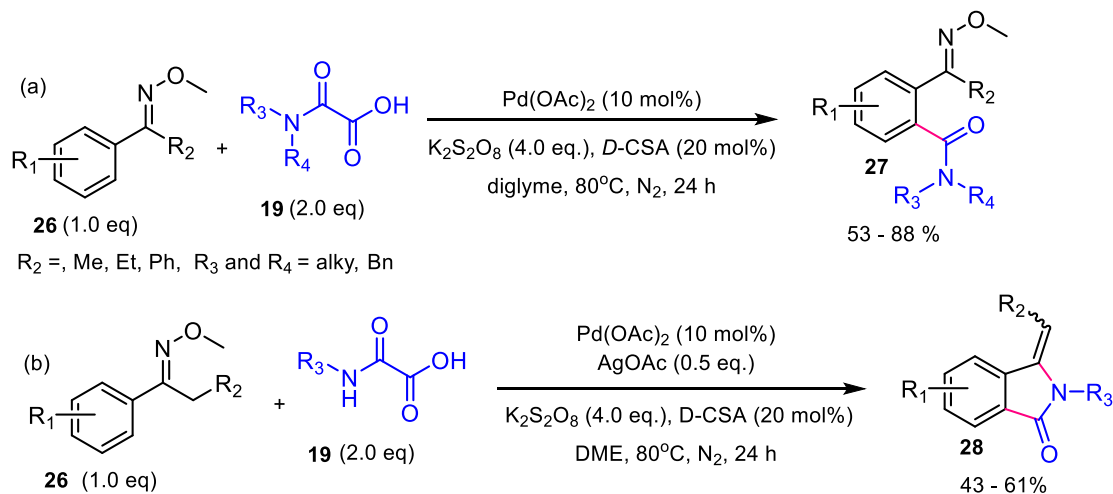
Besides heteroarenes as the coupling partner, several other compounds can serve as competent coupling partners with oxamic acids, providing useful and efficient synthetic methods for the synthesis of amides. Ge and co-worker reported a Pd(II)-catalyzed decarboxylative cross-coupling between oxamic acids and potassium phenyltrifluoroborates **24** to furnish arylamides **25** (Scheme 2.6).<sup>80</sup> This procedure gave access to a wide range of both acyclic and cyclic benzamides with diverse substituents in moderate to good yields. *N,N*-disubstituted acyclic oxamic acids demonstrated better reactivity in this reaction as compared to monosubstituted or *N,N*-cyclic counterparts which required heating up at 70°C and a catalytic amount of Ag<sub>2</sub>CO<sub>3</sub> to accelerate the decarboxylation step. The reaction failed when primary oxamic acid **19a** was used.<sup>80a</sup> Also, ortho-substituted potassium aryl trifluoroborates are not good candidates for the reaction possibly due to steric hindrance.



**Scheme 2.6:** Pd(II)-catalyzed decarboxylative cross-coupling of oxamic acids potassium phenyltrifluoroborates

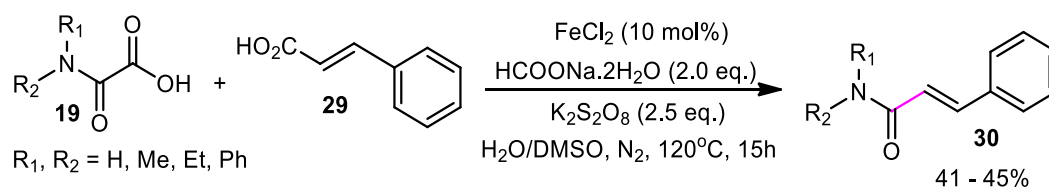
Furthermore, Wang group presented a palladium-catalyzed decarboxylative amidation using oxamic acids and arenes with ketoxime group **26** as a coupling partner (Scheme 2.7).<sup>81</sup> The reaction works well with a wide range of *N,N*-disubstituted oxamic acids including cyclic ones to give the corresponding ortho-amidated ketoximes **27** in good yields and regioselectivity. With *N*-monosubstituted oxamic acids, isoindolinone **28** was obtained instead through an intramolecular cyclization of the ortho-amidated ketoximes formed.

The authors proposed that reaction proceeds through the formation of a five membered palladacycle **I**. This is followed by oxidative addition of the carbamoyl radical, issued from oxamic acid decarboxylation, to the complex to form Pd(IV) intermediate **II**. The reductive elimination of **II** would furnish product **27**, and regenerate the Pd(II). When monosubstituted oxamic acid is used, the ortho-amidated ketoximes formed can further complex with Pd(II) to give a Pd(III) complex **III**, which undergoes intramolecular insertion to give intermediate **IV**. Then, removal of methoxyamine via  $\beta$ -H elimination will give 3-methyleneisindolinone **28**.



**Scheme 2.7:** Pd(II)-catalyzed C–H amidation of arenes with ketoxime directing group oxamic acid. Furthermore, Fe(II) mediated oxidative decarboxylative cross-coupling of oxamic acids and acrylic acids **29** to afford  $\alpha,\beta$ -unsaturated amides **30** has also been reported (Scheme 2.8).<sup>92</sup> However, the yields were generally moderate with few examples represented.

<sup>92</sup> Q. Jiang, J. Jia, B. Xu, A. Zhao, C.-C. Guo, *J. Org. Chem.* **2015**, *80*, 3586-3596.

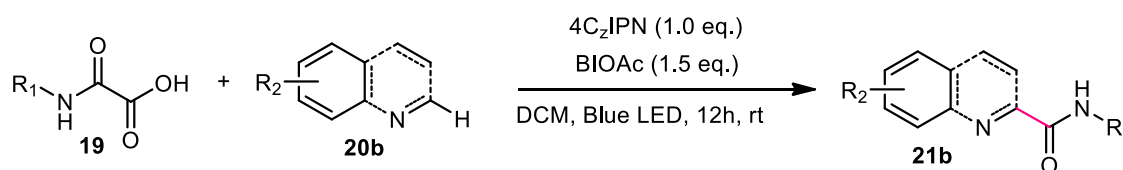


**Scheme 2.8:** Fe(II) mediated oxidative decarboxylative cross-coupling of oxamic acids for  $\alpha,\beta$ -unsaturated amide synthesis

### 3.2. Photocatalyzed Minisci reaction using oxamic acids for Csp<sup>2</sup>-Csp<sup>2</sup> bond formation

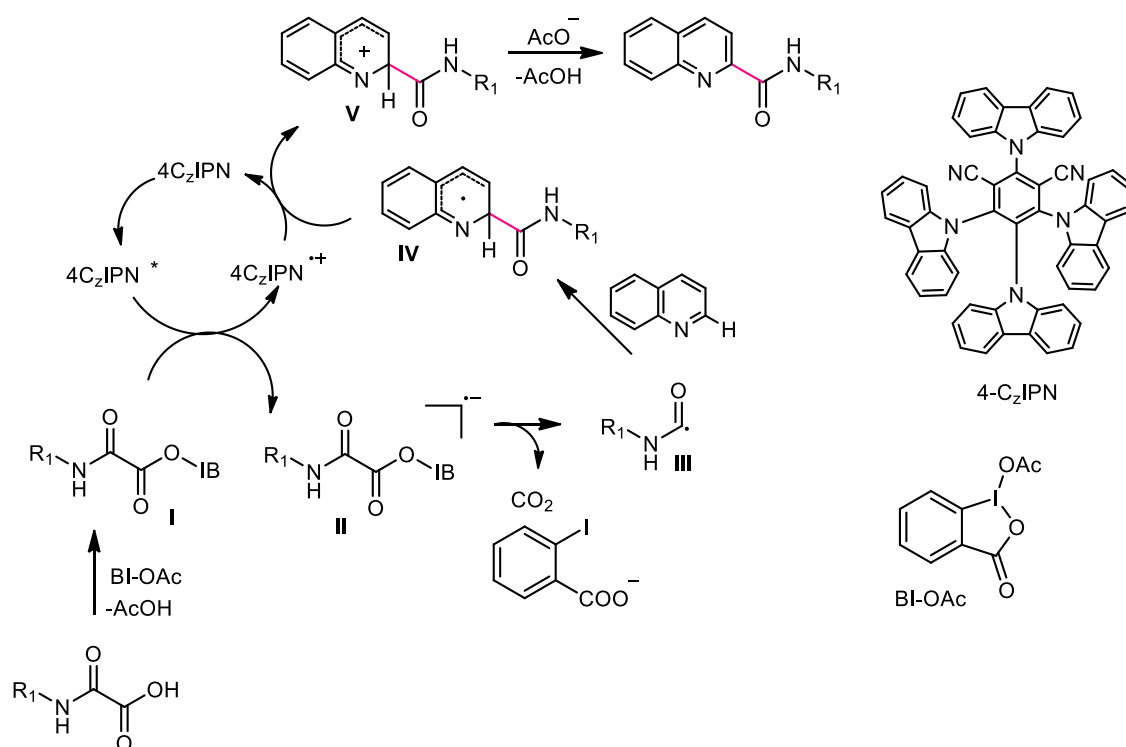
Our group recently developed a visible light-mediated carbamoyl radical addition to heteroarenes using oxamic acids (Scheme 2.9).<sup>65</sup> This mild, metal-free and efficient process operates at room temperature, using a hypervalent iodine (BI-OAc) and an organic dye (4CzIPN) to mediate oxidative decarboxylation of oxamic acids to carbamoyl radical, which in the presence of heteroaromatic base delivered the corresponding amides **3** in good to high yields. The procedure is compatible with a wide range of oxamic acids including chiral ones to furnish the desired chiral amides without racemization. As expected, the involvement of carbamoyl radical intermediate in the visible light-mediated process was unambiguously confirmed by various trapping experiments involving TEMPO, alkynylsulfone, and allylsilane where the respective TEMPO adducts were isolated.<sup>79</sup> A plausible mechanism for the transformation suggests that the photoexcited catalyst (4CzIPN\*) was quenched by a hypoiodite species **I** formed by a ligand exchange between oxamic acid and BI-OAc. The generated unstable radical anion **II** collapses to give a carbamoyl radical **III**. Then, the generated carbamoyl radical undergoes radical addition to the heteroaromatic base to give a radical intermediate **IV** which is oxidized by the photocatalyst radical cation (4CzIPN<sup>+</sup>) to give cationic species **V**. Deprotonation and rearomatization of **V** would furnish the product. Also, there is a possibility that the reaction followed the putative mechanism as proposed by Minisci<sup>58</sup> where the carbamoyl radical addition to the heteroaromatic base is promoted by the protonation of the base.<sup>58,93</sup>

Jouffroy and co-worker, shortly after, reported a similar visible light mediated decarboxylative carbamoylation of heteroaromatic bases using oxamic acids and their potassium oxamate.<sup>94</sup> Their method employs potassium persulfate as oxidant in aqueous DMSO to achieve the decarboxylative carbamoylation under visible light irradiation using acridinium based photocatalyst. The desired amide was obtained in moderate to good yields using aliphatic oxamic acids.



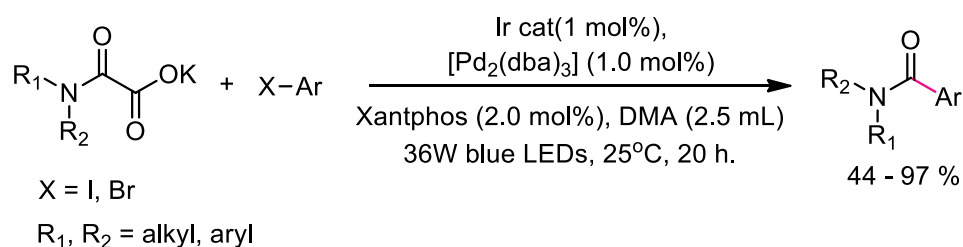
<sup>93</sup> F. Minisci, A. Citterio, E. Vismara, C. Giordano, *Tetrahedron*, **1985**, *41*, 4157.

<sup>94</sup> M. Jouffroy, J. Kong, *Chem. Eur. J.* **2019**, *25*, 2217-2221.



**Scheme 2.9:** Photocatalyzed decarboxylative carbamoylation using oxamic acids

Similarly, Fu and co-worker<sup>82</sup> reported a decarboxylative coupling of oxamic acids and aryl halides using a combination of iridium photoredox and palladium dual catalytic system (Scheme 2.10). The authors showed that both catalytic partners were necessary for the reaction, as desired product was not observed in the absence of either one of them. Although the authors proposed different possible mechanistic pathways for the transformation, in all, the photoexcited iridium ( $\text{Ir}^{\text{III}*}$ ) is implicated for the decarboxylation of the oxamic acid into carbamoyl radical which participates in the  $\text{Pd}^0$ - $\text{Pd}^{\text{II}}$  -  $\text{Pd}^{\text{III}}$  catalytic cycle in which  $\text{Ir}^{\text{II}}$  is re-oxidized by  $\text{Pd}^{\text{III}}$  to complete the catalytic cycle.<sup>82</sup>

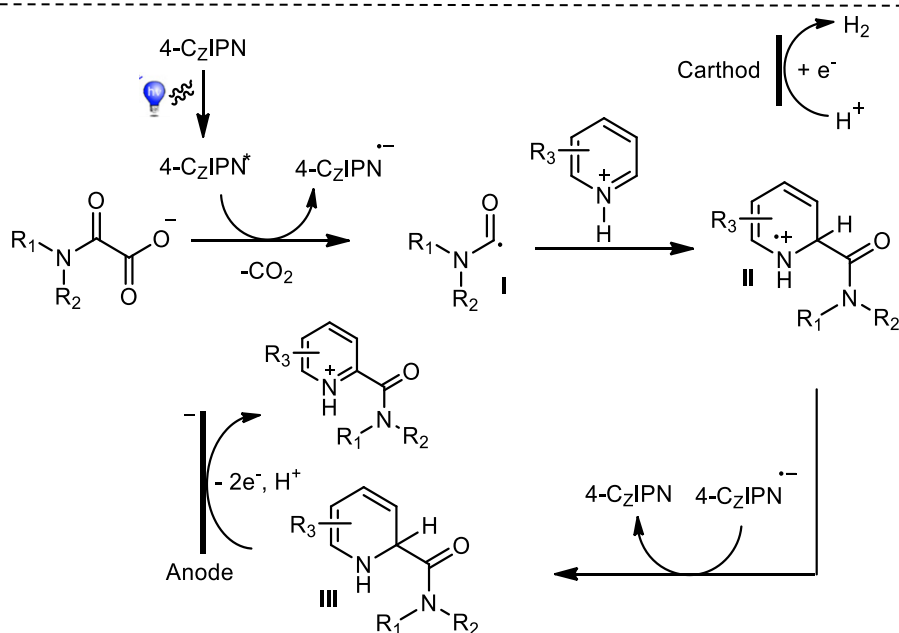
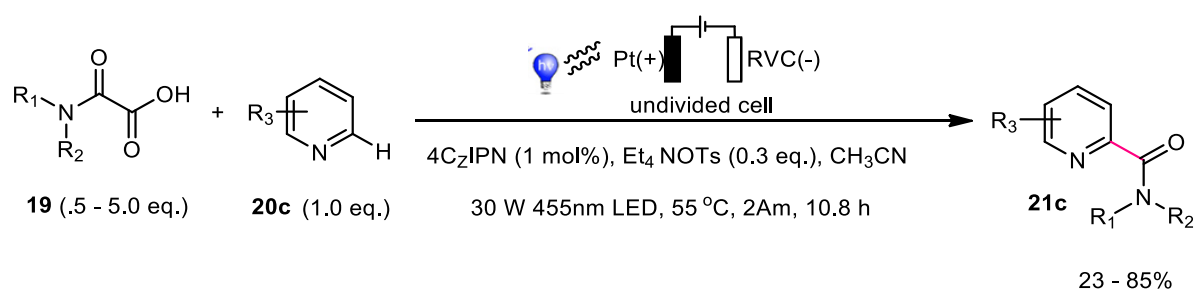


**Scheme 2.10:** Ir-Pd dual photoredox catalytic decarboxylative cross coupling of oxamic acids and aryl halides

In 2020, Song and co-workers unveiled an electrophotocatalytic decarboxylative Minisci reaction between heteroarenes and oxamic acids (Scheme 2.11).<sup>95</sup> This strategy, that combined organic electrochemistry and photocatalysis with anodic oxidation playing the role of chemical oxidant, was

<sup>95</sup> X.-L. Lai, X.-M. Shu, J. Song, H.-C. Xu, *Angew. Chem. Int. Ed.* **2020**, *59*, 10626-10632.

shown to be efficient for preparation of various amides. The authors demonstrated that both the light and electricity were essential for the transformation as only 3 to 18% of the desired product was observed in the absence of either of them. The procedure was compatible with a wide range of oxamic acids and heteroarenes with good functional group tolerance. A plausible mechanism for the transformation, as proposed by the authors, involves a single electron oxidative decarboxylation of the oxamate ion ( $E_{p/2}^{ox} = 1.17$  V vs SCE) by the photoexcited catalyst 4CzIPN\* ( $E_{p/2}^{red} = 1.35$  V vs SCE), followed by the addition of the generated carbamoyl radical **I** to protonated heteroarenes to give a radical cation intermediate **II**. The latter accepts an electron from the highly reducing photocatalyst radical anion (4CzIPN<sup>-</sup>) to give an intermediate **III** with the regenerated photocatalyst. Finally, anodic oxidation of **III** furnished the final product.



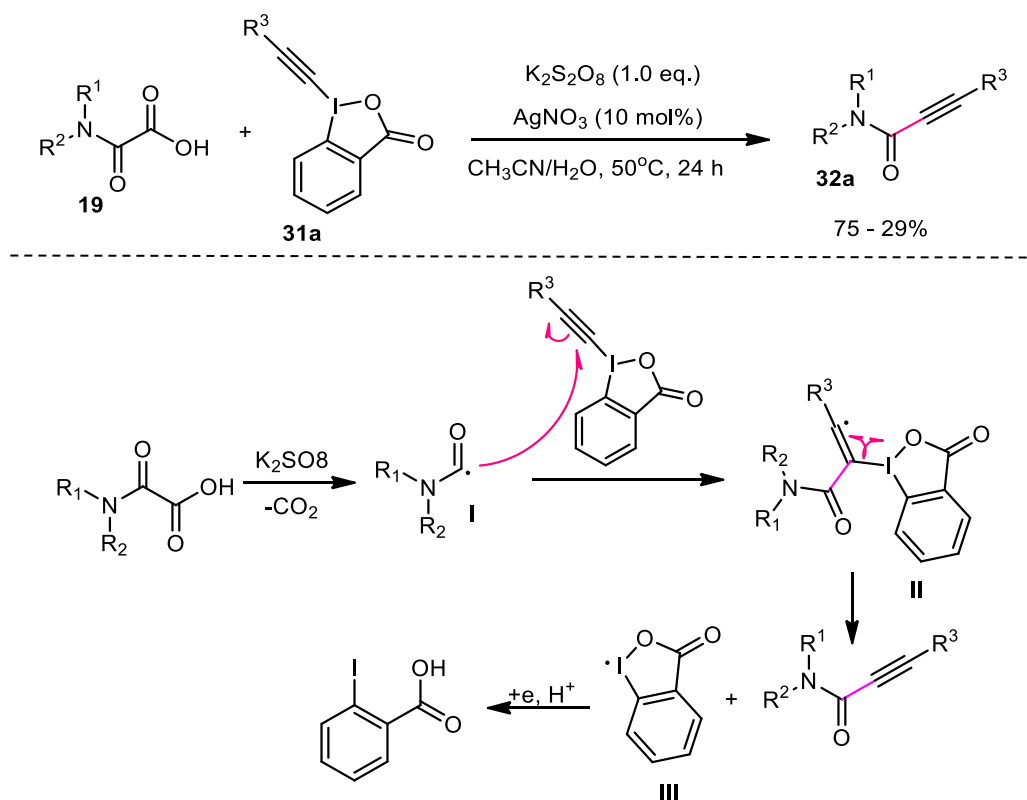
**Scheme 2.11:** Electrocatalytic decarboxylative Minisci reaction of oxamic acids

#### 4. Csp<sup>2</sup>-Csp bond formation

Oxamic acids can also be used for the formation of Csp<sup>2</sup>-Csp bonds through decarboxylative coupling with alkynyl compounds. In 2015, Duan group presented a decarboxylative alkylation of oxamic acids using hypervalent alkynyl iodide reagent **31a** as the alkylating agent (Scheme 2.12).<sup>96</sup> This procedure gave access to a wide range of propiolamides **32b** in moderate yields using

<sup>96</sup> H. Wang, L.-N. Guo, S. Wang, X.-H. Duan, *Org. Lett.* **2015**, *17*, 3054-3057.

different oxamic acids and alkynyl coupling partners. Propiolamides are important synthons for organic synthesis and interesting building blocks for natural product synthesis.<sup>96,97</sup> The authors proposed that the reaction proceeds through  $K_2S_2O_8$  mediated decarboxylation of oxamic acid to generate carbamoyl radical **I** which adds to the triple bond of the hypervalent iodine species, leading to radical intermediate **II** capable of undergoing  $\beta$ -elimination to deliver the desired product and benzoiodoxolonyl radical **III**. The latter is converted into benzoic acid through a reduction/protonation process.



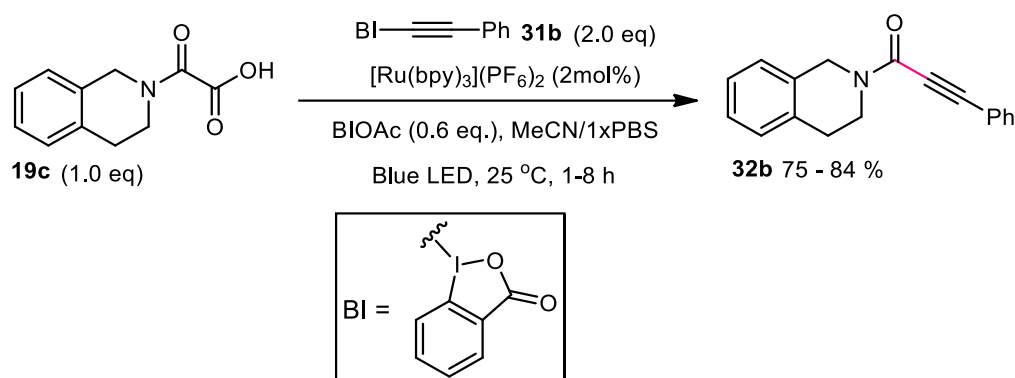
**Scheme 2.12:** Decarboxylation alkylation of oxamic acid

#### 4.1. Photocatalyzed decarboxylation of oxamic acids for $Csp^2$ - $Csp$ bond formation

Chen's group also in 2015 described a visible light catalyzed decarboxylative coupling of oxamic acids with hypervalent alkynyl iodine species **31b** for the preparation of ynamides **32b** (Scheme 2.13).<sup>98</sup> They demonstrated that the reaction was compatible with a wide range of oxamic acids, furnishing the corresponding ynamides in high yields with excellent chemoselectivity.

<sup>97</sup> a) A. C. Mantovani, T. A. C. Goulart, D. F. Back, P. H. Menezes, G. J. Zeni, *J. Org. Chem.* **2014**, *79*, 10526-10536. b) W.-T. Wei, R.-J. Song, X.-H. Ouyang, Y. Li, H.-B. Li, J.-H. Li, *Org. Chem. Front.* **2014**, *1*, 484-489.

<sup>98</sup> H. Huang, G. Zhang, Y. Chen, *Angew. Chem. Int. Ed.* **2015**, *54*, 7872-7876.

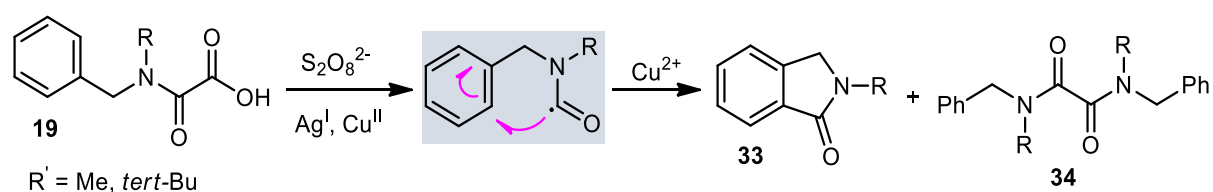


**Scheme 2.13:** Photocatalyzed decarboxylative alkylation of oxamic acid for preparation of ynamides. PBS = phosphate buffered saline.

## 5. Decarboxylative cyclization of oxamic acids for heterocycles synthesis

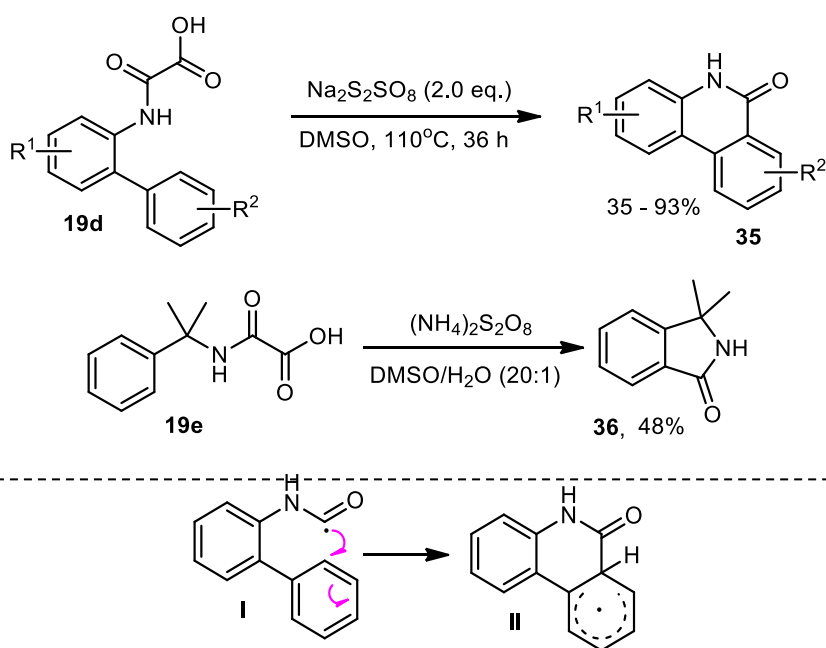
Recent years have witnessed lots of simple and useful synthetic procedures developed based on decarboxylative cyclization of oxamic acids for accessing heterocycles through C–C and C–X bonds formation. The progress in this area of study is summarized in this section.

The first decarboxylative cyclization of oxamic acids resulting in the formation of heterocyclic compound was reported by Minisci and co-workers<sup>58</sup> in 1994. They showed that Ag-catalyzed radical decarboxylation of *N*-methyl (or *tert*-butyl) -*N*-benzyl-oxamic acid **19** resulted in an intramolecular cyclization product **33** alongside homocoupling product **34**, though the details for the yields of the product were not available (Scheme 2.14).



**Scheme 2.14:**  $\text{Ag}^{2+}$ - mediated decarboxylative cyclization of oxamic acid

Zhang group in 2015 developed an efficient transition-metal-free procedure for accessing phenanthridinones **35** via  $\text{Na}_2\text{S}_2\text{O}_8$ -mediated decarboxylative intramolecular cyclization of biphenyl-2-oxamic acid **19d-e** (Scheme 2.15).<sup>77</sup> This simple procedure was shown to be efficient with different biphenyl-2-oxamic acids having both electron-withdrawing and electron-donating groups, furnishing the target compounds in moderate to high yields without precautions to exclude air from the reaction mixture. The procedure was also applicable for the synthesis of isoindolinone **36** as well as isoquinolinone. The authors proposed that the reaction possibly progressed through a carbamoyl radical aromatic substitution route involving intermediate radical **II**.

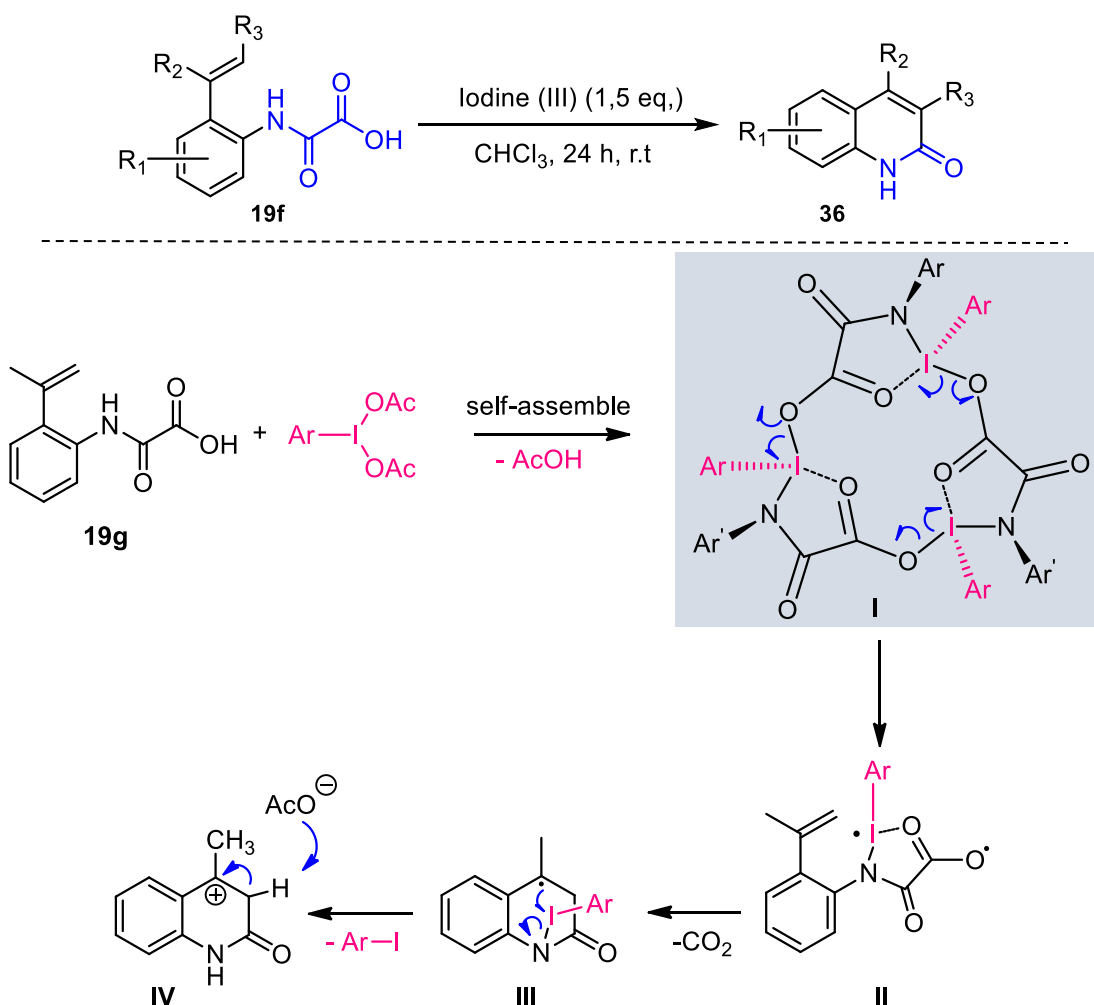


**Scheme 2.15:** Decarboxylative cyclization of oxamic acids for phenanthridinones synthesis

Furthermore, in 2018 Wang *et al.*,<sup>83</sup> reported a hypervalent iodine (III)-mediated decarboxylative intramolecular Heck-type reactions of oxamic acid for the synthesis of 2-quinolinones (Scheme 2.16). This mild and metal-free procedure delivered a wide range of 2-quinolinones **36** in good yields and excellent chemoselectivity using the corresponding 2-vinyl-phenyl oxamic acid **19f**. However, *N,N*-disubstituted oxamic acids were not compatible with this system. 2-Quinolinone is a well-known structural motif in many natural products and pharmaceutical agents.<sup>83,99</sup> The authors showed that the presence of TEMPO in the reaction mixture significantly suppressed the formation of 2-quinolinones, which suggests the involvement of a radical pathway in the transformation. Based on this and other related literatures,<sup>100</sup> they proposed a ring-strain-enabled radical decarboxylation mechanism, in which the hypervalent iodine reagent first forms a macrocyclic iodine (III) trimer **I** through self-assembly. A significant high ring strain in this macrocyclic species would facilitate the homolysis of its iodine-oxygen bond to generate diradical intermediate **II**. This is followed by decarboxylative radical addition to the olefin and cyclization. Subsequent intramolecular radical oxidation of **III** by the aryl iodine radical leads to benzylic cation intermediate **IV**. They also observed that when the  $-\text{CH}_3$  in **IV** was replaced by  $-\text{CF}_3$ , the reaction was completely shut down, supporting the possible involvement of a cationic species **IV** in the transformation. Also, NH group in the oxamic acid proved very important, as the desired product was not observed when *N*-methyl substituted oxamic acid was used.

<sup>99</sup> J. Schwan, M. Kleoff, B. Hartmayer, P. Heretsch, M. Christmann, *Org. Lett.* **2018**, *20*, 7661-7664.

<sup>100</sup> V. V. Zhdankin, A. E. Koposov, J. T. Smart, R. R. Tykwinski, R. McDonald, A. Morales-Izquierdo, *J. Am. Chem. Soc.* **2001**, *123*, 4095-4096.



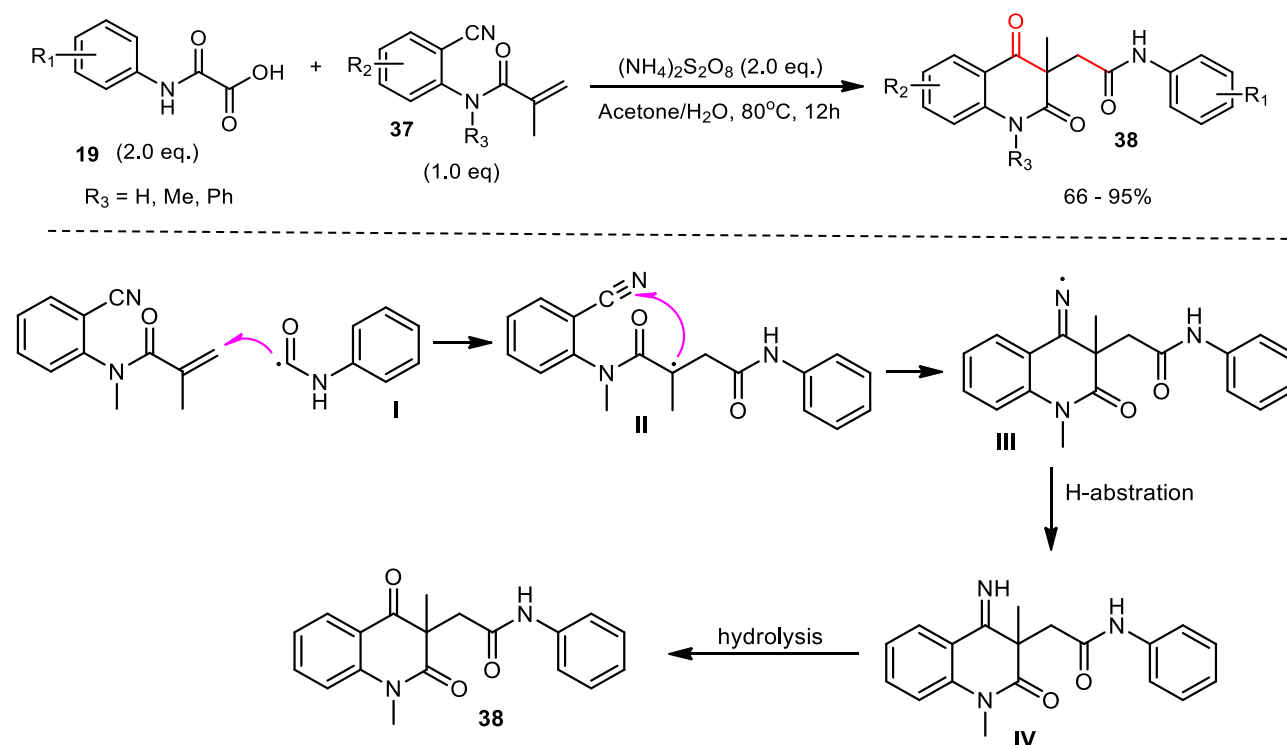
**Scheme 2.16:** Intramolecular decarboxylative Heck-type reactions of oxamic acids

## 6. Decarboxylative intermolecular addition-cyclization of oxamic acids for heterocycles synthesis

Apart from intramolecular decarboxylative cyclization, a lot of novel and simple synthetic procedures for synthesis of heterocycles have been developed over the years based on decarboxylative intermolecular addition-cyclization cascade reactions using oxamic acids. These reactions are summarized in this section.

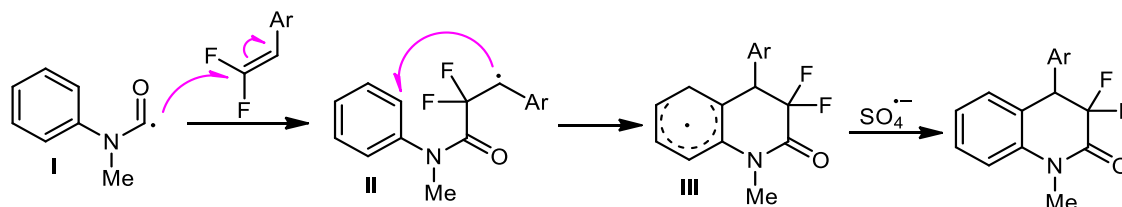
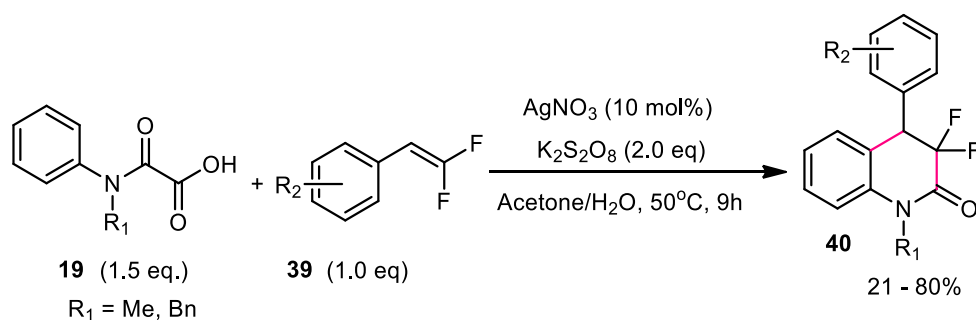
A new and efficient procedure for the synthesis of carbamoyl quinoline-2,4-diones **38** based on persulfate mediated tandem radical cyclization of *ortho*-cyanoarylacrylamides **37** with oxamic acids was reported (Scheme 2.17).<sup>85</sup> A wide range of oxamic acids with different substituents on the phenyl ring and *N*-(2-cyanoaryl)acrylamides were compatible with the reaction conditions, providing the desired product in moderate to high yields. However, acrylamide with a free N–H bond was not suitable. It was proposed that the transformation probably proceeds through  $(\text{NH}_4)_2\text{S}_2\text{O}_8$  mediated decarboxylation of oxamic acid generating carbamoyl radical **I**, which adds to *ortho*-cyanoarylacrylamides to give an alkyl radical intermediate **II**, the latter undergoing an intermolecular

cyclization at the nitrile group to give an imine radical **III**, followed by H-abstraction to give imine **IV**. The latter would undergo hydrolysis to deliver the final product **38**.



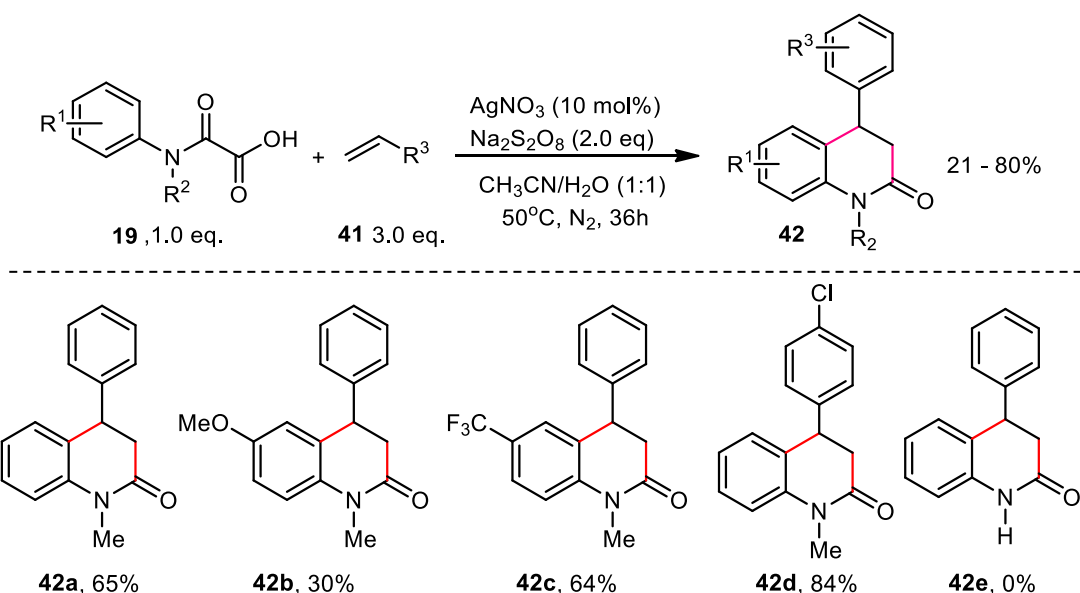
**Scheme 2.17:** Persulfate mediated tandem radical cyclization of ortho-cyanoarylacrylamides with oxamic acids

Liu *et al.*<sup>84</sup> have also reported a silver-promoted decarboxylative radical addition/annulation of oxamic acids with gem-difluoro-olefins **27** for the synthesis of  $\text{CF}_2$ -containing 3,4-dihydroquinolin-2-ones **40** (Scheme 2.18). Various *N*-substituted aniline-derived oxamic acids **19** and gem-difluoroalkenes **39** bearing electron-withdrawing and electron-donating groups on the benzene ring were compatible with the reaction, furnishing the desired product in moderate to good yields. Aliphatic gem-difluoroalkenes were however not compatible with reaction. Control experiment showed that Ag(I) catalyst was essential for the reaction, as the product was not observed in its absence. Furthermore, the reaction was inhibited by radical scavengers including TEMPO and BHT, indicating the involvement of carbamoyl radical in the transformation. Based on these and related literatures, the authors proposed that the reaction probably proceeds by generation of carbamoyl radical **I** mediated by Ag(II) as originally proposed by Minisci,<sup>58</sup> followed by an intermolecular radical addition gem-difluoroalkene resulting in a benzyl radical intermediate **II**, which undergoes intramolecular cyclization to generate intermediate **III**. Dehydroaromatization of the latter by the highly oxidizing  $\text{SO}_4^{\cdot-}$  would furnish the final product.

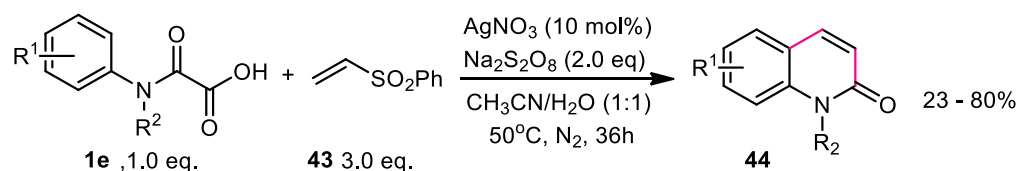


**Scheme 2.18:** Intermolecular addition/annulation of oxamic acids with *gem*-difluoroolefins

A similar silver-catalyzed tandem decarboxylative radical addition/cyclization of oxamic acids with alkenes for the synthesis of substituted 3,4-dihydroquinolin-2(1*H*)-ones **42** was also reported by the Feng group.<sup>86</sup> Their method demonstrated a wide substrates scope; styrenes and various electron-deficient alkenes **41** including ethyl vinyl ketone, ethyl acrylate, and  $\alpha$ -methylene- $\gamma$ -butyrolactone were competent partners for the reaction, furnishing the expected dihydroquinolin-2-ones in moderate yields (Scheme 2.19). Phenyl vinyl sulfones **43** were also good candidates for the reaction but delivered quinolin-2(1*H*)-ones **44** instead (Scheme 2.20). The authors explained that the generated 4-(phenylsulfonyl)-3,4-dihydroquinolin-2(1*H*)-ones possibly underwent Julia–Lythgoe elimination at high temperature to give the corresponding quinolin-2(1*H*)-ones. Furthermore, controlled experiment indicated that  $\text{AgNO}_3$  was necessary for the reaction, as the product was not observed in its absence. The transformation also requires *N*-protected oxamic acids; secondary oxamic acids failed in the reaction (*i.e.* **42e**). Also, methyl- and phenyl-*N*-protected oxamic acids displayed interesting chemoselectivity while the benzyl counterpart gave a mixture of two products including a radical rearrangement product.<sup>86</sup>

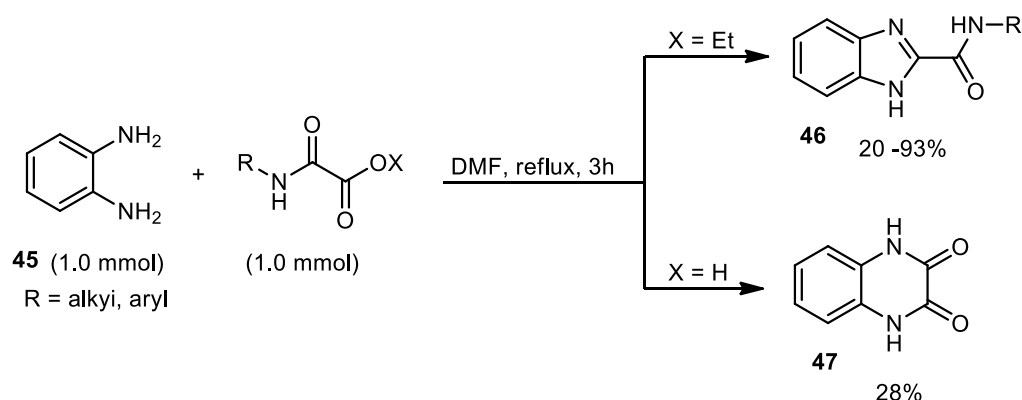


**Scheme 2.19:** Intermolecular addition/annulation of oxamic acids with styrenes and electron-deficient alkenes



**Scheme 2.20:** Intermolecular addition/annulation of oxamic acids with phenyl vinyl sulfones

It has also been shown that oxamic acid ethyl ester can undergo intermolecular cyclization with *o*-phenylenediamine **45** to furnish benzimidazole-2-carboxamide **46** (Scheme 2.21).<sup>101</sup> This simple procedure gave access to a wide range of benzimidazole-2-carboxamide in moderate to high yields with a wide range of ethyl oxamates. When oxamic acid was used instead of the ester, quinoxalinedione **47** was obtained albeit a low yield.



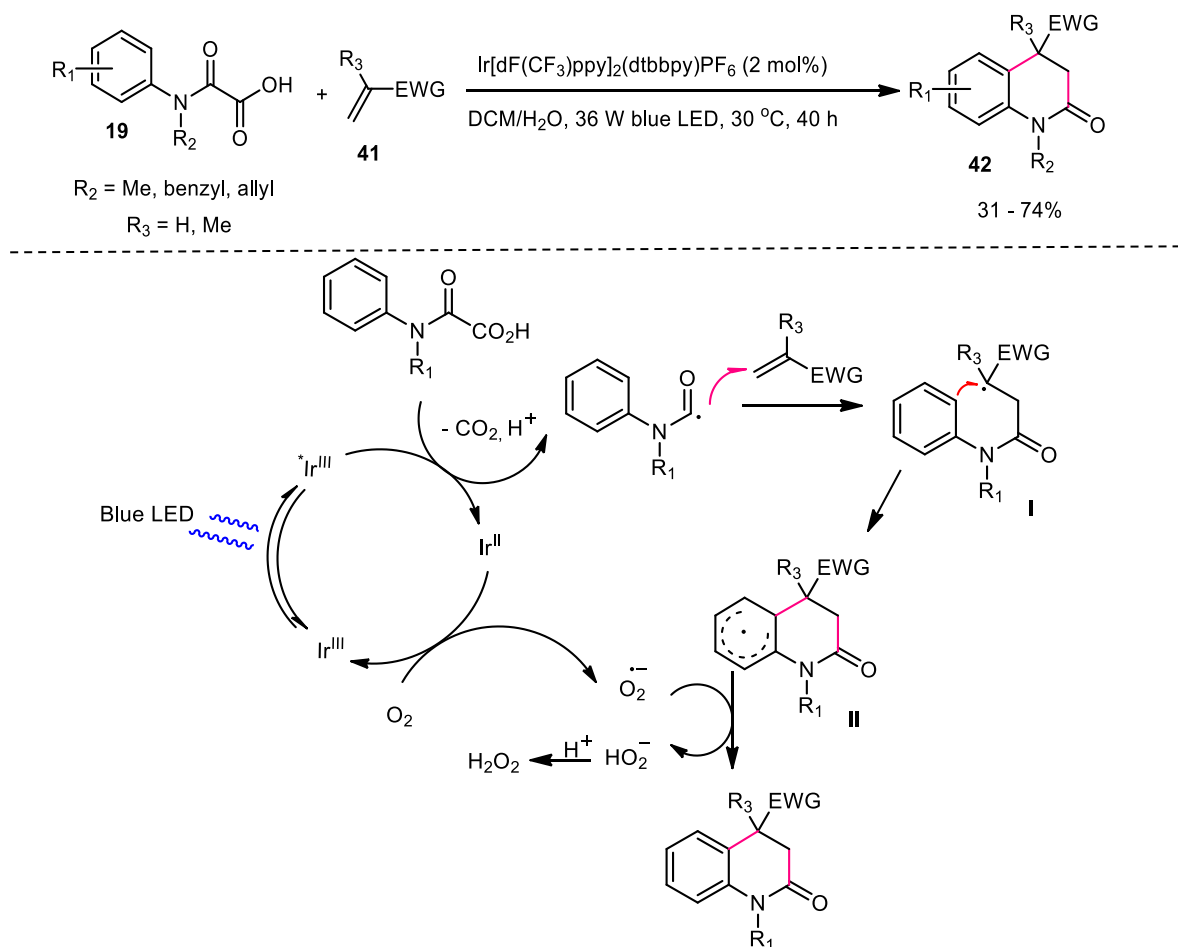
**Scheme 2.21:** Intermolecular addition/annulation of oxamic acids with phenyl vinyl sulfones

<sup>101</sup> a) P. A. Petyunin, A. M. Choudry, *Chem. Heterocycl. Compd.* **1982**, *18*, 519-521. b) I. Borza, S. Kolok, A. Gere, J. Nagy, L. Fodor, K. Galgoczy, J. Fetter, F. Bertha, B. Agai, C. Horvath, S. Farkas, G. Domanya, *Bioorganic Med. Chem. Lett.* **2006**, *16*, 4638-4640.

## 7. Photocatalyzed decarboxylative cyclization reaction for heterocycles formation

A visible light mediated decarboxylation addition/cyclization of oxamic acid for the synthesis of 3,4-dihydroquinolin-2(1*H*)-ones was reported by Feng and co-workers<sup>102</sup> in 2018 (Scheme 2.22). Various aniline derived oxamic acids with different substituents and different electron deficient alkenes **41** including acrylonitrile, phenyl vinyl sulfone, butyl acrylate, ethyl vinyl ketone and *N,N*-dimethylacrylamide were suitable for the reaction, leading to diverse 3,4-dihydroquinolin-2(1*H*)-ones **42** in moderate yields. The authors proposed that the transformation proceeds by oxamic acid decarboxylation mediated by the photoexcited iridium catalyst Ir<sup>III\*</sup>. The generated carbamoyl radical would undergo intermolecular addition to the electron deficient alkene to give a radical intermediate **I**, which would give cyclohexadienyl radical **II** by intramolecular cyclization. Then, the residual oxygen in the system plays the role of external oxidant by regenerating the reduced catalyst (Ir<sup>II</sup>) to its original state (Ir<sup>III</sup>). The oxygen radical anion generated would then abstract a proton from **II** to afford the product and H<sub>2</sub>O<sub>2</sub>.

This reactivity is quite different from the photocatalyzed version the authors reported earlier (Scheme 2.19),<sup>86</sup> where 4-(phenylsulfonyl)-3,4-dihydroquinolin-2(1*H*)-ones were obtained using the same substrates.



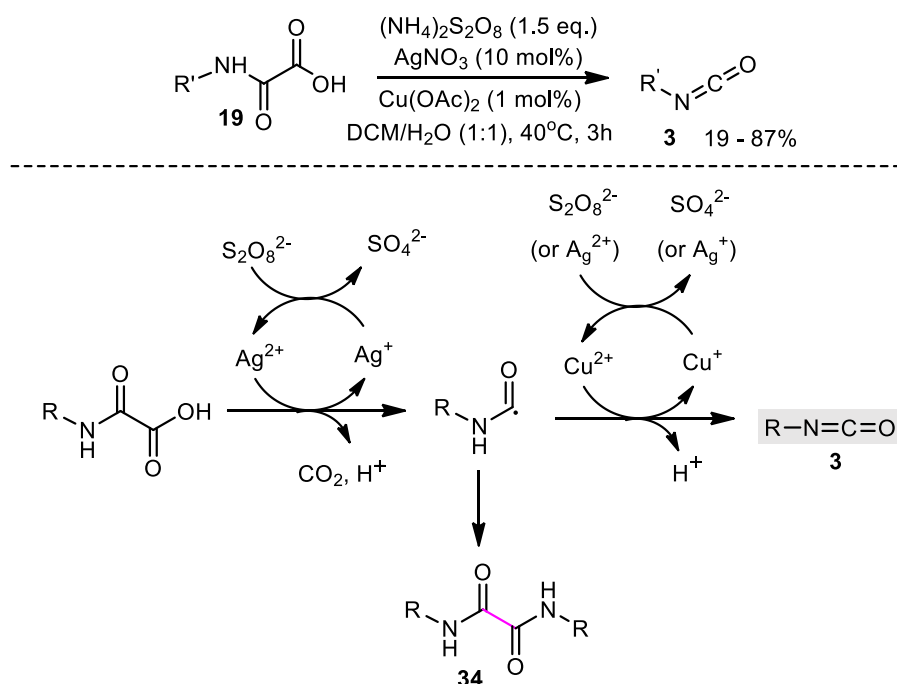
**Scheme 2.22:** visible-light-mediated decarboxylation for 3,4-Dihydroquinolin-2(1*H*)-ones synthesis

<sup>102</sup> Q.-F. Bai, C. Jin, J.-Y. He, G. Feng, *Org. Lett.* **2018**, *20*, 2172-2175.

## 8. Oxamic acids as a precursor for isocyanate and urethane

Oxamic acids have also been designated as a potent green precursor for the synthesis of non-phosgene carbamates and ureas through *in-situ* generation of isocyanate.<sup>79</sup> Minisci<sup>58</sup> originally showed that oxamic acids can be oxidized into isocyanate using  $S_2O_8^{2-}$  as an oxidant,  $AgNO_3$  and  $Cu(OAc)_2$  as catalysts, and a biphasic medium involving water and an organic solvent (Scheme 2.23). Various isocyanates could be accessed with their method in moderate yields using different monoxamic acids. They indicated that oxidation of secondary oxamic acid to isocyanate was not feasible, due to the importance of  $-NHCO-$  group in the second oxidation process. The silver salt was vital for the reaction as no isocyanates were observed in its absence, while copper salt was needed to favor selective oxidation of the carbamoyl radical into isocyanate, thereby minimizing the homocoupling of the generated carbamoyl radical into diamide.

Although this method gave access to isocyanates, the yields were generally moderate due to partial hydrolysis of the generated isocyanate into amine in the aqueous medium. Moreover, direct access to urethane using this method was not feasible, leaving the option of isolating and purifying the generated isocyanate.



**Scheme 2.23:** Generation of isocyanate from oxamic acids

Recently our group developed a metal-free photocatalyzed procedure for direct access to urethanes and ureas from oxamic acids.<sup>79</sup> This mild and efficient method uses an organic dye as photocatalyst, hypervalent iodine reagent as oxidant and visible-light irradiation to trigger the free-radical oxidation of oxamic acids into *in-situ* generated isocyanates in an organic solvent. In the presence of alcohol the reaction furnished urethane in a one-pot process, thereby avoiding isolation and purification of the generated isocyanate. The details of this process will be discussed in the next chapter.

## 9. Conclusion

Oxamic acids have been shown to be versatile greener precursors for generation of carbamoyl radicals. They can easily undergo single electron oxidative decarboxylation to liberate these reactive species. These bench stable and relatively non-toxic compounds have been shown to be competent for efficient construction of C–C, C–O or C–N bonds in the synthesis of diverse organic molecules including amides and heterocycles and can circumvent the regioselectivity problem usually encountered in classical routes developed to generate carbamoyl radicals. Also, the two-electron oxidation of oxamic acid is quite promising as a greener route to non-phosgene urethanes through the *in-situ* generation of isocyanate. Finally, oxamic acids can easily be accessed in excellent yields by direct coupling of amines and commercially available oxalic acid derivatives and their synthesis do not require any tedious purification step.

## Chapter 3

### Urethane and PUs synthesis by visible light-mediated decarboxylation of oxamic acids

A new photocatalyzed procedure for the synthesis of urethanes and polyurethanes from oxamic acids is described in this chapter. The chapter is divided into two parts. The first part highlights some basic concepts of visible light photoredox catalysis necessary for a better understanding of this project while the details of the work accomplished during this project are described in a second part.

#### **PART I: Basic concepts of visible-light photoredox catalysis**

##### **1. Introduction**

Interest in the use of visible-light photoredox catalysis for organic synthesis has increased over the years due to its efficiency and the fact that it can be conducted using cheap light sources without any specialized equipment. Unlike UV photocatalysis, visible-light photoredox catalysis relies on lower energy photon, and makes use of photocatalyst to mediate electron and/or energy transfer during a photochemical transformation and hence, the technique is milder and more selective.<sup>103</sup> Moreover, it has been shown that with visible-light photoredox catalysis, some reactions that are rather difficult with a conventional organic chemistry can easily be accomplished.<sup>103,104</sup> Among other factors, this can be attributed to the fact that excited photocatalysts (PC<sup>\*</sup>) can function as both reducing and oxidizing agents depending on the nature of the reacting species.<sup>103</sup>

##### **2. Common photocatalysts for visible-light photoredox catalysis**

Visible-light photocatalysts are usually transition metal complexes or organic dyes which absorb visible light and become electronically excited (PC<sup>\*</sup>). At its excited state, a photocatalyst is more reactive than when on ground state and is capable of triggering a chemical transformation *via* electron transfer and/or energy transfer.<sup>105</sup> Although visible-light photoredox catalysis originally relied mainly on transition metal complexes including ruthenium and iridium complexes due to their efficiency, recent years have witnessed an increasing interest in organic dyes because of their environmental friendliness, lower cost, and the fact that their photophysical properties can easily be tuned.<sup>106</sup> Besides, some organic dyes can exhibit better catalytic performance than their metal-based counterparts.<sup>104</sup> Common visible-light photoredox catalysts usually employed in organic synthesis

---

<sup>103</sup> C. K. Prier, D. A. Rankic, D.W. C. MacMillan, *Chem. Rev.* **2013**, *113*, 5322-5363.

<sup>104</sup> N. A. Romero, D. A. Nicewicz, *Chem. Rev.* **2016**, *116*, 10075-10166.

<sup>105</sup> J. M. R. Narayanam, C. R. J. Stephenson, *Chem. Soc. Rev.* **2011**, *40*, 102-113. b) L. Marzo, S. K. Pagire, O. Reiser, B. König, *Angew. Chem. Int. Ed.* **2018**, *57*, 10034-10072.

<sup>106</sup> D. A. Nicewicz, T. M. Nguyen, *ACS Catal.* **2014**, *4*, 355-360. b) S. Fukuzumi, K. Ohkubo, *Org. Biomol. Chem.* **2014**, *12*, 6059-6071.

are represented in (Figure 3.1). Among the organic dyes, 4-CzIPN appeared to be the mostly used because it is a potent oxidant and reductant when photoactivated (Table 3.1).

The reducing or oxidizing power of excited photoredox catalysts is often measured using standard reduction potentials  $E_{1/2}(M^+/M^*)$ , which is an electrochemical half reaction written in the direction from the oxidized to the reduced species.<sup>107</sup> This property is very important in the choice of photoredox catalyst for a particular reaction. The more negative the reduction potentials of a catalyst the more reducing power it has, and vice versa. For instance,  $^*Ru(bpy)_3^{2+}$  ( $E_{1/2}^{III/*II} = -0.81$  V vs SCE) is much better reducing agent than in its ground-state  $Ru(bpy)_3^{2+}$  ( $E_{1/2}^{III/II} = +1.29$  V vs SCE).

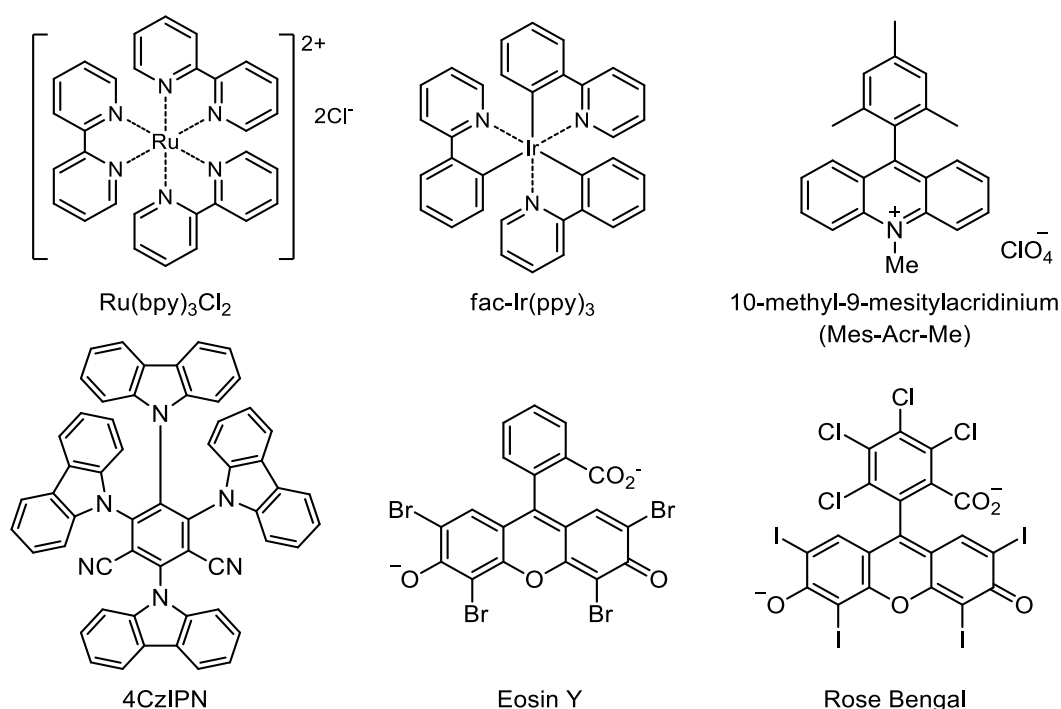


**Figure 3.1:** Some common visible light photocatalysts

Entry	$E_{ox}^*$	$E_{red}^*$	$\lambda_{max}$ (nm)	Excited-state lifetime $\tau$ (ns)
Ru(bpy) <sub>3</sub> Cl <sub>2</sub>	-0.81 vs SCE	+0.77 v SCE	452	1100
fac-Ir(ppy) <sub>3</sub>	-1.73 vs SCE	+0.31 vs SCE	375	1900
4-CzIPN	-1.18 vs SCE	+1.43 vs SCE	375	20.4
Mes-Acr-Me	-0.49 vs SCE	+2.18 vs SCE	430	6.0
Eosin Y	$ES_1^*_{red} = +1.23$ vs SCE	$ET_1^*_{red} = +0.83$ vs SCE	539	2.1
Rose Bengal	$ES_1^*_{red} = +1.18$ vs SCE	$ET_1^*_{red} = +0.81$ vs SCE	549	-

**Table 3.1:** Redox potentials of some common visible light photocatalysts.<sup>103,104</sup>

<sup>107</sup> C. R. Bock, J. A. Connor, A. R. Gutierrez, T. J. Meyer, D. G. Whitten, B. P. Sullivan, J. K. J. Nagle, *J. Am. Chem. Soc.* **1979**, *101*, 4815-4824.

### 3. Jablonski Diagram

Jablonski Diagram<sup>108</sup> describes the electronic states of a molecule and the transition processes during photoexcitation. For instance, when a photocatalyst is irradiated with light of appropriate wavelength, promotion of an electron from the ground state ( $S_0$ ) to the singlet-excited state ( $S_1$ ) takes place (Figure 3.2). The molecule in an excited electronic state can relax back (decay) to ground state and this can occur through different photophysical processes:  $S_1$  can return to ground state by emission of light (fluorescence, F) or it can undergo nonradiative transitions such as internal conversion (IC), or intersystem crossing (ISC)- a spin-forbidden transition of an excited singlet state to an excited triplet state ( $T_1$ ). Both  $S_1$  and  $T_1$  excited states can engage in electron transfer with a substrate, resulting in a bimolecular reaction. The lifetime of  $T_1$  is however longer than that of  $S_1$  due to the fact that it is a product of spin-forbidden transition,<sup>109</sup> and hence is considered a more useful excited state for single-electron transfer or energy transfer during photocatalysis.<sup>103,104</sup> Lastly, if not usefully quenched *via* electron transfer or energy transfer with the reacting species,  $T_1$  can decay to ground state by emission of light (phosphorescence, P) or through nonradiative internal conversion.

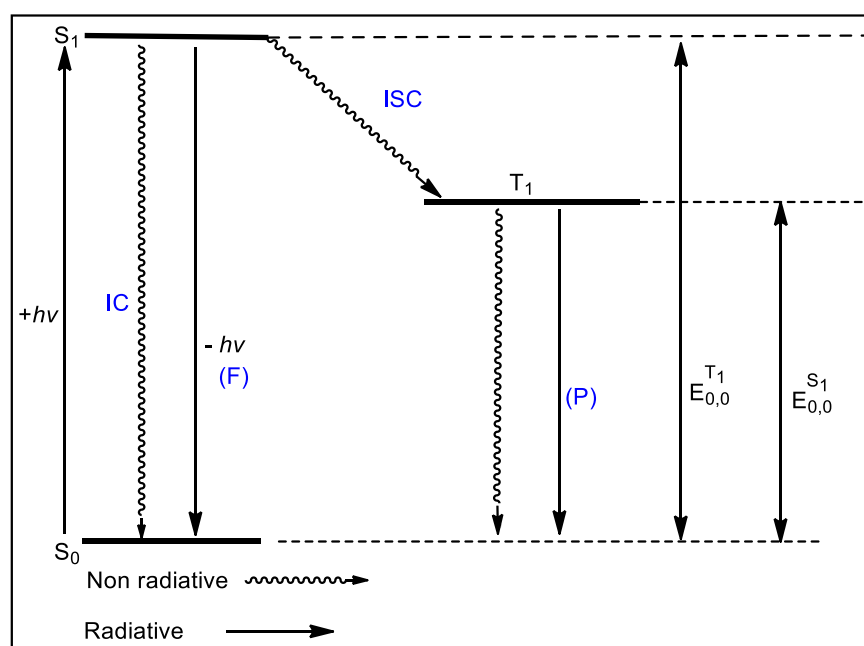


Figure 3.2: Jablonski Diagram

### 4. Mechanism of visible-light photoredox catalysis

Visible-light photoredox catalysis can mediate organic transformation through different mechanisms including electron transfer, energy transfer and hydrogen atom transfer (HAT).

#### 4.1. Electron transfer

The mechanism of visible-light photoredox catalysis is mainly based on the ability of the excited photocatalyst ( $cat^*$ ) to donate or accept an electron from organic substrates, thereby generating

<sup>108</sup> A. Jablonski, *Nature* **1933**, 131, 839-840.

<sup>109</sup> T. J. Penfold, E. Gindensperger, C. Daniel, C. M. Marian, *Chem. Rev.* **2018**, 118, 6975-7025.

reactive radical ions, which can engage in different chemical transformations. When a photoredox catalyst (cat) absorbs a photon from visible region, it undergoes electronic transition from ground state to singlet-excited state as explained earlier. For instance, when  $\text{Ru}(\text{bpy})_3^{2+}$  absorbs visible light, an electron from the metal-centered orbitals can be promoted to a ligand-centered orbital, resulting in species in which Ru(II) has been oxidized to Ru(III) and the ligand part has undergone a single electron reduction; this electronic transition being known as metal to ligand charge transfer (MLCT).<sup>110</sup> This singlet-excited species can further rapidly decay to longer-lived triplet state ( $T_1$ ) via intersystem crossing (ISC). Intersystem crossing basically involves change of the spin multiplicity of a compound, normally from the lowest excited singlet state to the lowest excited triplet state<sup>111,112</sup> (Figure 3.3).

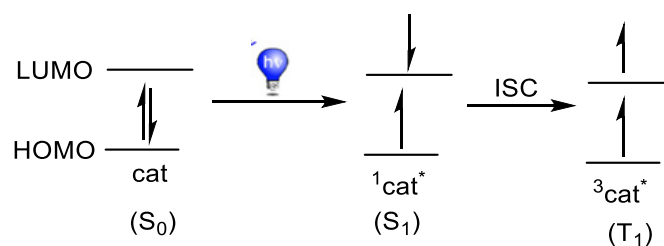


**Figure 3.3:** Electron excitation of photocatalyst

The photoexcited catalyst ( $\text{cat}^*$ ) can react through two mechanistic pathways: it can undergo “oxidative quenching” by donating an electron to an oxidant (ox) present in the reaction mixture or “reductive quenching” by accepting an electron from a reductant [Red] in the reaction mixture (Figure 3.4). Normally, Stern-Volmer or fluorescence quenching experiment could be used to ascertain if a particular reaction proceeds by reductive or oxidative quenching cycle.<sup>103</sup> Note that  $\text{cat}^*$  refers to either the  $S_1$  or  $T_1$  excited states, both excited species can mediate organic transformations. While  $T_1$  has longer lifetime,  $S_1$  is reported to exhibit more oxidizing and reducing power.<sup>104</sup> Nevertheless, reports suggest that photoexcited catalyst requires at least an excited state lifetime of 1 ns to mediate a single electron transfer (SET).<sup>111</sup>

To ensure catalyst turnover, the oxidized species ( $\text{cat}^{*+}$ ) in the oxidative quenching cycle requires a reducing agent (Red) to return to its ground state while the reduced species ( $\text{cat}^{*-}$ ) in the reductive quenching cycle needs an oxidizing agent (OX) to return to its ground state. Electron transfer between the photoexcited catalyst and substrate ultimately results in radical ions, which are ready for further reactions.

<sup>110</sup> R. S. Lumpkin, E. M. Kober, L. A. Worl, Z. Murtaza, T. J. Meyer, *J. Phys. Chem.* **1990**, *94*, 1, 239-243.

<sup>111</sup> J. D. Bell, J. A. Murphy, *Chem. Soc. Rev.* **2021**, *50*, 9540-9685.

<sup>112</sup> M. Kasha, *Discuss. Faraday Soc.* **1950**, *9*, 14-19.

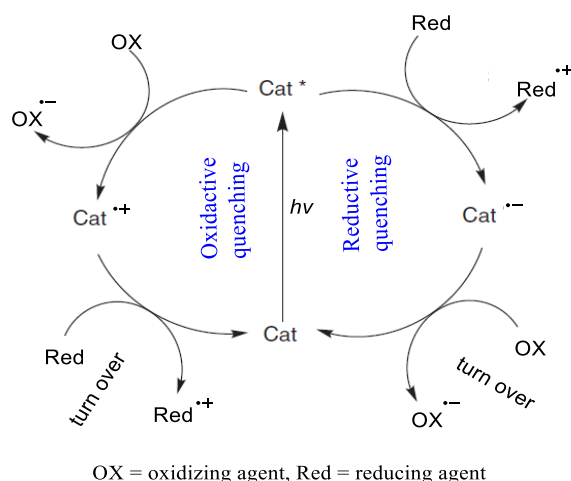


**Figure 3.4:** Oxidative and reductive quenching cycle of a photocatalyst

The comparison of electron transfer between  $\text{cat}^*$  and substrate (sub) for triplet state and singlet states in a reductive quenching process is represented in (Figure 3.5). In both cases, spin multiplicity of the excited photocatalyst is maintained in contact radical ion pairs. Also, in the contact radical ion pairs, back electron transfer (BET) can occur which can neutralize the radical ions generated back to ground state,<sup>113</sup> while cage escape will furnish reactive radical ions. BET usually occurs through recombination reaction and it is not favorable for catalytic performance. It has also been shown that BET occurs faster in singlet contact radical ion pairs (SCRIP) than in the triplet contact radical ion pairs (TCRIP),<sup>104,114</sup> corroborating more catalytic relevance of  $T_1$  over  $S_1$ .

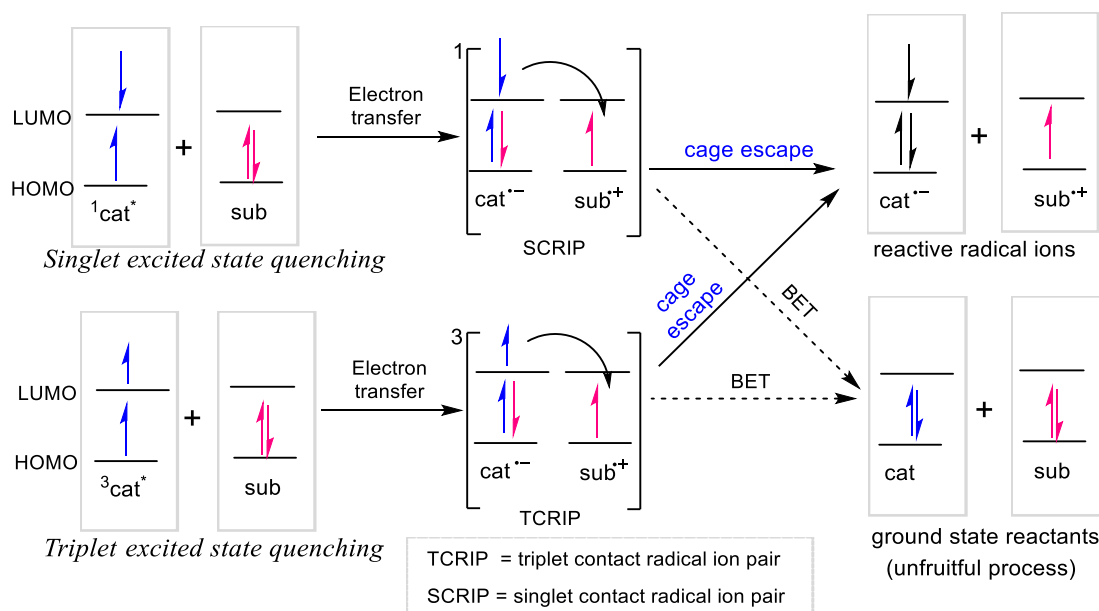


**Figure 3.5:** Electron transfer between substrate (sub) and excited photocatalyst ( $^*\text{cat}$ ) during a reductive quenching process: comparison between  $S_1$  and  $T_1$  states quenching.<sup>104</sup>

<sup>113</sup> S. Narra, Y. Nishimura, H. A. Witek, S. Shigeto, *Chem. Phys. Chem.* **2014**, *15*, 2945-2950.

<sup>114</sup> Y. Kuriyama, T. Arai, H. Sakuragi, K. Tokumaru, *Chem. Lett.* **1988**, *17*, 1193-1196.

## 4.2. Energy transfer

Another pathway through which photoexcited catalyst can trigger organic transformation is through energy transfer. However, this pathway is less common compared to electron transfer. Aside being quenched by electron transfer, triplet excited photocatalyst can be quenched by energy transfer to substrate *via* triplet-triplet energy transfer (TTET), resulting in chemical transformation<sup>115</sup> (Figure 3.6). Visible-light photocatalysis involving energy transfer mechanism have been reported for some common photocatalysts like  $\text{Ru}(\text{bpy})_3^{2+}$ ,  $\text{Ir}[\text{dF}(\text{CF}_3)\text{ppy}]_2(\text{dtbbpy})^+$ , Rose Bengal and Eosin<sup>115b,116,117</sup>. In this capacity, the photocatalysts are often referred to as photosensitizers (sen).

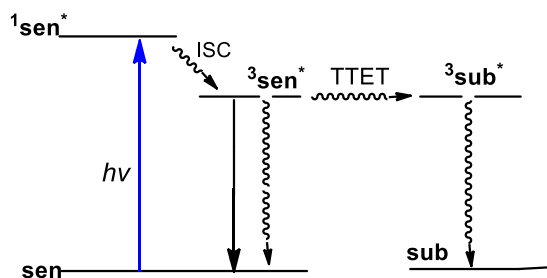


**Figure 3.6:** Triplet state quenching by energy transfer

## 4.3. Hydrogen atom transfer

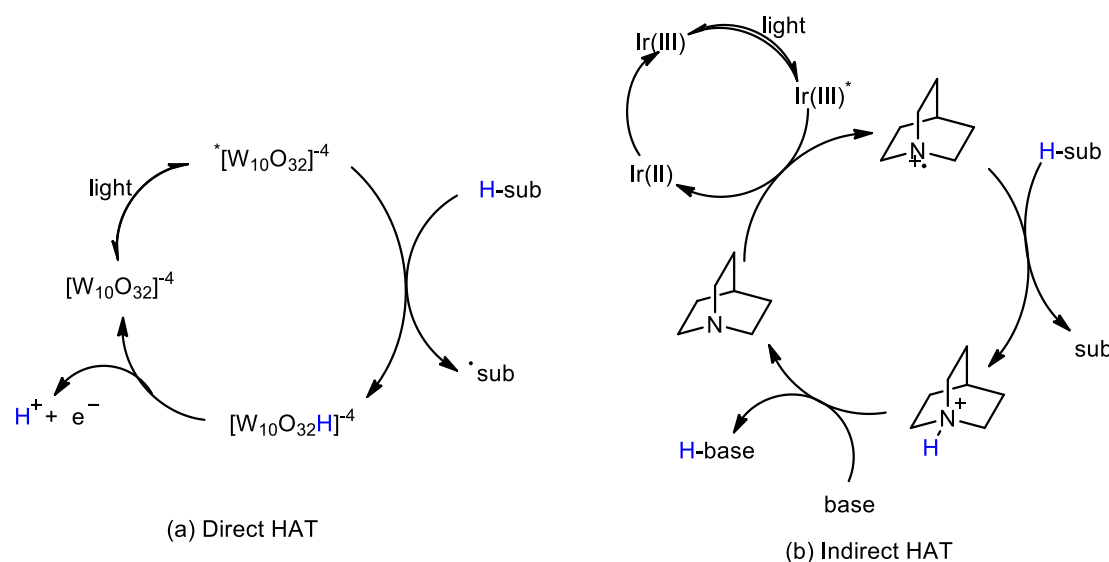
Hydrogen atom transfer (HAT) is another mechanism through which photoexcited catalyst can trigger a chemical transformation and this can be by direct or indirect HAT.<sup>111,118</sup> In direct HAT, the photoexcited catalyst abstracts hydrogen atom directly from the substrate resulting in a radical species. Sodium decatungstate  $[\text{W}_{10}\text{O}_{32}]$  is a typical example of such visible light photocatalyst proceeding through this mechanism (Figure 3.7a).<sup>111</sup> In an indirect HAT, a HAT reagent such as quinuclidine or DABCO are used in combination with the photocatalyst to accomplish HAT (Figure 3.7b). HAT is determined by bond energy of the resulting bond between the catalyst and the abstracted hydrogen atom, compared to the original H-substrate bond. Generally, HAT pathway is the best choice for substrates that have very high oxidation potential such that they are not easily oxidized using photoredox catalysts.<sup>111</sup> Some substrates that can be activated by HAT are presented in Figure 3.7.

<sup>115</sup> a) H. Ikezawa, C. Kutal, K. Yasufuku, H. Yamazaki, *J. Am. Chem. Soc.* **1986**, *108*, 1589-1594. b) R. R. Islangulov, F. N. Castellano, *Angew. Chem. Int. Ed.* **2006**, *45*, 5957-5959.

<sup>116</sup> M. Wrighton, J. Markham, *J. Phys. Chem.* **1973**, *77*, 3042-2043.

<sup>117</sup> M. S. Lowry, J. I. Goldsmith, J. D. Slinker, R. Rohl, R. A. Pascal, G. G. Malliaras, S. Bernhard, *Chem. Mater.* **2005**, *17*, 5712-5719.

<sup>118</sup> L. Capaldo, D. Ravelli, *Eur. J. Org. Chem.* **2017**, *15*, 2056-2071.



Examples of substrates (H-sub) and their bond energy

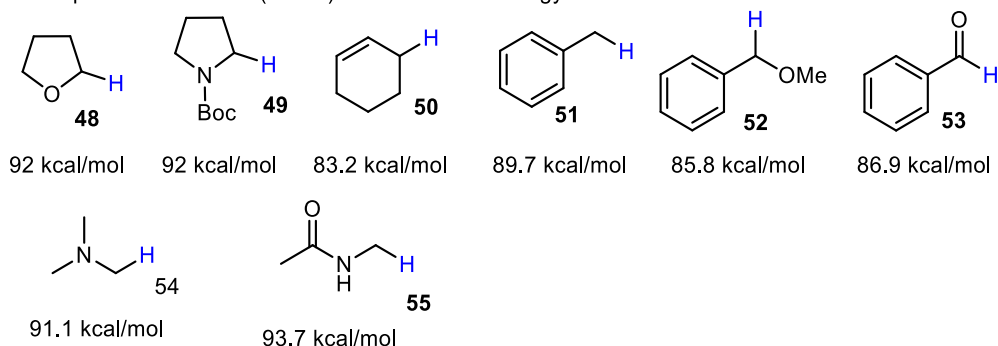


**Figure 3.7:** Substrate that can be activated by visible-light mediated HAT<sup>111</sup>

## 5. Conclusion

Visible-light photoredox catalysis has been shown to be a benign and efficient alternative procedure for organic synthesis. The technique uses relatively low energy photons in the range 380-600 nm to activate a photocatalyst, which then mediates a chemical transformation. This makes it more selective as compared to the UV-based photochemistry where reagents, solvents and products are often indiscriminately irradiated leading to potential undesired by-products. Moreover, visible-light photocatalysis uses cheap light source such as LEDs or household compact fluorescent lamps (CFLs) and does not require specialized equipment as in the case of UV irradiation. Photocatalysis finally allows to attain unique reactivities of molecules in their excited states, which often lead to distinct behaviors from those generally observed using classical thermal activation.

## **PART 2: Urethanes and PUs synthesis by visible light-mediated decarboxylation of oxamic acids**

### **1. Introduction**

As discussed in the preceding chapter, oxamic acids can serve as a greener alternative to phosgene for the synthesis of isocyanates. Minisci<sup>119</sup> first demonstrated the radical oxidation of this safer starting material to isocyanates in moderate to good yields. Their method however was not suitable for direct access to urethanes due to the involvement of water as solvent, leaving the option of isolation and purification of the carcinogenic isocyanate before being transformed to urethanes. Partial hydrolysis of the generated isocyanate into amine was equally observed which has a detrimental effect on the product yield.

To address this problem, our group recently developed a metal-free photocatalyzed procedure that permits direct access to urethanes and ureas from oxamic acids (Scheme 3.1).<sup>120</sup> This mild and efficient procedure uses organic dye photocatalyst, hypervalent iodine reagent and visible-light activation to trigger the free-radical oxidation of oxamic acids into *in-situ* generated isocyanates, which in the presence of alcohols furnished urethanes in a one-pot process, thereby avoiding isolation and purification of the generated isocyanate. 4-CzIPN was shown to be the most efficient organic photocatalyst for the reaction though Ru(bpy)<sub>3</sub>Cl<sub>2</sub> and AcrMes<sup>+</sup>ClO<sub>4</sub><sup>-</sup> could also serve as competent photocatalysts for the reaction. On the other hand, Eosin-Y and rose-Bengal gave only trace amount of the desired product. Furthermore, acetoxybenziodoxole (BI-OAc) demonstrated superior performance as an oxidant for the reaction compared to other hypervalent iodine reagents tested including BI-OH, PIDA and PIFA. The reaction worked efficiently with DCE or DCM as solvent while THF, CH<sub>3</sub>CN or DMF resulted in low product yield and DMSO failed to provide the product.

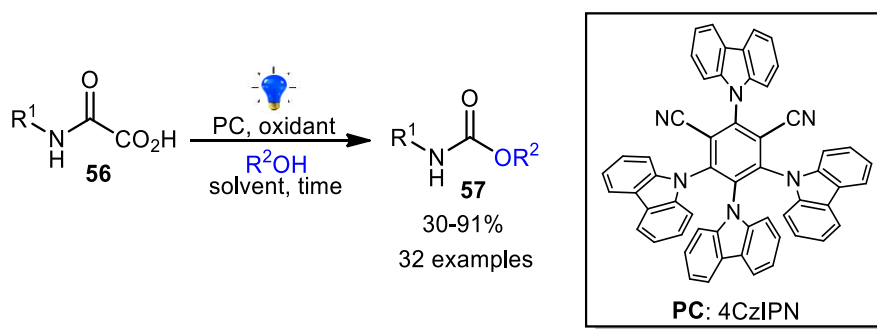
This new photocatalyzed procedure exhibited a wide substrate scope; varieties of oxamic acids and alcohols were compatible with the system furnishing the desired urethanes in good to excellent yields with high functional group tolerance.<sup>120</sup>

Furthermore, extension of this greener process to the preparation of unsymmetrical ureas was also successfully. However, a two-step one pot strategy was adopted here, in which isocyanate was first generated under photocatalytic conditions and then the amine was added to furnish the corresponding urea without isolation and purification of the generated isocyanate.<sup>120</sup>

---

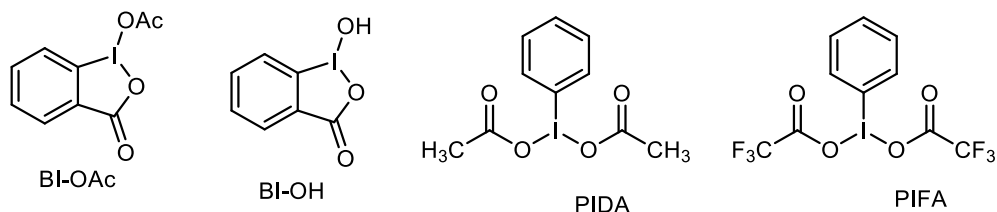
<sup>119</sup> a) F. Minisci, F. Coppa, F. Fontana, *Chem. Commun.* **1994**, 679. b) F. Minisci, F. Fontana, F. Coppa, M. Y. Yan, *J. Org. Chem.* **1995**, *60*, 5430-5433.

<sup>120</sup> G. G. Pawar, F. Robert, E. Grau, H. Cramail, Y. Landais, *Chem. Commun.* **2018**, *54*, 9337-9340.



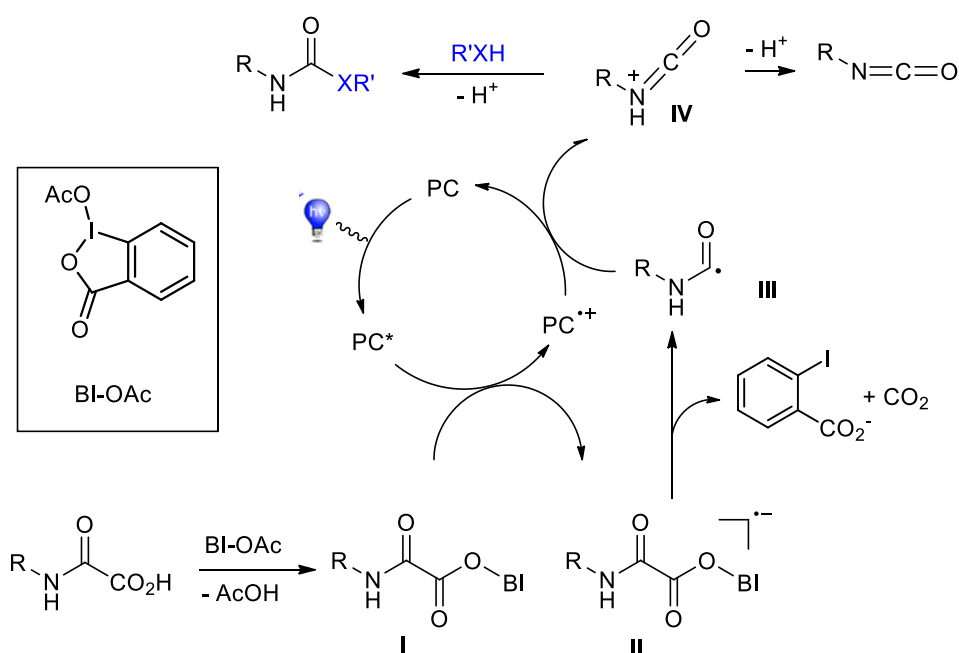
-----

**Oxidants**



**Scheme 3.1:** Urethane synthesis through visible-light mediated decarboxylation of oxamic acids.<sup>18</sup>

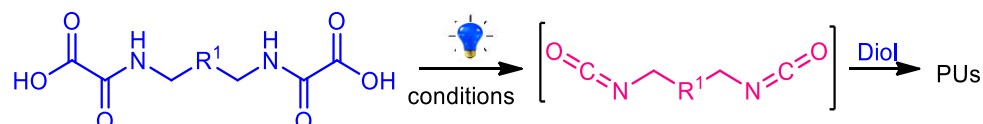
The proposed mechanism suggests that the photoexcited catalyst ( $PC^*$ ) is quenched by intermediate **I** which is formed through ligand exchange between oxamic acid **56** and BI-OAc, resulting in an unstable radical-anion **II** which collapses to release carbamoyl radical **III** and *o*-iodobenzoic acid anion (Scheme 3.2). Further oxidation of **III** by the photocatalyst radical cation  $PC^{*+}$  would give the corresponding protonated isocyanate **IV** while the photocatalyst is regenerated. The protonated isocyanate can either react *in-situ* with the nucleophile to furnish the desired product or loses a proton to give isocyanate. It is worth mentioning that when the reaction is performed in the absence of alcohols, the isocyanate is isolated in good yield, further supporting the mechanism below.



**Scheme 3.2:** Mechanism of the photocatalyzed urethane synthesis from oxamic acid

## 2. The objective of this Project

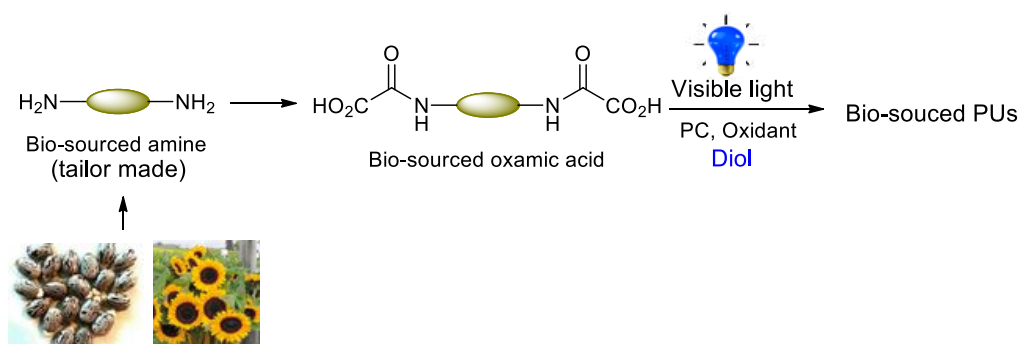
The main objective of this project was to develop a sustainable route to polyurethanes based on this new photocatalyzed process. We envisaged that with a bifunctional or polyfunctional oxamic acids, diisocyanates or polyisocyanates could be generated *in-situ*, and in the presence of diols or polyols would afford PUs through a one pot process, without isolation and purification of the generated isocyanate (Scheme 3.3).



**Scheme 3.3:** New photocatalyzed process for PUs synthesis from oxamic acid

This project relies on the following pillars:

- ❖ The use of oxamic acids as non-toxic starting material to generate isocyanates *in-situ*, thereby avoiding the direct handling of the carcinogenic isocyanates, and most importantly the use of hazardous phosgene as isocyanate precursor is circumvented.
- ❖ Secondly, CO<sub>2</sub> released during the process is targeted to serve as a blowing agent for the preparation of self-blown PU-foams from oxamic acids.
- ❖ Finally, this procedure could serve as another gateway for the synthesis of bio-sourced PUs, whereby oxamic acids could be derived from bio-based amine precursors and then be transformed into bio-sourced polyurethanes (Scheme 3.4).



**Scheme 3.4:** Possible route to bio-sourced PUs based bio-sourced oxamic acids

## 3. Further process optimization using PIDA as oxidant

In the new photocatalyzed procedure for the synthesis of urethane from oxamic acids described above, BI-OAc was used as oxidant, though most efficient of all the oxidants studied, the by-product (2-iodobenzoic acid) is solid. This solid by-product may be problematic to remove during polymer purification. For this reason, we considered PIDA more suitable for polyurethane synthesis; it's by-

products (iodobenzene and acetic acid) are liquids at room temperature and could easily be removed from reaction mixture during polymer precipitation or by simple evaporation at reduced pressure. However, as mentioned earlier, PIDA was less efficient as an oxidant for the visible-light mediated process compared to BI-OAc. We first tried to optimize the performance of PIDA as an oxidant for the photocatalyzed reaction, by varying process parameters and different activation strategies reported in literature.

For a start, we chose mono-oxamic acid **56a** as our model compound and EtOH (Table 3.1). Under the optimal conditions developed previously, PIDA expectedly delivered only a moderate amount of the desired urethane **57a** (64 %, entry 1), while its derivative PIFA was even less efficient for the reaction (entry 2). Conducting the reaction at 40°C showed no significant improvement in the product yield (entry 3), neither did extending the reaction time to 48 h improved the reaction (entry 4). Also, DCE displayed similar reactivity as DCM as solvent for the reaction (entry 5). Using 2.0 equivalent of PIDA equally did not help to improve the product yield (entry 6). Then, the alcohol equivalent was varied, though the effect was not very significant, it showed that the reaction could still progress satisfyingly with just 1.0 eq. of alcohol (entry 9) which is quite interesting for polymer synthesis using AA- BB-type monomers.<sup>121</sup>

At this point, we turned our attention to some strategies that can be used to enhance the reactivity of PIDA. It has been shown that the oxidative capacity of PIDA can be enhanced by acid activation using BF<sub>3</sub>·Et<sub>2</sub>O, Me<sub>3</sub>SiOTf, HOTf or Me<sub>3</sub>SiBr.<sup>122</sup> Although the mechanism of this activation is not yet clear, there are some speculations that it could be due to the formation of more reactive cationic species [PhI(OAc)]<sup>+</sup> through the interaction between the Lewis acid and the hypervalent iodine (Scheme 3.5, **I**). There was also a suggestion that Me<sub>3</sub>SiOTf activation could be due to formation of more reactive species PhI(OTf)<sub>2</sub> **II** through ligand exchange.<sup>123</sup> We tried these strategies in our system, unfortunately they were detrimental to the urethane yield (entry 10-11).

Furthermore, it was reported that PIDA can be activated using HFIP *via* formation of strong hydrogen bond adduct (Scheme 3.5, **III**).<sup>124</sup> This strategy was equally tried in our reaction using 3.0 eq. of HFIP, but it was not effective (entry 12). Also, the use of PIDA in combination with a catalytic amount of iodine has been reported to exhibit special reactivity towards oxidative decarboxylation of carboxylic acids; the activation works through the formation of acetyl hypoiodite **IV** (AcOI).<sup>125</sup> It is believed that AcOI would react with the organic acid to generate of RCO<sub>2</sub>I bearing a weak iodine-oxygen bond which can easily be cleaved under photocatalyzed conditions to trigger the decarboxylation.<sup>125a</sup> When we tried this strategy in our reaction, interestingly a significant improvement in the urethane yield was observed, resulting in 89% conversion (entry 13).

<sup>121</sup> Y. Ye, K. Y. Choi, *Polymer* **2008**, *49*, 2817–2824.

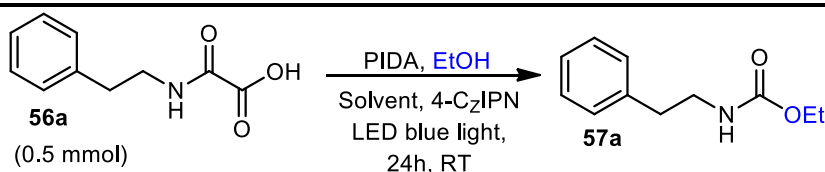
<sup>122</sup> S. Izquierdo, S. Essafi, I. del Rosal, P. Vidossich, R. Pleixats, A. Vallribera, G. Ujaque, A. Lledós, A. Shafir, *J. Am. Chem. Soc.* **2016**, *138*, 12747–12750.

<sup>123</sup> K. Kiyokawa, K. Takemoto, S. Yahata, T. Kojima, S. Minakata, *Synthesis* **2017**, *49*, 2907–2912.

<sup>124</sup> I. Colomer, C. Batchelor-McAuley, B. Odell, T. J. Donohoe, R. G. Compton, *J. Am. Chem. Soc.* **2016**, *138*, 8855–8861.

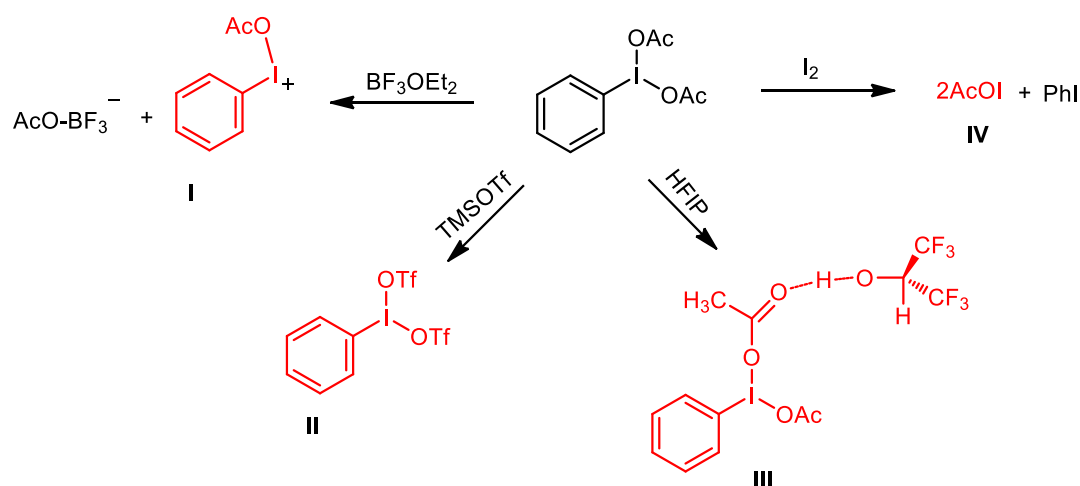
<sup>125</sup> a) K. Kiyokawa, T. Watanabe, L. Fra, T. Kojima, S. Minakata, *J. Org. Chem.* **2017**, *82*, 11711–11720. b) M. Stateman, E. A. Wappes, K. M. Nakafuku, K. M. Edwards, D. A. Nagib, *Chem. Sci.*, **2019**, *10*, 2693–2699. c) A. F. Prusinowski, R. K. Twumasi, E. A. Wappes, D. A. Nagib, *Am. Chem. Soc.* **2020**, *142*, 5429–5438.

Application of these optimized PIDA conditions for the synthesis of bicarbamates **59** using bis-oxamic acids **58**, resulted in 72 - 77% conversion (Scheme 3.6), which also confirmed some improved reactivity compared to the reaction using PIDA alone which gave 69%.

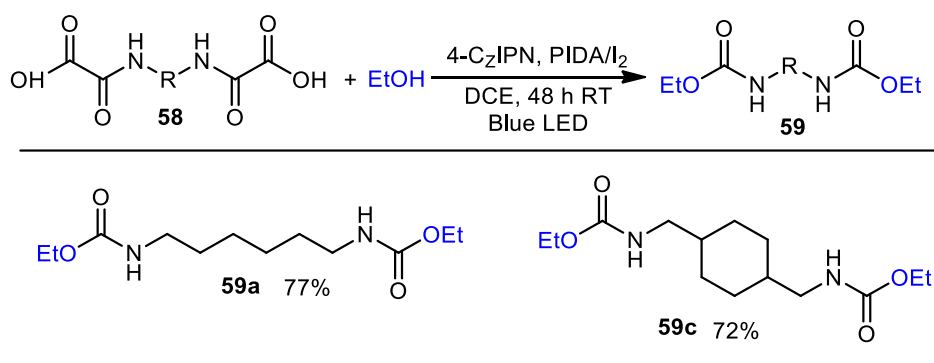


Entry <sup>a</sup>	PC	Oxidant	Additive	Solvent	EtOH (eq.)	Time (h)	% Yield <sup>b</sup>
1	4C <sub>z</sub> IPN	PIDA	-	DCM	3.0	24	64
2	4C <sub>z</sub> IPN	PIFA	-	DCM	3.0	24	50
3 <sup>c</sup>	4C <sub>z</sub> IPN	PIDA	-	DCM	3.0	24	68
4	4C <sub>z</sub> IPN	PIDA	-	DCM	3.0	48	69
5	4C <sub>z</sub> IPN	PIDA	-	DCE	3.0	48	69
6 <sup>d</sup>	4C <sub>z</sub> IPN	PIDA	-	DCM	3.0	48	70
7	4C <sub>z</sub> IPN	PIDA	-	DCM	2.0	24	73
8	4C <sub>z</sub> IPN	PIDA	-	DCM	1.5	24	70
9	4C <sub>z</sub> IPN	PIDA	-	DCM	1.0	24	68
10	4C <sub>z</sub> IPN	PIDA	BF <sub>3</sub> OEt <sub>2</sub>	DCM	3.0	24	42
11	4C <sub>z</sub> IPN	PIDA	TMSOTf	DCM	3.0	24	24
12	4C <sub>z</sub> IPN	PIDA	HFIP (1:3)	DCM	3.0	24	68
13	4C <sub>z</sub> IPN	PIDA	I <sub>2</sub> (0.05 eq.)	DCM	1.5	24	89(76) <sup>e</sup>
14	4C <sub>z</sub> IPN	PIDA	I <sub>2</sub> (0.1 eq.)	DCM	1.5	24	86
15	4C <sub>z</sub> IPN	BI-OAc	-	DCM	3.0	24	92(88) <sup>e</sup>

**Table 3.1:** <sup>a</sup> Unless otherwise stated, all reactions were carried out in a sealed tube using mono-oxamic acid **56a** (0.5mmol.), EtOH (3 eq.), photocatalyst: **PC** (1 mol%), oxidant (1.5 eq.). <sup>b</sup> Yields of **57a** determined by <sup>1</sup>H NMR using 1,3,5-trimethylbenzene as an external standard. <sup>c</sup> Isolated yields of **57a**. <sup>e</sup> Reaction performed at 40 °C. <sup>d</sup> Reaction using 2.0 eq. of PIDA. <sup>e</sup> Isolated yield.



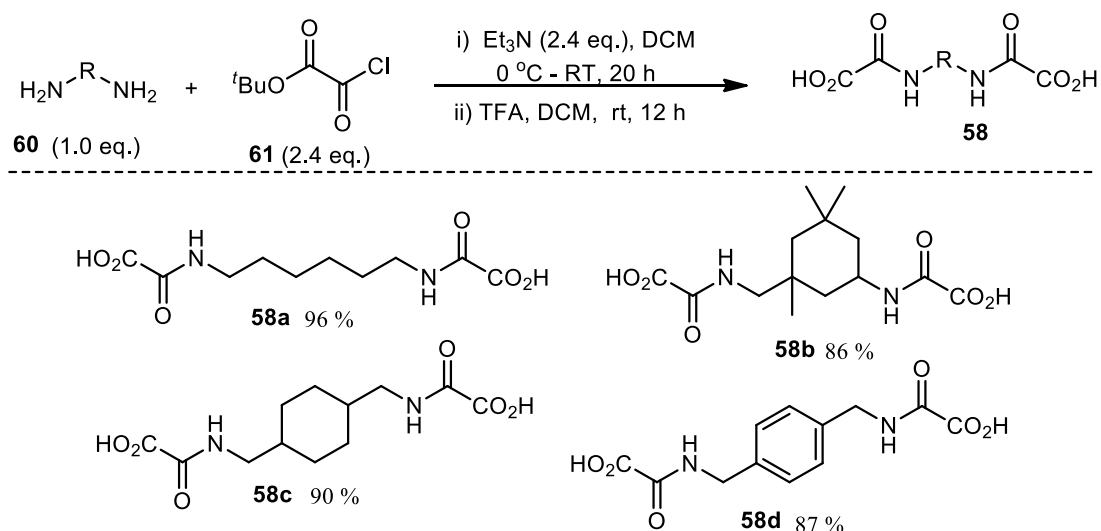
**Scheme 3.5 :** Activation of PIDA reactivity using additives.



**Scheme 3.6:** Photocatalyzed bicarbamate synthesis from bis-oxamic acid using PIDA/I<sub>2</sub> as oxidant

#### 4. Bis-oxamic acids used for the photocatalyzed polyurethane synthesis

For the scope of this project, we started with bis-oxamic acids synthesized from commercially available diamines by direct coupling with *t*-butyl 2-chloro-2-oxoacetate (ClCOCO<sub>2</sub>*t*-Bu) (Scheme 3.7). The synthesis involves two-steps: the amine was treated with ClCOCO<sub>2</sub>*t*-Bu to form the corresponding *t*-butyl oxamate, which was followed by the removal of the *t*-Bu group using TFA in the second step. The expected bis-oxamic acids were obtained in excellent yields.



**Scheme 3.7:** Bis-oxamic acids from commercially available diamines

#### 5. Design of a new photocatalyzed procedure for the thermoplastic PU synthesis from bis-oxamic acids

Bis-oxamic acid **58a** was chosen as a model compound, PEG-1500 **62** as a polyol, BI-OAc was first used as the oxidant and 4-CzIPN as photocatalyst following the optimized conditions previously determined using mono-oxamic acid (Scheme 3.8).<sup>120</sup>



**Scheme 3.8:** New photocatalyzed procedure for the synthesis of polyurethane from bis-oxamic acids **58a**: (1.0 mmol), PEG-1500 **62** (1.0 eq.), BI-OAc (2.5 eq.), 4-CzIPN (5 mol%), DCE (0.2 M), 72h, RT.

The reaction was monitored using FT-IR (Figure 3.8a) where the *in-situ* generation and consumption of diisocyanate during the polymerization was observed around  $2270\text{ cm}^{-1}$ , and the corresponding urethane linkage formation at about  $1702\text{ cm}^{-1}$ . The concentration of the *in-situ* generated diisocyanate in the reaction mixture appeared to be higher between 8 to 15 h (Figure 3.8b), suggesting that its rate of generation probably was higher than its consumption within that time. Nevertheless, it took between 48 to 72 h for complete disappearance of isocyanate from the reaction mixture. Furthermore, bis-oxamic acid conversion during the reaction was indicated by the disappearance of its two C=O bands at  $1678\text{ cm}^{-1}$  and  $1762\text{ cm}^{-1}$  and formation of new C=O of urethane linkage at about  $1702\text{ cm}^{-1}$  (Figure 3.8b).

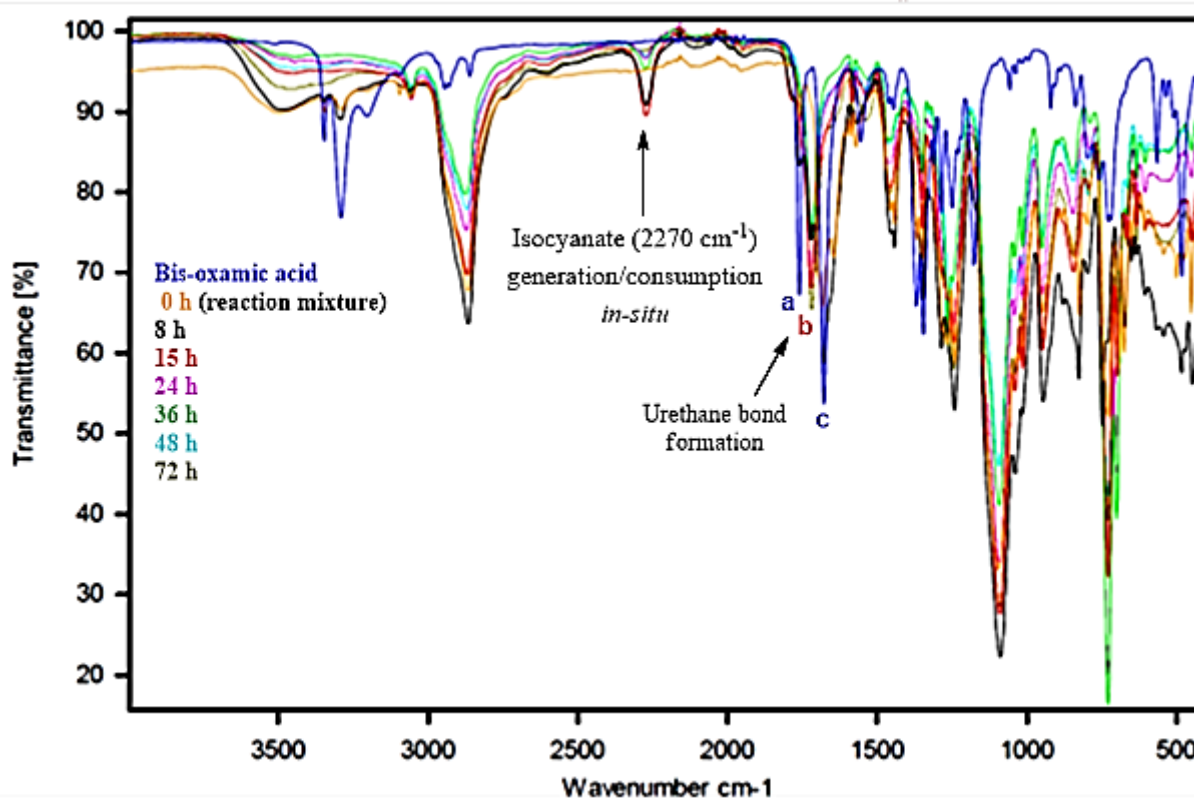
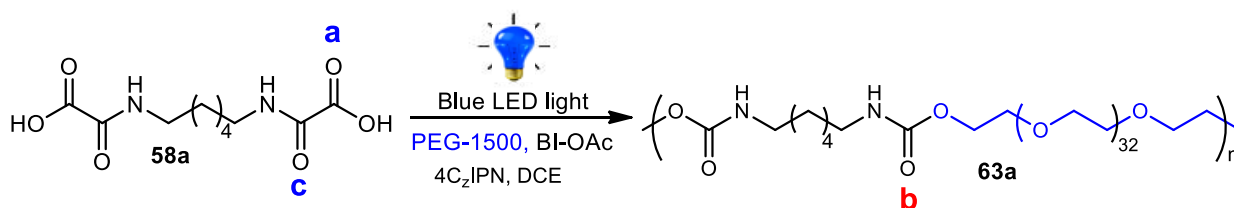


**Figure 3.8a:** FT-IR monitoring of photocatalyzed synthesis of PUs using bis-oxamic acids

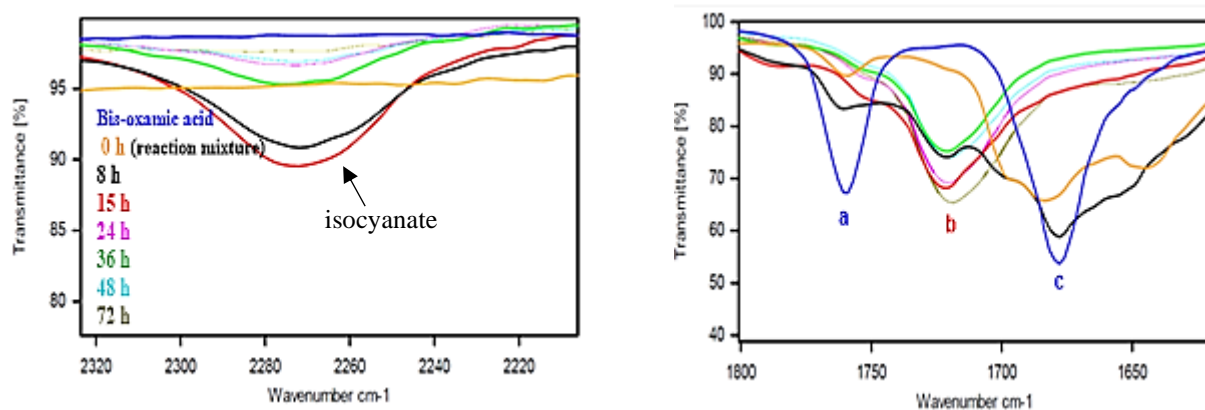
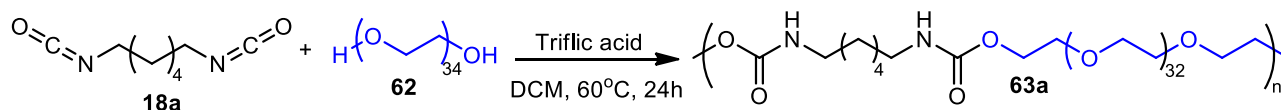


**Figure 3.8b:** FT-IR monitor of photocatalyzed synthesis of PUs using bis-oxamic acid (magnified spectra). **a:** oxamic acid C(OH)=O; **b:** urethane C=O; **c:** oxamic acid NH-C=O

After the reaction, the polyurethane was precipitated in diethyl ether and dried in *vacuo*. For structural comparison and properties, a similar PU was synthesized from the traditional diisocyanate route using PEG-1500 as polyol using acid catalysis (Scheme 3.9).<sup>126</sup>



**Scheme 3.9:** Polyurethane synthesis from diisocyanate **18a**: (1.0 mmol), PEG-1500 **62** (1.0 eq.), triflic acid (5 mol%), DCM (0.5 mL), precipitated using diethyl ether.

### 5.1. Characterization of the synthesized PUs

The <sup>1</sup>H NMR comparison of structural similarities of both PUs from the bis-oxamic acid and diisocyanate routes are represented in Figure 3.9. As expected, the peak at 4.12 ppm due to the two protons adjacent to the urethane function (-NHCO-O-CH<sub>2</sub>-) indicated urethane linkage formation between the isocyanate and polyol and this signal was the same in both PUs. Also, the FT-IR spectra of both PUs showed close resemblance, indicating the C=O bond around 1700 cm<sup>-1</sup> (Figure 3.10).

Furthermore, the molecular weight and polydispersity of the synthesized PUs were determined using size exclusion chromatography (SEC), DMF as eluent and polystyrene as standard. The molecular weight was determined based on differential refractive index (dRI). Figure 3.11 shows the SEC trace of the PU obtained from the photocatalyzed process. It was clear that the expected PU formed, though relatively of lower molecular weight compared to the one prepared using standard diisocyanate (Figure 3.12). The SEC trace also indicated that the photocatalyzed PU comprised different

<sup>126</sup> H. Sardon, A. C. Engler, J. M. W. Chan, J. M. García, D. J. Coady, A. Pascual, D. Mecerreyes, G. O. Jones, J. E. Rice, H. W. Horn, J. L. Hedrick, *J. Am. Chem. Soc.* **2013**, *135*, 16235-16241.

populations which probably include some oligomers. A little peak of the remaining unconverted PEG-1500 was also observed from the SEC trace.

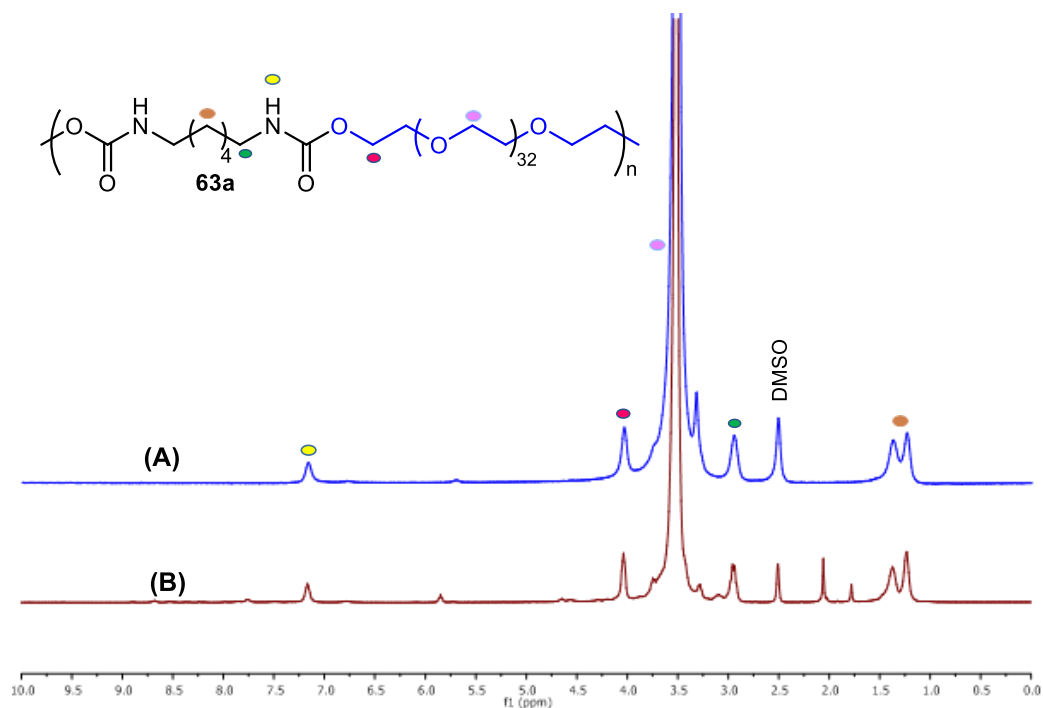


**Figure 3.9:** <sup>1</sup>H NMR comparing PU from diisocyanate route (A) with that from bis-oxamic acid route (B).

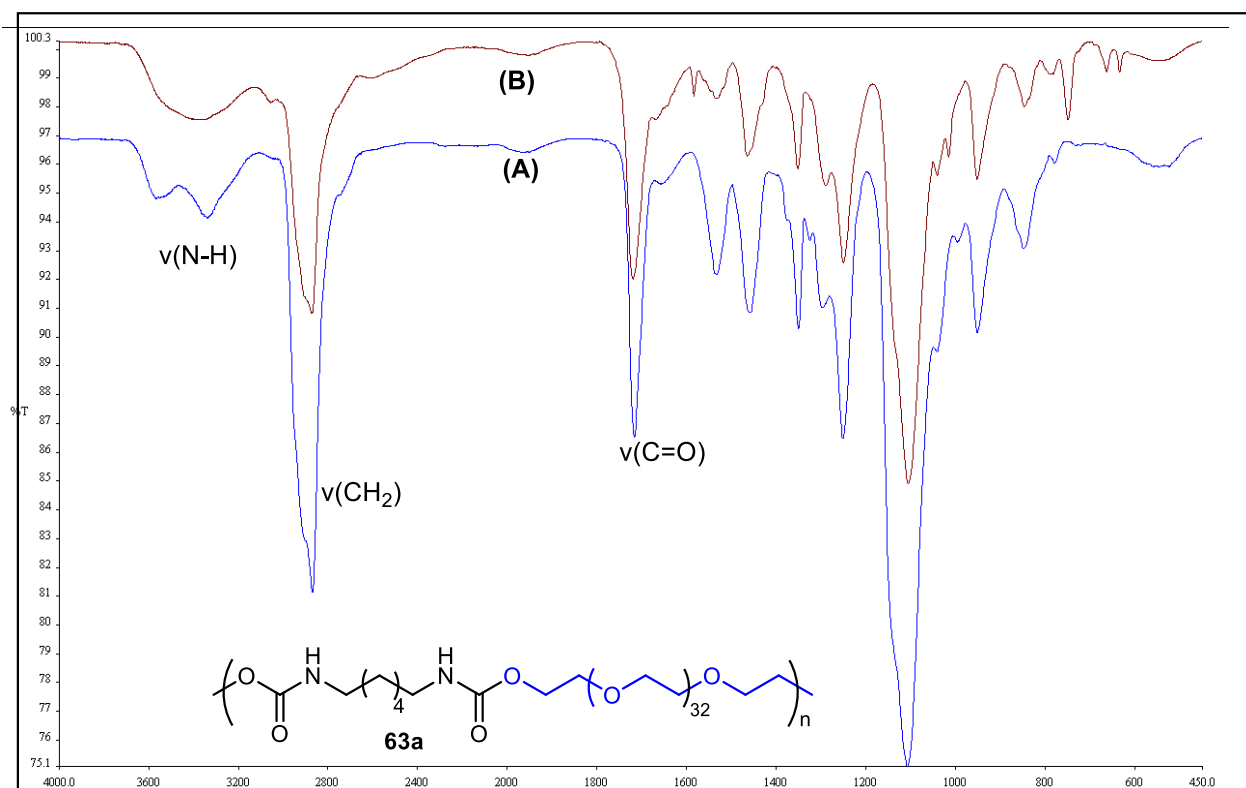
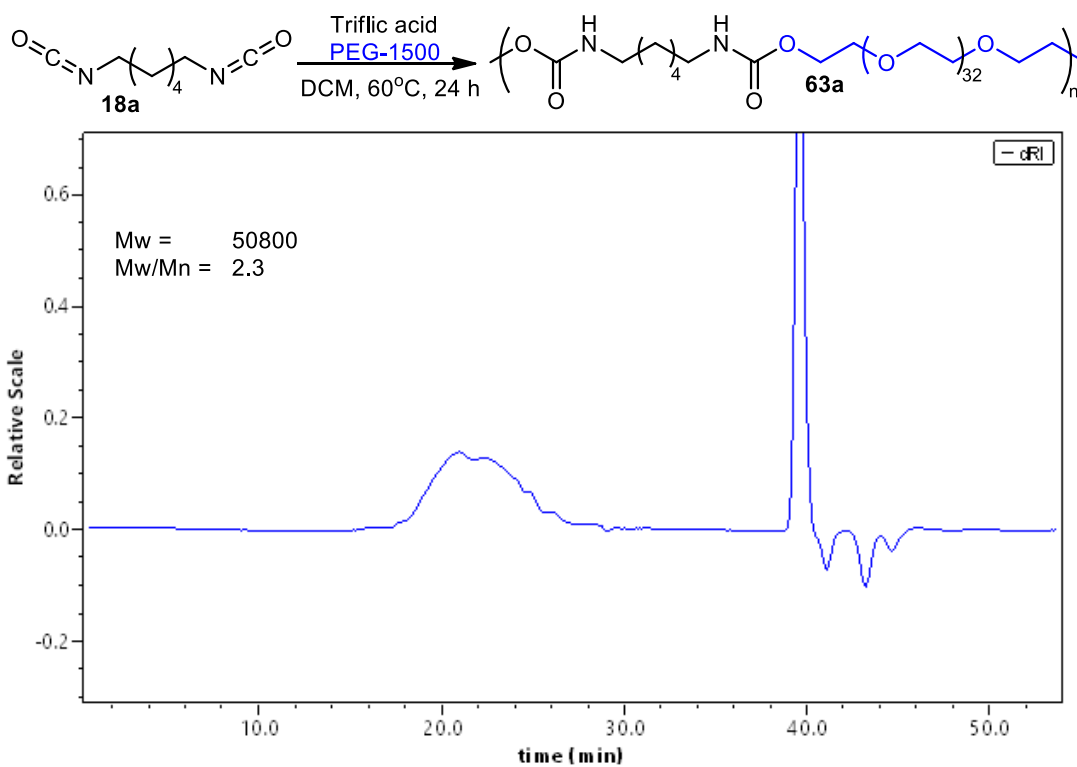
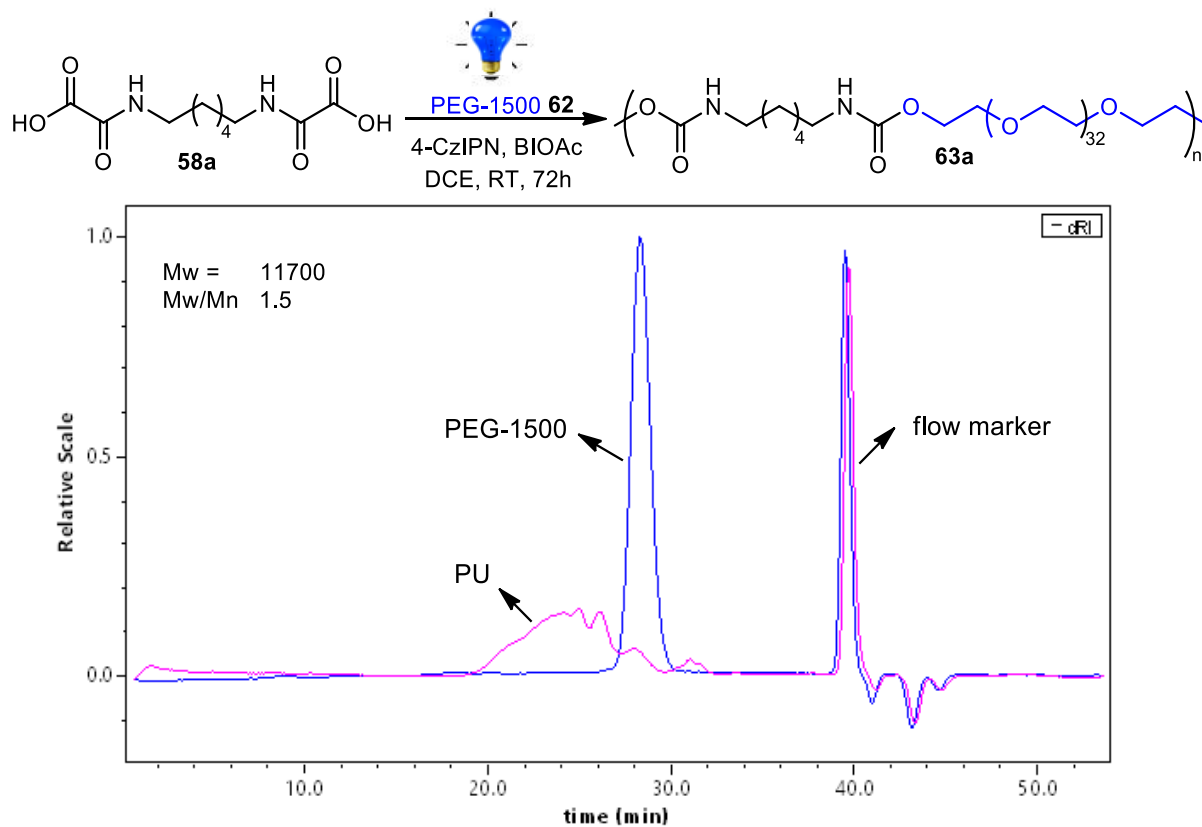


**Figure 3.10:** FT-IR comparing PU from diisocyanate route (A) with that from bis-oxamic acid routes (B).



## 5.2. Optimization of photocatalyzed PU synthesis

Encouraged by these results, we sought to optimize the photocatalyzed polymerization by varying different parameters. With BI-OAc as the oxidant, 4-CzIPN as photocatalyst and DCM as solvent, PU with molecular weight 11700 g/mol and polydispersity of 1.5 was obtained after 72 h (Table 3.2., entry 1). Extending the reaction time to 5 days did not help to improve the molecular weight. Unfortunately, our optimized PIDA/I<sub>2</sub> system was not efficient for the polymerization as only 8320 g/mol molecular weight was attained (entry 2), likewise PIDA alone (entry 3).

Moreover, we observed that unlike mono-oxamic acids, bis-oxamic acids were less soluble in DCM or DCE leading to reaction mixture, which were always heterogeneous at the beginning, but tending to homogenize as reaction progressed. We thought that this could be at the origin of the low molecular weight observed and long reaction time required. In order to solve this problem, we tried to use DMF (10%, v/v) as a co-solvent, although optimization studies showed that it is not a competent solvent for the photocatalyzed reaction just as THF and CH<sub>3</sub>CN (Table 3.3). Nevertheless, a better solubility of bis-oxamic acids in DMF endeared us to try it to achieve a better homogeneity of the reaction mixture. Unfortunately, this did not work as PU obtained displayed even lower molecular weight as compared to DCM or DCE alone (entry 4). We also tried to accelerate the nucleophilic addition of the polyol to the *in-situ* generated diisocyanate by using different types of catalysts reported in the literature including MTBD and DBU,<sup>127</sup> but their presence was even deleterious to the photocatalyzed process (data not shown). Interestingly, the use of acridinium salt as photocatalyst showed some improvement in the molecular weight (entry 5-6) but it was not reproducible. Also, decreasing the polyol equivalent (from 1.0 to 0.9 or 0.8 eq.) in an attempt to achieve a better stoichiometry for the AA- BB-type monomers did not show any significant improvement in the molecular weight, just that the recovered polyol after the reaction significantly reduced. The polyol was recovered using centrifugation after the PU precipitation.

Furthermore, we explored the possibility of conducting the polymerization using a two-step one pot process in which diisocyanate was first generated from the bis-oxamic acid under the photocatalytic conditions without the polyol, thereafter polyol was added with triflic acid (5 mol%) to complete the polymerization process (Figure 3.13). However, this strategy was not effective as even lower molecular weight PUs was obtained (entry 7). Probably part of the *in-situ* generated diisocyanate underwent some side reactions (formation of allophanates,.....) before the polyol was added since isocyanate is a reactive group (and particularly when activated as proposed in the mechanism); isocyanate can also be hydrolyzed by trace of water in the reaction mixture resulting in amine which can further consume more isocyanate to form urea.<sup>128</sup> The SEC trace of the two-step process indicated different populations probably comprising mainly oligomers (Figure 3.13).

Our original target was to accomplish the photocatalyzed polymerization at room temperature. Nevertheless, we tried to apply mild heating (60°C) on the photocatalyzed process to know if it could improve the polymerization process, probably by speeding up the addition of the polyol to the *in-situ*

<sup>127</sup> J. Alsarraf, Y. A. Ammar, F. Robert, E. Cloutet, H. Cramail, Y. Landais, *Macromolecules*, **2012**, *45*, 2249–2256.

<sup>128</sup> O. Kreye, H. Mutlu, M. A. R. Meier, *Green Chem.*, **2013**, *15*, 1431-1455

generated diisocyanate. This strategy interestingly allowed us to perform the polymerization in bulk with improved molecular weight (entry 9-10). Particularly, with PIDA as oxidant under this condition, a significantly high molecular weight PU was observed (Figure 3.14). However, the PUs obtained under this combined heat and light conditions were difficult to precipitate and, in some cases, insoluble and could not be analyzed by SEC. A simultaneous crosslinking probably occurred alongside the polymerization under the heat and light conditions.



Entry <sup>a</sup>	PC (5.0 mol%)	Oxidant (2.5 eq.)	Conversion <sup>b</sup> (%)	Solvent (0.1 M)	Mw <sup>c</sup> (g/mol)	Đ <sup>c</sup> (Mw/Mn)
1	4CzIPN	BI-OAc	90	DCM	11700	1.5
2	4CzIPN	PIDA/I <sub>2</sub>	75	DCM	8320	1.4
3	4CzIPN	PIDA	69	DCM	8590	1.4
4 <sup>d</sup>	4CzIPN	BI-OAc	-	DCM/DMF	8220	1.2
5	AcrMes <sup>+</sup> ClO <sub>4</sub> <sup>-</sup>	BI-OAc	82	DCM	16700	2.2
6	AcrMes <sup>+</sup> ClO <sub>4</sub> <sup>-</sup>	PIDA	76	DCM	9780	1.8
7 <sup>e</sup>	4CzIPN	BI-OAc	87	DCE	4230	1.3
8 <sup>f</sup>	4CzIPN	BI-OAc	91	DCE	14100	1.9
9 <sup>g</sup>	4CzIPN	BI-OAc	89	DCE	19500	2.0
10 <sup>g</sup>	4CzIPN	PIDA	91	-	42300	3.0
11	Diisocyanate route				50800	2.3

**Table 3.2:** PUs from bis-oxamic acids using photocatalyzed procedure. <sup>a</sup> All reactions were performed with bis-oxamic acid **58a** (1.0 eq.), PEG-1500 **62** (1.0 eq.), PC (5.0 mol %) and oxidant (2.5 eq.) in the indicated solvent (0.1 M), in a sealed tube for 72 h. <sup>b</sup> Determined from <sup>1</sup>H NMR. <sup>c</sup> Obtained from SEC (DMF) using polystyrene standards, <sup>d</sup> Reaction using DCM/DMF (9:10), <sup>e</sup> Reaction using two-steps method. <sup>f</sup> Reaction performed at 60°C, <sup>g</sup> Reaction performed at 60°C in bulk with only 0.5 ml of DCE as solvent.

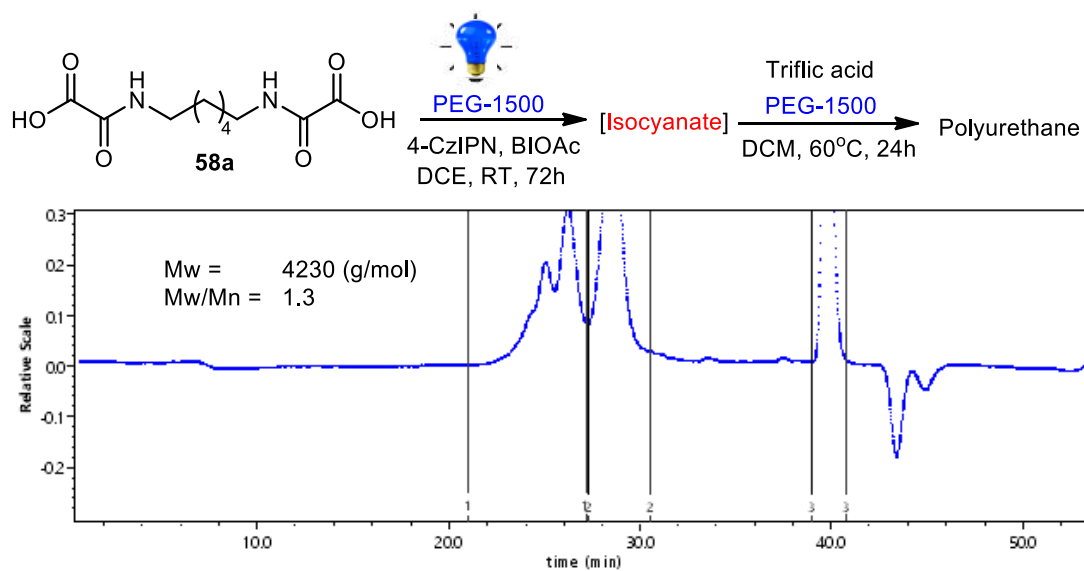


**Figure 3.13:** PU synthesis from bis-oxamic acid using two-step process

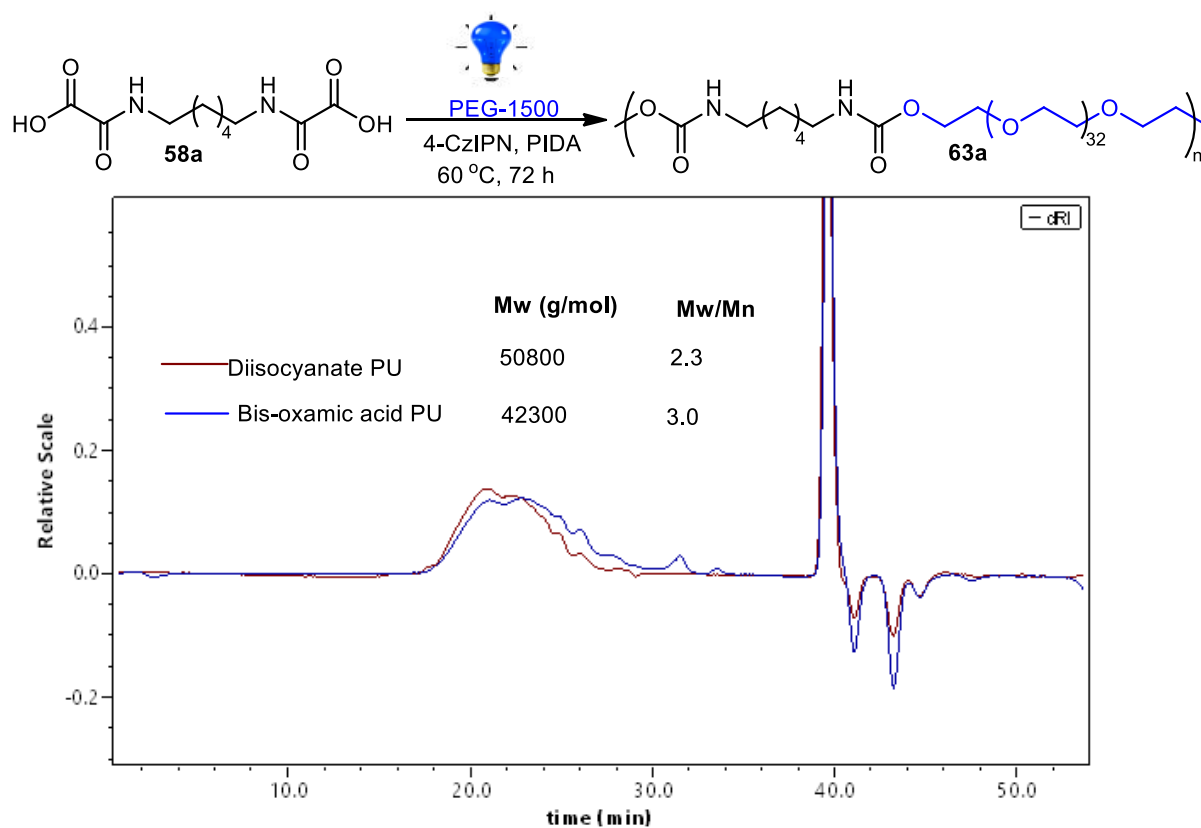


**Figure 3.14:** Comparing the SEC (DMF) traces of photocatalyzed PU obtained from bis-oxamic acid under bulk method and that from standard diisocyanate route

Entry <sup>a</sup>	PC (1 mol %)	Oxidant	Solvent	EtOH (Eq.)	Time (h)	% Yield <sup>b</sup>
1	4C <sub>z</sub> IPN	PIDA	DCM	3.0	24	69
2	4C <sub>z</sub> IPN	PIDA	DMF	3.0	24	08
3	4C <sub>z</sub> IPN	PIDA	THF	3.0	24	33
4	4C <sub>z</sub> IPN	PIDA	CH <sub>3</sub> CN	3.0	24	20

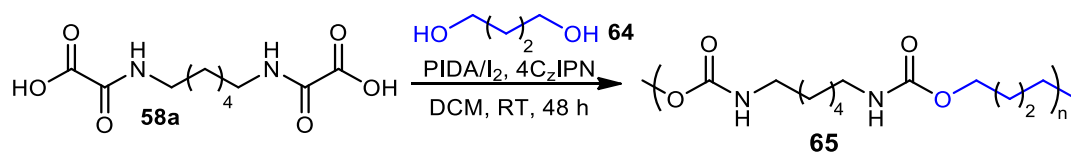
**Table 3.3:** Effect of solvent on bi-carbamate yield under visible-light mediated decarboxylation of bis-oxamic acid. <sup>a</sup> Unless otherwise stated, all reactions were carried out in a sealed tube using bis-oxamic acid **58a** (0.25mmol.), Ethanol (3 eq.), photocatalyst: **PC** (1.0 mol%), oxidant (2.5 eq.). <sup>b</sup> Yields of **59a** determined by <sup>1</sup>H NMR using 1,3,5-trimethylbenzene as an external standard.

## 6. Photocatalyzed PU synthesis from bis-oxamic acids using 1,4-butanediol

The new photocatalyzed process was also applied for the synthesis of “hard segment” PUs using bis-oxamic acid **58a** and 1,4-butanediol **64**. The reaction was conducted using DCE as solvent, PIDA/I<sub>2</sub> as oxidant. (Scheme 3.10). It is worth noting that, this reaction was part of our preliminary photocatalyzed polyurethane synthesis; it was intended to serve as our model reaction for the optimization, but the obtained PUs were very challenging to characterize by SEC analysis; they were only partially soluble in DMF, THF, DMSO or HFIP even when mild heating and/or a long dissolution time (48h) was applied. This same challenge was equally encountered with the standard diisocyanate derived PU using the same short chain diol. Nevertheless, after filtration, SEC (DMF) analysis (Figure 3.15) indicated a molecular weight of 3830 g/mol and polydispersity of 2.8 for the PU.

With <sup>1</sup>H NMR (Figure 3.16) and FT-IR (Figure 3.17), it was shown that the PU from the photocatalyzed process has similar structure with that from standard diisocyanate. The <sup>1</sup>H NMR clearly indicated the urethane linkage formation around 4.1 ppm in a similar manner with that of commercial diisocyanate derived PU. A possible urea peak<sup>129</sup> (~ 2.0 %) was also observed at about 6.7 ppm in both PUs. As mentioned earlier, urea is among the common by-product during urethane synthesis using isocyanate<sup>128</sup>; it is mainly triggered by traces of water in the reaction mixture. There is also another by-product peak around 7.6 ppm (~ 8.0 %) that is yet to be identified. From the FT-IR, C=O band of urethane was also clearly shown at around 1687 cm<sup>-1</sup> which corresponds to that of diisocyanate route (Figure 3.18).

<sup>129</sup> A. Lapprand, F. Boisson, F. Delolme, F. Mechin, J.-P. Pascault, *Polym. Degrad. Stab.* **2005**, *90*, 363-373.



**Scheme 3.10:** Photocatalyzed PU synthesis from bis-oxamic acid **58a** (1.0 mmol) and 1,4-Butanediol **64** (1.0 eq.), PIDA (2.5 eq.), I<sub>2</sub> (5mol%), 4CzIPN (5 mol%), DCE (0.2 M), 48h, RT.

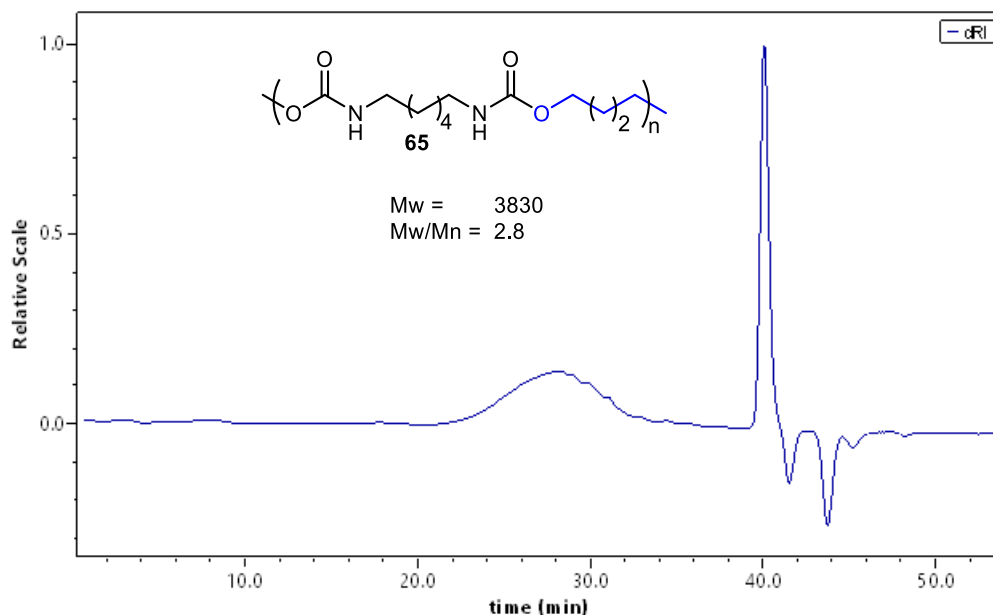


**Figure 3.15:** SEC trace (DMF) of photocatalyzed PU **65** from bis-oxamic acid **58a** and 1,4-butanediol

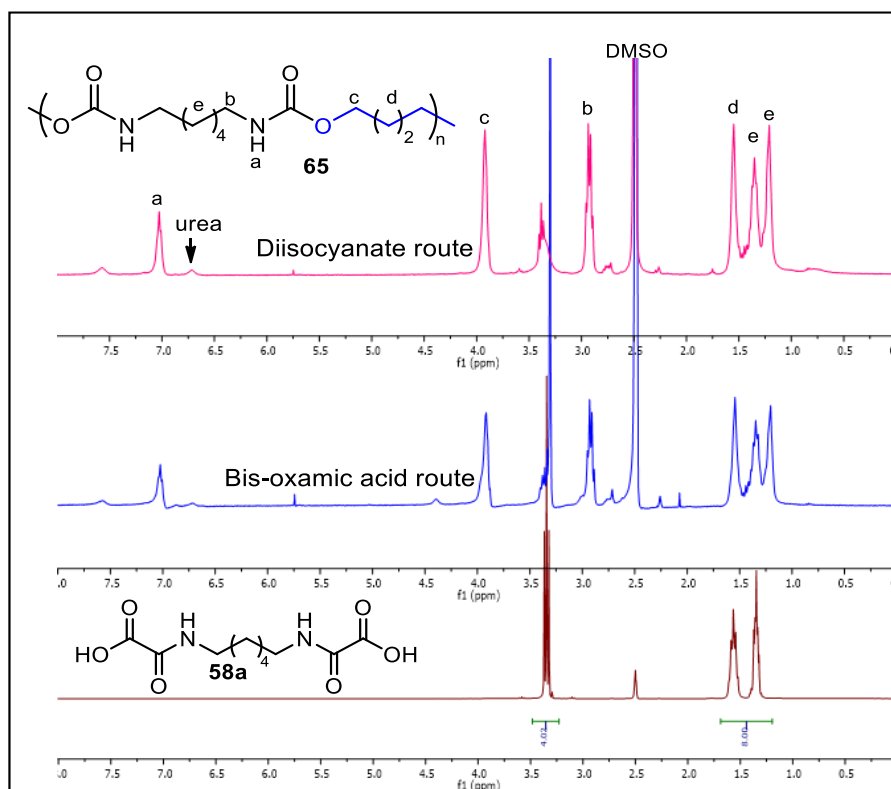


**Figure 3.16:** <sup>1</sup>H NMR of photocatalyzed PU **65** from bis-oxamic acid **58a** and 1,4-butanediol

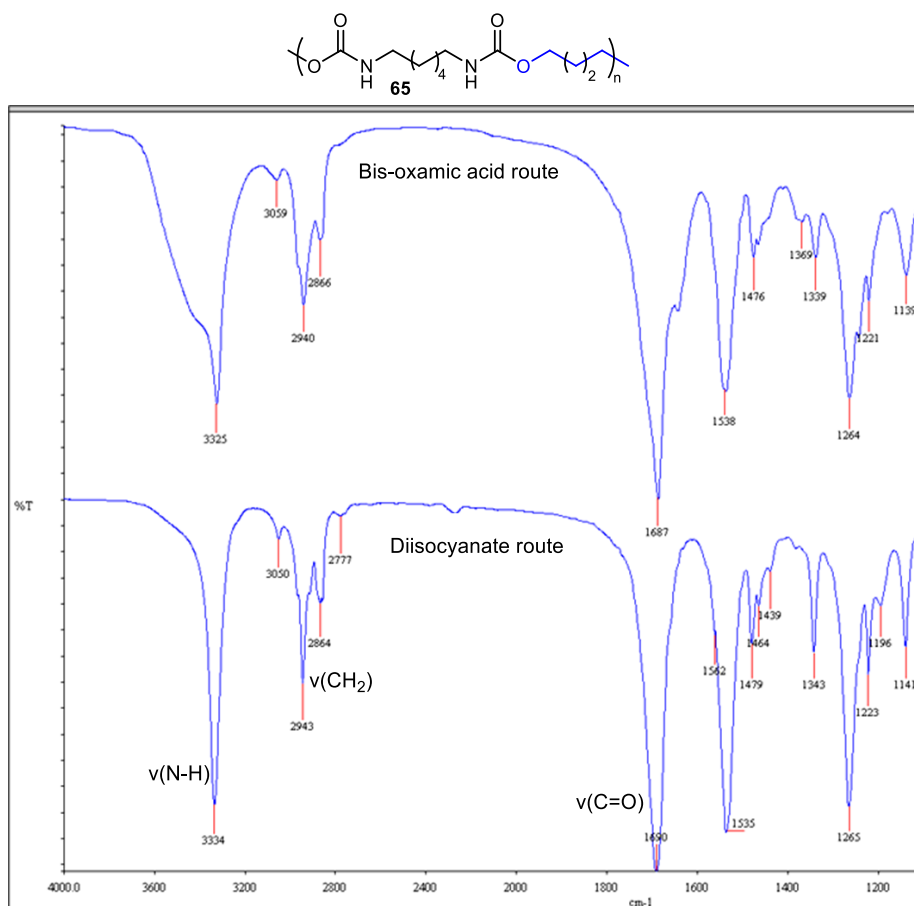
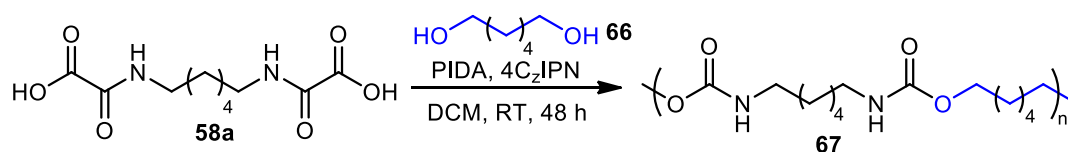


**Figure 3.17:** FT-IR of photocatalyzed PU **65** from bis-oxamic acid **58a** and 1,4-butanediol

### 7. Photocatalyzed PU synthesis from bis-oxamic acids using 1,6-hexanediol

Furthermore, 1,6-hexanediol was also subjected to the photocatalyzed reaction with bis-oxamic acid **58a** resulting in molecular weight of 4083 g/mol and polydispersity of 2.8 (Scheme 3.11). Just as in 1,4-butanediol, the obtained PU was difficult to solubilize during the SEC analysis.



**Scheme 3.11:** Photocatalyzed PU synthesis from bis-oxamic acid **58a** and 1,6-hexanediol **66** (1.0 mmol) PIDA (2.5 eq.), I<sub>2</sub> (5mol%), 4CzIPN (5 mol%), DCE (0.2 M), 48h, RT.

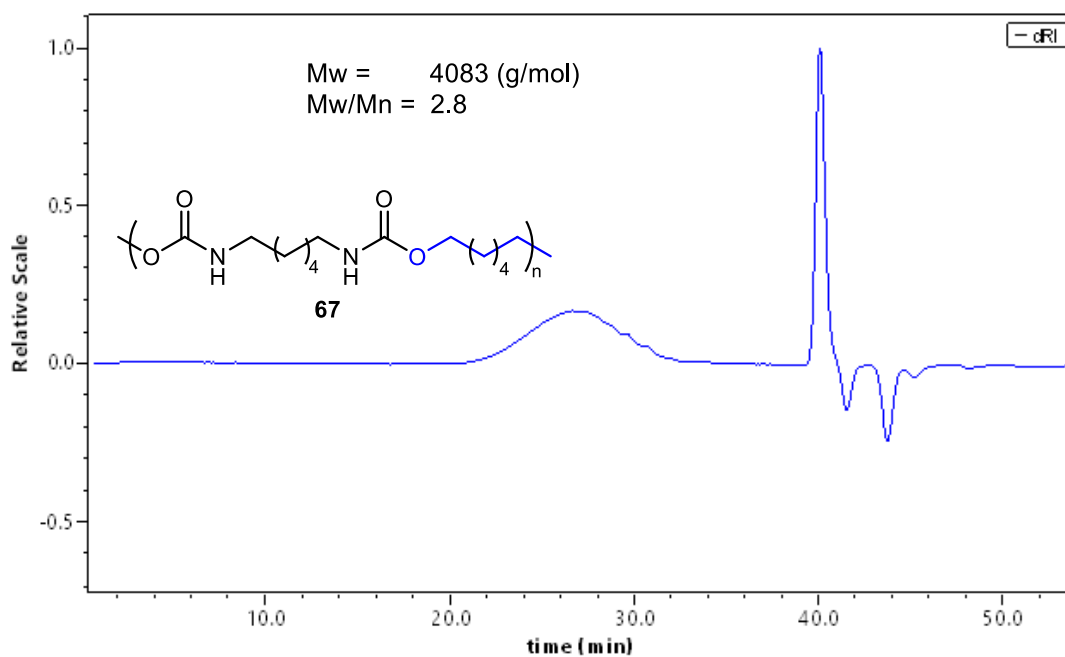


**Figure 3.18:** SEC trace (DMF) of photocatalyzed PU **64** from bis-oxamic acid **58a** and 1,6-hexanediol **66**

## 8. Conclusion

A new photocatalyzed procedure for synthesis of polyurethane from bis-oxamic acids has been reported.  $^1\text{H}$  NMR and FT-IR indicated that the obtained PUs have similar structures with one prepared through the standard diisocyanate route. SEC analysis also indicated the PUs formation with molecular weight up to 16700 g/mol and  $\bar{D}$  of 2.3 at room temperature using PEG-1500 as the polyol. A mild heating up of the photocatalyzed system during the polymerization resulted in a significant improvement in the molecular weight probably by accelerating the addition of the polyol to the generated diisocyanate; however, problem of precipitating the obtained PUs was encountered and in most cases, they were unusually insoluble in most of common organic solvent tried and hence could not be characterized by SEC. This probably could be due to a simultaneous crosslinking during the polymerization under the influence heat and light. Nevertheless, this served as a foundation for the development of a more efficient synthetic route to PUs using oxamic acids as greener precursors.

# Chapter 4

## Near-infrared light photocatalysis. Application to the oxidative decarboxylation of oxamic acids

### 1. Near-infrared light photocatalysis

There is a growing interest in the use of near infrared (NIR) light in photocatalysis due to its promising advantages over UV-visible light counterparts. Although visible light photocatalysis has been shown to be efficient, its shallow penetration into reaction media limits its application in large-scale synthesis and photopolymerization.<sup>130,131</sup> NIR light on the other hand has deeper penetration into reaction media due to its longer wavelength.<sup>132</sup> As illustrated in Figure 4.1, the longer the wavelength, the lesser the optical density in a given medium;<sup>133</sup> optical density is a measure of how much the light is blocked (or diffused) by the medium. It was recently demonstrated that NIR light could penetrate as far as about 300 times deeper into a reaction medium compared to blue light,<sup>131</sup> making it more attractive for photopolymerization and large-scale photocatalyzed reactions. Besides photocatalysis, NIR light has equally attracted a growing attention in biological fields including photodynamic therapy, drug release and bio-imaging, where its deeper penetration into biological tissue, better tissue transparency and minimal phototoxicity are valued over UV-visible light.<sup>134</sup>

Furthermore, many organic molecules do not absorb NIR light, hence NIR-based photocatalysis is promising to avoid an unwanted competition for the incident light between the photocatalyst and other co-components from the reaction mixture, and this would limit side reactions and enhance catalytic efficiency.<sup>131,135</sup> Moreover, the health risk associated with the exposure to highly energetic UV-visible light during photochemical reaction can be curtailed by using NIR light.<sup>136</sup>

---

<sup>130</sup> H. Mokbel, G. Noirbent, D. Gigmes, F. Dumur, J. Lalevée, *Beilstein J. Org. Chem.* **2021**, *17*, 2067–2076.

<sup>131</sup> B. D. Ravetz, A. B. Pun, E. M. Churchill, D. N. Congreve, T. Rovis, L. M. Campos, *Nature*, **2019**, *565*, 342–346.

<sup>132</sup> a) M. L. Viger, M. Grossman, N. Fomina, A. Almutairi, *Adv. Mater.* **2013**, *25*, 3733–3738. b) A.M. Smith, M.C. Mancini, S. Nie, *Nat. Nanotechnol.* **2009**, *4*, 710–711.

<sup>133</sup> A. H. Bonardi, F. Dumur, T. M. Grant, G. Noirbent, D. Gigmes, B. H. Lessard, J.-P. Fouassier, J. Lalevée, *Macromolecules* **2018**, *51*, 1314–1324.

<sup>134</sup> a) J. Zhou, Q. Liu, W. Feng, Y. Sun, F. Li, *Chem. Rev.* **2015**, *115*, 395–465. b) S. He, K. Krippes, S. Ritz, Z. Chen, A. Best, H.-J. Butt, V. Mailander, S. Wu, *Chem. Commun.* **2015**, *51*, 431–434.

<sup>135</sup> M. Irikura, Y. Tamaki, O. Ishitani, *Chem. Sci.* **2021**, *12*, 13888–13896.

<sup>136</sup> a) Y. Kuse, K. Ogawa, K. Tsuruma, M. Shimazawa, *Sci. Rep.* **2014**, *4*, 5223. b) K. Szaciłowski, W. Macyk, A. Drzewiecka-Matuszek, M. Brindell, G. Stochel, *Chem. Rev.* **2005**, *105*, 2647–2694.

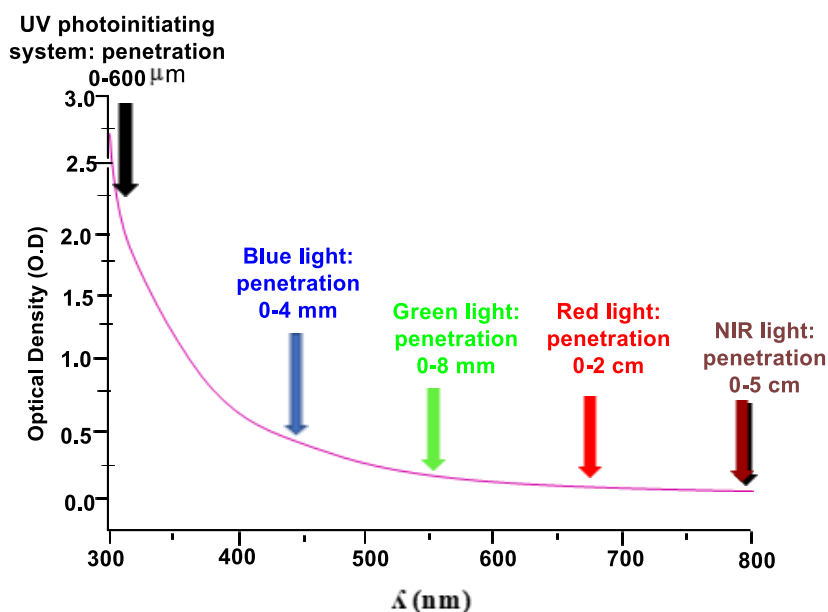


**Figure 4.1:** UV–vis diffusion of light for a polystyrene latex (112 nm of average diameter) and calculated penetrations of selected photons.<sup>133</sup>

Although NIR light has a higher penetration depth, its energy is usually too weak to trigger organic transformations compared to UV-visible light. For instance, the energy of the first excited-state of many visible-light-activated photocatalysts is in the range of 50 to 80 kcal/mol, which is usually enough to stimulate chemical transformations, whereas photoexcitation using NIR generates only about 35 kcal/mol, which is generally too low for chemical reactions.<sup>131</sup> Only few reports are available on direct NIR light photocatalysis and they are mainly on photoinduced radical polymerization. Nevertheless, there is a growing interest in the use of photon up-conversion (UC)<sup>137</sup> to solve this limitation. UC is a process that converts lower-energy photons to higher-energy photons. In the concept of NIR photocatalysis based on UC, the reaction mixture is irradiated with NIR light and once the light penetrates inside the medium, it would be converted into a more energetic photon such as blue light, which is capable of triggering the desired chemical transformation.<sup>131,138</sup> Up-conversion of low energy photon to higher energy photon can be achieved using different strategies including: upconverting nanoparticles (UCNPs),<sup>139</sup> two-photon absorption up-conversion (TPA-UC)<sup>140</sup> and triplet–triplet annihilation up-conversion (TTA-UC).<sup>131</sup> However, TTA-UC is considered the most attractive among these approaches due to its ability to work with incoherent incident light even at low intensities.<sup>141</sup>

<sup>137</sup> a) Q. Tian, W. Yao, W. Wu, C. Jianga, *Nanoscale Horiz.* **2019**, *4*, 10-25.

<sup>138</sup> a) M. Majek, U. Faltermeier, B. Dick, R. Pérez-Ruiz, A. Jacobi von Wangelin *Chem. Eur. J.* **2015**, *21*, 15496-15501. b) M. Häring, R. Pérez-Ruiz, A. J. von Wangelin, D. D. Díaz, *Chem. Commun.* **2015**, *51*, 16848-16851.

<sup>139</sup> a) X. Meng, H. Lu, Z. Li, C. Wang, R. Liu, X. Guana, Y. Yagci, *Polym. Chem.* **2019**, *10*, 5574-5577. b) B. Chen, F. Wang, *Inorg. Chem. Front.* **2020**, *7*, 1067-1081.

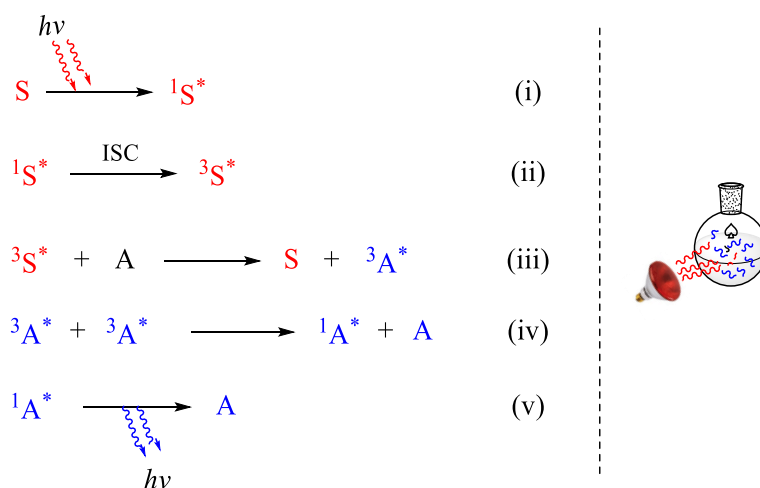
<sup>140</sup> C. Ye, L. Zhou, X. Wang, Z. Liang, *Phys. Chem. Chem. Phys.* **2016**, *18*, 10818-10835.

<sup>141</sup> P. Bharmoria, H. Bildirir, K. Moth-Poulsen, *Chem. Soc. Rev.* **2020**, *49*, 6529-6554.

## 2. Triplet–triplet annihilation upconversion (TTA-UC)

TTA-UC can be regarded as a bimolecular non-linear process involving two pairs of chromophores: a sensitizer (donor) and an annihilator (acceptor). A sensitizer is capable of absorbing low-energy photons such as NIR light and becomes excited to singlet ( $S_1$ ) state and then to triplet state ( $T_1$ ) through a spin-forbidden intersystem crossing (ISC). Sensitizers usually have a narrow singlet-triplet gap which permit easy triplet excitons by low-energy photons.<sup>142</sup> On the other hand, annihilator is a triplet energy accepting chromophore. Although it is not capable of absorbing low energy photons to become triplet excited, it can accept triplet energy from a triplet excited sensitizer usually through a Dexter-type energy transfer,<sup>142</sup> and can become triplet excited. Triplet excited annihilators can easily undergo self-quenching (annihilation) resulting in the release of photon of higher energy (Scheme 4.1).<sup>143,144,145</sup> TTA-UC has over the years been widely studied for its promising applications in photovoltaics, photodynamic therapy and drug release.<sup>146</sup>

TTA-UC up-conversion essentially involves five main steps (Scheme 4.1): (i) the sensitizer (donor) absorbs long wavelength light such as NIR light and becomes excited to singlet state ( $^1S^*$ ), (ii) intersystem crossing (ISC) from the  $^1S$  to a triplet state ( $^3T$ ), (iii) triplet–triplet energy transfer (TTET) from the triplet excited sensitizer to an annihilator (A) (iv) triplet–triplet annihilation (TTA) between two annihilator triplets ( $^3A^*$ ), resulting in a higher-energy singlet exciton on one of the annihilators ( $^1A^*$ ), (v) upconverted delayed fluorescence (emission of shorter wavelength such as blue light) by the decay of  $^1A^*$  to the ground state. This blue light emitted inside the reaction mixture for instance, can then be absorbed by a visible light photocatalyst present in the mixture for a normal visible light photoredox catalytic transformation.



**Scheme 4.1:** TTA-UC involving a sensitizer (**S**) and an annihilator (**A**).

<sup>142</sup> M. K. Manna, S. Shokri, G. P. Wiederrecht, D. J. Gosztola A. J.-L. Ayitou, *Chem. Commun.* **2018**, 54, 5809–5818.

<sup>143</sup> T. N. Singh-Rachford, F. N. Castellano, *Coord. Chem. Rev.* **2010**, 254, 2560–2573.

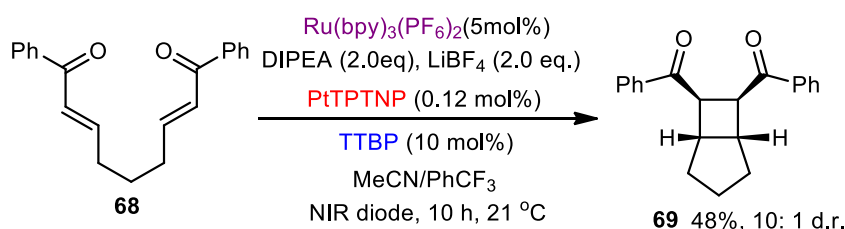
<sup>144</sup> a) N. Yanai, N. Kimizuka, *Chem. Commun.* **2016**, 52, 5354–5370. b) T. F. Schulze, T. W. Schmidt, *Energy Environ. Sci.* **2015**, 8, 103–125. c) Y. C. Simon, C. Weder, *J. Mater. Chem.* **2012**, 22, 20817–20830. d) N. Yanai, N. Kimizuka, *Chem. Commun.* **2016**, 52, 5354–5370.

<sup>145</sup> W. Wu, H. Guo, W. Wu, S. Ji, J. Zhao, *J. Org. Chem.* **2011**, 76, 7056–7064.

<sup>146</sup> J. Zhou, Q. Liu, W. Feng, Y. Sun, F. Li, *Chem. Rev.* **2015**, 115, 395–465.

### 3. TTA-UC from red/NIR light to blue light

The few reported sensitizer/annihilator pairs for TTA-UC of deep red/NIR light to blue light are highlighted in this section. Zhao and co-workers<sup>145</sup> in 2011 reported a novel TTA-UC from red (~618 nm) to blue light (~475 nm) using a boron-dipyrromethene (BODIPY) based sensitizer and 1-chloro-9,10-bis(phenylethynyl)anthracene (1CBPEA) as annihilator, with a quantum yield ( $\Phi_{UC}$ ) up to 6.1 % (Figure 4.2). This appeared to be the first all-organic sensitizer/annihilator for up-conversion of red light to blue light. However, there is no record on its application for photocatalysis yet. Castellano *et al.*,<sup>147</sup> has also shown that red-blue TTA-UC (635 nm to 475 nm) can be accomplished using Pt(II) *meso* tetraphenyltetraenzoporphyrin (PtPh<sub>4</sub>TBP) as sensitizer and perylene as an annihilator (Figure 4.2). A similar TTA-UC was equally reported by Monguzzi and co-workers<sup>148</sup> but using the palladium (II) complex (PdPh<sub>4</sub>TBP). A TTA-UC of NIR to blue light using Pt(II) tetraphenyltetranaphthoporphyrin (PtTPTNP) as sensitizer and tetraterbutylperylene (TTBP) as annihilator (Figure 4.3) was recently reported by Rovis group<sup>131</sup> where they demonstrated the usefulness of the technique in some photoredox catalysis including intramolecular [2+2] cyclization of diene **68** (Scheme 4.2); they showed the deeper penetration depth of the TTA-UC photocatalytic system in the reaction mixture which they carried out using a hemoglobin solution (0.2 mM) as a barrier, where the TTA-UC provided 48% of the desired product **69** whereas blue light delivered only 1% of the product under similar conditions.



**Scheme 4. 2:** Intramolecular [2+2] cyclization by TTA-UC using PTTPTNP as sensitizer, TTBP as annihilator and  $\text{Ru}(\text{bpy})_2(\text{PF}_6)_2$  as visible light photocatalyst.<sup>131</sup>

<sup>147</sup> T. N. Singh-Rachford, F. N. Castellano, *J. Phys. Chem. Lett.* **2010**, *1*, 195-200.

<sup>148</sup> S. Hoseinkhani, R. Tubino, F. Meinardi, A. Monguzzi, *Phys. Chem. Chem. Phys.* **2015**, *17*, 4020-4024.

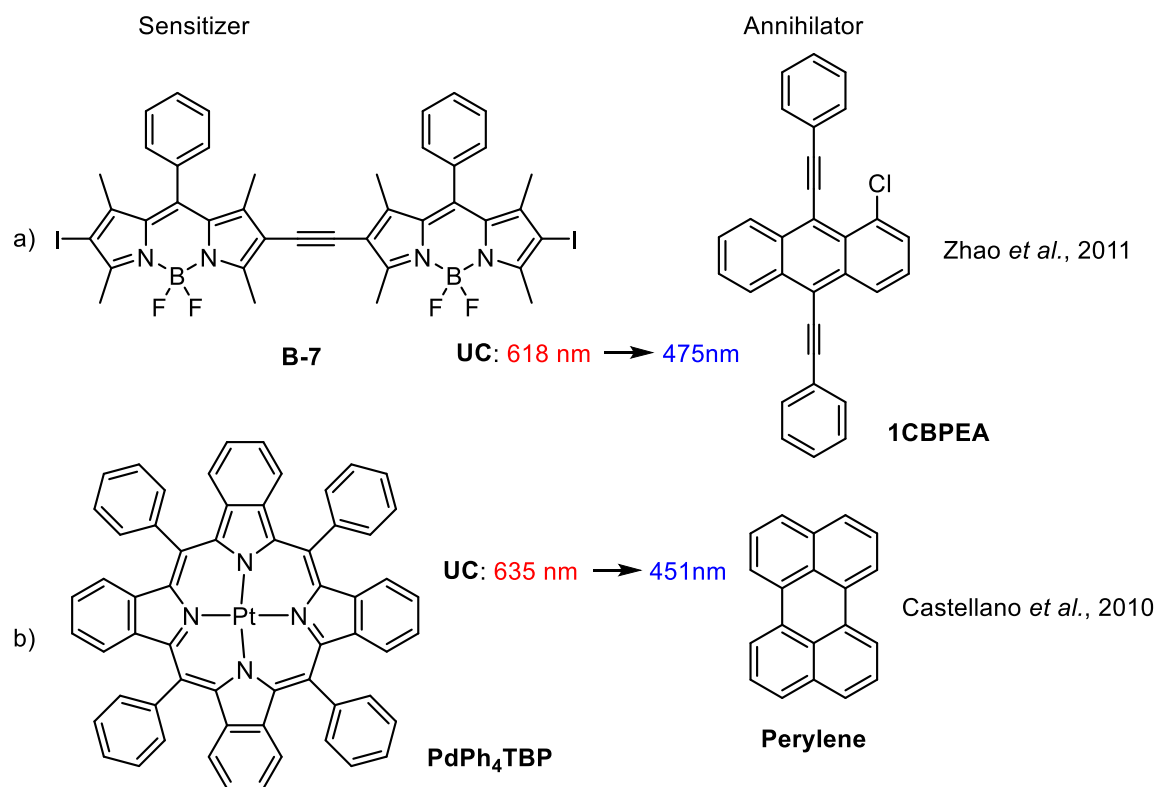


**Figure 4. 2:** Pairs of sensitizers and annihilators for up-conversion of NIR to blue light

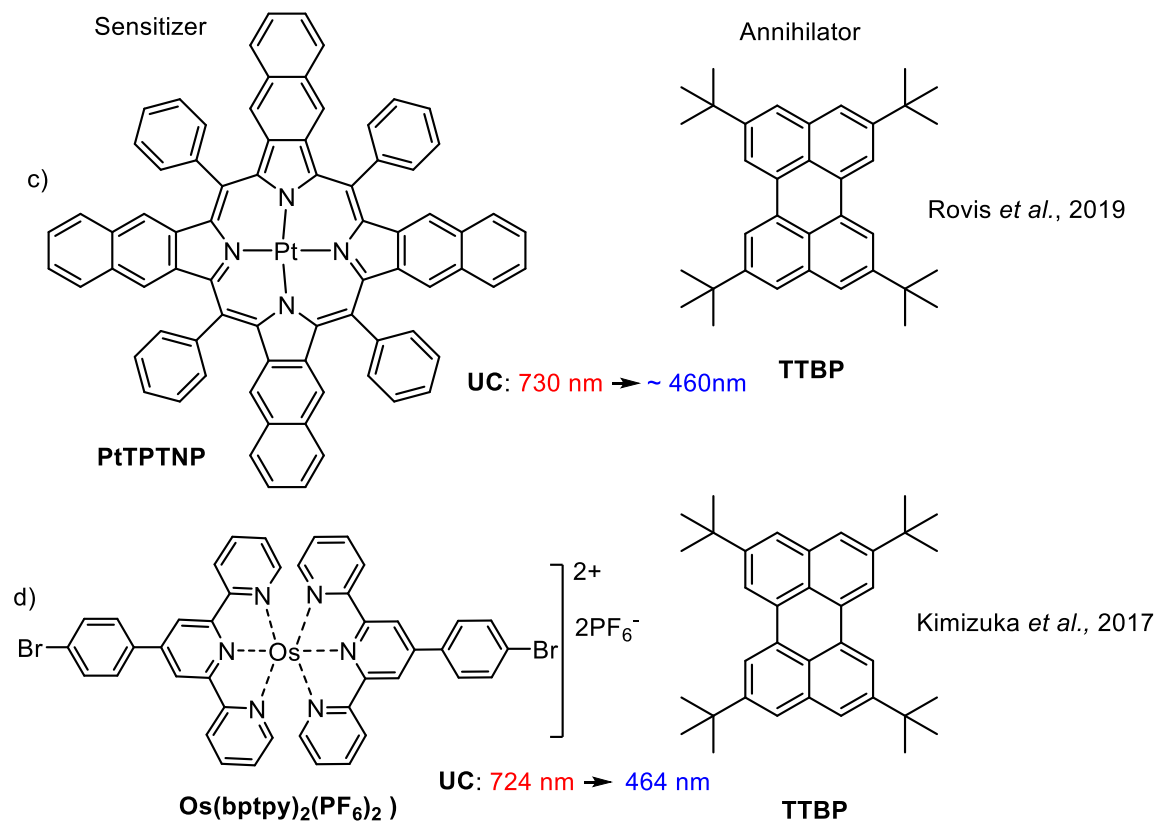


**Figure 4.3:** Pairs of sensitizers and annihilators for up-conversion of NIR to blue light.

Furthermore, Kimizuka and co-worker<sup>149</sup> in 2017 unveiled an Os(btpy)<sub>2</sub>(PF<sub>6</sub>)<sub>2</sub> based TTA-UC from NIR-to-blue light with a large anti-Stokes shift (0.97 eV) and quantum yield ( $\phi_{UC}$ ) = 2.7% (Figure 4.3). Interestingly, the authors showed that the up-conversion could be observed both in solution as well as when encapsulated in a poly(vinyl alcohol) (PVA) matrix, which is promising for photopolymerization. This TTA-UC strategy is based on direct excitation of sensitizer (Os(btpy)<sub>2</sub>(PF<sub>6</sub>)<sub>2</sub>) from singlet to triplet state (S→T), thereby avoiding energy loss during ISC. Energy loss during ISC of sensitizer has been identified as one of the major drawbacks in TTA-UC from red-blue light. This restricts the use of annihilators with large triplet and singlet energy gap, which ordinarily should favor high anti-Stokes shift.<sup>149</sup> Anti-Stokes shift is the difference in energy or wavelength between absorption peak and emission peak. The energy loss during ISC in a “classical” TTA-UC using Pd(II) porphyrin sensitizer is represented in Figure 4.4 as compared to direct singlet to triplet state transition (S→T) using Os(II) complex (Figure 4.5). Energy loss due to ISC is very significant at NIR region considering the low energy content of photon at that region.

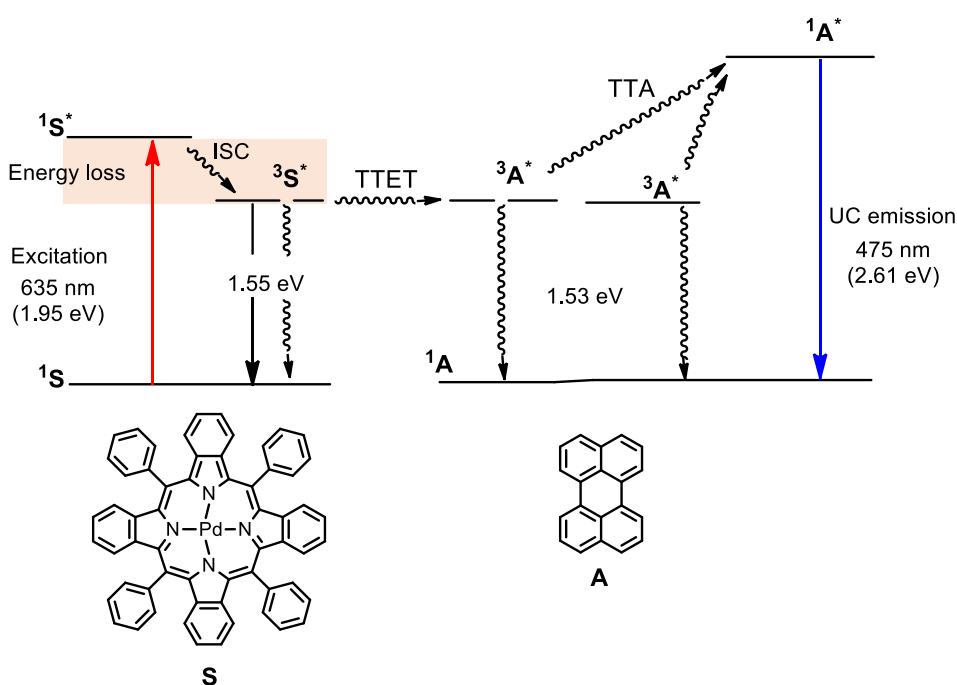


**Figure 4.4:** Energy diagram of the “classical” TTA-UC showing energy during ISC. Sensitizer (S): PdPh<sub>4</sub>TBP, annihilator (A): perylene

<sup>149</sup> a) Y. Sasaki, S. Amemori, H. Kouno, N. Yanai, N. Kimizuka, *J. Mater. Chem. C*, **2017**, *5*, 5063-5067. b) N. Yanai, N. Kimizuka, *Acc. Chem. Res.* **2017**, *50*, 2487-2495.

Direct population of triplet state from the ground state is a spin-forbidden transition; however, osmium (II) complexes display this unique ability due to its strong spin-orbit coupling associated with the presence of a heavy atom effect.<sup>135,150,151</sup> Os (II) complexes show triplet metal-to-ligand charge transfer (MLCT) absorption in the visible<sup>135</sup> and NIR region.<sup>149,152</sup> Nevertheless, excitation using longer wavelength tends to favor direct  $S_0 \rightarrow T_1$  transition more than  $S_0 \rightarrow S_1$  state and this is due to the fact that triplet excited state has lower energy than the singlet excited state.<sup>153</sup> Thus, osmium complexes exhibit high photoconversion efficiencies in the NIR region of electromagnetic radiation.<sup>149</sup> Although Fe(II)<sup>154</sup>, Ru (II)<sup>155</sup> and Ir(III)<sup>156</sup> can undergo  $S_0 \rightarrow T_1$  photoexcitation, their photoredox catalysis at NIR region is limited probably due to insignificant extinction coefficients. Anti-Stoke shift of up-converted NIR to blue light is presented in Figure 4.6.

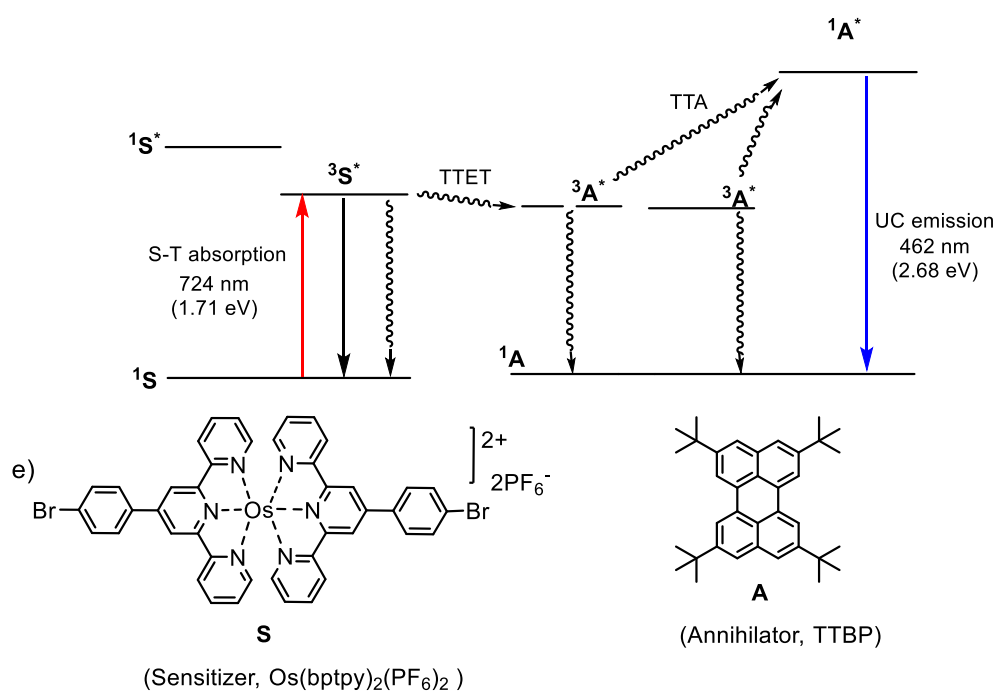


**Figure 4.5:** Energy diagram of TTA-UC based on the direct singlet to triplet absorption of  $\text{Os}(\text{btpy})_2(\text{PF}_6)_2$  as sensitizer (**S**) using TTET as annihilator (**A**)

- <sup>150</sup> a) S. Altobello, R. Argazzi, S. Caramori, C. Contado, S. Da Fre, P. Rubino, C. Chone, G. Larramona, C. A. Bignozzi, *J. Am. Chem. Soc.* **2005**, *127*, 15342-15343. b) T. Kinoshita, J. Fujisawa, J. Nakazaki, S. Uchida, T. Kubo, H. J. Segawa, *Phys. Chem. Lett.* **2012**, *3*, 394-398. c) D. Kuciauskas, M. S. Freund, H. B. Gray, J. R. Winkler, N. S. Lewis, *J. Phys. Chem. B* **2001**, *105*, 392-403. d) M. Alebbi, C. A. Bignozzi, T. A. Heimer, G. M. Hasselmann, G. J. Meyer, *J. Phys. Chem. B* **1998**, *102*, 7577-7581. e) X. Zhang, S. E. Canton, G. Smolentsev, C.-J. Wallentin, Y. Liu, Q. Kong, K. Attenkofer, A. B. Stickrath, M. W. Mara, L. X. Chen, K. Wärnmark, V. Sundström, *J. Am. Chem. Soc.* **2014**, *136*, 8804-8809.
- <sup>151</sup> a) S. Amemori, Y. Sasaki, N. Yanai and N. Kimizuka, *J. Am. Chem. Soc.* **2016**, *138*, 8702-8705. b) P. P. Laine, F. Bedioui, F. Loiseau, C. Chiorboli and S. Campagna, *J. Am. Chem. Soc.* **2006**, *128*, 7510-7521.
- <sup>152</sup> a) J.-P. Sauvage, J.-P. Collin, J.-C. Chambron, S. Guillerez, C. Coudret, V. Balzani, F. Barigelletti, L. De Cola L. Flamigni, *Chem. Rev.* **1994**, *94*, 993-1019. b) Y. Imamura, M. Kamiya, T. Nakajima, *Chem. Phys. Lett.* **2016**, *648*, 60-65.
- <sup>153</sup> M. Nakajima, S. Nagasawa, K. Matsumoto, T. Kuribara, A. Muranaka, M. Uchiyama, T. Nemoto, *Angew. Chem. Int. Ed.* **2020**, *59*, 6847-6852.
- <sup>154</sup> A. B. Maurer, G. J. Meyer, *J. Am. Chem. Soc.* **2020**, *142*, 6847-6851.
- <sup>155</sup> D. W. Thompson, A. Ito, T. J. Meyer, *Pure Appl. Chem.* **2013**, *85*, 1257-1305.
- <sup>156</sup> T. Hofbeck, H. Yersin, *Inorg. Chem.* **2010**, *49*, 9290-9299.

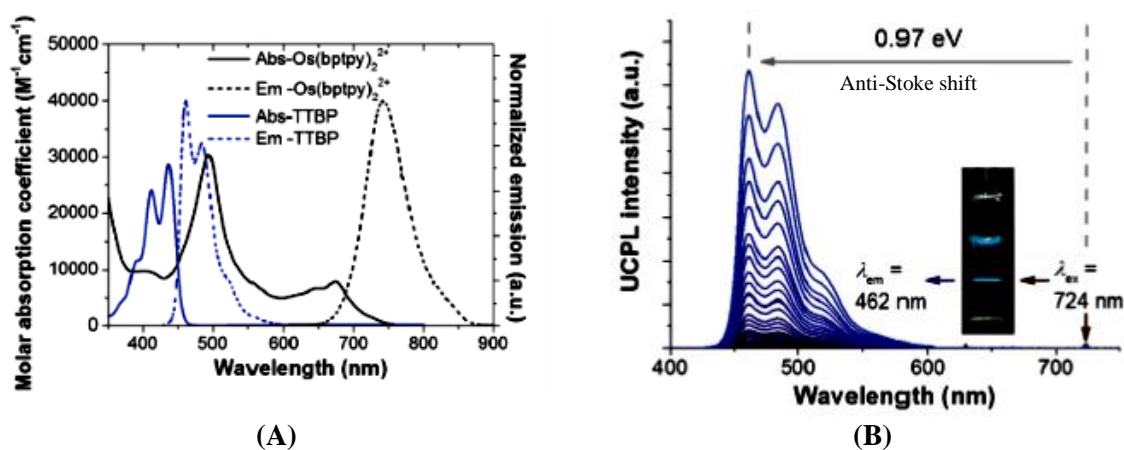


**Figure 4.6:** (A) Absorption and photoluminescence spectra<sup>149</sup> of  $\text{Os}(\text{btpy})_2(\text{PF}_6)_2$  and TTBP in DMF. (B) Photoluminescence spectra of  $\text{Os}(\text{btpy})_2(\text{PF}_6)_2$  and TTBP (2 mM) in deuterated DMF

#### 4. Direct red/NIR light photocatalysis

There are some reports where deep red/NIR light (655–850 nm) have been applied directly for photocatalysis despite their relatively low energy content compared to UV-visible light. As mentioned earlier, most of reported work in this area are mainly on photoinduced radical polymerization. Some of them are highlighted in this section.

##### 4.1. Metalloporphyrins as direct NIR photocatalyst

Direct NIR light photoinduced radical polymerization has been reported by different research groups using metalloporphyrins as photocatalysts. Boyer *et al*<sup>157</sup> in 2015 showed that ZnTPP could serve as a competent photocatalyst for electron transfer–reversible addition–fragmentation chain transfer (PET-RAFT) polymerization of styrene, (meth)acrylates and (meth)acrylamides under deep red light (655 nm) irradiation, leveraging its weak Q-band around 600 nm (Figure 4.7).<sup>157,158</sup> Recently, Lalevée and co-workers<sup>159</sup> equally presented a direct NIR light initiated free radical polymerization of methacrylate resin using a series of metalloporphyrins including FeTPP, ZnTPP-2 and ZnTPP-4 (Figure 4.7). These photocatalysts mediated the free radical polymerization despite their weak absorption at the NIR region.

<sup>157</sup> S. Shanmugam, J. Xu, C. Boyer, *J. Am. Chem. Soc.* **2015**, *137*, 9174–9185.

<sup>158</sup> a) K. A. Nguyen, P. N. Day, R. Pachter, S. Tretiak, V. Chernyak, S. Mukamel, *J. Phys. Chem. A* **2002**, *106*, 10285–10293. (b) M.M. El-Nahass, H.M. Zeyada, M. S. Aziz, M. M. Makhlof, *Spectrochim. Acta A Mol. Biomol. Spectrosc.* **2005**, *62*, 11-15.

<sup>159</sup> G. Noirbent, Y. Xu, A.-H. Bonardi, D. Gigmes, J. Lalevée, F. Dumur, *Eur. Polym. J.* **2020**, *139*, 110019.

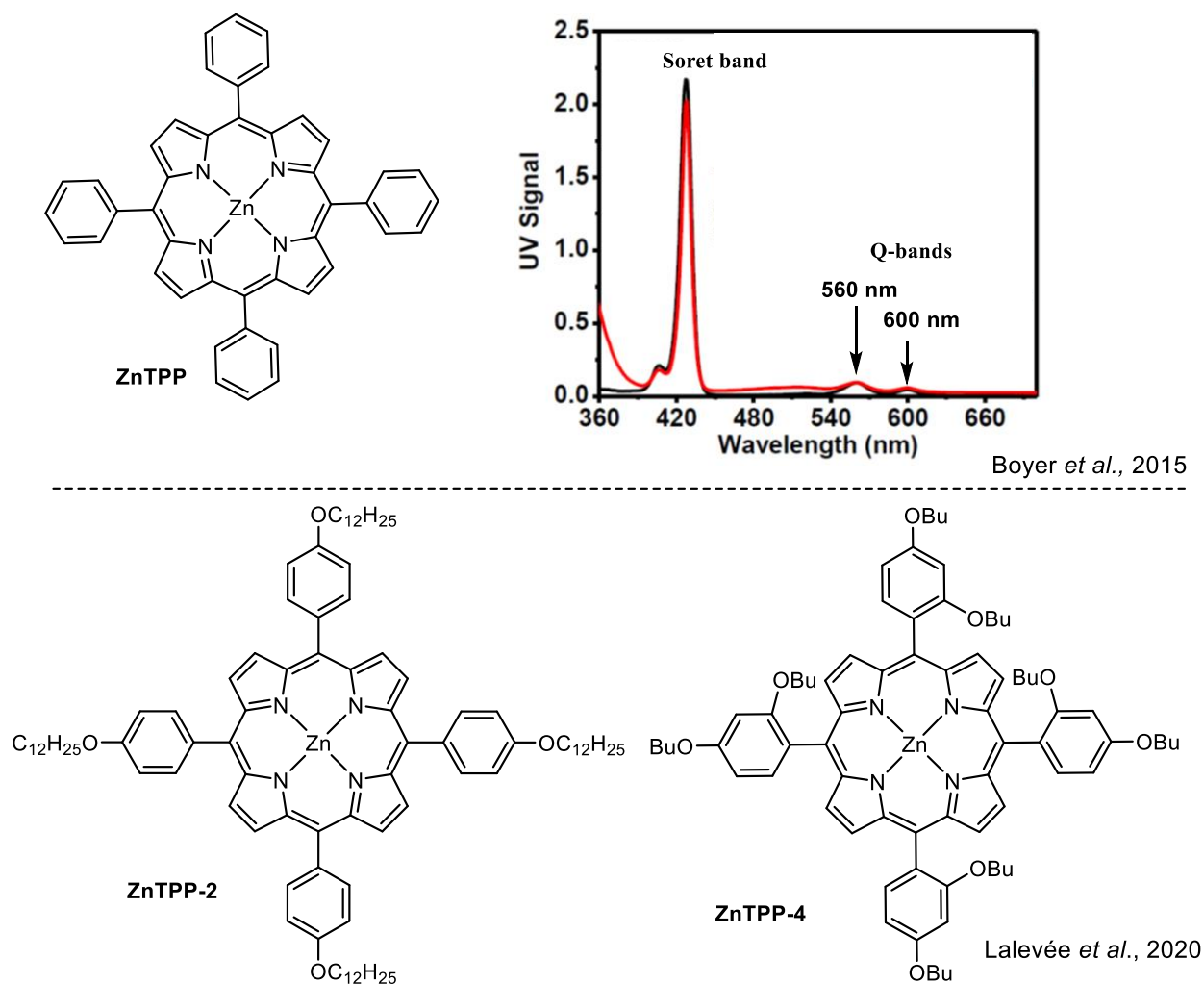


**Figure 4.7:** Metalloporphyrins as photocatalysts for direct NIR initiated free radical polymerization.

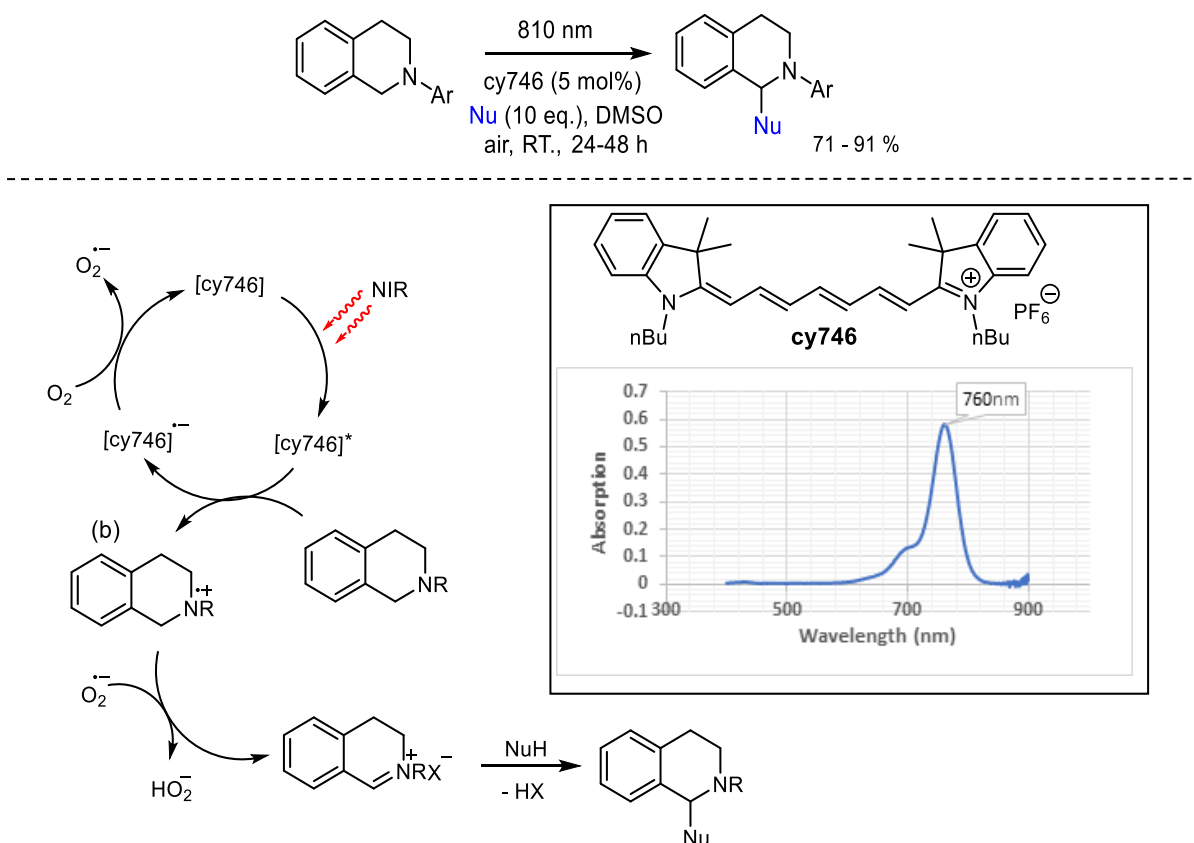
## 4.2. Indocyanine dye as NIR photocatalyst

Recently Goddard *et al.*<sup>160</sup> reported a direct NIR light (810 nm) organic photoredox catalysis using indocyanine dye as the photocatalyst (Scheme 4.2). They demonstrated that the procedure was efficient for some photoredox reactions including aza-Henry reaction and oxidation of boronic acids. Based on Stern-Volmer quenching experiments, the authors proposed single electron transfer pathway involving molecular oxygen as an oxidant for the aza-Henry reaction and for boronic acid oxidation, they suggested energy transfer *via* photosensitization. However, a short excited state lifetime of 1.2 ns was reported for the catalyst<sup>161</sup>. Meanwhile there are few other reports on NIR polymerization using cyanine dyes as photoinitiators.<sup>162</sup>

<sup>160</sup> A. R. O. Kosso, N. Sellet, A. Baralle, M. Cormier, J.-P. Goddard, *Chem. Sci.* **2021**, *12*, 6964-6968.

<sup>161</sup> J. K. G. Karlsson, O. Woodford, H. Mustroph, A. Harriman, *Photochem. Photobiol. Sci.* **2018**, *17*, 99-106.

<sup>162</sup> a) B. Strehmel, C. Schmitz, C. Kütahya, C. Kütahya, Y. Pang, A. Drewitz, H. Mustroph, *Beilstein J. Org. Chem.* **2020**, *16*, 415-444. b) A. H. Bonardi, F. Dumur, T. M. Grant, G. Noirbent, D. Gigmes, B. H. Lessard, J.-P. Fouassier, J. Lalevée, *Macromolecules*, **2018**, *51*, 1314-1324. c) T. Brömme, C. Schmitz, D. Oprych, A. Wenda, V. Strehmel, M. Grabolle, U. Resh-Genger, S. Ernt, D. Keil, P. Lüs, H. Baumann, B. Strehmel, *Chem. Eng. Technol.* **2016**, *39*, 13-25. d) B. Strehmel, C. Schmitz, K. Cremanns, J. Göttert, *Chem. Eur. J.* **2019**, *25*, 12855-12864.



**Scheme 4.2:** Direct NIR photoredox catalysis for aza-Henry reaction using 1,1'-dibutyl-3,3,3',3'-tetramethylindotricarbocyanine hexafluorophosphate (cy746) as photocatalyst.

## 5. Urethanes synthesis by NIR-mediated decarboxylation of oxamic acids

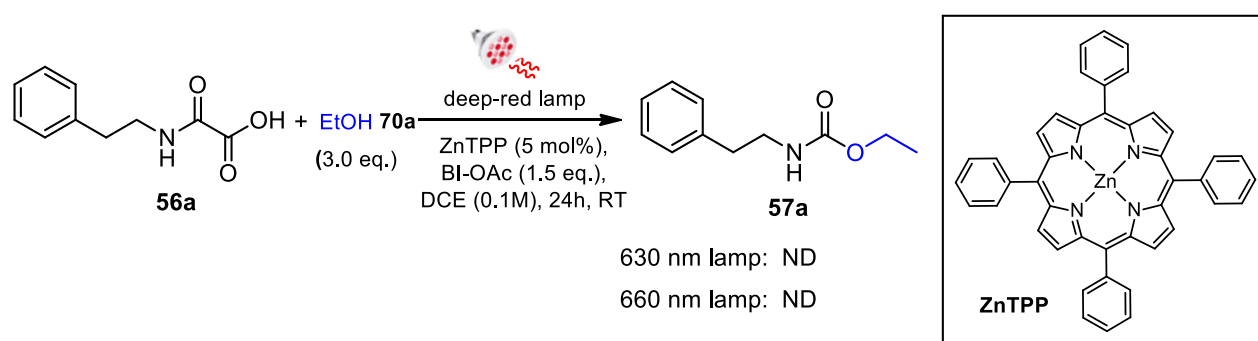
As mentioned earlier, there is a growing interest in NIR photocatalysis due to its deeper penetration depth, which is beneficial for large scale photochemical reaction and photopolymerization compared to UV-visible light photocatalysis.<sup>130,131</sup> The visible light-mediated decarboxylation of oxamic acids for urethane synthesis recently developed by our group was shown to be efficient for urethane synthesis using mono-oxamic acids. However, extension of this greener procedure to polyurethane (PUs) synthesis was less efficient as the molecular weights of PUs obtained were generally low compared to classic route. We envisioned that developing a system that would use NIR light could improve the new non-phosgene route to polyurethanes taking advantage of the deeper penetration depth of NIR light. This could also facilitate performing the photopolymerization using bulk method, a strategy that is promising for improved molecular weight.

Thus, we sought to develop a NIR photoredox catalytic system for the urethane synthesis from oxamic acids. According to literature precedence, NIR light can be used directly for photoredox catalysis; certain photocatalysts can absorb NIR light to access the redox active excited state, which can mediate redox transformations.<sup>160</sup> Also, NIR light photoredox catalysis can be achieved using triplet fusion up-conversion.<sup>131</sup> In this project, different deep-red to NIR light based photoredox catalysis, both by direct activation and triplet fusion up-conversion were investigated for their ability to mediate urethane synthesis from oxamic acids and these attempts are presented in this section.

## 5.1 Urethane synthesis from oxamic acids by direct red/NIR light photocatalysis

### 5.1.1. Urethane synthesis from oxamic acids using ZnTPP as a photocatalyst

As discussed earlier, zinc *meso*-tetraphenylporphyrin (ZnTPP) has been reported as an efficient photocatalyst for photoinitiated electron transfer-reversible addition-fragmentation chain transfer (PET-RAFT) polymerization under deep-red light irradiation,<sup>157</sup> leveraging its Q-band absorption around 630 nm (Figure 4.7). We tried this photocatalyst to mediate the urethane synthesis from oxamic acid **56a** under deep red irradiation (Scheme 4.3). However, the expected product **57a** was not observed, oxamic acid remaining unconverted when irradiated at 630 or 660 nm, and this probably could be due to short lifetime of the triplet excited state of the photocatalyst, which was shown to be around 2.7 ns.<sup>163</sup> The longer a photocatalyst stays in its redox active excited state the higher the probability of it mediating a redox transformation.



**Scheme 4.3:** Urethane synthesis from oxamic acids under deep-red irradiation using ZnTPP as photocatalyst ( $\lambda_{\max} = 630$  nm,  $E_{\text{ox}}^*(\text{ZnTPP}^*/\text{ZnTPP}^{+\bullet}) = -1.32$  V,  $E_{\text{ox}}(\text{ZnTPP}/\text{ZnTPP}^{+\bullet}) = +0.75$  V).

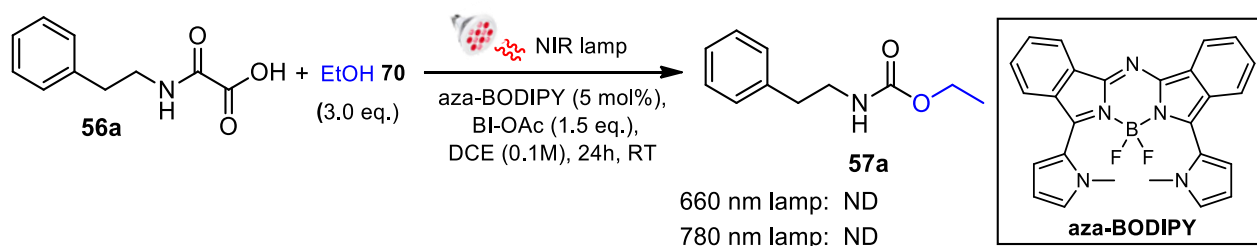
### 5.2.2. Urethane synthesis from oxamic acids using aza-BODIPY as a photocatalyst

Aza-BODIPY dyes (ABP) with heterocyclic substituents including N-methyl pyrrole displays a remarkable molar extinction coefficient in the NIR region and are promising for solar energy harvesting in the NIR region.<sup>164</sup> Although, there is no report on its application in photoredox catalysis, but looking at its redox potential ( $\lambda_{\max} = 762$  nm,  $E_{\text{ox}}^*(\text{ABP}^*/\text{ABP}^{+\bullet}) = -1.04$  V,  $E_{\text{ox}}(\text{ABP}/\text{ABP}^{+\bullet}) = +0.50$  V), it is a good reductant at excited state. As proposed in our visible light mediated procedure, oxamic acid decarboxylation probably proceeds *via* an oxidative quenching of photoexcited catalyst by an oxamic acid-BI-OAc adduct (*vide infra*),<sup>120</sup> though the redox potential of this adduct has not been well established. We tried the photocatalyst in our system to know if it could mediate the decarboxylation of oxamic acids using NIR light (660 – 780 nm) (Scheme 4.4). However, the reaction was not successful as oxamic acids remained unconverted and no other product was observed in the reaction mixture. Complete discoloration of the photocatalyst was observed at the

<sup>163</sup> A. Harriman, *J. Chem. Soc., Faraday Trans. 1*, **1981**, 77, 369-377.

<sup>164</sup> T.-Y. Li, T. Meyer, R. Meerheim, M. Hoppner, C. Korner, K. Vandewal, O. Zeika, K. Leo, *J. Mater. Chem. A*, **2017**, 5, 10696-10703.

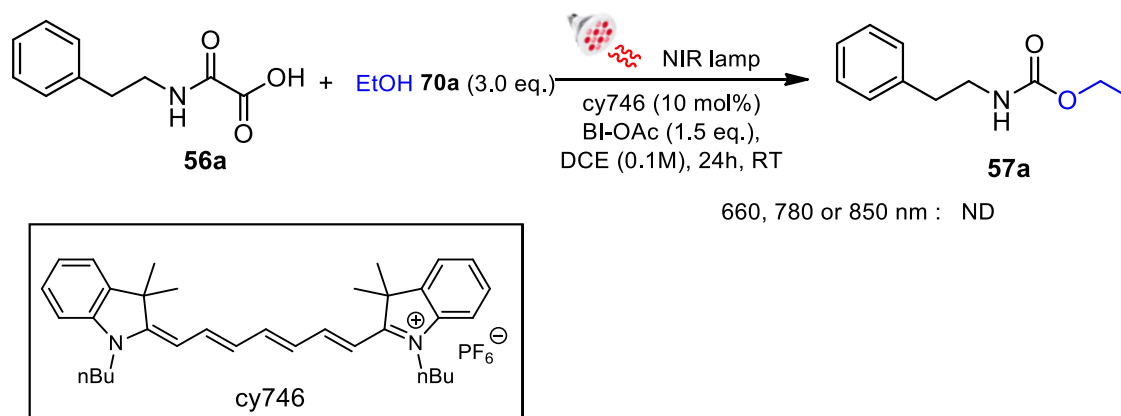
end of the reaction, suggesting that the catalyst was not stable under the reaction conditions, possibly due to the oxidation of the electron-rich pyrrole system by BI-OAc.



**Scheme 4.4:** Urethane synthesis from oxamic acids using aza-BODIPY as photocatalyst

### 5.2.3. Urethane synthesis from oxamic acids using indocyanine dye as a photocatalyst

As discussed earlier, indocyanine dye cy746 (CAS: 134339-08-5) has been reported as efficient direct NIR photocatalyst for some photoredox transformations.<sup>160</sup> We equally tried this photocatalyst to activate the oxidative decarboxylation of oxamic acid **56a** for urethane synthesis under NIR conditions (Scheme 4.5). The expected product did not form, the starting oxamic acid remaining unconverted whatever the wavelength (660, 780 or 850 nm) and no other side product was detected. The lifetime of triplet-excited state of this catalyst was shown to be about 1.0 ns,<sup>152,161</sup> which may be the limiting factor to its catalytic activity in this reaction.



**Scheme 4.5:** (a) Urethane synthesis from oxamic acids using indocyanine dye as photocatalyst (b) cy746 ( $\lambda_{\max} = 760$  nm).<sup>160</sup>

## 5.2. Towards triplet-triplet annihilation up-conversion (TTA-UC)

As discussed earlier, TTA-UC is another strategy by which NIR light photoredox catalysis can be achieved. In this case, the reaction mixture is irradiated with NIR light taking advantage of its deep penetration depth, and once the light gets inside the reaction mixture it would be up-converted to higher energy photon such as blue light capable of triggering a chemical transformation in the presence of normal visible light photocatalyst.<sup>131</sup> In this work, some NIR-blue light TTA-UC

strategies reported in the literature were tried for the urethane synthesis from oxamic acids under NIR light irradiation and such efforts are discussed in this section.

### 5.2.1. Towards urethane synthesis from oxamic acids by TTA-UC using methylene blue as sensitizer and tetracene as annihilator

Methylene blue (MB) is a sensitizer with a strong absorption in the red to NIR regions.<sup>165</sup> In this study, we imagined that this dye could serve as a competent photosensitizer in combination with tetracene as an annihilator, to achieve a NIR-blue TTA-UC based photoredox catalysis for the synthesis of urethane from oxamic acids (Scheme 4.6). Among the factors considered in the choice of sensitizer/annihilator pair for TTA-UC is that, the triplet excited sensitizer must have a higher energy level ( $E_T$ ) than that of the annihilator excited triplet state.<sup>166</sup> Looking at the energy of the triplet state of MB ( $\lambda_{\max} = 660 \text{ nm}$ ;  $S_0 \rightarrow S_1 = 1.83 \text{ eV}$  and  $S_0 \rightarrow T_1 = 1.44 \text{ eV}$  for a  $\tau_T$  (triplet state lifetime) = 77  $\mu\text{s}$ ) and that of tetracene ( $S_0 \rightarrow T_1 = 1.25 \text{ eV}$  for a  $\tau_T$  (triplet state lifetime) = 63 ms), it appeared that they have the prospect to mediated the desired red  $\rightarrow$  blue up-conversion (Figure 4.8).

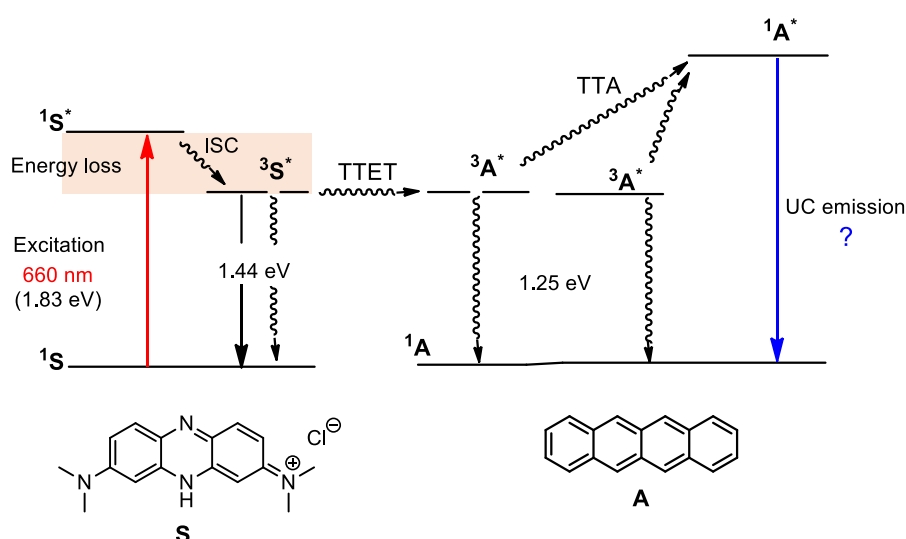


**Figure 4.8:** Energy diagram of expected TTA-UC methylene blue as sensitizer and tetracene as annihilator

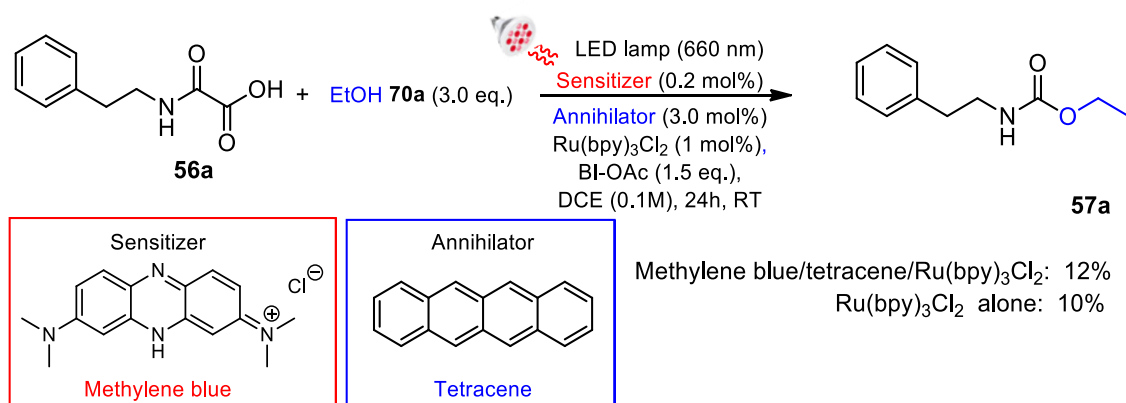
However, the reaction was not successful. A control experiment showed that the little amount of urethane observed in the reaction mixture was largely due to the presence of  $\text{Ru}(\text{bpy})_3\text{Cl}_2$ .  $\text{Ru}(\text{bpy})_3\text{Cl}_2$  works efficiently as a visible light photocatalyst for urethane synthesis from oxamic acids under blue light irradiation.<sup>167</sup> Nevertheless, it was also observed that it showed little activity towards the reaction under deep-red light (660 nm) irradiation, and this could be as a result of

<sup>165</sup> R. W. Redmond, J. N. Gamlin, *Photochem. Photobiol.* **1999**, 70, 391-475.

<sup>166</sup> a) T. N. Singh-Rachford, F. N. Castellano, *Coord. Chem. Rev.* **2010**, 254, 2560-2573. b) J. Zhu, Q. Liu, W. Feng, Y. Sun, F. Li *Chem. Rev.* **2015**, 115, 395 – 465.

<sup>167</sup> G. G. Pawar, F. Robert, E. Grau, H. Cramail, Y. Landais, *Chem. Commun.* **2018**, 54, 9337 - 9340.

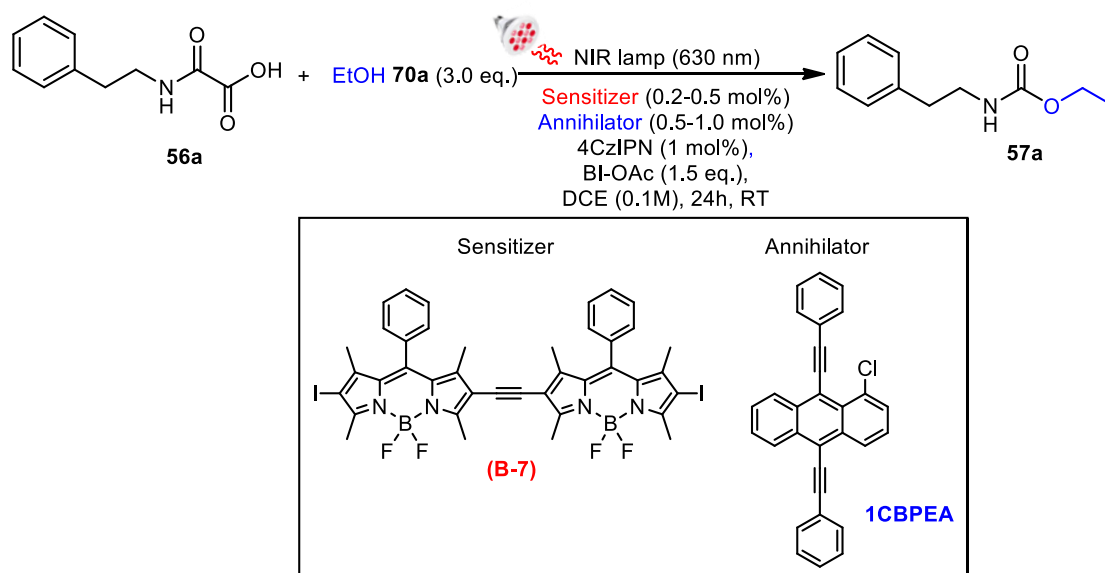
somewhat activation by the tail end lamp emission; Ru(bpy)<sub>3</sub>Cl<sub>2</sub> absorption band extends up to 553 nm (Figure S6).



**Scheme 4.6:** Urethane synthesis from oxamic acids using methylene blue as sensitizer and tetracene as annihilator.

### 5.2.2. Towards urethane synthesis from oxamic acids by TTA-UC using BODIPY as sensitizer and ICBPEA as an annihilator

We also tried BODIPY (B-7) as a sensitizer and 1-Chloro-9,10-bis(phenylethynyl)anthracene (ICBPEA) as annihilator as reported by Zhao *et al.*,<sup>145</sup> using some selected visible light photocatalysts (Scheme 4.7). The B-7 ( $\lambda_{\text{max}} = 629$  nm,  $S_0 \rightarrow T_1 = 1.43$  eV,  $\tau_T = 66.3$   $\mu\text{s}$ ) and ICBPEA ( $S_0 \rightarrow T_1 = 1.20$  eV), satisfied the triplet energy requirements for TTA-UC.<sup>166</sup> As mentioned earlier, Zhao and co-workers<sup>145</sup> reported a significant red-blue up-conversion for this pair of chromophores with quantum yield of ( $\Phi_{\text{UC}}$ ) up to 6.1% and anti-Stokes shift of about 0.56 eV both in solution and in a polymer films. However, this TTA-UC strategy was not successful in our reaction; oxamic acid remained unconverted in most cases. Urethane was not detected in the reaction mixture except when Ru(bpy)<sub>3</sub>Cl<sub>2</sub> or AcrMes<sup>+</sup>ClO<sub>4</sub><sup>-</sup> were used as visible light photocatalyst component, where their little-known activities at deep-red light was also observed, resulting in traces of urethane (Scheme 4.7). Furthermore, there was a discoloration of the reaction mixture, from bluish to yellowish/purplish at the end of the reaction, indicating that the B-7 was probably not stable under the reaction condition. B-7 is originally blue in color.



Entry <sup>a</sup>	PC	Yield <sup>b</sup> (%)
1	B-7/1CBPEA/4CzIPN	ND
2 <sup>c</sup>	B-7/1CBPEA/4CzIPN	ND
3	B-7/1CBPEA/AcrMes <sup>+</sup> ClO <sub>4</sub> <sup>-</sup>	ND
4 <sup>d</sup>	B-7/1CBPEA/AcrMes <sup>+</sup> ClO <sub>4</sub> <sup>-</sup>	ND
5	B-7/1CBPEA/Ru(bpy) <sub>3</sub> Cl <sub>2</sub>	5
6	Ru(bpy) <sub>3</sub> Cl <sub>2</sub>	15
7	4CzIPN	ND

**Scheme 4.7:** <sup>a</sup> Urethane synthesis from oxamic acids using BODIPY B-7 as sensitizer and 1CBPEA as annihilator. <sup>b</sup> Yields of **57a** determined by <sup>1</sup>H NMR with 1,3,5-trimethylbenzene as an external standard. <sup>c</sup> Reaction using 0.5 mol% sensitizer and 1.0 mol% annihilator. <sup>d</sup> Reaction mixture degassed by freeze-pump-thaw technique.

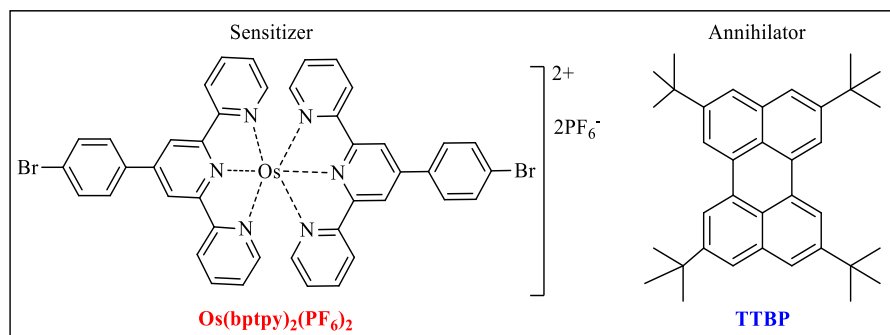
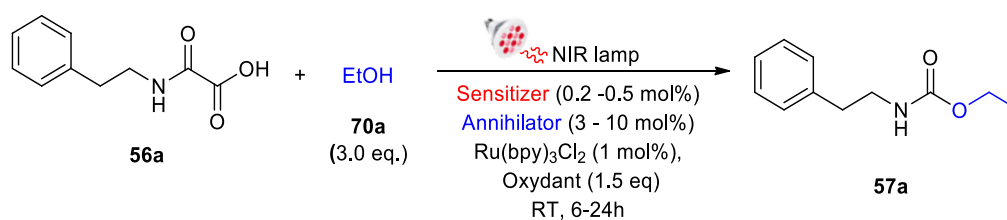
### 5.2.3. Towards urethane synthesis from oxamic acids by TTA-UC using Os(bptpy)<sub>2</sub>(PF<sub>6</sub>)<sub>2</sub> as sensitizer and TTBP as an annihilator

Attempts were also made to achieve a TTA-UC from NIR to blue light for the urethane synthesis from oxamic acids using osmium terpyridine [Os(bptpy)<sub>2</sub>(PF<sub>6</sub>)<sub>2</sub>] as a sensitizer and TTBP as annihilator as reported by Kimizuka *et al.*<sup>149</sup> (Scheme 4.8). We started by applying this pair of chromophores for the reaction using Ru(bpy)<sub>3</sub>Cl<sub>2</sub> as a visible light photocatalyst component ( $\lambda_{\max}$  452 nm). Gratifyingly 88% conversion was observed with 82% urethane isolated (Table 1, entry 1). Replacing Ru(bpy)<sub>3</sub>Cl<sub>2</sub> with other visible light photocatalysts such as 4CzIPN or AcrMes<sup>+</sup>ClO<sub>4</sub><sup>-</sup> resulted in lower urethane yield (entry 2-3). PIDA as an oxidant instead of BI-OAc was less efficient (entry 4). However, some control experiments (entry 5-8) showed that neither the presence of annihilator nor visible light photocatalyst was important for the reaction. Interestingly, the reaction proceeded even more efficiently with the Os(bptpy)<sub>2</sub>(PF<sub>6</sub>)<sub>2</sub> alone, furnishing the corresponding urethane in an excellent yield (entry 9). This makes the reaction even simpler. Rovis and co-

workers<sup>168</sup> recently reported a similar observation where they used the osmium (II) terpyridine catalyst to achieve some photoredox catalyzed reactions under NIR light irradiation. Further optimization studies also showed that no urethane was observed in the absence of the osmium (II) catalyst (entry 10), light (entry 11) or BI-OAc (entry 12), indicating that each of these components was essential for the transformation. The reaction still worked efficiently even with catalyst loading as low as 0.3 mol% (entry 13). With a longer wavelength NIR lamp ( $\lambda_{\text{max}} = 780$  nm), the procedure still delivered the urethane in moderate yield, 60% (entry 14). In this case, although the absorption band of Os(btpy)<sub>2</sub>(PF<sub>6</sub>)<sub>2</sub> extended only to 724 nm (Figure S7), the emission spectrum of the lamp was between 700 to 860 nm, which still allowed the photocatalyst to be activated by the tail end of the spectrum (Figure S10). With blue LED lamp (450 nm) urethane was also observed in a moderate 75% yield (Entry 15) and this can be explained by the fact that Os(II) terpyridine is also panchromatic; it absorbs strongly at all wavelength of visible light, generating the same triplet lowest excited state.<sup>135</sup> With 1.0 eq. of BI-OAc, 89% urethane was obtained (entry 16). Finally, reducing the reaction time to 6 h still led to 90 % urethane conversion (entry 17). Just as with our visible light procedure, the reaction did not work efficiently with CH<sub>3</sub>CN as a solvent (entry 18).

---

<sup>168</sup> B. D. Ravetz, N. E. S. Tay, C. L. Joe, M. Sezen-Edmonds, M.A. Schmidt, Y. Tan, J. M. Janey, M.D. Eastgate, T. Rovis, *ACS Cent. Sci.* **2020**, *6*, 2053-2059.



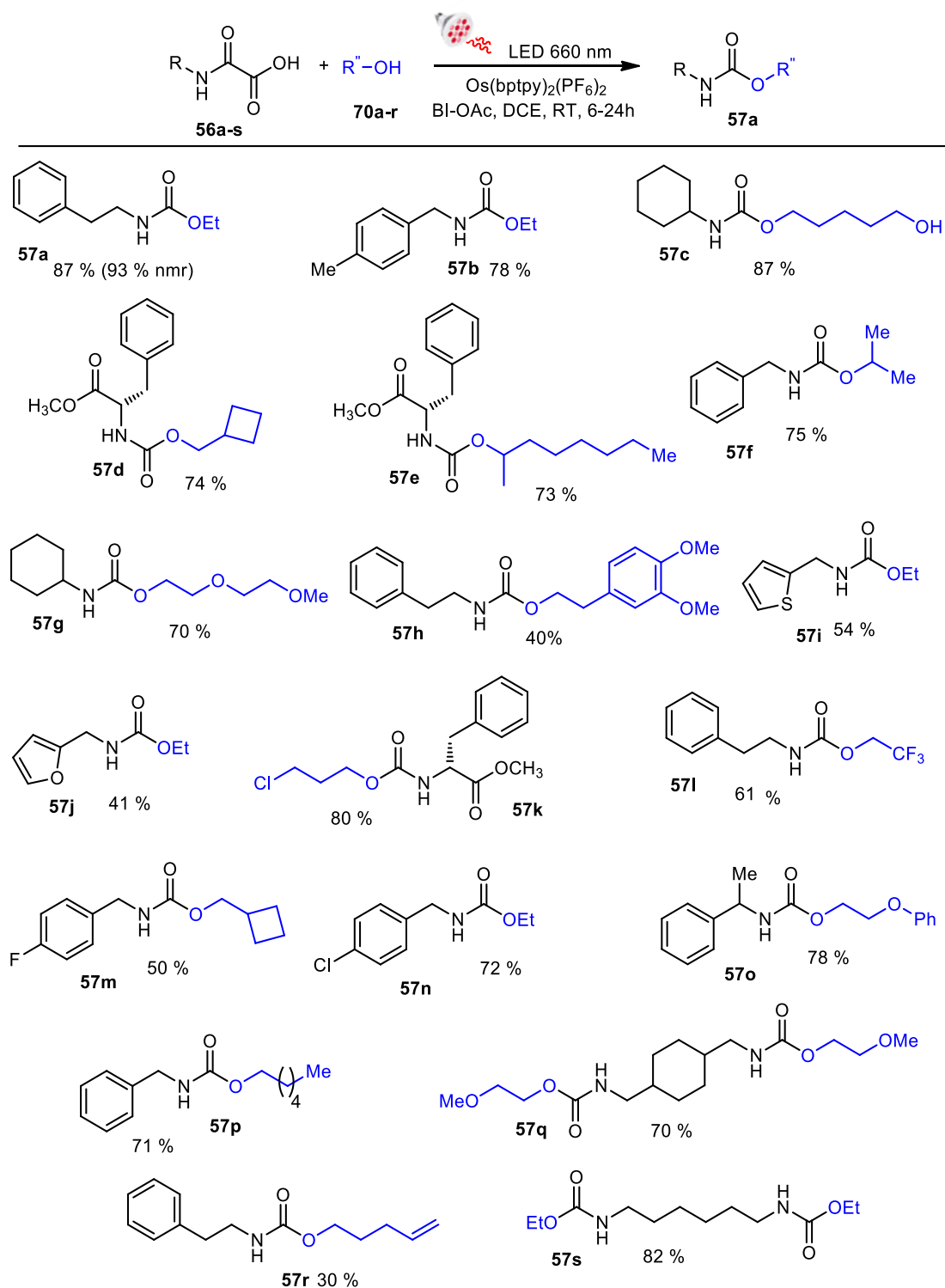
Entry <sup>a</sup>	PC	Oxidant (1.5 eq.)	Time (h)	Solvent (0.1 M)	Yield <sup>b</sup> (%)
1	Os(btpy) <sub>2</sub> (PF <sub>6</sub> ) <sub>2</sub> / TTBP / Ru(bpy) <sub>3</sub> Cl <sub>2</sub>	BI-OAc	24	DCE	88 (82)
2	Os(btpy) <sub>2</sub> (PF <sub>6</sub> ) <sub>2</sub> / TTBP / 4C <sub>2</sub> IPN	BI-OAc	24	DCE	42
3 <sup>c</sup>	Os(btpy) <sub>2</sub> (PF <sub>6</sub> ) <sub>2</sub> / TTBP / AcrMes <sup>+</sup> ClO <sub>4</sub> <sup>-</sup>	BI-OAc	24	DCE	80
4	Os(btpy) <sub>2</sub> (PF <sub>6</sub> ) <sub>2</sub> / TTBP / Ru(bpy) <sub>3</sub> Cl <sub>2</sub>	PIDA	24	DCE	64
5	Os(btpy) <sub>2</sub> (PF <sub>6</sub> ) <sub>2</sub> / AcrMes <sup>+</sup> ClO <sub>4</sub> <sup>-</sup> (2)	BI-OAc	24	DCE	77
6	Os(btpy) <sub>2</sub> (PF <sub>6</sub> ) <sub>2</sub> / Ru(bpy) <sub>3</sub> Cl <sub>2</sub>	BI-OAc	24	DCE	78
7	Ru(bpy) <sub>3</sub> Cl <sub>2</sub>	BI-OAc	24	DCE	09
8	TTBP	BI-OAc	24	DCE	ND
9	Os(btpy) <sub>2</sub> (PF <sub>6</sub> ) <sub>2</sub> (0.5)	BI-OAc	24	DCE	95 (87)
10	-	BI-OAc	24	DCE	ND
11 <sup>f</sup>	Os(btpy) <sub>2</sub> (PF <sub>6</sub> ) <sub>2</sub>	BI-OAc	24	DCE	ND
12	Os(btpy) <sub>2</sub> (PF <sub>6</sub> ) <sub>2</sub>	-	24	DCE	ND
13	Os(btpy) <sub>2</sub> (PF <sub>6</sub> ) <sub>2</sub> (0.3)	BI-OAc	24	DCE	93 (87)
14 <sup>d</sup>	Os(btpy) <sub>2</sub> (PF <sub>6</sub> ) <sub>2</sub> (0.3)	BI-OAc	24	DCE	60
15 <sup>e</sup>	Os(btpy) <sub>2</sub> (PF <sub>6</sub> ) <sub>2</sub>	BI-OAc	24	DCE	73
16 <sup>g</sup>	Os(btpy) <sub>2</sub> (PF <sub>6</sub> ) <sub>2</sub> (0.3)	BI-OAc	24	DCE	89
17	Os(btpy) <sub>2</sub> (PF <sub>6</sub> ) <sub>2</sub> (0.3)	BI-OAc	6	DCE	90
18	Os(btpy) <sub>2</sub> (PF <sub>6</sub> ) <sub>2</sub> (0.3)	BI-OAc	6	CH <sub>3</sub> CN	45

<sup>a</sup> Unless otherwise stated, all reactions were performed with **56a** (0.25 mmol), **70a** (3.0 eq.), Os(btpy)<sub>2</sub>(PF<sub>6</sub>)<sub>2</sub> (0.2 mol%), TTBP (3 mol%), PC: visible light photocatalyst (1.0 mol%). Lamp of 660 nm. <sup>b</sup> Yields of **57a** determined by <sup>1</sup>H NMR with 1,3,5-trimethylbenzene as an external standard (Isolated yields of **57a** under brackets). <sup>c</sup> AcrMes<sup>+</sup>ClO<sub>4</sub><sup>-</sup> (2.0 mol%) was used. <sup>d</sup> Reaction performed using 780 nm NIR. <sup>e</sup> Reaction performed using blue LED (455 nm). <sup>f</sup> Reaction without light. <sup>g</sup> Reaction using 1.0 eq. of BI-OAc.

**Table 4.8:** Urethane synthesis from oxamic acids using Os(btpy)<sub>2</sub>(PF<sub>6</sub>)<sub>2</sub> as sensitizer and TTBP as annihilator

With these optimal conditions (entry 13) in hand, the substrate scope was evaluated. Gratifyingly, different oxamic acids with different substituted arenes, bearing both electron-withdrawing group and electron donating groups, were compatible with the NIR photocatalyzed procedure, furnishing

the desired urethane in moderate to high yields (Scheme 4.9). Also, alcohols with different functionalities including ether (**57g**, **57h**, **57o**, **57q**), CF<sub>3</sub> (**57l**) and Cl (**57k**) groups were compatible with the reaction and delivered the desired urethanes in moderate to high yields. With diol, only monofunctionalization occurred with a satisfying yield (**57c**), alcohol with terminal alkene also delivered the urethane albeit low yield (**57r**). With chiral oxamic acids, the corresponding chiral urethanes were obtained in moderate to high yields (**57d-e**, **57k**) without racemization as confirmed using chiral HPLC (Figure 4.9).



**Scheme 4.9:** Urethane synthesis from oxamic acids using 660 nm LED: Substrate scope. Oxamic acid (0.25 mmol), alcohol (3.0 eq.), Os(btpy)<sub>2</sub>(PF<sub>6</sub>)<sub>2</sub> (0.3 mol%), DCM (0.1M), BI-OAc (1.5 eq.).

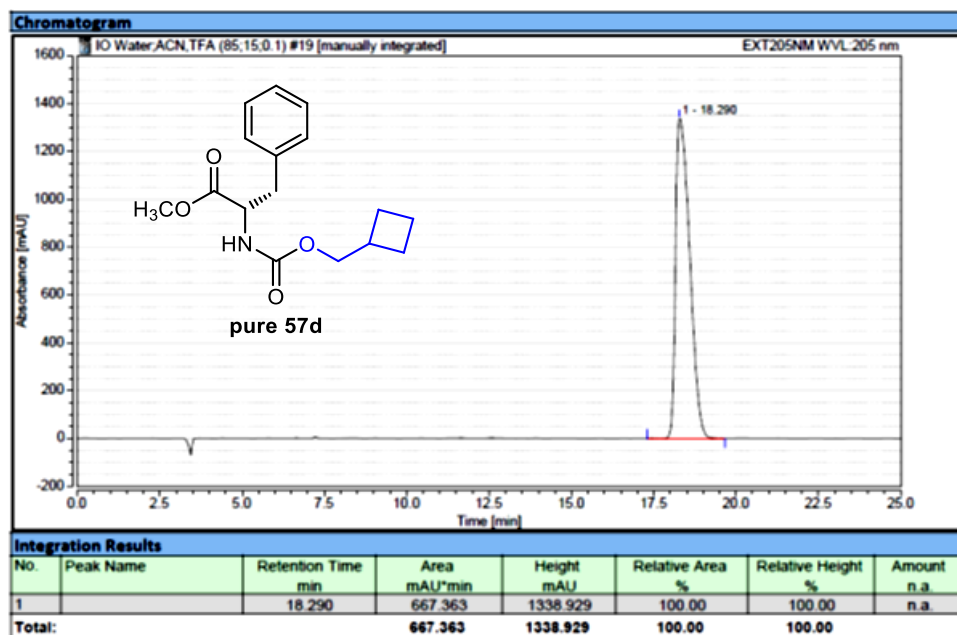


**Figure 4.9a:** HPLC Data for (*S*)-methyl 2-(((cyclobutylmethoxy)carbonyl)amino)-3-phenylpropanoate (pure **57d**). UltiMate-3000 (Water:CH<sub>3</sub>CN:TFA (65:35:0.1)).

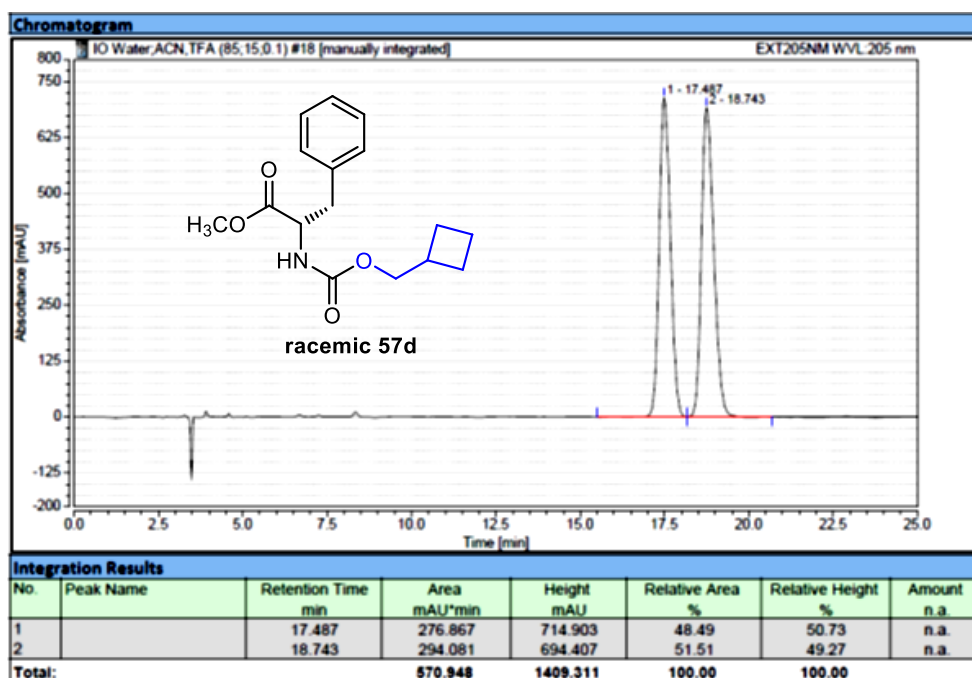
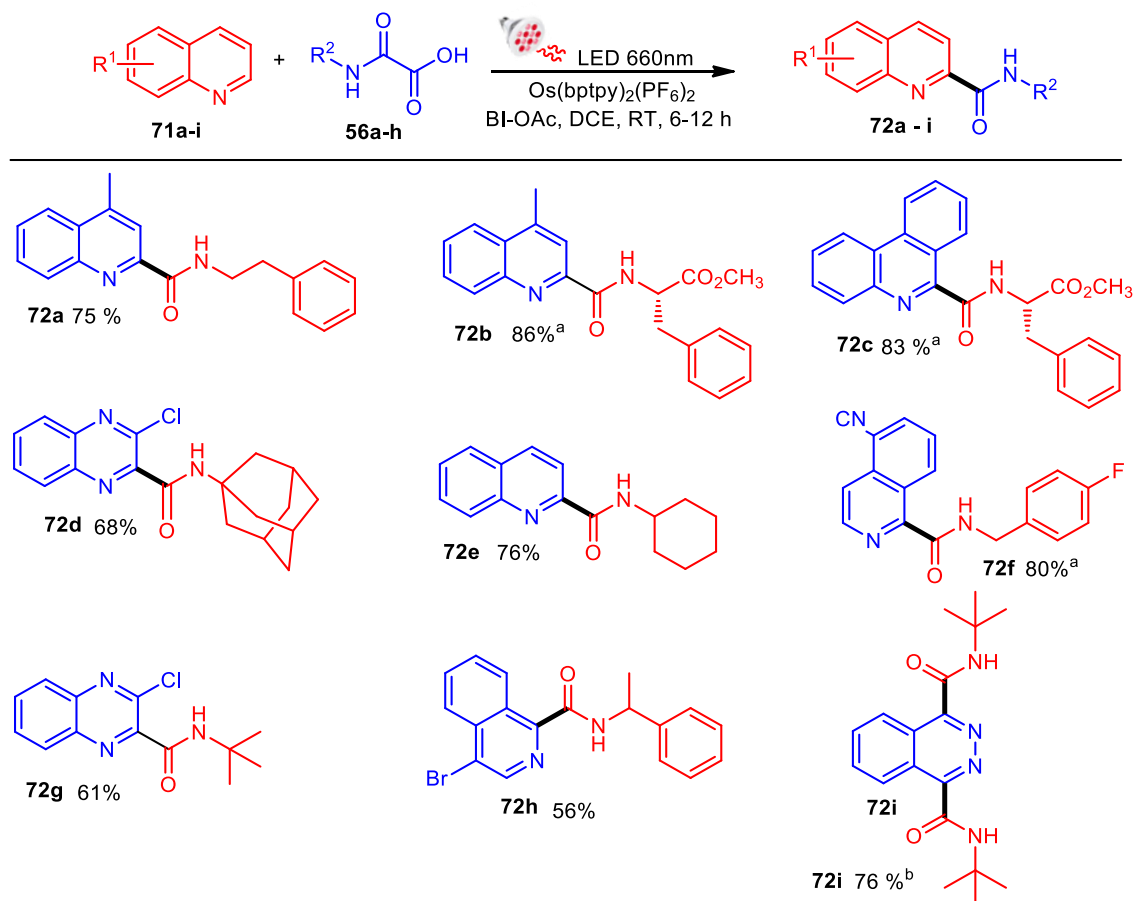


**Figure 4.9b:** HPLC Data for (*S*)-methyl 2-(((cyclobutylmethoxy)carbonyl)amino)-3-phenylpropanoate (racemic **57d**). UltiMate-3000 (Water:CH<sub>3</sub>CN:TFA (65:35:0.1)).

Next, the new NIR light photocatalyzed process was also applied for carbamoyl radical addition to heteroarenes, and it was shown to be efficient, providing the corresponding amides in satisfying yields with good functional group tolerance (Scheme 4.10). With phthalazine, a selective double

addition was observed in reasonable yield (**72i**); no mono addition product was detected even when only 2.0 equivalent of oxamic acid was used, though the yield was relatively low (51%) in this case. Double amidation of phthalazine using oxamic acid has been shown to be more favored than the monofunctionalization;<sup>169</sup> the mono-amide probably is much more reactive than the starting oxamic acid, resulting that the first amidation increasing the electron-deficiency of the heteroarene, and hence accelerating the second addition. Just as with urethane synthesis, chiral oxamic acid furnished chiral amides (**72b-c**) without racemization as determined with chiral HPLC (Figure 4.10).



**Scheme 4.10:** Oxamic acid decarboxylative carbamylation of heteroarenes using 660 nm LED. Heteroarene (0.25 mmol), oxamic acid (2.0 eq.), BI-OAc (1.5 eq.), DCE (0.1M), <sup>a</sup> Oxamic acid (3.0 eq.) was used. <sup>b</sup> Oxamic acid (4.0 eq.) was used.

Toxicity concerns about osmium are mainly attributed to osmium tetroxide.<sup>170</sup> While more information is still needed on the level of toxicity of osmium (II) complexes, they have been reported to be much less toxic, studies using osmium (II) bipyridine complex for cellular imaging probes showing that the toxicity of the complex was comparable to that of ruthenium (II) counterpart.<sup>171</sup> Also, possible oxidation of osmium (II) terpyridines to osmium tetroxide during the use as a

<sup>169</sup> A. H. Jatoi, G. G. Pawar, F. Robert, Y. Landais, *Chem. Commun.* **2019**, 55, 466-469.

<sup>170</sup> A. I. G. McLaughlin, R. Milton, K. M. A. Perry, *Br. J. Ind. Med.* **1946**, 3, 183-186.

<sup>171</sup> A. Byrne, C. Dolan, R. D. Moriarty, A. Martin, U. Neugebauer, R. J. Forster, A. Davies, Y. Volkov, T. E. Keyes, *Dalton Trans.* **2015**, 44, 14323-14332. b) R. Huang, F.-P. Feng, C.-C. Huang, L. Mao, M. Tang, Z.-Y. Yan, B. Shao, L. Qin, T. Xu, Y.-H. Xue, B.-Z. Zhu, *ACS Appl. Mater. Interfaces*, **2020**, 12, 3465-3473.

photocatalyst was not detected even when exposed to oxygen under light irradiation or mild heating,<sup>168</sup> confirming its high stability.

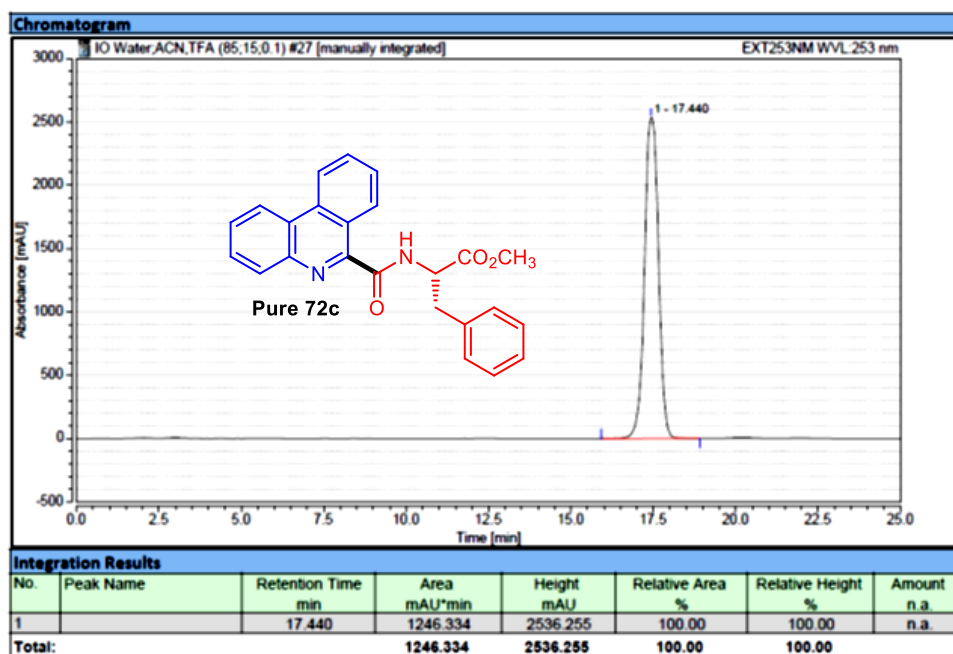


**Figure 4.10a:** HPLC Data for (*S*)-methyl 2-(phenanthridine-6-carboxamido)-3-phenylpropanoate (pure **72c**). UltiMate-3000 (Water:CH<sub>3</sub>CN:TFA (85:15:0.1)).

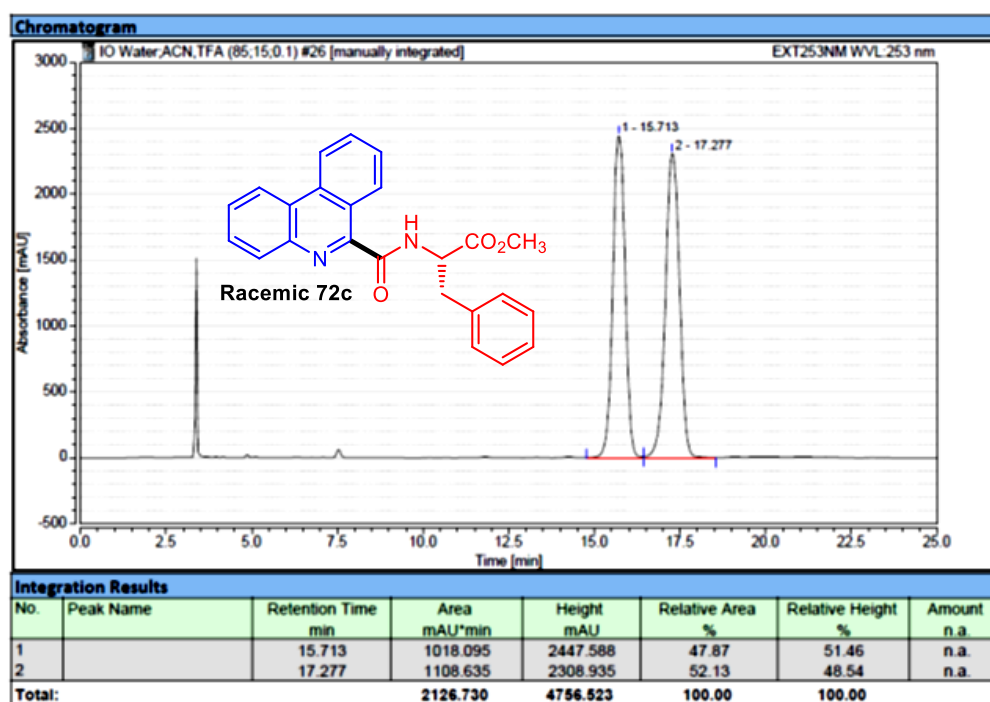
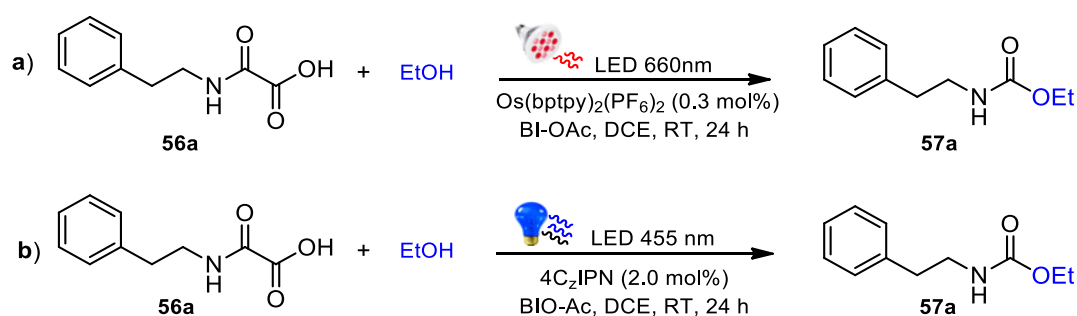


**Figure 4.10b:** HPLC Data for (*S*)-methyl 2-(phenanthridine-6-carboxamido)-3-phenylpropanoate (racemic **72c**). UltiMate-3000 (Water:CH<sub>3</sub>CN:TFA (85:15:0.1)).

## 6. Comparing the penetration depth of the NIR light and blue LED light

The penetration depth of the optimal NIR light photocatalytic procedure was compared with that of the visible light process developed earlier<sup>167</sup> (Scheme 4.11). Different "barricades" were used including paraffin wax of different diameters, white paper, pig skin and hemoglobin solution. The light source was placed 13cm behind the barrier (Figure 4.11) and the reaction was performed using our optimized conditions. The NIR procedure clearly demonstrated a superior penetration through these barriers to perform the photocatalytic reaction efficiently while with blue procedure, only trace amount of the desired urethane was observed in most cases. Very remarkable among them is the reaction performed in a hemoglobin solution, where penetration of the blue light through the solution was completely blocked, resulting in no urethane being observed. Hemoglobin belongs to heme family (porphyrin derivative) which absorbs strongly in the visible region; visible light is characterized by a short penetration depth when traveling through a visible light absorbing medium.



Entry	Barrier	NIR	Blue light
		LED 660nm (a)	LED 455 nm (b)
1	None	93%	94%
2	Paraffin wax (1 mm)	92%	89%
3	Paraffin wax (7 mm)	85%	trace
4	Paraffin wax (1.5 cm)	71%	trace
5	White paper (3 sheets)	80%	12%
6	Pig skin (1 cm)	86%	35%
7	Hemoglobin	87%	ND

**Scheme 4.11:** Comparing the penetration depth of the Red LED 660 nm and blue LED light 455 nm. BI-OAc (1.5 eq.).

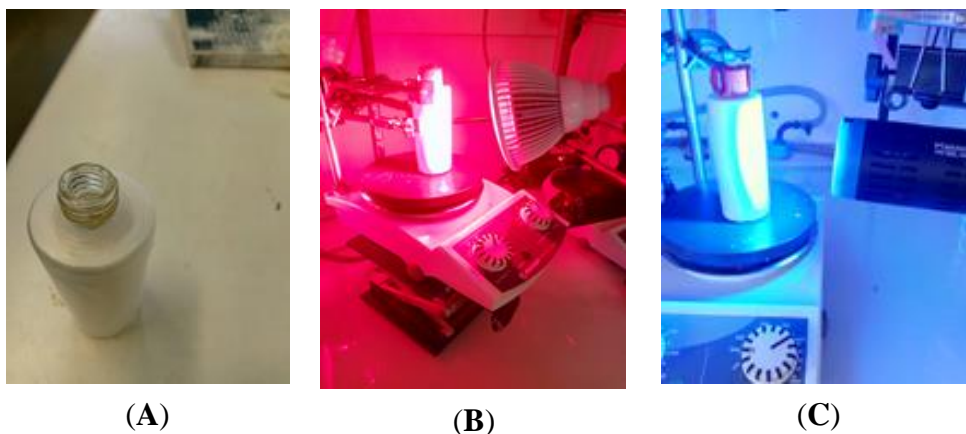


**Figure 4.11a:** Resealable tube with paraffin barricade used for the reaction (A), the reaction using the red light ( B) reaction using blue light (C).

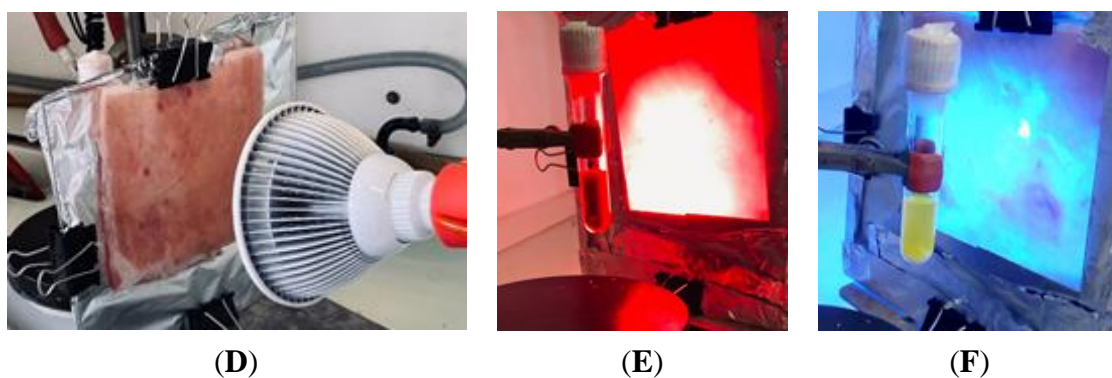


**Figure 4.11b:** Reaction setup using pig skin (1.0 cm) as a barricade (D): Reaction using red light (E), reaction using blue light (F).

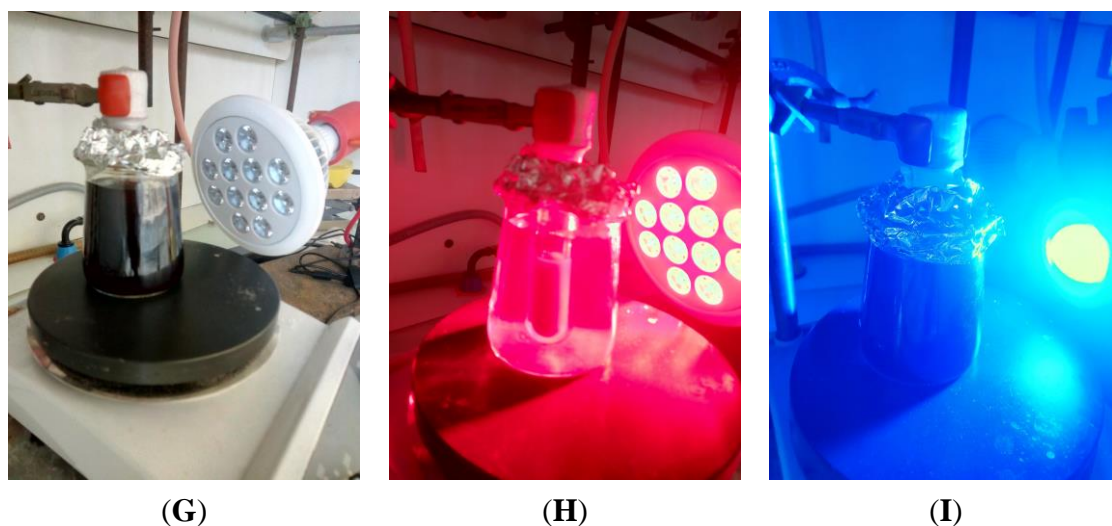
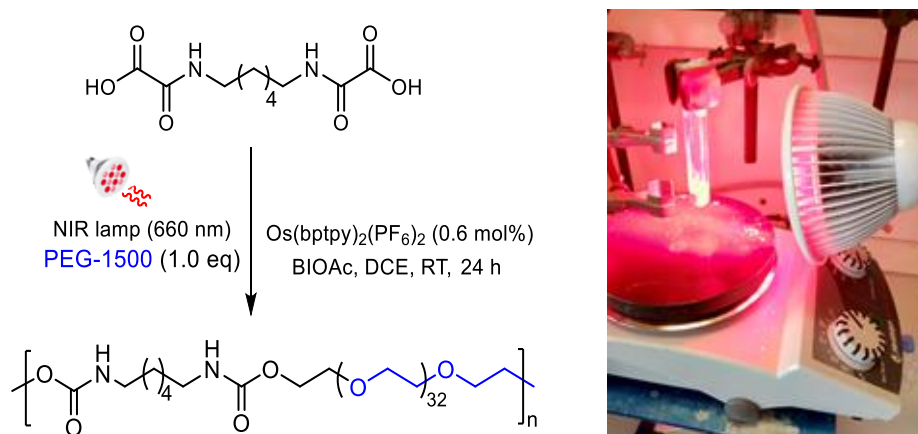


**Figure 4.11c:** Reaction setup with hemoglobin solution (G). Reaction using red light (H), reaction using blue light (I).

## 7. Towards polyurethane synthesis from bis-oxamic acids using bulk polymerization method and 660 nm LED light.

As mentioned earlier, our main goal was to leverage the deeper penetration depth of NIR light system to perform the polyurethane synthesis from bis-oxamic acids under bulk conditions. We applied the optimized NIR procedure for PUs synthesis using bulk method as represented in Scheme 4.12. In this case, little quantity of DCE (0.5 mL, 1.0 M) was used to solubilize the reaction mixture to form a paste which was irradiated with a 660 nm LED light for 72 h. However, the reaction was not successful;  $^1\text{H}$  NMR showed that only trace amount of urethane linkage was formed while oxamic acids remained largely unconverted. This probably could be due to the insolubility of bis-oxamic acids under the reaction conditions. Bis-oxamic acids are sparingly soluble in DCE or DCM even at 0.2 M. These are the only efficient solvents for the reaction. Very closed contact between the reacting species is key for efficient chemical transformation. In an attempt to solve this problem, the polymerization was also repeated using more diluted system (0.2 M) but this did not help to solve the problem of low oxamic acid conversion

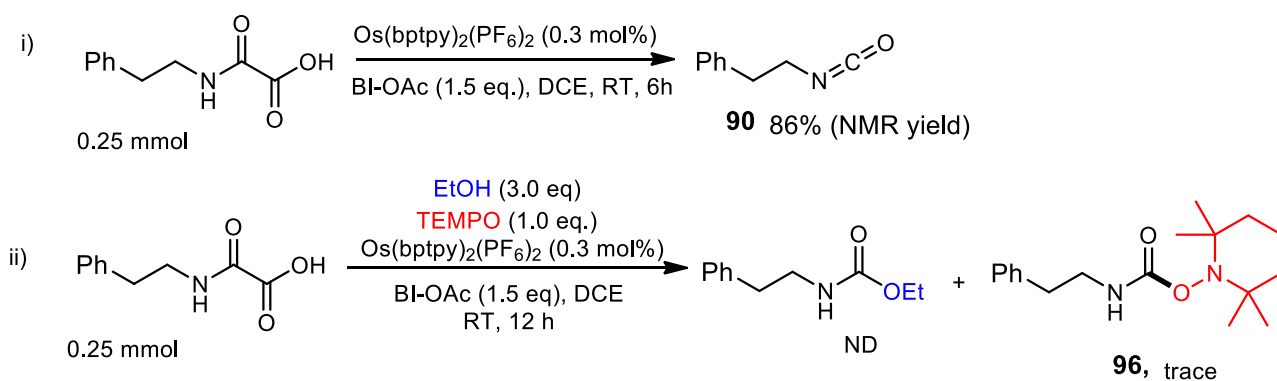


**Scheme 4.12:** Polyurethane synthesis from bis-oxamic acids using NIR light conditions: Bis-oxamic acids (0.25 mmol), BI-OAc (2.5 eq.), DCE (0.5 mL).

## 8. Towards Reaction Mechanism

### 8.1 Intermediate trapping and identification experiments

With  $^1\text{H}$  NMR and FT-IR, the *in-situ* generation of an isocyanate during the reaction was unambiguously confirmed (Scheme 4.13, i). A radical trapping experiment showed that urethane **57a** formation was completely shut down in the presence of TEMPO, indicating that the reaction probably followed a radical pathway.



**Scheme 4.13:** Radical trapping experiment using TEMPO

## 8.2. Fluorescence Quenching Experiment

Steady state luminescence, Figure 4.12, showed that a mixture of oxamic acid (OA) and BI-OAc significantly quenched the emission of  $\text{Os}(\text{btpy})_2(\text{PF}_6)_2$ , possibly due to cleavage of the weak O-I bond (of oxamic-acid-BI-OAc adduct formed *in-situ*<sup>167</sup>) by the excited catalyst. Oxamic acid alone did not decrease the intensity of the osmium catalyst emission, while BI-OAc surprisingly magnified the emission, a phenomenon that is not yet very clear.

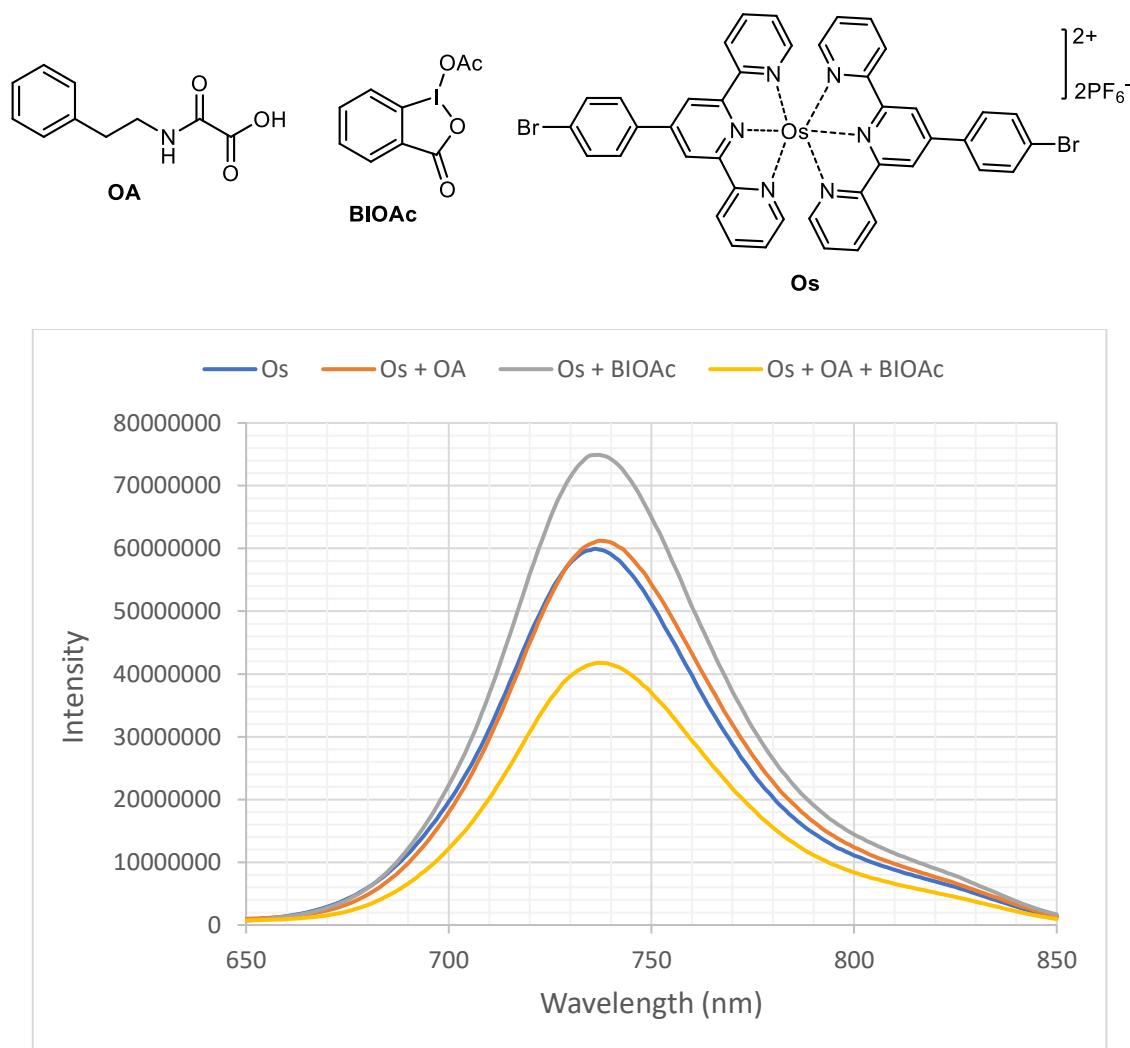


**Figure 4.12:** Steady state luminescence of  $\text{Os}(\text{btpy})_2(\text{PF}_6)_2$  in the presence of oxamic acid and BI-OAc.

### 8.3. Proposed mechanism

Based on the intermediates trapping experiments, fluorescence quenching experiment, and our previous work on visible-light mediated oxamic acid decarboxylation,<sup>167</sup> a tentative mechanism for the NIR light based urethane synthesis was proposed (Figure 4.13). The reaction between oxamic acid and BI-OAc would provide the oxamic-acid-BI-OAc adduct,<sup>167</sup> **I**. Quenching of Os(II) in its excited state by the intermediate **I** would generate Os(III) and result in an unstable radical-anion intermediate **II**, which collapses to generate carbamoyl radical **III**, CO<sub>2</sub> and *o*-iodobenzoic acid anion. Further oxidation of **III** by the Os(III) would give protonated isocyanate **IV** while regenerating the Os(II) catalyst. Then the protonated isocyanate will be trapped by the alcohol to furnish the corresponding urethane.

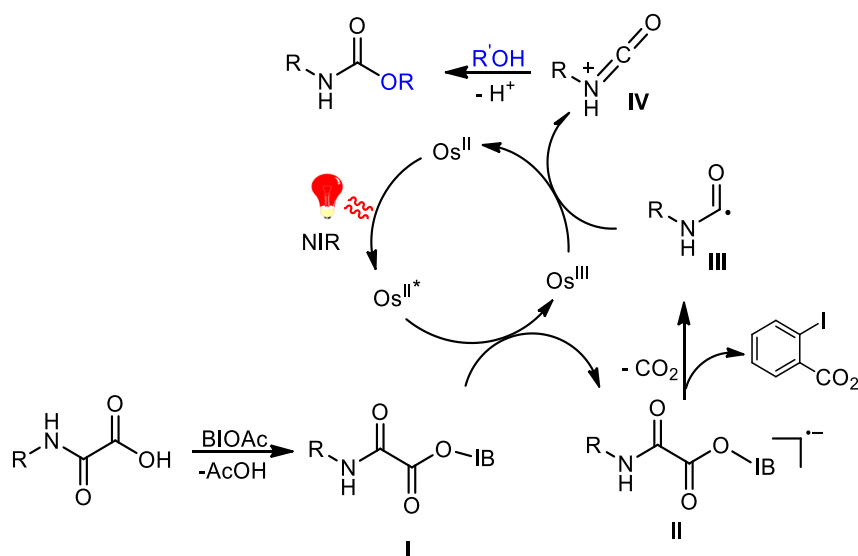


**Figure 4.13:** Tentative mechanism for the NIR infrared light mediated decarboxylation of oxamic acids for urethane synthesis

For the carbamoylation of heteroarenes, the carbamoyl radical **III** generated from the decarboxylation of the intermediate **II**, would add to the heteroarenes to form radical intermediate **V** (Figure 4.14). Oxidation of the latter by Os(III) would generate cationic species **VI** that undergoes deprotonation and rearomatization to furnish the amide.

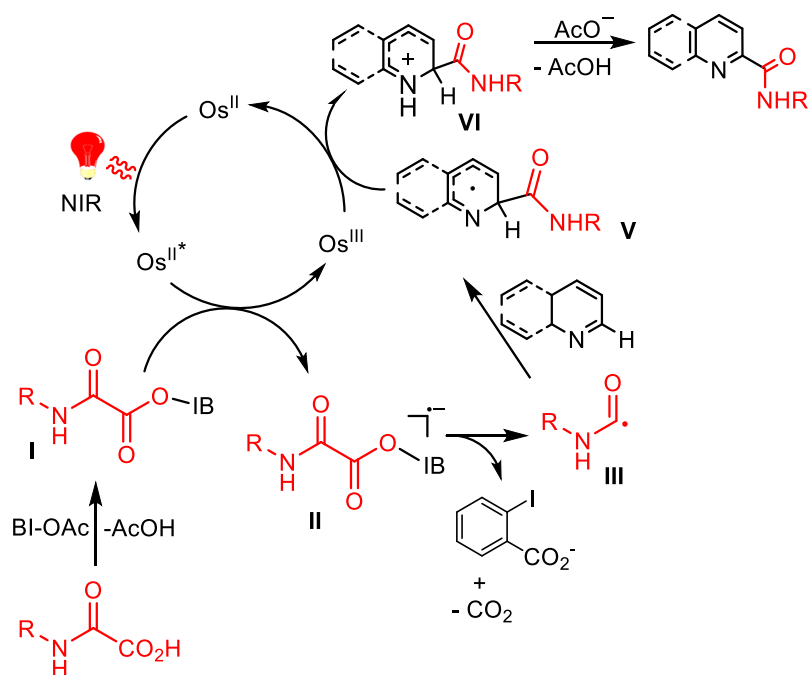


**Figure 4.14:** Tentative mechanism for the NIR light mediated decarboxylative carbamoylation of heteroarenes.

## 9. Conclusion

Urethane synthesis from oxamic acids using near infrared (NIR) light photoredox catalysis has been developed. This new procedure uses very small amount of  $\text{Os}(\text{btpy})_2(\text{PF}_6)_2$  (0.3 mol%) as catalyst to furnish urethane in an excellent yield. Application of this procedure for carbamoylation of heteroarenes using oxamic acids was also successful. With mono-oxamic acid, the NIR light procedure demonstrated superior penetration depth into media. It was able to penetrate through different barriers and highly absorbing solution to accomplish the desired reaction, which could not be achieved using the visible light based photocatalysis. However, it was not suitable for polyurethane synthesis from bis-oxamic acid using bulk method, which was the main target of this study. Nevertheless, this procedure can serve as a useful tool for synthesis of carbamates and amides from oxamic acids with advantage of relying on a very mild light source and low catalyst load. Although this has not been carried out here, NIR-photocatalyzed large-scale oxidative decarboxylation of oxamic acids should be at hand following this strategy.



## Chapter 5

### Urethanes and polyurethanes synthesis through PIDA-mediated decarboxylation of oxamic acids under thermal conditions

#### Introduction

As shown in the proceeding chapters, urethanes can efficiently be synthesized from oxamic acids under visible- or near-infrared (NIR) light mediated oxidative decarboxylation of oxamic acids. These photocatalyzed methods furnished urethanes through a one-pot process thereby avoiding isolation, purification and storage of toxic isocyanates. A wide range of carbamates of pharmaceutical interest could be accessed in moderate to excellent yields using either of the methods. In addition, it was shown that these photocatalyzed procedures were suitable for carbamoylation of heteroarenes, giving access to a wide variety of amides of biological interests. Extension of the photocatalyzed procedures to polyurethane synthesis using bifunctional oxamic acids and polyols was also demonstrated with some level of success; however, the obtained polyurethanes were generally of lower molecular weights. Efforts to perform the photopolymerization at room temperature in bulk also provided low or modest molecular weights polyurethanes, probably due to poor mobility of the reacting monomers. Under bulk conditions, application of heat (60-70°C) during the photocatalyzed process to enhance the molecular mobility and kinetics of the reaction was also tried. Although this strategy resulted in reasonable improvement in the molecular weight, especially when PIDA was used as the oxidant, problem of precipitating the obtained polymer was encountered, probably due to a simultaneous crosslinking process under the influence of the heat and light. Also, the insolubility of the obtained PUs, hampered its characterization in most cases. Polymerization by bulk or solvent free method is however crucial for preparation of polyurethane foams.<sup>172</sup>

Moreover, the near-infrared light photocatalyzed procedure, which was aimed at improving the efficiency of the polyurethane synthesis from bis-oxamic acids due to its known deeper penetration depth into media, was not successful. Just as with visible-light method, the NIR light-based photocatalytic procedure was very efficient for preparation of urethanes from mono-oxamic acids, but its application to polymerization of bis-oxamic acids and polyol was inefficient.

In the process of solving this problem, we discovered that PIDA under thermal conditions could efficiently mediate the decarboxylation of oxamic acids into *in-situ* generated isocyanate without the need for photocatalyst and light, thereby making the process simpler.

In our photocatalyzed procedure discussed earlier, BI-OAc was found the most efficient of all the oxidants tested, furnishing the desired urethane in excellent yield (~ 94%), while PIDA and its derivative PIFA gave only moderate yield of the product (< 70%). However, in this new thermal

---

<sup>172</sup> A. Ivdre, A. Abolins, I. Sevastyanova, M. Kirpluks, U. Cabulis, R. Merijs-Meri, *Polymers (Basel)* 2020, 12, 738, 1-8.

procedure, PIDA surprisingly exhibited a unique reactivity under optimized conditions, resulting in a straightforward access to urethanes from oxamic acids without the need for a photocatalyst. This new procedure is described in this chapter.

The chapter is divided into two parts; the first one deals with process optimization and synthesis of thermoplastic polyurethanes from oxamic acids using the PIDA-mediated procedure while the extension of the work to thermoset PUs is discussed in the second part.

## **PART 1: Thermoplastic polyurethane synthesis from bis-oxamic acids using the PIDA-mediated decarboxylation**

### **1. Process optimization**

During our optimization of the photocatalyzed decarboxylation of oxamic acids, we discovered that hypervalent iodine reagent PIDA was able to trigger the oxidative decarboxylation in the absence of the photocatalyst and that the reaction was sensitive to temperature. A direct access to urethanes from oxamic acids was thus accomplished using PIDA as an oxidant, which under mild heating activation was shown to initiate the oxidative decarboxylation of oxamic acids to afford urethanes in one-pot process in the presence of alcohols. This new reaction condition was first optimized using mono-oxamic acid **56a** as a model compound and ethanol **70a** as summarized in Table 5.1. At 60°C, with PIDA as the oxidant and DCE as solvent, the expected urethane **57a** was observed in 88% conversion after 12h (Table 5.1, entry 1). Decreasing the reaction time to 6h still delivered the urethane in high yield (entry 2). PIFA as an alternative oxidant was less efficient for the reaction (entry 3), while BI-OAc or BI-OH resulted in very low to trace amount of the urethane (entry 4-5). The hypervalent iodine was shown to be essential for the reaction as no urethane was observed in its absence (entry 6). At 40°C, 75% of urethane was observed (entry 7). At room temperature (23°C), the expected urethane was not detected within 12h. However, after a prolonged reaction time of five days, the product was observed in satisfying amount (79%) indicating that the reaction still proceeded at room temperature but with low kinetics. Using 1.1 eq. of PIDA, 82% conversion was obtained after 6h (entry 9). But the reaction did not progress with catalytic amount of PIDA (entry 10).

Interestingly, unlike our photocatalyzed procedure which works efficiently only with DCE or DCM as solvents, the PIDA-mediated procedure progressed smoothly with other organic solvents such as DMF and CH<sub>3</sub>CN (entry 11-12). The use of DABCO<sup>173</sup> (to accelerate the putative addition of the alcohol onto the isocyanate) as a catalyst did not show any significant effect on the urethane yield (entry 13), while classical urethane catalyst DBTDL<sup>174</sup> improved the product yield to 92 % (entry 14). Using Bis(trifluoromethanesulfonyl)imide (TFMI)<sup>175</sup> as a catalyst led to 95% conversion (entry 15). This catalytic effect of TFMI on the reaction was also observed when the reaction was conducted in CH<sub>3</sub>CN as the solvent (entry 16). Triflic acid (TfOH) was less efficient as an alternative acid

<sup>173</sup> A. L. Silva, J. C. Bordado, *Catal. Rev.* **2004**, *46*, 31–51.

<sup>174</sup> H. Sardon, A. Pascual, D. Mecerreyes, D. Taton, H. Cramail, J. L. Hedrick, *Macromolecules* **2015**, *48*, 3153–3165.

<sup>175</sup> H. Sardon, A. C. Engler, J. M. W. Chan, J. M. García, D. J. Coady, A. Pascual, D. Mecerreyes, G. O. Jones, J. E. Rice, H. W. Horn, J. L. Hedrick, *J. Am. Chem. Soc.* **2013**, *135*, 16235–16241.

catalyst for the reaction.<sup>4</sup> Lastly, when 1.0 eq. of Brønsted base ( $K_2CO_3$ ) was used as an additive, the reaction was drastically suppressed (entry 19) possibly due to formation of an insoluble salt of the oxamic acid.

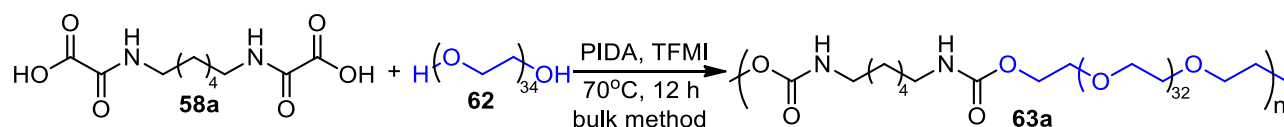
Entry <sup>a</sup>	Oxidant (1.5 eq.)	Time (h)	Temp (°C)	Additive (5mol%)	Solvent	Yield (%) <sup>b</sup>
1	PIDA	12	60	-	DCE	88 (78)
2	PIDA	6	60	-	DCE	86
3	PIFA	6	60	-	DCE	63
4	BI-OAc	6	60	-	DCE	16
5	BI-OH	6	60	-	DCE	trace
6	-	12	60	-	DCE	ND
7	PIDA	12	40	-	DCE	75
8	PIDA	12	23	-	DCE	ND
9 <sup>c</sup>	PIDA	6	60	-	DCE	82 (74)
10 <sup>d</sup>	PIDA	12	60	-	DCE	Trace
11	PIDA	12	60	-	CH <sub>3</sub> CN	87
12	PIDA	12	60	-	DMF	85
13	PIDA	6	60	DABCO	DCE	86
14	PIDA	6	60	DBTDL	DCE	92
15	PIDA	6	60	TFMI	DCE	95 (84)
16	PIDA	6	60	TFMI	CH <sub>3</sub> CN	91
17 <sup>e</sup>	PIDA	6	60	TFMI	DCE	95
18	PIDA	6	60	TFOH	DCE	87
19 <sup>f</sup>	PIDA	6	60	K <sub>2</sub> CO <sub>3</sub>	DCE	08

**Table 5.1:** Urethane synthesis from oxamic acid using PIDA-mediated oxidative decarboxylation. <sup>a</sup> Unless otherwise stated, all reactions were performed with **56a** (0.5 mmol), **70a** (3.0 eq.), oxidant (1.5 eq.), solvent (1.0 mL), in a sealable test tube. The heating was done in an oil bath. <sup>b</sup> Yields of **57a** were determined by <sup>1</sup>H NMR with 1,3,5-trimethylbenzene as an external standard, isolated yields of **57a** inside brackets. <sup>c</sup> Reaction using 1.1 eq. of PIDA. <sup>d</sup> Reaction using 10 mol% of PIDA. <sup>e</sup> Reaction using 1.0 eq. of EtOH. <sup>f</sup> Reaction using K<sub>2</sub>CO<sub>3</sub> (1.0 eq.). TFMI = Bis(trifluoromethanesulfonyl)imide, TFOH = Triflic acid.

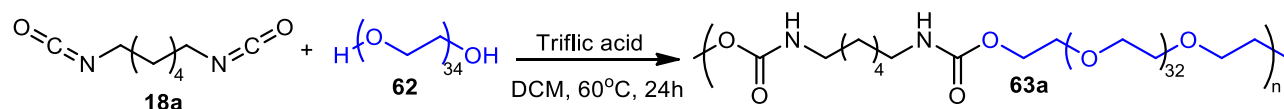
## 2. Thermoplastic polyurethane synthesis using PIDA-mediated decarboxylation of bis-oxamic acids

The PIDA-mediated oxidative decarboxylation of oxamic acids was then applied to the synthesis of thermoplastic polyurethanes. Using bis-oxamic acid **58a** as a model compound and PEG-1500 **62** as a polyol, the polymerization was conducted under solvent-free conditions (in bulk) at 70°C (Scheme 5.1). FTIR (Figure 5.1) and <sup>1</sup>H NMR (Figure 5.2) analyses confirmed the formation of the urethane linkage, and that the chemical structure was in good agreement with its counterpart prepared from commercial diisocyanate using acid catalysis<sup>175</sup> (Scheme 5.2). The urethane linkage formation in the

PUs was indicated by the peak around 4.1 ppm in the  $^1\text{H}$  NMR and a signal around  $1700\text{ cm}^{-1}$  in the FTIR.<sup>176</sup> Gratifyingly, Sized Exclusion Chromatography (SEC) analysis (Figure 5.3) confirmed polyurethane formation with reasonable molecular weight. The SEC analysis was performed using different solvents including DMF, THF and HFIP, where HFIP gave better results in terms of molecular weight and polydispersity, probably due to better solubility of the PUs in the solvent (Figure S16a-c).



**Scheme 5.1:** Thermoplastic polyurethane synthesis using PIDA-mediated decarboxylation of bis-oxamic acid **58a**: (1.0 mmol), PEG-1500 **62** (1.0 eq.), PIDA (2.5 eq.), TFMI (5 mol%). Precipitated using diethyl ether.



**Scheme 5.2:** Polyurethane synthesis from diisocyanate **18a**: (1.0 mmol), PEG-1500 **62** (1.0 eq.), triflic acid (5 mol%), DCM (0.5 mL), precipitated using diethyl ether.

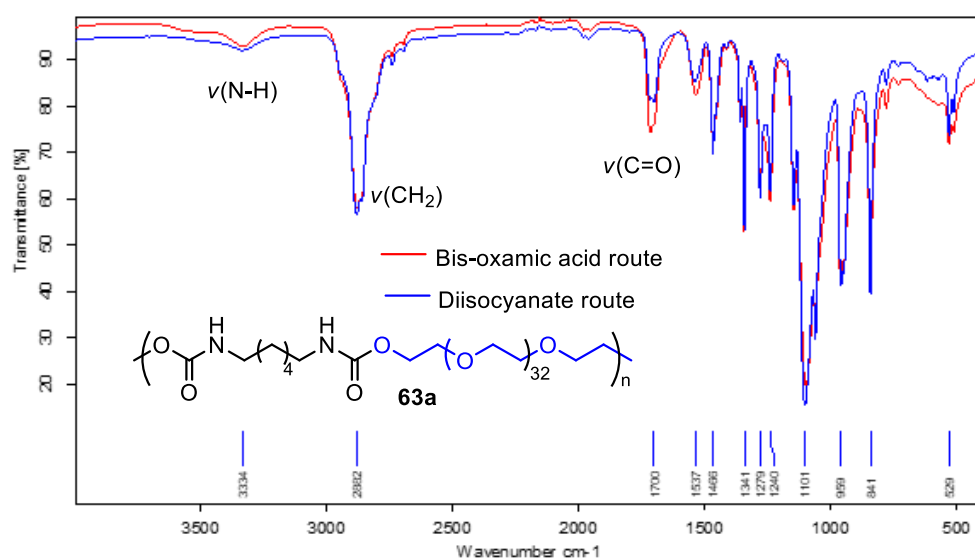


**Figure 5.1:** FTIR of PUs issued from bis-oxamic acid **58a** (red) or from diisocyanates (blue)

<sup>176</sup> L. Gu, B. Cui, Q.-Y. Wub, H. Yu, *RSC Adv.*, **2016**, *6*, 17888–17895.

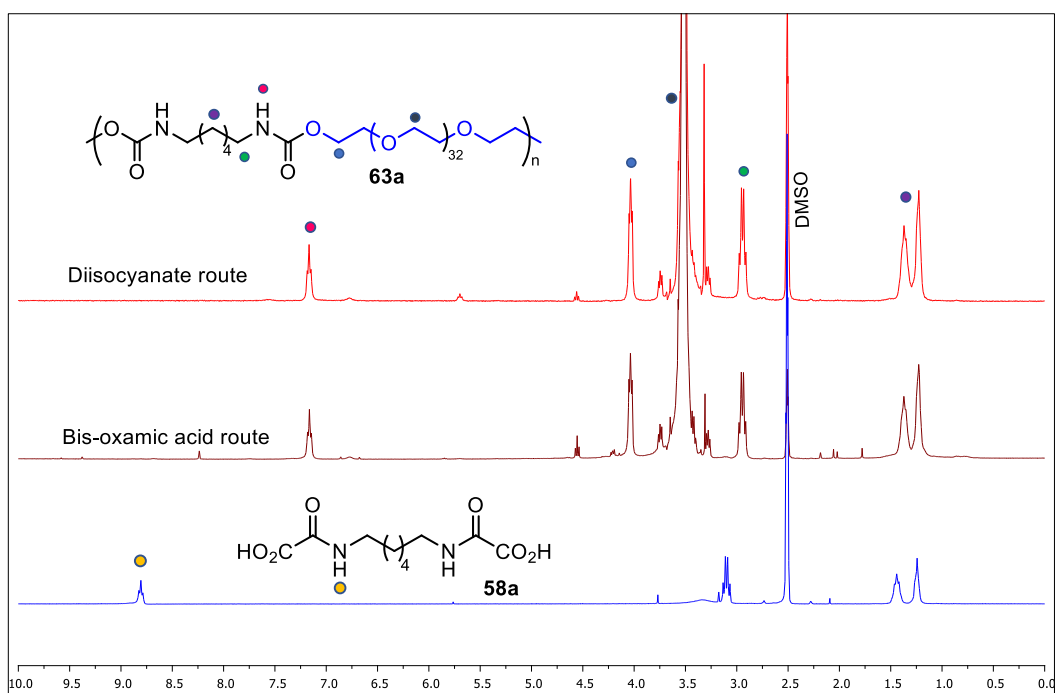


**Figure 5.2:**  $^1\text{H}$  NMR of PUs issued from bis-oxamic acid **58a** (brown) or from diisocyanates (red)

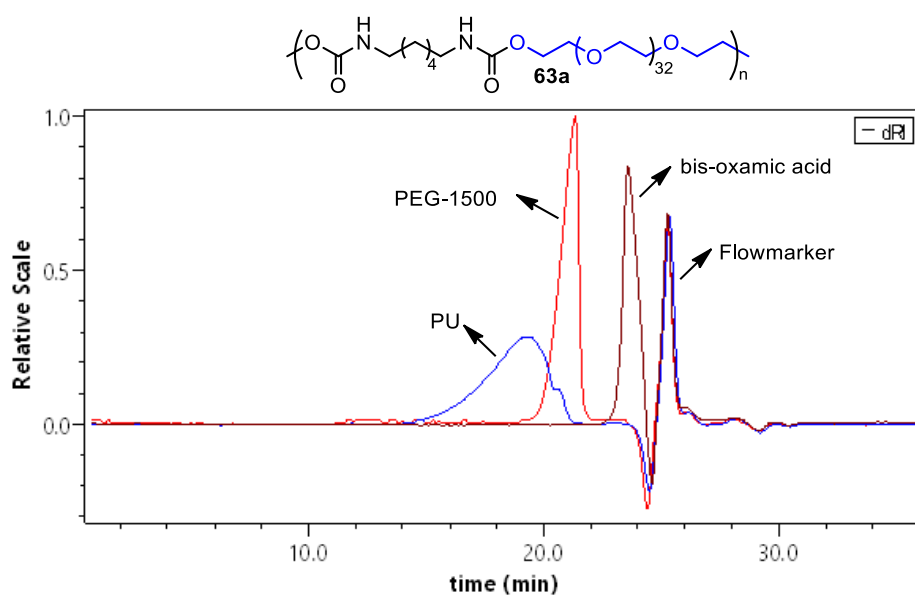


**Figure 5.3:** SEC (in HFIP) of PU prepared from PIDA-mediated decarboxylation of bis-oxamic acid **58a**

### 3. Optimization of the PIDA-mediated synthesis of thermoplastic PU from bis-oxamic acids

Process parameters were varied to determine the optimal conditions for the polymerization. All the reactions were performed using bis-oxamic acid **58a** and PEG-1500 as a polyol, in bulk conditions and at 70°C. First, when the polymerization was conducted using a 1:1 mixture of bis-oxamic acid **58a** and polyol, PU **63a** of molecular weight 34600 g/mol and polydispersity 1.8 was obtained (Table 5.2, entry 1). Extending the reaction time to 48h under these conditions did not show any significant effect in the molecular weight (data not shown). From the optimization using mono-oxamic acid discussed earlier, it was shown that conversion of oxamic acid to urethane was not quantitative; the

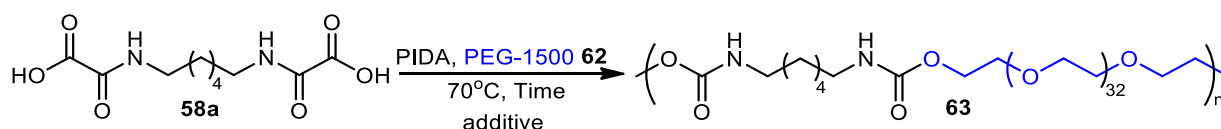
highest conversion attained was 95%. Also, from the SEC trace of the obtained PUs (Figure 5.3), some unconverted PEG-1500 was observed, indicating that it was probably in excess. Stoichiometric balance is very crucial for polymer synthesis using AA-BB-type monomers.<sup>177</sup> In consideration of this, we then dropped the polyol equivalent to 0.9 and this resulted in a significant improvement in the molecular weight after 12h (entry 2). Extending the reaction time to 48h showed no significant effect on the molecular weight (entry 3). Further decrease of polyol equivalent to 0.8 did not help to increase the molecular weight (entry 4). Therefore, a **58a** / polyol stoichiometry of 1:0.9 was adopted for the rest of the study.

When TFMI (5 mol%) was used as a catalyst for the polymerization, a remarkable improvement on the molecular weight was observed, while the polydispersity of the obtained PU was broader compared to the uncatalyzed reaction (entry 5). Interestingly, decreasing the reaction time to 6h with the acid catalysis resulted in PUs with reasonably high molecular weight (84800 g/mol) and excellent polydispersity (entry 6). Hedrick and co-workers earlier reported the efficacy of TFMI to catalyze polyaddition of poly(ethylene glycol) and diisocyanate, possibly through dual activation mechanism.<sup>178</sup> The strong acid catalyst possibly exhibited similar catalytic activity towards this oxamic acid route by speeding up the addition of polyol onto the *in-situ* generated isocyanate. Moreover, 2 mol% of TFMI still exhibited some catalytic effect on the reaction although with less efficiency as compared to 5 mol% (entry 7). Other catalysts including TfOH, DABCO and TBTDL were also tried on the polymerization, but were all ineffective for the reaction (entry 8-10). As observed on mono-functional system **56a**, DABCO was obviously detrimental to the polymerization. Without any catalyst, relatively high molecular weights could be accessed at 100°C though with broader polydispersity (entry 11).

---

<sup>177</sup> J. K. Stille, *J. Chem. Educ.* **1981**, 58, 862-865.

<sup>178</sup> H. Sardon, A. C. Engler, J. M. W. Chan, J. M. García, D. J. Coady, A. Pascual, D. Mecerreyes, G. O. Jones, J. E. Rice, H.W. Horn, J. L. Hedrick, *J. Am. Chem. Soc.* **2013**, 135, 16235–16241.



Entry <sup>a</sup>	62 : 58a	Time (h)	Additive (5mol%)	Mw <sup>b</sup> (g/mol)	Mn <sup>b</sup> (g/mol)	Đ <sup>b</sup> Mw/Mn
1	1:1	12	-	34600	19700	1.8
2	0.9:1	12	-	45000	25000	1.8
3	0.9:1	48	-	47200	26900	1.8
4	0.8:1	48	-	44300	24400	1.8
5	0.9:1	12	TFMI	93700	32300	2.9
6	0.9:1	6	TFMI	84800	39300	2.0
7 <sup>c</sup>	0.9:1	6	TFMI	62600	36800	1.7
8	0.9:1	6	TfOH	46100	24900	1.8
9	0.9:1	6	DABCO	24400	16100	1.5
10	0.9:1	6	DBTDL	35800	21100	1.7
11 <sup>d</sup>	0.9:1	6	-	86900	36900	2.4

**Table 5.2:** <sup>a</sup> Unless otherwise indicated, all the reactions were performed under solvent free conditions, using a Schlenk tube equipped with magnetic stirrer. <sup>b</sup> Determined from SEC (in HFIP) using polystyrene as standard. <sup>c</sup> TFMI (2 mol%) was used. <sup>d</sup> Reaction performed at 100°C.

## 4. Kinetics studies

Some kinetic studies were also undertaken on the PIDA-mediated thermoplastic PU synthesis to gain more insight into the mechanism of the process and search for optimal reaction conditions. For this study, mechanical stirrer was chosen to ensure a more uniform mixing throughout the studies. The reaction was conducted under continuous N<sub>2</sub> flow. Samples were drawn from the reaction mixture at interval of time and analyzed using <sup>1</sup>H NMR, SEC and FTIR. Information on the oxamic acid conversion, urethane linkage formation and molecular weight evolution as a function of time and temperature were determined.

### 4.1. Kinetic studies on the oxamic acid conversion/urethane linkage formation as a function of time

<sup>1</sup>H NMR was used to monitor bis-oxamic acid **58a** consumption and urethane linkage formation during the polymerization. Oxamic acid conversion was quantified by integration of the two methylene groups adjacent to the oxamic acid function (3.1 ppm) which showed an upfield shift (2.9 ppm) as it was converted into urethane (Figure 5.4). Also, urethane linkage formation was quantified by integrating the peak around 4.1ppm. The peak around 1.2 ppm due to the four protons (two CH<sub>2</sub>) at the middle of the bis-oxamic acid carbon chain was used as an internal standard.

Conversion of oxamic acid **58a** appeared to be fast, taking only about 2-3h to hit a plateau (Figure 5.5, **A**). Likewise, urethane linkage formation evolved in a similar manner (**B**), suggesting that, probably there is no very slow intermediary steps involved between the oxamic acid conversion and urethane formation. Meanwhile, it is important to note that the urethane linkage include polymers

having long chains, oligomers and even dimers that would later join to form longer polymer chains since polycondensation of diisocyanates and polyols involves a step-growth mechanism.<sup>179</sup>

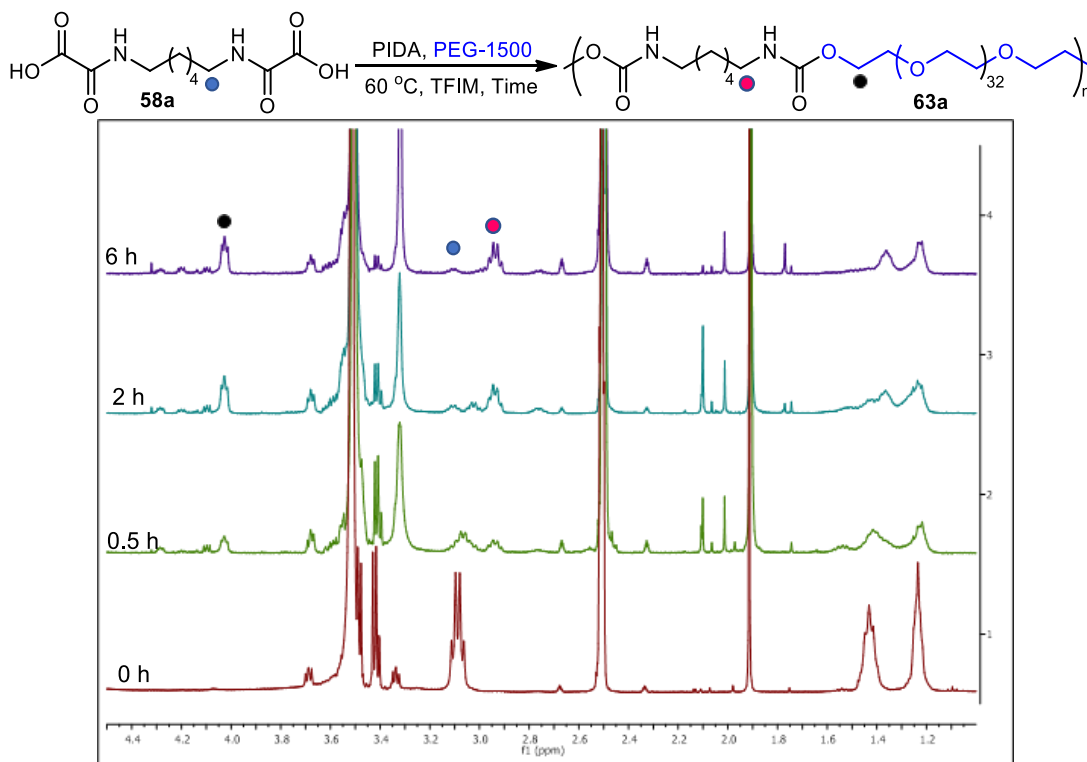


**Figure 5.4:** <sup>1</sup>H NMR monitored oxamic acid **58a** conversion and urethane linkage formation during PIDA-mediated bis-oxamic acid decarboxylation

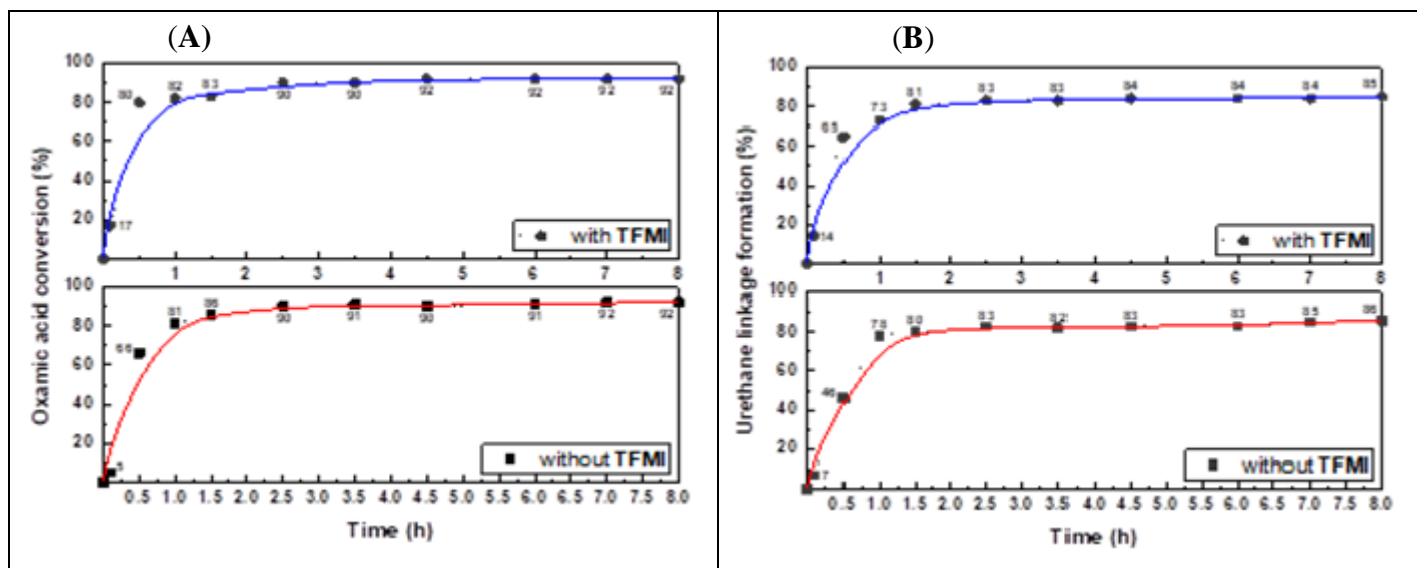


**Figure 5.5:** Oxamic acid conversion (A) and urethane linkage formation (B) at 70°C during thermoplastic PU synthesis from bis-oxamic acid

Furthermore, effect of temperature on the polymerization was also studied. The polymerization was conducted using the optimal conditions determined earlier but varying the temperature: 50, 60 and 70°C. Going below this temperature range was not feasible due to the melting point range of PEG-

<sup>179</sup> A. D. Padsalgikar, *Plastics in Medical Devices for Cardiovascular Applications*, Elsevier Inc. Oxford, 2017. pp 2-3.

1500 (43-49°C). The reaction was performed again in bulk conditions. It was shown that temperature has great influence on the polymerization as indicated by the rate of bis-oxamic acid conversion (Figure 5.6, A) and urethane linkage formation (B). The reaction progressed appreciably fast at 60 and 70°C, taking about 3h for oxamic acid conversion and urethane linkage formation to reach a maximum peak. However, the reaction was significantly slower at 50°C and took up to 12h to attain saturation (data not shown).

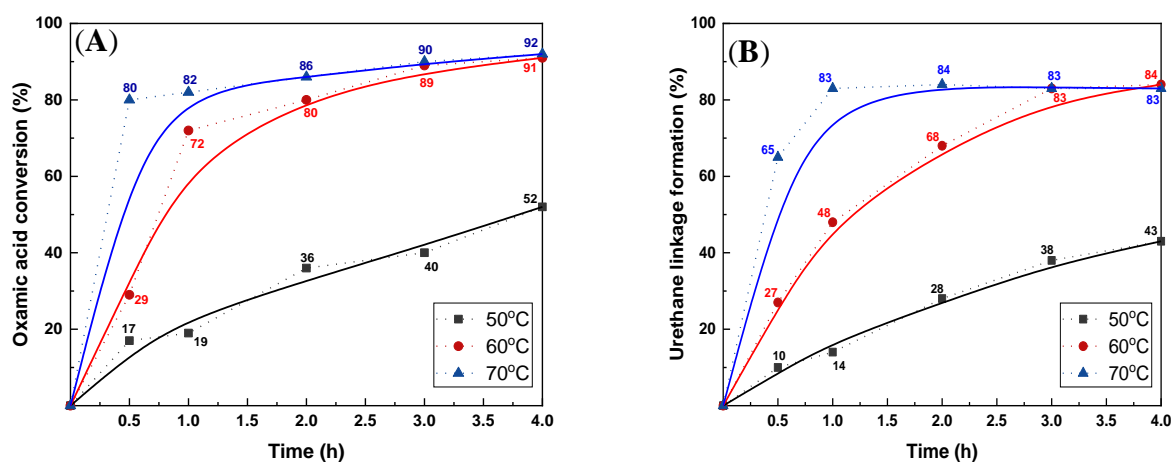


**Figure 5.6:** Effect of temperature on oxamic acid conversion (A) and urethane linkage formation (B) during PU synthesis from bis-oxamic acid **58a**

#### 4.2. Molecular weight evolution during the kinetic studies

The evaluation of molecular weight and polydispersity during the kinetic study was also monitored by SEC (Figure 5.7, Table 5.3). It was shown that molecular weight and polydispersity evolved with time. The SEC trace clearly showed the gradual conversion of the polyol (PEG-1500) to PUs as the reaction progressed (Figure 5.7). PUs formation became obvious on SEC at about 1.5h, as the PEG-1500 apparently disappeared after about 12h. The retention time of the polymers gradually decreased as the molecular weight evolved, and this is in line with the principle of Size Exclusion Chromatography (SEC). Smaller molecules are trapped within the pores on the column beads, thereby taking a longer time to elute while larger molecules elute faster since they cannot pass into many pores in the column.<sup>180</sup> It was shown in Table 5.3 that molecular weight of the polymers reached near saturation in 12h without the TFMI. However, with TFMI (5 mol%), the reaction was monitored only for 8h as the mixture solidified and could not be stirred further. Maybe the reaction was not compatible with the continuous N<sub>2</sub> flow or some impurities present in the flow interfered with the polymerization.

The results of these kinetic investigations using mechanical stirrer have provided some useful insight into the polyurethane synthesis using oxamic acids, especially the rate of monomer conversion and molecular weight evolution. However, molecular weights of PUs obtained from the mechanical

<sup>180</sup> S. Paul-Dauphin, F. Karaca, T. J. Morgan, M. Millan-Agorio, A. A. Herod, R. Kandiyoti, *Energy and Fuels* **2007**, *21*, 3484-3489.

stirring under continuous N<sub>2</sub> stream were lower compared to the ones got using a closed system discussed earlier. Hence, we chose to use the optimal conditions determined earlier with a closed system (Table 5.2, entry 6).

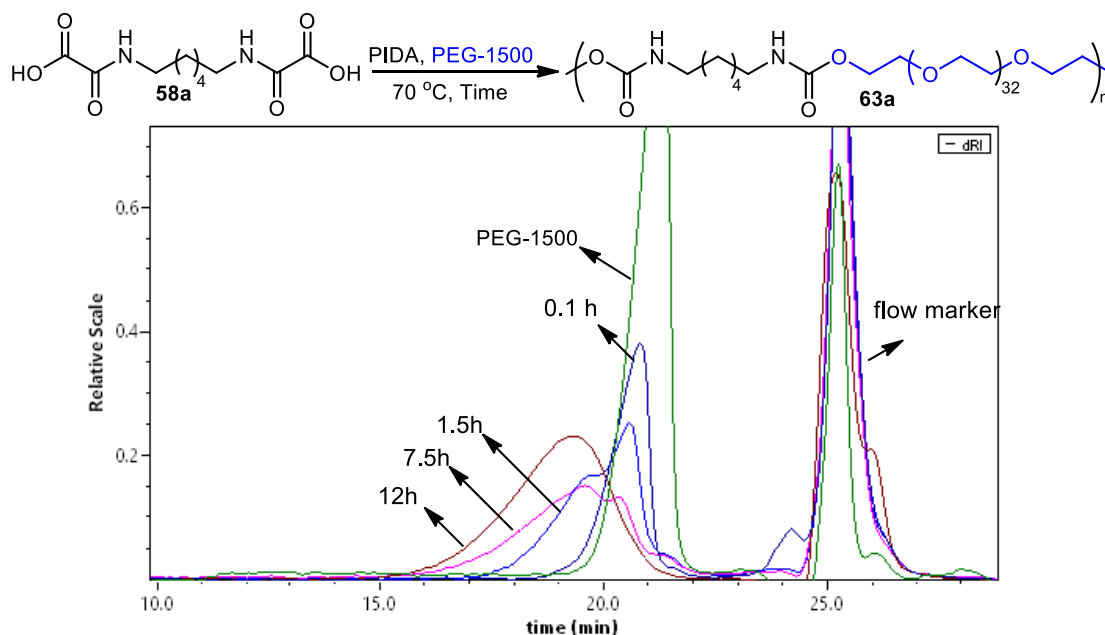


**Figure 5.7:** SEC (in HFIP) trace of molecular weight evolution during the synthesis of PU **63a** from bis-oxamic acid **58a** as a function of the time.

S/No.	Time (h)	Mw (kDa)	Mn (kDa)	Đ (Mw/Mn)
1	0.1	11.1	10.0	1.1
2	0.5	20.1	14.6	1.4
3	1.5	23.3	16.0	1.5
4	2.5	27.8	16.3	1.7
5	4.5	26.4	17.8	1.5
6	6.5	27.7	17.6	1.6
7	7.5	32.5	18.2	1.9
8	12	40.4	23.7	1.7
9	60	42.2	23.1	1.8

**Table 5.3:** SEC (in HFIP) monitored molecular weights evolution during the synthesis of PU **63a** from bis-oxamic acid **58a** as a function of the time. **58a** (1 eq.), PEG-1500 (0.9 eq.), PIDA (2.5 eq.). Mechanical stirrer under continuous N<sub>2</sub> flow. (Note: 1.0 kDa = 1000 g/mol).

Time (h)	Mw (kDa)	Mn (kDa)	Đ (Mw/Mn)
0.1	15.0	12.9	1.2
0.5	20.3	14.4	1.4
1.0	22.7	15.5	1.5
2.0	23.9	15.4	1.6
3.0	28.6	17.5	1.6
4.0	31.4	18.1	1.7
6.0	34.2	21.1	1.6
8.0	79.0	30.0	2.7

**Table 5.4:** SEC (in HFIP) monitor of molecular weight evolution during the synthesis of PU **63a** from bis-oxamic acid **58a** as a function of the time. TFMI (5 mol%), **58a** (1 eq.), PEG-1500 (0.9 eq.), PIDA (2.5 eq.). Mechanical stirrer under continuous N<sub>2</sub> flow.

## 5. Investigation of thermal behavior of the bis-oxamic acid derived PUs

The thermal behavior of PU **63a** from bis-oxamic acid **58a** was analyzed alongside its counterpart prepared following the diisocyanate route using Thermogravimetric Analysis (TGA) and Differential Scanning Calorimetry (DSC). TGA primarily gives information on the thermal stability<sup>181</sup> of polymers while other thermal behaviors including melting point and glass transition temperature can be accessed from DSC analysis.

The bis-oxamic acid PU was prepared using the optimal conditions: 0.9:1 mole ratio of polyol/bis-oxamic acids, 5mol% TFMI, 2.5 eq. of PIDA, 70°C and 6h (Table 5.2. entry 6). DSC revealed a melting temperature ( $T_m$ ) of 40.3°C for the bis-oxamic acid derived PU **63a**, which coincided with that of the PU made through the diisocyanate route (40.4°C). Crystalline melting temperature ( $T_m$ ) is useful for identification of polymers.<sup>182</sup> Also, the glass transition temperature ( $T_g$ ) of the bis-oxamic acid PUs was observed around -40.8°C, which is close to that of its diisocyanate counterpart (-48.8°C), though the plateau were not quite conspicuous (Figure 5.8). However, a similar observation was reported by Gao and co-workers<sup>183</sup> for a similar PUs prepared using the classical route.  $T_g$  is a glass-to-rubber transition; a temperature at which amorphous or semicrystalline polymers change from hard to soft.

Furthermore, thermogravimetric analysis (TGA) was used to investigate the thermostability of the PU samples. PU **63a** from bis-oxamic acid **58a** was shown to be thermostable with a  $T_{d5\%}$  of 314°C, which compared favorably with that of the PU issued from the diisocyanate *i.e.* 291°C (Figure 5.9).  $T_{d5\%}$  is the temperature at which 5% weight loss is recorded during thermogravimetric analysis and

<sup>181</sup> A. W. Coats, J. P. Redfern, *Analyst*, **1963**,88, 906-924.

<sup>182</sup> A. Rudin, P. Choi: in *The Elements of Polymer Science and Engineering*, Elsevier Inc., 3<sup>rd</sup> Ed., 2013, 149-229.

<sup>183</sup> H. Fu, H. Gao, G. Wu, Y. Wang, Y. Fan, J. Ma, *Soft Matter* **2011**, 7, 3546-3552.

is usually used as an index of thermostability.<sup>184</sup> The similarities in the thermal behavior of the PU derived from bis-oxamic acid and that of commercial diisocyanate is also a confirmation of their structural similarities.

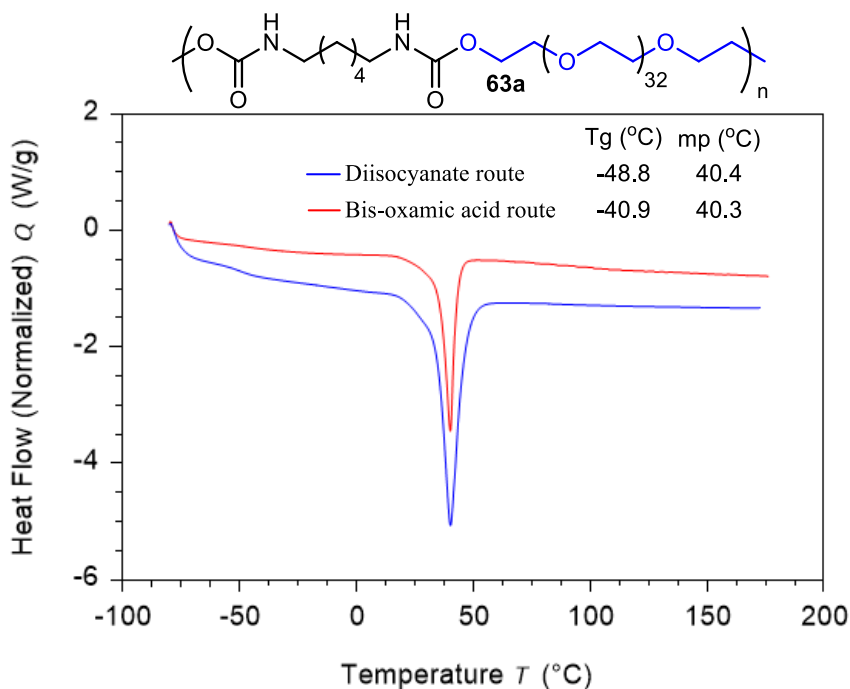


**Figure 5.8:** DSC comparing the thermal behavior of bis-oxamic acid (red) and diisocyanate (blue) derived PUs.

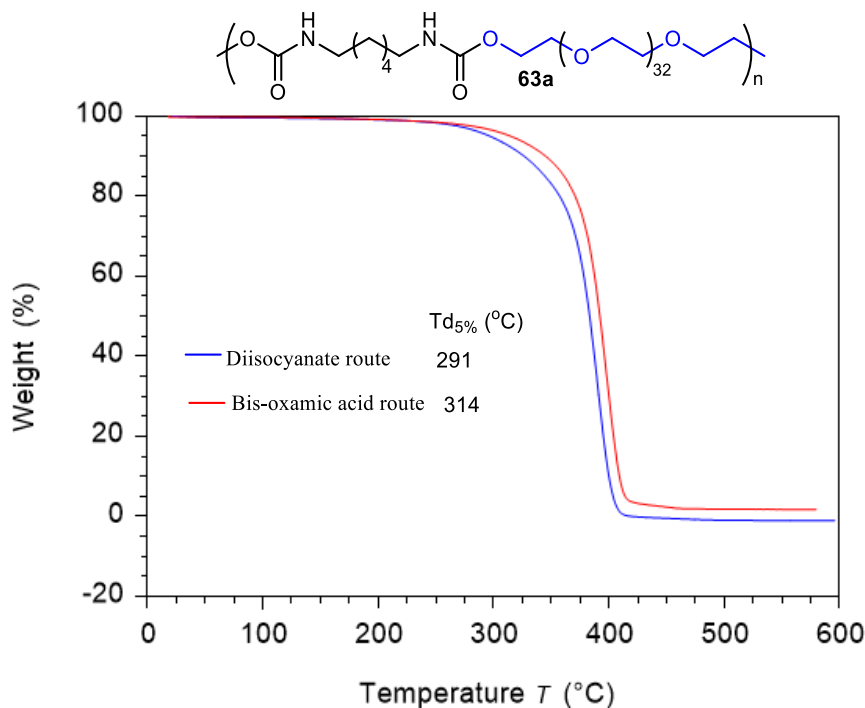


**Figure 5.9:** TGA comparing the thermal behavior of bis-oxamic acid (red) and diisocyanate (blue) derived PUs.

<sup>184</sup> a) X. Wang, B. Li, J. Peng, B. Wang, A. Qin, B. Z. Tang, *Macromolecules* **2021**, *54*, 6753–6761. b) H.-J. Han, S. Zhang, R.-Y. Sun, J.-H. Wu, M.-R. Xie, X.-J. Liao. *Chin. J. Polym. Sci.* **2016**, *34*, 378–389.

## 6. Thermoplastic PUs from different bis-oxamic acids

Excited about these results, we extended this new non-phosgene route to PUs using additional three bis-oxamic acids **58b-d**, PEG-1500 as the polyol and applying the optimal conditions determined earlier. All the bis-oxamic acids were shown to be competent monomers for the polymerization, delivering the corresponding PUs **63b-d** with molecular weight ranging from 32200 to 95700 g/mol and polydispersity between 1.6 and 2.3 (Table 5.5). The SEC traces of the thermoplastic PUs are displayed in Figure 5.10, 5.13 and 5.16. It was observed however that the molecular weight of PUs **63d** obtained from aromatic bis-oxamic acid **58d** was relatively modest compared to the aliphatic counterparts. This probably could be due to less stability of the bis-oxamic under the reaction conditions; it has been shown that oxamic acids from benzylamines tend to oxidize at the benzylic position to form the corresponding aldehyde.<sup>185</sup> However, only trace of (supposedly) aldehyde peak (10 ppm) was observed in the <sup>1</sup>H NMR of the crude PU (data not shown).

Furthermore, the <sup>1</sup>H NMR spectra of the thermoplastic PUs from various bis-oxamic acids clearly showed urethane linkage formation around 4.1 ppm, which is typical for PUs derived from PEG polyols (Figure 5.11, 5.14, 5.17). The structures of the PUs were also confirmed by FTIR analysis, indicating the C=O vibration typical of PUs at about 1700 cm<sup>-1</sup> (Figure 5.12, 5.15, 5.18).

Thermal behavior of the various PU samples were studied using TGA and DSC. TGA indicated that the PUs with aromatic ring **63d** expectedly exhibited the highest thermal stability with Td<sub>5%</sub> of 341°C compared to the aliphatic PUs with Td<sub>5%</sub> between 277 and 314 (Table 5.5, Figure 5.19). This could be due to the fact that aromatic rings generally exhibit higher resistance to thermal degradation compared to the aliphatic counterpart. A similar trend was also observed for the TGA of the starting materials where the aromatic bis-oxamic acids showed higher thermal stability than the aliphatic ones (Figure S15).

Furthermore, DSC results showed that all PUs prepared from different bis-oxamic acids have melting point (T<sub>m</sub>), indicating that they are all semicrystalline (Table 5.5, Figure 5.20). The sample synthesized from linear bis-oxamic acid **63a** has the highest melting point (40.3 °C), possibly due to a higher molecular packing, which favors intermolecular attractions, including hydrogen bonds, between polymer chains.

---

<sup>185</sup> G. G. Pawar, F. Robert, E. Grau, H. Cramail, Y. Landais, *Chem. Commun.* **2018**, 54, 9337-9340

PU Sample <sup>a</sup>	Bis-oxamic acid	Conv. <sup>b</sup> (%)	M <sub>w</sub> <sup>c</sup> (g/mol)	M <sub>n</sub> <sup>c</sup> (g/mol)	Đ <sup>c</sup> (M <sub>w</sub> /M <sub>n</sub> )	T <sub>d5%</sub> <sup>d</sup> (°C)	T <sub>g</sub> <sup>e</sup> (°C)	T <sub>m</sub> (°C)
<b>63a</b>		94	84800	39300	2.0	314	-40.9	40.3
<b>63b</b>		93	48600	29500	1.7	294	-43.8	32.2
<b>63c</b>		92	95700	38400	2.5	277	-41.6	35.5
<b>63d</b>		91	32200	19600	1.6	341	-43.0	37.0

**Table 5.5:** Thermoplastic PUs prepared from bis-oxamic acids **58a-d** using PIDA-mediated decarboxylation. <sup>a</sup> All reactions were carried out in a Schlenk tube equipped with magnetic stirrer under solvent free conditions. The corresponding bis-oxamic acid (1.0 mmol), PEG-1500 (0.9 mmol.), PIDA (2.5 mmol.) and TFMI (5 mol%) were used. <sup>b</sup> Determined from <sup>1</sup>H NMR. <sup>c</sup> Determined from SEC in HFIP using polystyrene as standard. <sup>d</sup> Determined from TGA, 10°C min<sup>-1</sup> under N<sub>2</sub> atmosphere. <sup>e</sup> Determined from DSC second heating cycle, 10°C min<sup>-1</sup>.

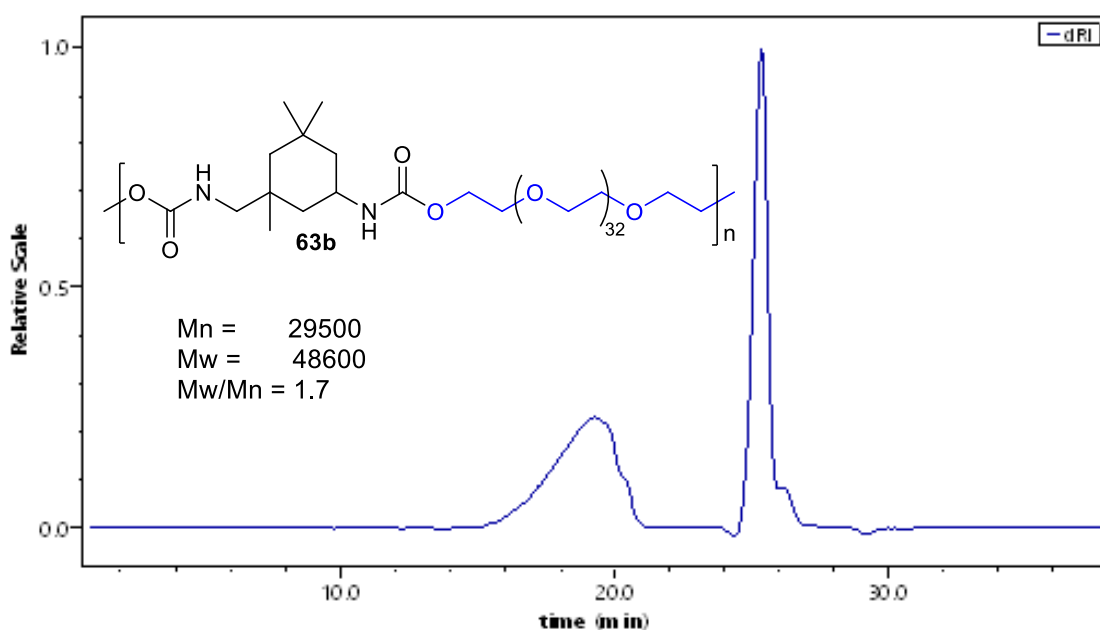


**Figure 5.10:** SEC trace (HFIP) of **63b**

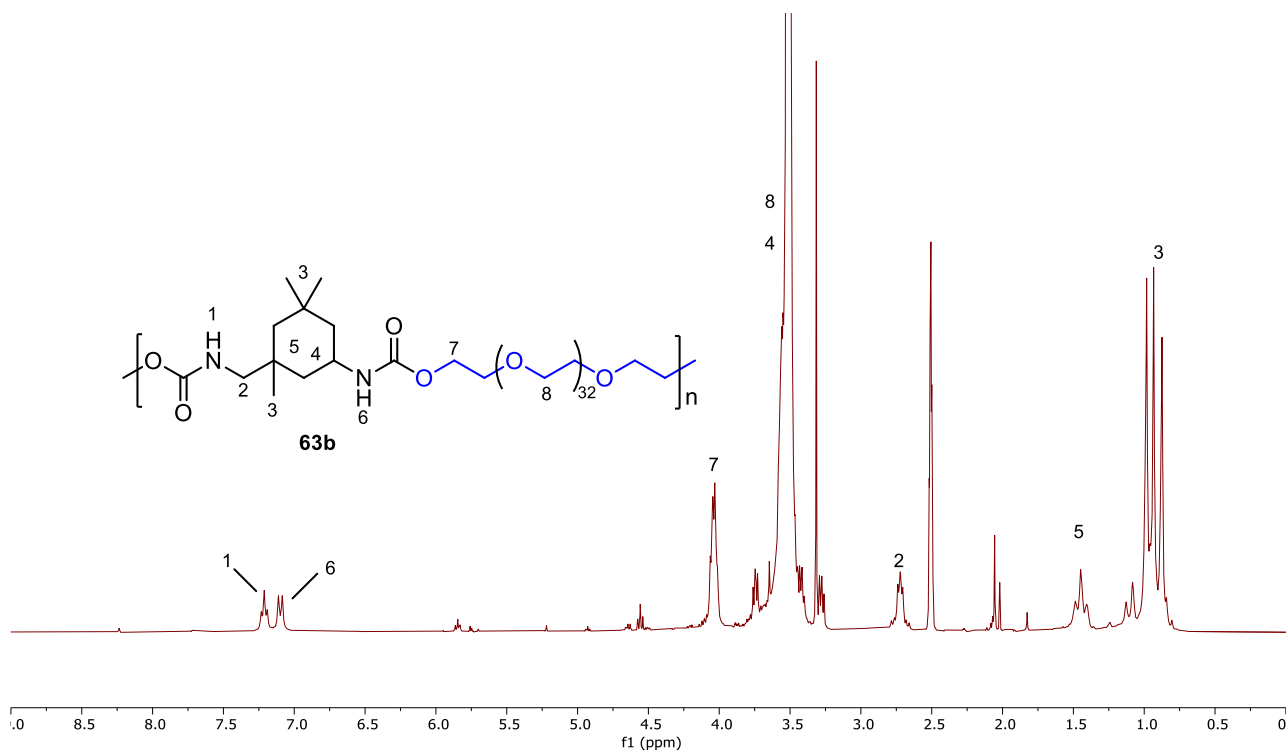


**Figure 5.11: <sup>1</sup>H NMR of 63b**

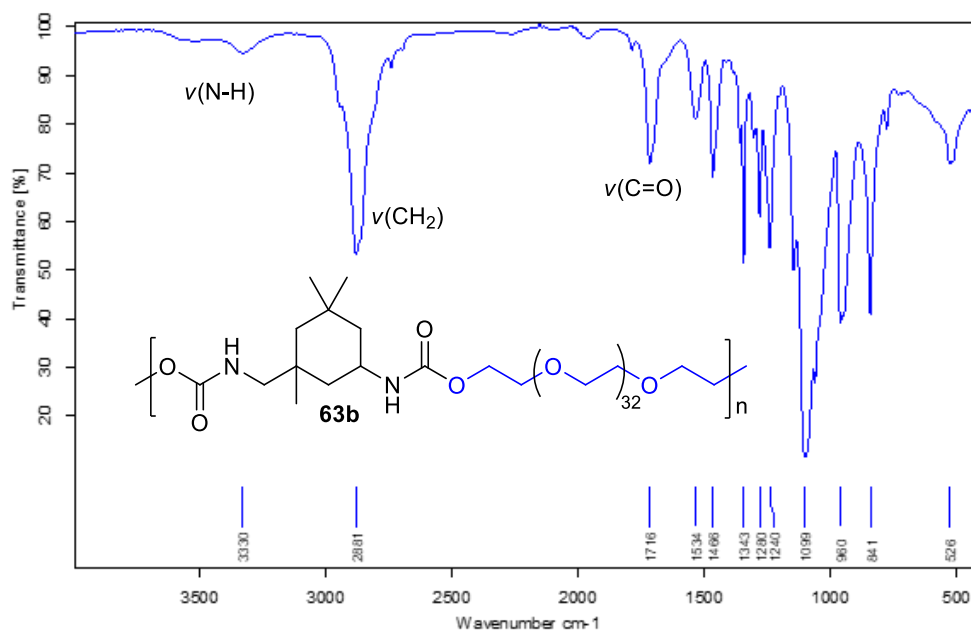


**Figure 5.12: FTIR of 63b**

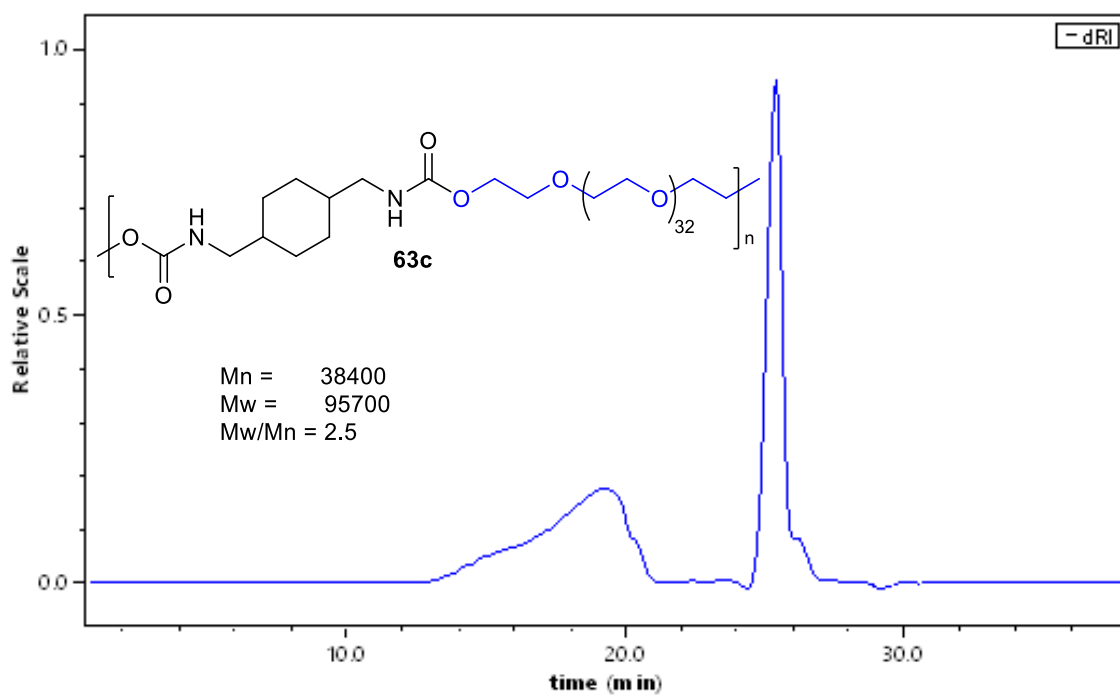


**Figure 5.13:** SEC trace (HFIP) of **63c**

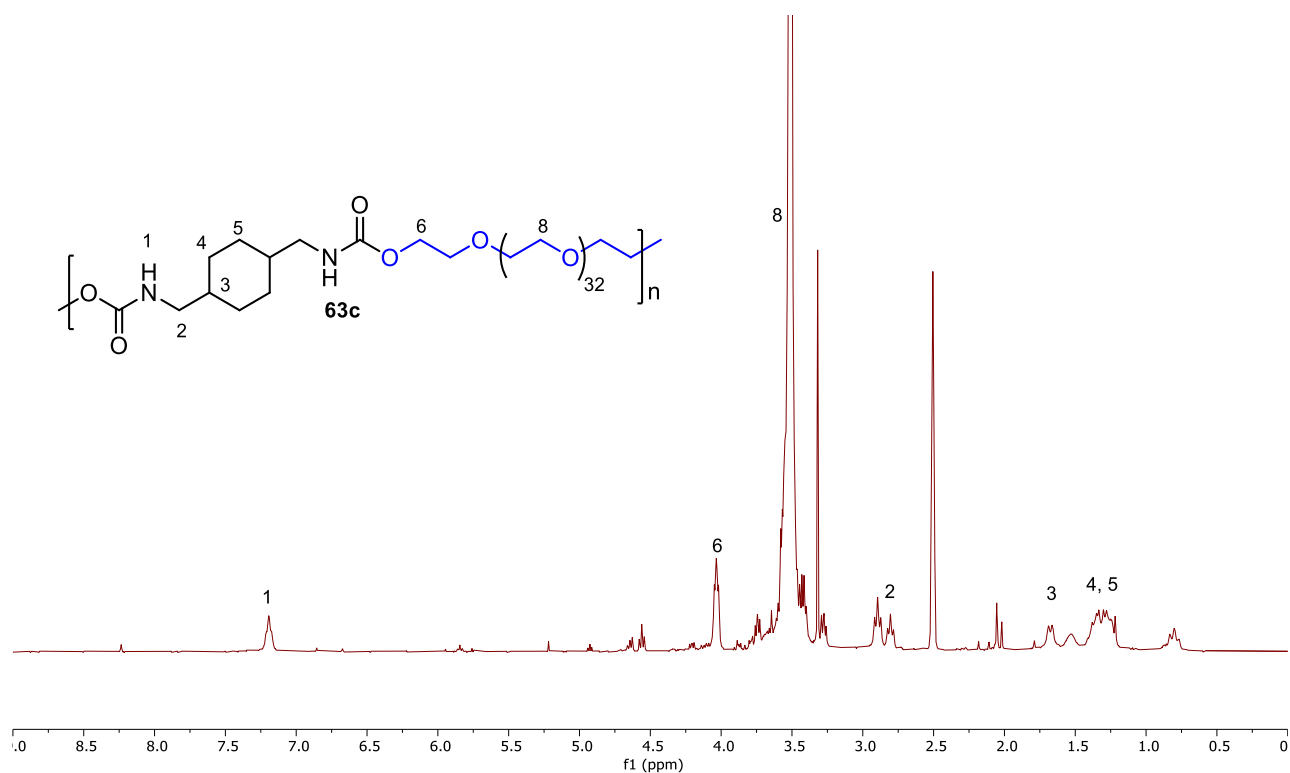


**Figure 5.14:** <sup>1</sup>H NMR of **63c**

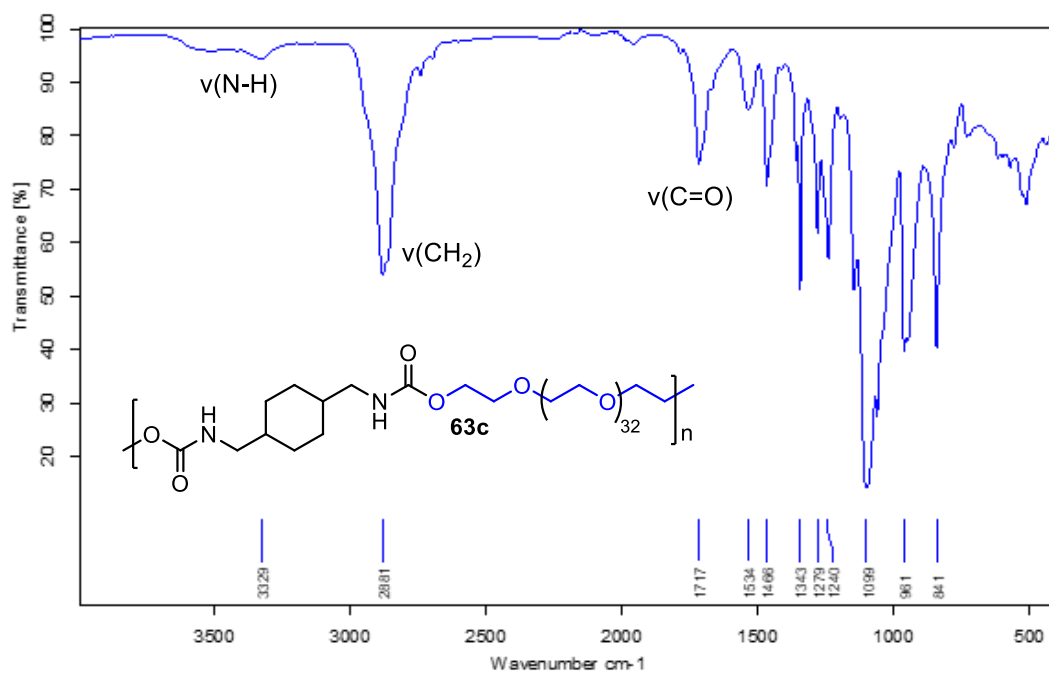


**Figure 5.15: FTIR of 63c**

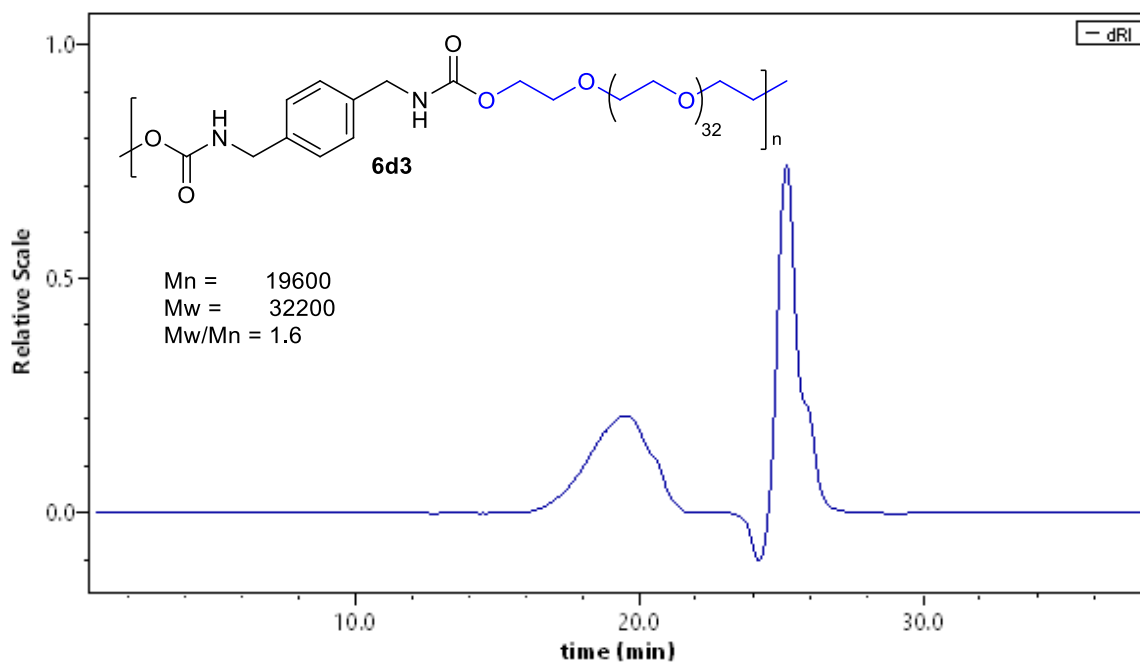


**Figure 5.16: SEC trace (HFIP) of 63d**

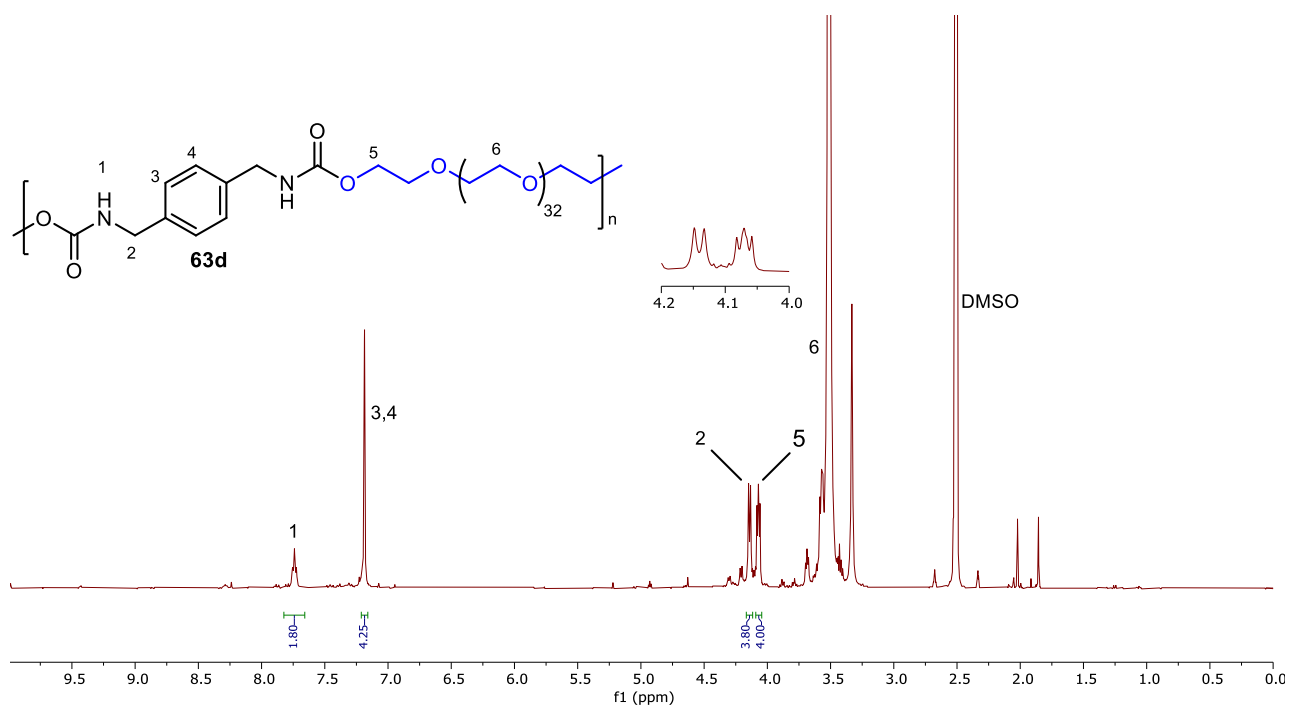


**Figure 5.17:**  $^1\text{H}$  NMR of **63d**

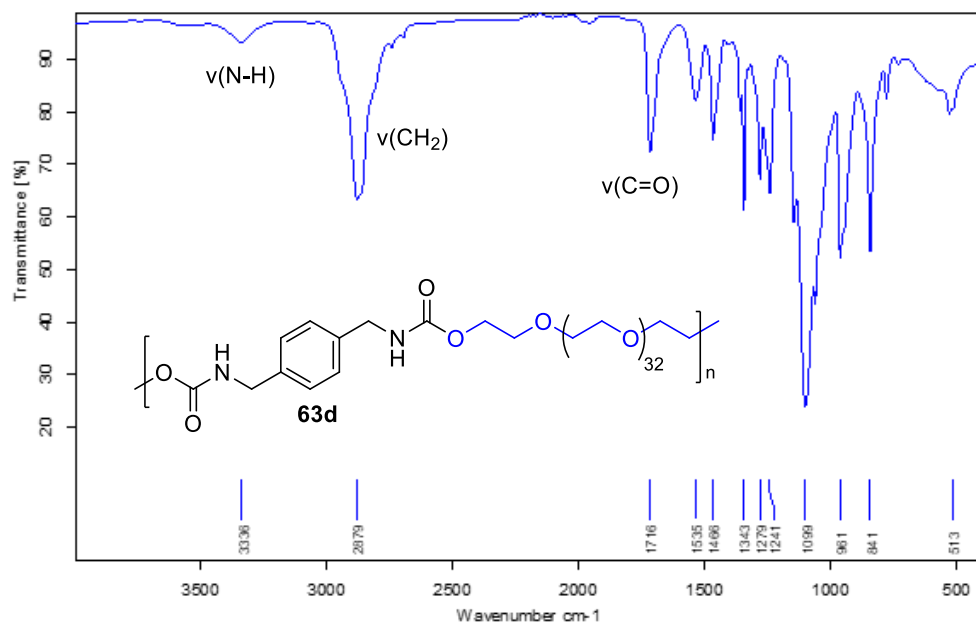


**Figure 5.18:** FTIR of **63d**

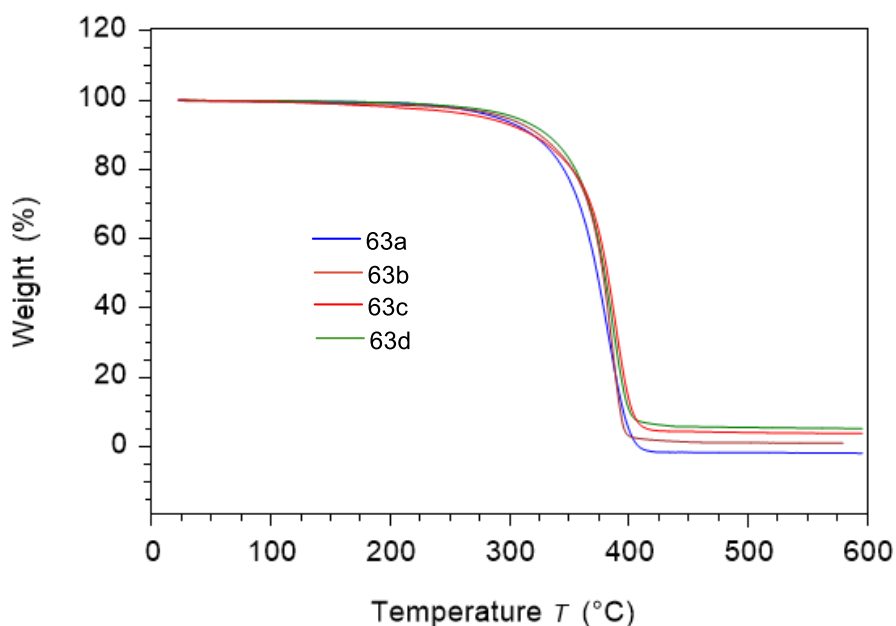


**Figure 5.19:** TGA of the thermoplastic PUs from different bis-oxamic acids **58a-d**

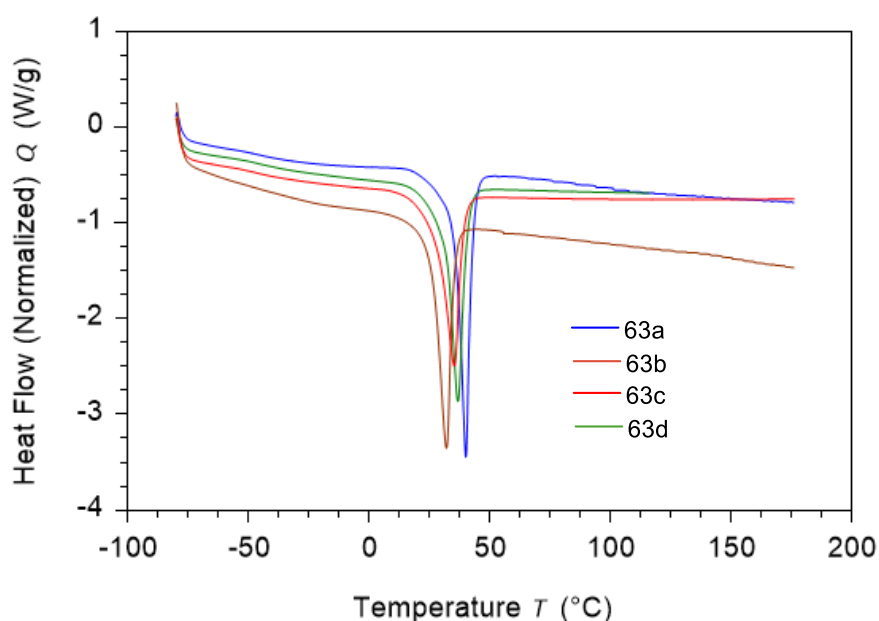


**Figure 5.20:** DSC of the thermoplastic PUs from different bis-oxamic acids **58a-d**

## 7. Thermoplastic PUs from bis-oxamic acid using different polyols/diols

To further test the generality of this new process, different diols were also subjected to the polymerization using **58a** as the model bis-oxamic acid (Table 5.6). All the polymerizations were performed without the TFMI catalyst. The results of these experimental also provided information about the generality of the polymerization without TFMI catalyst. Although TFMI catalyst improves molecular weight of the bis-oxamic acid route, the presence of such strong acid in some applications include PU foam synthesis may not be necessary.

Each PUs were identified by comparing them with their commercial diisocyanate derived counterparts using SEC, FTIR and  $^1\text{H}$  NMR analyses. Expectedly, the size of the diol influenced the values of PUs molecular weights. PUs derived from 1,4-butanediol (Table 5.6, entry 1) and 1,5-pentanediol (entry 2) have molecular weight of 2590 and 2650 g/mol respectively with polydispersity of 1.9. Besides the influence of the short-chain diols, difficulty in solubilizing these PUs from the short-chain diols during the SEC analysis probably contributed to the observed low molecular weights. The PUs were very difficult to be solubilized in any of the solvents used for SEC analysis including DMF, THF, DMSO and HFIP. Although HFIP provided a better solubility of the PUs compared to the other solvents, the additional peaks (in the light scattering signal, Figure S17), probably due to aggregation, was an indication that the PUs were not well solubilized compared to other PUs obtained from polyols that were very soluble in HFIP (Figure S16a). It is important to note that such short-chain diols are usually used in PU synthesis just as chain extenders.<sup>186</sup>

Furthermore, with PTMO-1000 as polyol, PU of molecular weight 46800 g/mol was obtained with polydispersity of 2.3 (entry 3). The SEC trace comparison showed that the obtained PU matched the one obtained from standard diisocyanate route (Figure 5.21). Also,  $^1\text{H}$  NMR confirmed that both PUs have similar structures (Figure 5.22). The molecular weight of PUs from PEG-2060 and PEG-4600 using the bis-oxamic acid route were 58300 and 110000 g/mol respectively (entry 5 and 6), which were very similar to their mates from the commercial diisocyanate as indicated by the SEC traces (Figure 5.23, 5.25); their  $^1\text{H}$  NMR equally confirmed their chemical similarities  $^1\text{H}$  NMR (Figure 5.24, 5.26).

---

<sup>186</sup> T.J. Touchet, E.M. Cosgriff-Hernandez, *Advances in Polyurethane Biomaterials*, Elsevier, **2016**, 3-22.

$$\text{HOOC-CO-NH-(CH}_2\text{)}_4\text{-NH-CO-COOH} + \text{HO-R-OH} \xrightarrow[70^\circ\text{C, 12 h}]{\text{PIDA}} \left( \text{O-CO-NH-(CH}_2\text{)}_4\text{-NH-CO-O-R} \right)_n$$

Entry	Sample <sup>a</sup>	Diol/polyol (name/structure)	Conv. <sup>b</sup> (%)	Mw <sup>c</sup> (g/mol)	Mn <sup>c</sup> (g/mol)	Đ <sup>c</sup> (Mw/Mn)
1 <sup>d</sup>	PU-But.diol	1,4-Butanediol HO-(CH <sub>2</sub> ) <sub>4</sub> -OH	93	2590	1380	1.9
2 <sup>d</sup>	PU-Pent.diol	1,5-Pentanediol HO-(CH <sub>2</sub> ) <sub>5</sub> -OH	94	2650	1390	1.9
3	PU-PTMO-1000	PTMO-1000 H(OCH <sub>2</sub> CH <sub>2</sub> CH <sub>2</sub> CH <sub>2</sub> ) <sub>14</sub> OH	93	46800	20500	2.3
4	PU-PEG-1500	PEG-1500 H(OCH <sub>2</sub> CH <sub>2</sub> ) <sub>34</sub> OH	94	44300	24400	1.8
5	PU-PEG-2060	PEG-2060 H(OCH <sub>2</sub> CH <sub>2</sub> ) <sub>46</sub> OH	93	58300	34200	1.7
6	PU-PEG-4600	PEG-4600 H(OCH <sub>2</sub> CH <sub>2</sub> ) <sub>104</sub> OH	92	110000	54000	2.0

**Table 5.6:** Thermoplastic PUs from bis-oxamic acid **58a** using different diols. <sup>a</sup> All reactions were carried out in a Schlenk tube equipped with magnetic stirrer under solvent free conditions. Bis-oxamic acid **58a** (1.0 mmol), PIDA (2.5 eq.). Diol (0.9 eq.). <sup>b</sup> Determined from <sup>1</sup>H NMR. <sup>c</sup> Determined from SEC in HFIP using polystyrene as standard. <sup>d</sup> Reaction carried out using anhydrous DMF (0.5mL) as solvent.

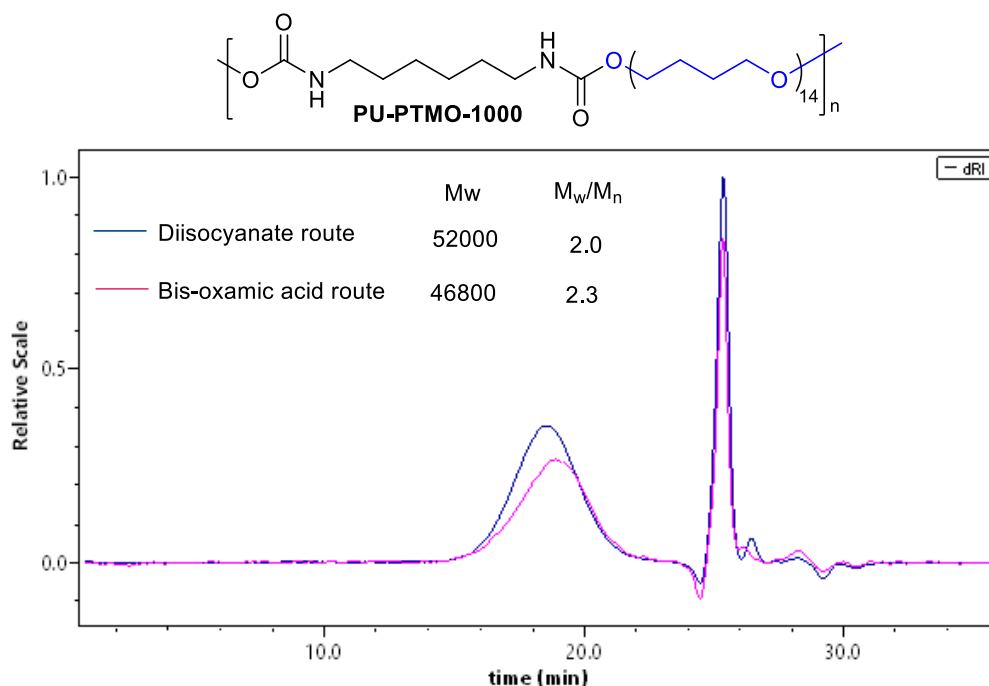


**Figure 5.21:** SEC (in HFIP) comparing PTMO-1000 based PUs obtained from bis-oxamic acid **58a** and diisocyanate.

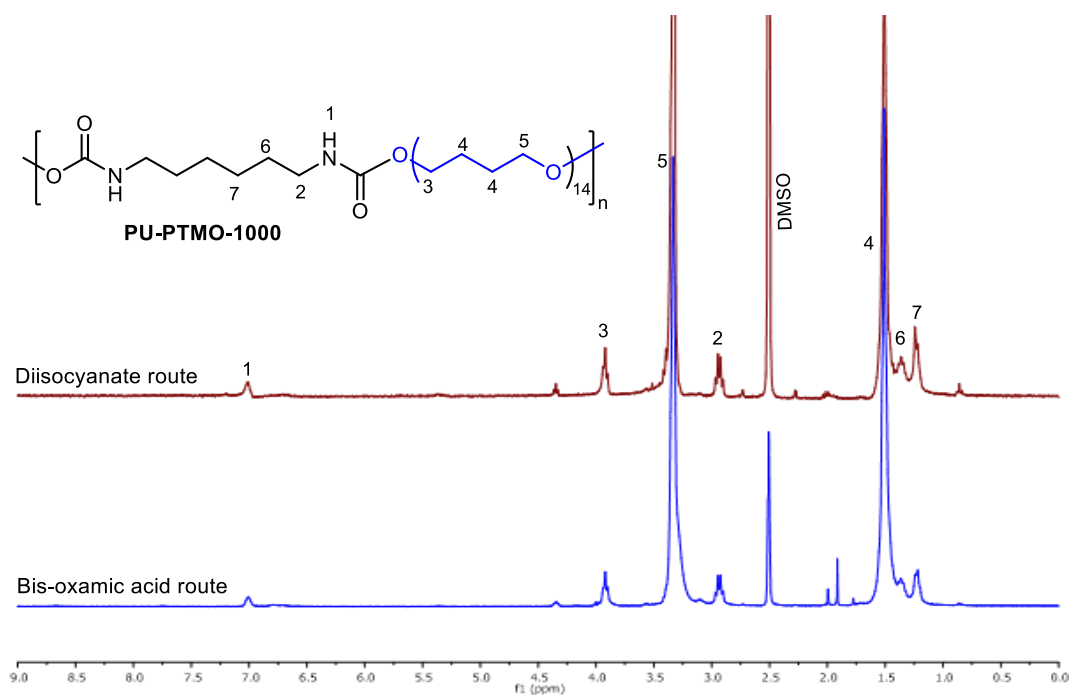


**Figure 5.22:**  $^1\text{H}$  NMR comparing PTMO-1000 based PUs obtained from bis-oxamic acid **58a** and diisocyanate routes

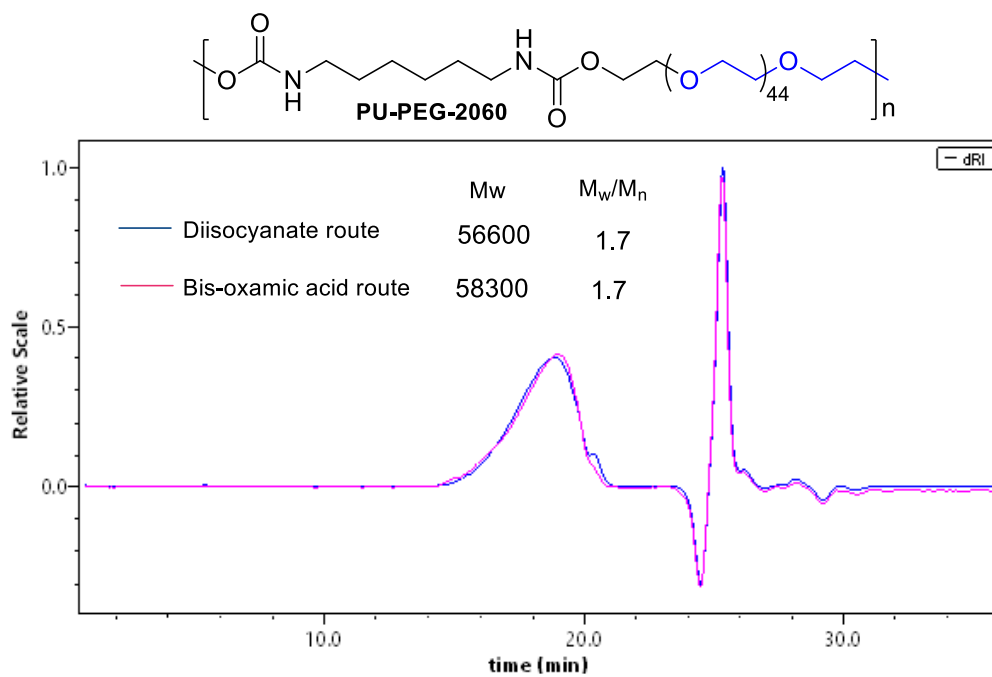


**Figure 5.23:** SEC (in HFIP) comparing PEG-2060 based PUs obtained from bis-oxamic acid **58a** and diisocyanate routes

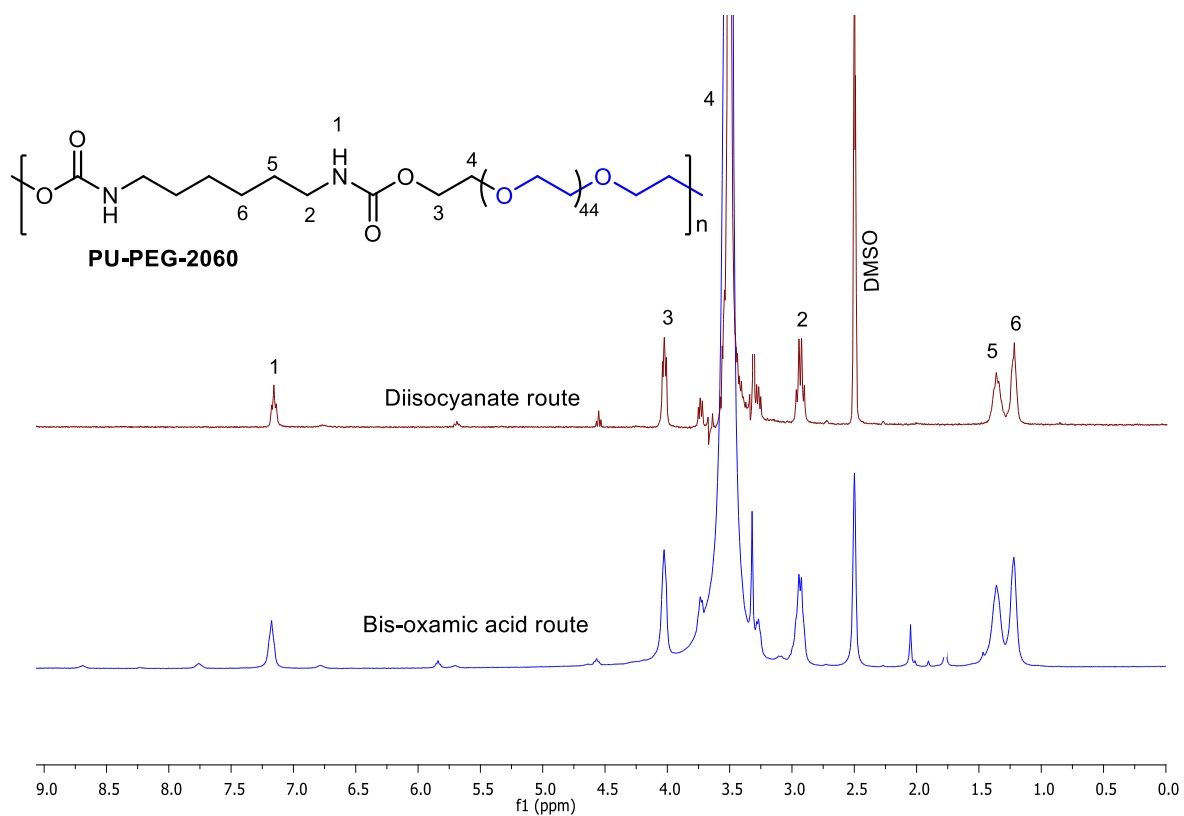


**Figure 5.24:**  $^1\text{H}$  NMR comparing PEG-2060 based PUs obtained from bis-oxamic acid **58a** and diisocyanate routes

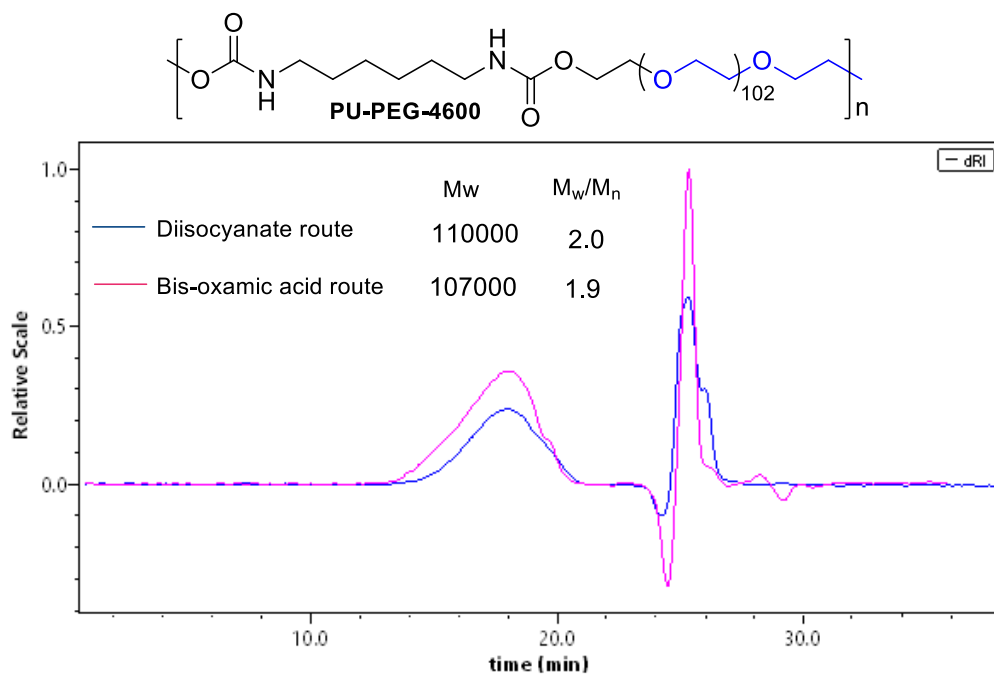


**Figure 5.25:** SEC (in HFIP) comparing PEG-4060 based PUs obtained from bis-oxamic acid **58a** and diisocyanate routes

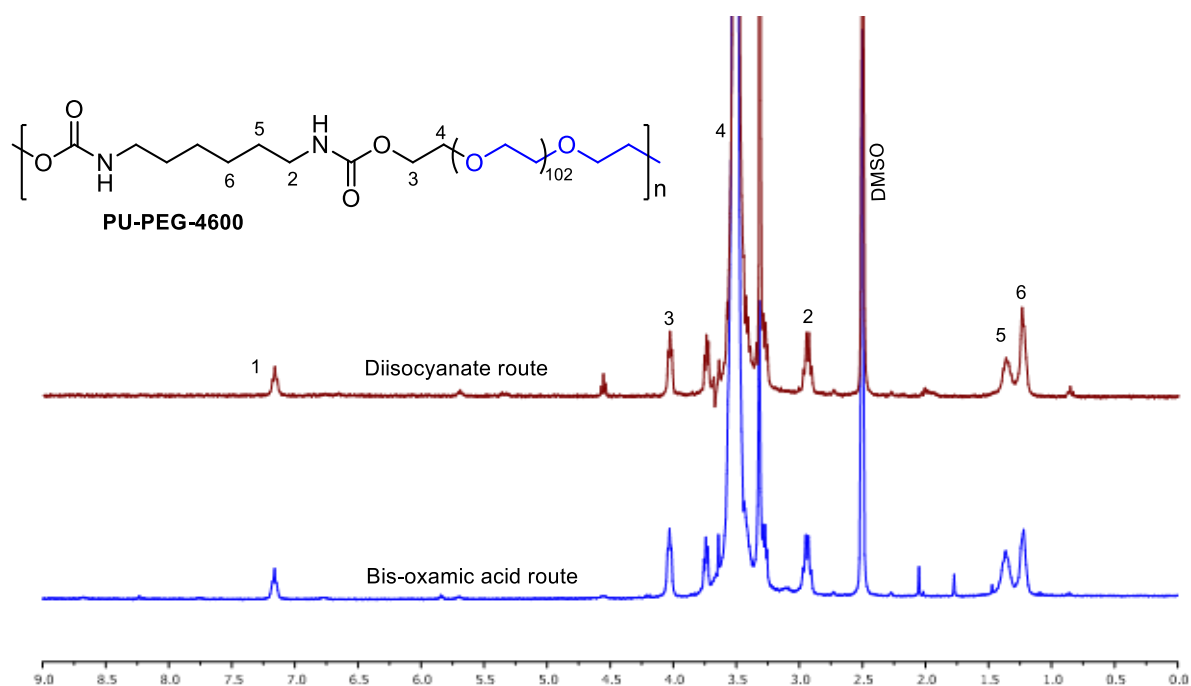


**Figure 5.26:** <sup>1</sup>H NMR comparing PEG-4600 based PUs obtained from bis-oxamic acid **58a** and diisocyanate routes

## 8. Conclusion

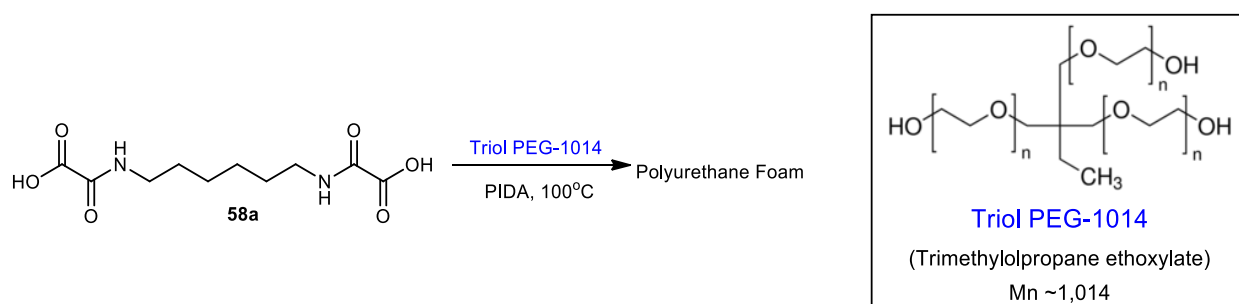
The bis-oxamic route provides thermoplastic PUs that are very similar in Mw, polydispersities and physical properties with those prepared using the Bayer diisocyanate-diol route. This is a very attractive feature as we have demonstrated that the oxidative decarboxylation process allows the one-pot preparation of PUs in the presence of polyols without the need to isolate the putative isocyanate. Given the relatively easy access to bis and polyoxamic acids from the corresponding amines and polyamines, this process constitutes a potent alternative to the Bayer process for the preparation of PUs of high molecular weight.

## PART 2: PIDA-mediated Synthesis of Thermoset PUs by decarboxylation of oxamic acids

### 1. Introduction

Encouraged by our results on thermoplastic PU synthesis from bis-oxamic acids using PIDA-mediated process, we sought to extend this greener procedure to the synthesis of polyurethane foams. In this case, the CO<sub>2</sub> released during the oxamic acid decarboxylation was targeted to serve as a blowing agent. CO<sub>2</sub> is a known blowing agent for PU foam synthesis; in classical method, CO<sub>2</sub> is released for the foaming process by adding water to the reaction mixture to induce hydrolysis of excess isocyanate into unstable carbamic acid, which decomposes to release the gas.<sup>187</sup> In our strategy, the use of water contamination is not required as oxamic acids releases *in-situ* both the isocyanate and CO<sub>2</sub> for the blowing.

As a proof of concept, bis-oxamic acid **58a** and a polyether triol (Triol Peg-1014) were mixed to polymerize under the optimized conditions established earlier, but raising the temperature to 100°C (Scheme 5.3). The reaction mixture evolved through a liquid phase transition, gelation and then formation of PU foam (Figure 5.27). The foam obtained in a closed system (*e.g.* vial sealed throughout the reaction) was very “compact” and did not rise from the liquid state (Figure 5.28, **A**). On the other hand, when the reaction was performed without covering the vial (open system) a foam with highly heterogeneous cells was formed (**B**). Gladly, performing the polymerization in a closed system and then dropping the pressure at the sol-gel transition delivered a flexible polyurethane foam (**C**). Interestingly, the polymerization was very fast at 100°C and took between 10 to 20 min to furnish the expected PU foam. Initial trials on the PU foam synthesis were performed at 70°C, but the process was less efficient, resulting in sticky PU foams probably due to incomplete conversion of the starting material. However, the reaction at 100°C was very fast, as mentioned earlier, it took just about 10 min for the solid starting materials to pass through the liquid transition state and then about another 10 min to crosslink. The obtained foam was cured at 80°C for 2h and thereafter, the curing continued under vacuum for additional 2h during which by-products from PIDA (acetic acid and phenyl iodine) were removed.



**Scheme 5.3:** PU foam synthesis from bis-oxamic acid **58a** and triol-PEG-1014 using PIDA-mediated decarboxylation procedure.

<sup>187</sup> a) F. Monie, T. Vidil, B. Grignard, H. Cramail, C. Detrembleur, *Mater. Sci. Eng. R.* **2021**, *145*, 100628. b) F. Monie, B. Grignard, J.-M. Thomassin, R. Mereau, T. Tassaing, C. Jerome, C. Detrembleur, *Angew. Chem. Int. Ed.* **2020**, *59*, 17033-17041.

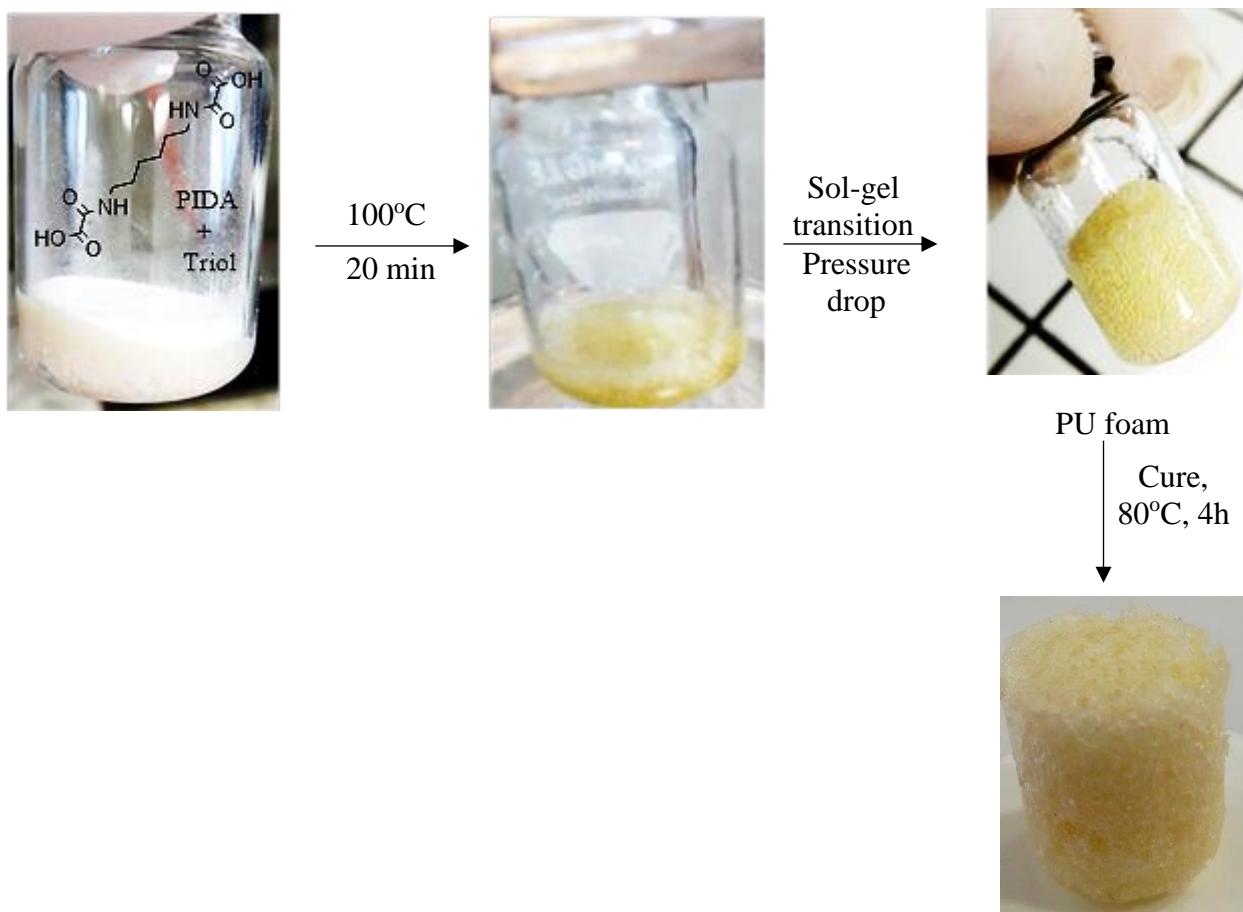


**Figure 5.27:** PU foam synthesis from bis-oxamic acid **58a** and triol-PEG-1014 showing different transitions

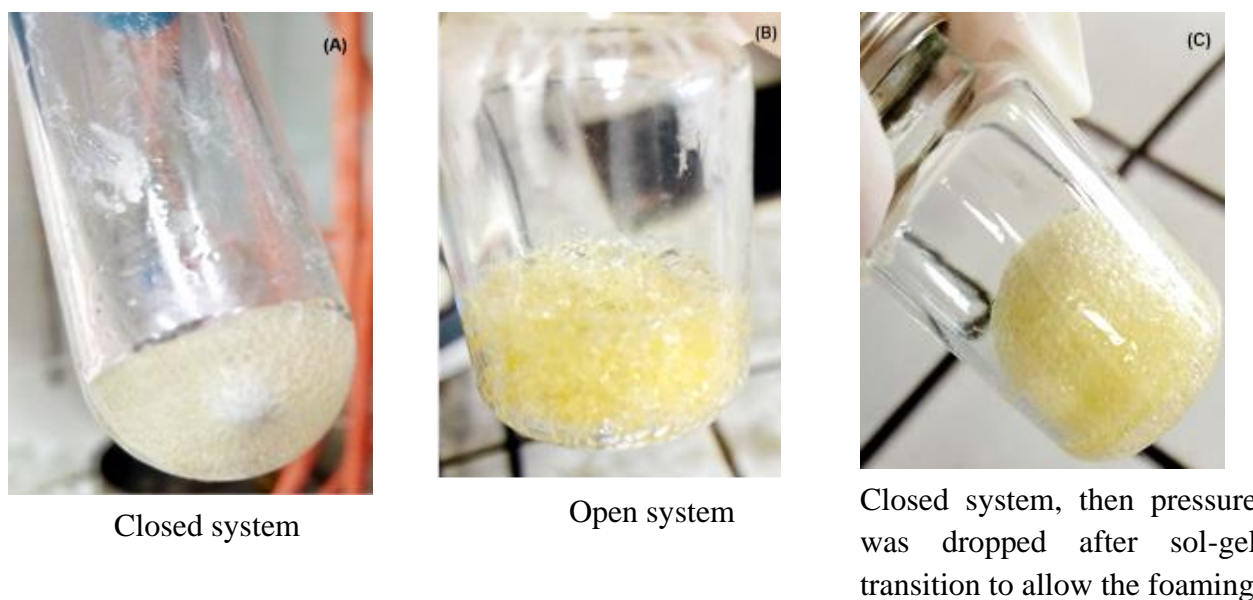


**Figure 5.28:** PU foam synthesis from bis-oxamic acid **58a** and triol-PEG-1014 under different reaction conditions.

## 2. Swelling test

A simple swelling test was carried out on the foam sample to ascertain its level of crosslinking. A piece of the foam (7.94 mg) was soaked in DCM (15 mL) for 20h. The solvent was removed with a pipette, then the swollen foam was rinsed with 10 mL of DCM and finally dried in *vacuo* for 12h. The difference in the mass of the foam before and after the test showed that the polymer was reasonably crosslinked with only 5% soluble fraction of the total mass of the foam (Figure 5.29).

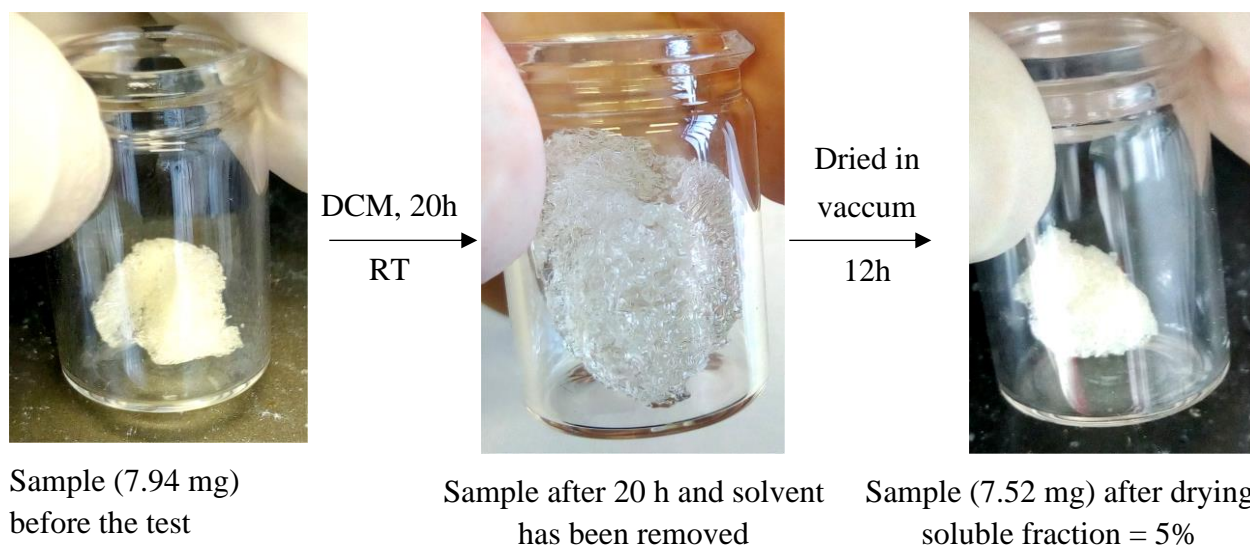


**Figure 5.29:** Swelling test of the synthesized PU-Foam from bis-oxamic acid **58a** and triol-PEG-1014

## 3. Characterization of PU foam from bis-oxamic acid

FTIR analysis of the synthesized PU foam indicated formation of urethane linkages in the PU foam (Figure 5.30). TGA (Figure 5.31) showed that the PU-foam has  $T_{d5\%}$  of 278°C, suggesting that it has reasonable thermal stability. Also, the DSC analysis showed the glass transition temperature of -44.8°C (Figure 5.32).

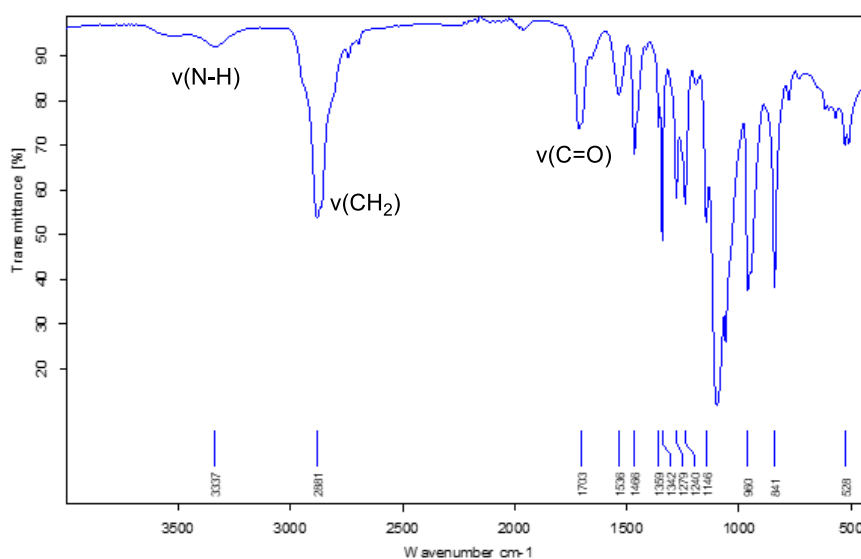


**Figure 5.30:** FT-IR spectrum of the obtained PU foam

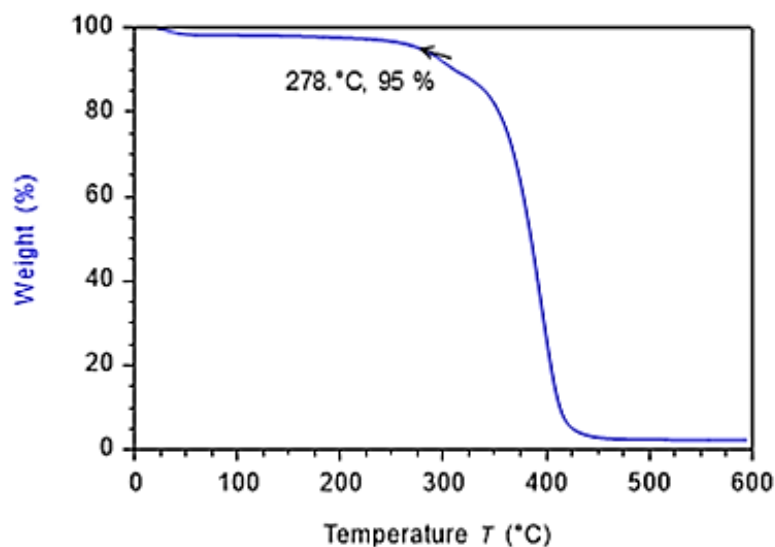


**Figure 5.31:** TGA analysis of PU foam from bis-oxamic acid **58a** and triol-PEG-1014

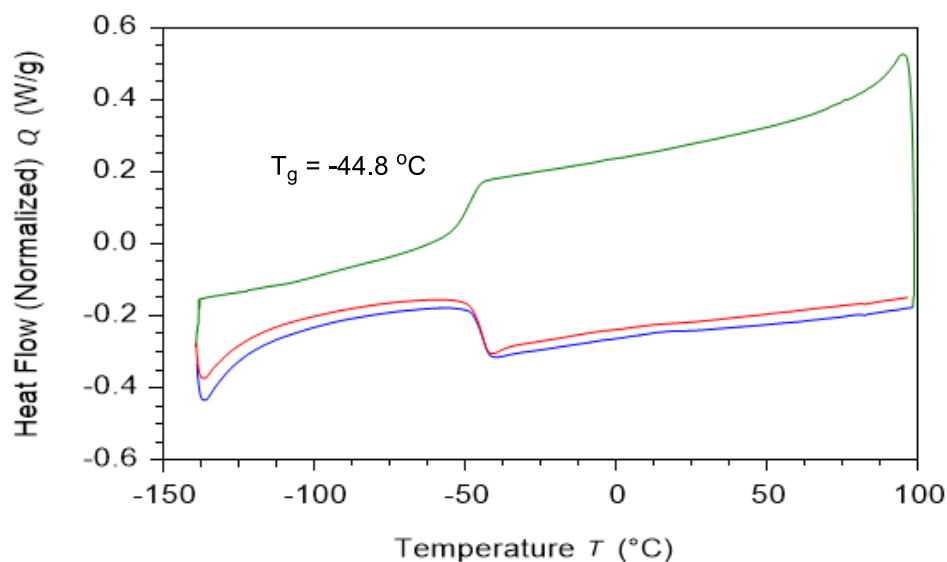


**Figure 5.32:** DSC analysis of PU foam from bis-oxamic acid **58a** and triol-PEG-1014, showing the first and second heating cycles ( $10^{\circ}\text{C min}^{-1}$ ). The glass transition temperature ( $T_g$ ) was determined from the second heating cycle. DSC data is usually taken from the second curve<sup>183,188</sup> since it is considered more accurate and precludes any changes that are not directly caused by the substance under investigation.

## Conclusion

The bis-oxamic route could provide self-blown PU foam whereby the  $\text{CO}_2$  released during the decarboxylation of oxamic acids functioned as blowing agent. Although more optimization processes are still required to determine the full performance of this procedure, swelling test indicated that the

<sup>188</sup> F. Magliozzi, A. Scali, G. Chollet, D. Montarnal, E. Grau, H. Cramail, *ACS Sustainable Chem. Eng.* **2020**, *8*, 9125-9135.

obtained foam has well cross-linked structure, and TGA analysis showed that the sample was thermally stable.

#### 4. Towards Reaction Mechanism of the PIDA-mediated urethane synthesis from oxamic acids

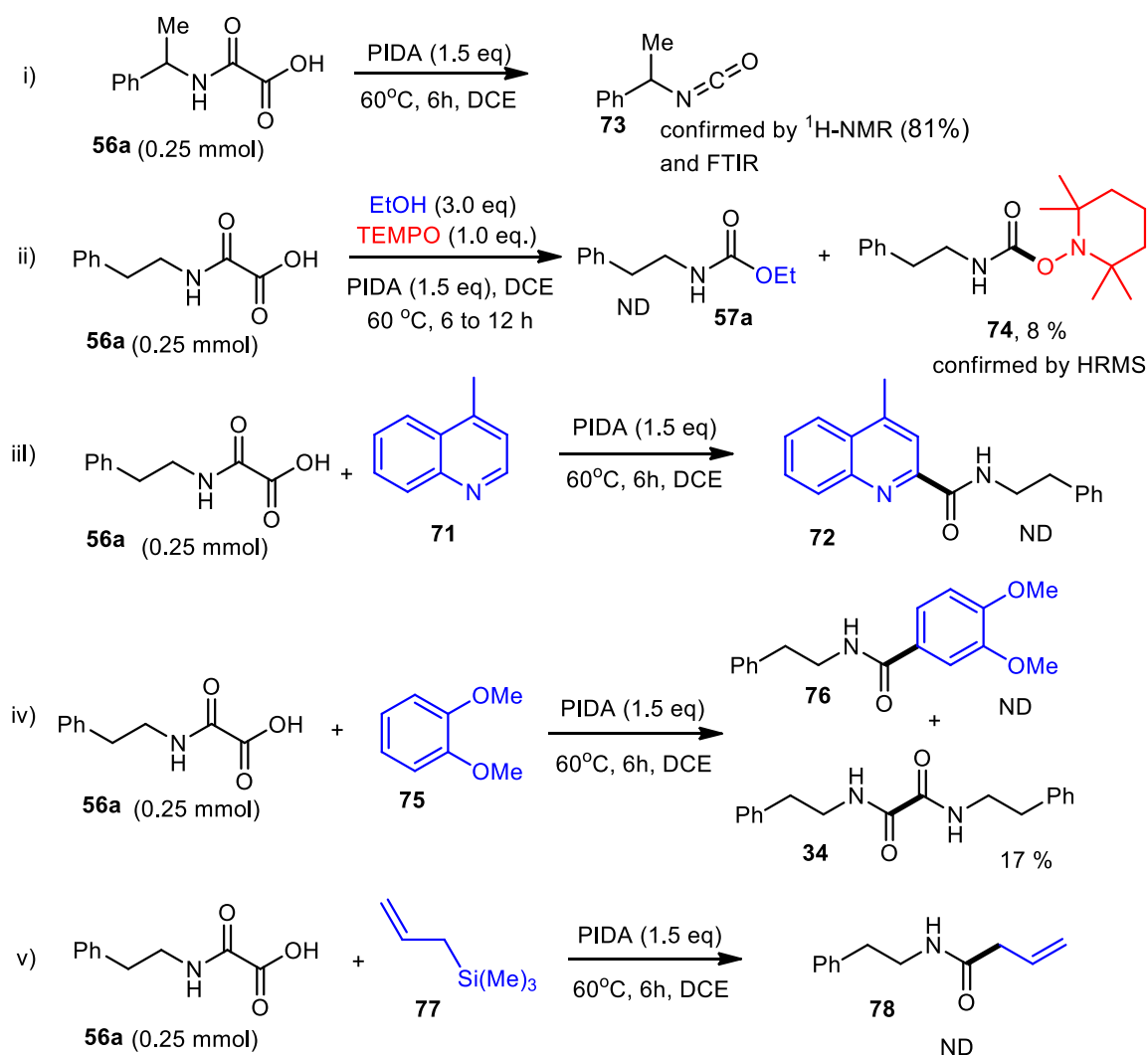
Several intermediates trapping and identification experiments were conducted to gain insight into possible reaction pathway for the PIDA-mediated process. Starting from mono-oxamic acid **56** using 1.5 eq. of PIDA under above reaction conditions, <sup>1</sup>H NMR and FTIR confirmed the *in-situ* generation of isocyanate **73**, which structure was unambiguously assigned through comparison with commercial **73**. In this case, the reaction was performed in the absence of a nucleophile (alcohol) and the crude mixture analyzed (> 90% conversion by <sup>1</sup>H NMR) (Scheme 5.4, **i**). Secondly, the radical nature of the reaction was investigated by using TEMPO as a radical trapping agent. The presence of TEMPO completely quenched the urethane formation (**ii**) and traces of carbamoyl radical-TEMPO adduct **74** was isolated from the reaction mixture confirmed using HRMS. Although the formation of the carbamoyl radical intermediate was assessed by the previous experiment, when the PIDA-mediated oxidation was repeated in the presence of methyl-quinoline **71**, no trace of amide **72** resulting from the addition of a carbamoyl radical onto **71**, was observed. It is worthy of note that this reaction proceeded efficiently using our visible light<sup>189</sup> or NIR light mediated procedures.

Several efforts made to achieve the carbamoylation of heteroarenes using the PIDA-mediated process failed, raising our suspicion that this process probably follows a reaction pathway, which is distinct from the one proposed earlier for our photocatalyzed system.<sup>189</sup>

To further interrogate the possible reaction pathway of this process, and the possible occurrence of a cationic carbamoyl species, intermolecular addition to electron rich arene (veratrole **75**) was tried but the expected amide **76** was equally not observed. The homocoupling product diamide **34** was isolated instead in 17% yield, as confirmed by NMR and HRMS (**iv**), again confirming the formation of the carbamoyl radical which dimerized. The reaction of oxamic acid **56a** with an allylsilane, which was reported to deliver the corresponding amide **78** in 22% with our photocatalyzed system<sup>185</sup> equally failed with this PIDA-mediated process (**v**).

---

<sup>189</sup> A. H. Jatoi, G. G. Pawar, F. Robert, Y. Landais, *Chem. Commun.*, **2019**, 55, 466-469.



**Scheme 5.4:** Intermediate trapping experiments

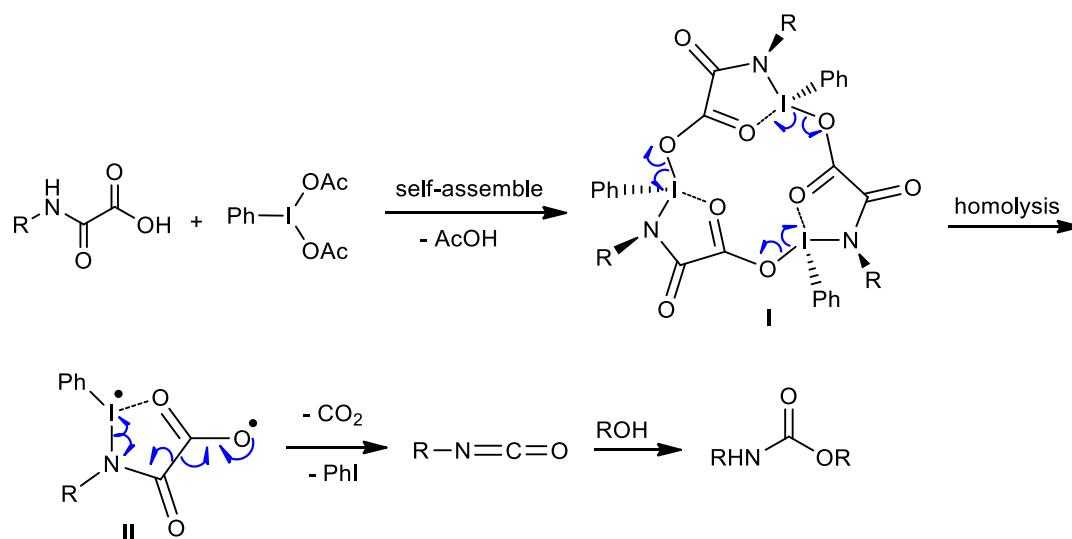
#### 4.1. Proposed mechanism

The mechanism of the PIDA-mediated decarboxylation of oxamic acids likely involves a carbamoyl radical as an intermediate as shown by its trapping by TEMPO. However, the absence of reactivity toward lepidine, while the same reaction is highly efficient using BI-OAc points toward a distinct mechanism with PIDA as compared to BI-OAc. In their recent studies on the decomposition of oxamic acids with PIDA in Heck-type cyclization processes (Scheme 5.5a), Fan and co-workers<sup>190</sup> proposed a mechanism where oxamic acid would react with PIDA to form a trimer **I** that would then decompose homolytically to produce a carbamoyl radical. The formation of such a trimer was proposed based on the occurrence of similar assembly between amino-acids and PIDA.<sup>191</sup>

Although this trimer has not been isolated nor its structure firmly established, the decomposition of a similar trimer **I** could well produce directly the isocyanate through several homolytic cleavages. Evidence for the formation of the isocyanate in the absence of alcohols in our PIDA-mediated process would support such a pathway.

<sup>190</sup> H. Fan, P. Pan, Y. Zhang, W. Wang, *Org. Lett.* **2018**, *20*, 7929-7932.

<sup>191</sup> V. V. Zhdankin, A. E. Koposov, J. T. Smart, R. P. Tykwinski, R. McDonald, A. Moreales-Izquierdo, *J. Am. Chem. Soc.* **2001**, *123*, 4095-4096.

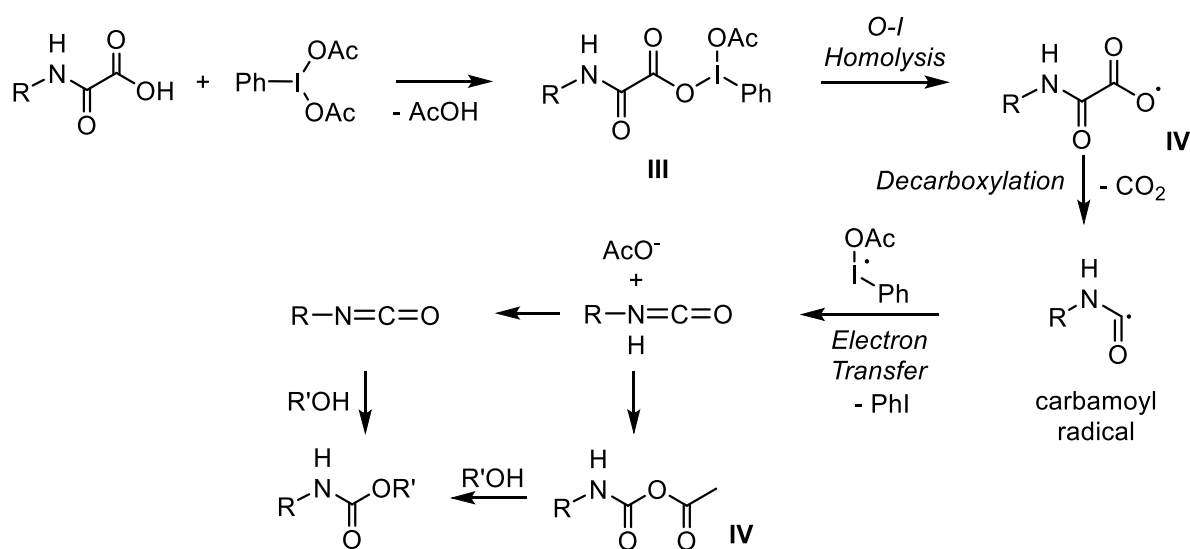


**Scheme 5.5a:** Tentative mechanism A

An alternative pathway not relying on trimer **I** may also be proposed that would be in good agreement with our experimental evidence (Scheme 5.5a). The reaction between PIDA and the oxamic acid would release acetic acid and generates an unstable hypoiodide intermediate **III**, which upon warming would decompose homolytically, leading to a carboxyl radical **IV**. Decarboxylation of the latter would then produce the carbamoyl radical and PhIOAc radical. Electron transfer from the carbamoyl radical to the latter would then afford the protonated isocyanate and PhI. Such an electron transfer is likely much faster than trapping of the carbamoyl radical with TEMPO, explaining the low yield of TEMPO trapping adduct observed. Lifetime of the carbamoyl radical under these oxidative conditions is thus very short also explaining the absence of reactivity toward lepidine. Protonated isocyanate would then react *in situ* with the alcohol R'OH to afford the urethane.

The reaction between an isocyanate and an alcohol is usually quite slow and often requires heating and a catalysis. In our case, we were surprised that in reactions using photocatalysis the addition of the alcohol was quite fast and proceeded at room temperature. This may be explained by the presence of a protonated isocyanate that is more electrophilic than a simple isocyanate or the *in-situ* formation of intermediate **IV** resulting from the addition of acetic acid onto isocyanate. Such an addition is well-known and compounds such as **IV** are generally not stable decomposing into anhydrides and amides upon warming.<sup>192</sup> In the presence of alcohols, **IV** might constitute a better electrophile than isocyanate alone. Experiments are currently on-going to examine this pathway and isolate possible by-products that might suggest the occurrence of this route. This would explain the unexpected reactivity of the *in-situ* generated isocyanates in photocatalyzed and thermal oxamic acids decarboxylations in the presence of alcohols.

<sup>192</sup> a) K. Sasaki, D. Crich, *Org. Lett.* **2011**, *13*, 2256-2259. b) P. Babusiaux, R. Longerey, J. Dreux, *Liebigs Ann. Chem.* **1976**, 487-495.



**Scheme 5.5b:** Tentative mechanism B

## 5. Conclusion

PIDA-mediated oxidative decarboxylation of oxamic acids under mild heating has been revealed. This practically simple procedure relies on the mild thermal activation of PIDA to trigger the decarboxylation of oxamic acids to generate urethanes in excellent yields in one-pot in the presence of alcohols, without isolation of the putative isocyanate intermediate. The method was shown to be competent for the synthesis of thermoplastic polyurethanes using a range of bis-oxamic acids and diols/polyols, furnishing polyurethanes with properties analogous to PU samples made from commercial diisocyanates. Application of this procedure to the preparation of a self-blown PU foam using a bis-oxamic acid and a triol, whereby the  $\text{CO}_2$  released during the decarboxylation process served as blowing agent, was demonstrated with success. High kinetics of this reaction combined with greener starting material make it quite attractive as an alternative procedure for polyurethane synthesis. Process optimization and characterization is ongoing within our group for the PU foam synthesis from oxamic acids.

# Chapter 6

## Urethane synthesis from Oxamic acids Under Electrochemical Conditions

In this project, we equally explored the potential to use organic electrochemistry to mediate single electron transfers during the oxamic acid decarboxylation and thus, simplifying this new non-phosgene route to urethane. Based on related literatures, we envisioned that we could use anodic oxidation to replace the chemical oxidant during oxamic acid decarboxylation, thereby making our reaction simpler.

This chapter is divided into two parts. Part 1 deals with some basic concepts in organic electrochemistry necessary for the understanding of this project. It is however not a comprehensive review of all about organic electrochemistry. Meanwhile some recent reviews in organic electrochemistry are cited for more information.

### PART 1: Basic concepts on Organic electrochemistry

#### 1. Introduction

Organic electrochemistry primarily deals with reduction and oxidation of organic compounds through electron transfer between the substrate and electrodes. There is an increasing interest and a renaissance in organic electrochemistry due to its promising advantages over conventional organic chemistry. First, organic electrochemistry is considered environmentally friendly because it uses electron as a mass-free reagent to replace excess or stoichiometric amounts of chemical oxidants and reductants normally employed in conventional organic reactions. Hence, the procedure holds potential to minimize waste generation during organic synthesis and a recourse to expensive reagents. Electrons serve as both reactants and energy source in this technique thereby ensuring high atom economy. Organic electrochemistry could play a significant role in sustainable chemistry.<sup>193</sup>

Furthermore, studies have shown that organic electrochemistry can facilitate some organic transformations that are rather difficult or impossible with conventional organic chemistry,<sup>194,195</sup> which makes it an interesting complimentary tool for traditional synthetic chemistry. Notably, electron transfer between electrode and organic molecules can lead to polarity reversal (umpolung), facilitating conventionally difficult or impossible reactions.<sup>196</sup> This technique has equally been shown to be promising for late-stage functionalization because of its mild nature and selectivity.<sup>197</sup>

---

<sup>193</sup> a) E. J. Horn, B. R. Rosen, P. S. Baran, *ACS Cent. Sci.* **2016**, *2*, 302–308. b) T. Wirtanen, E. Rodrigo, S. R. Waldvogel, *Adv. Synth. Catal.* **2020**, *362*, 2088–2100. b) T. H. Meyer, L. H. Finger, P. Gandeepan, L. Ackermann, *Trends Chem.* **2019**, *1*, 63–71.

<sup>194</sup> J. Xiang, M. Shang, Y. Kawamata, H. Lundberg, S. H. Reisberg, M. Chen, P. S. Baran *et al.*, *Nature* **2019**, *573*, 398–402.

<sup>195</sup> Y. Jiang, K. Xu, C. Zeng, *Chem. Rev.* **2018**, *118*, 4485–4540.

<sup>196</sup> F. Tang, C. Chen, K. D. Moeller, *Synthesis* **2007**, *21*, 3411–3420.

<sup>197</sup> a) C. Schotten, T. P. Nicholls, R. A. Bourne, N. Kapur, B. N. Nguyen, C. E. Willans, *Green Chem.* **2020**, *22*, 3358–3375. b) S. Mohle, M. Zirbes, E. Rodrigo, T. Gieshoff, A. Wiebe, S. R. Waldvogel, *Angew. Chem. Int. Ed.* **2018**, *57*, 6018–6041.

Today, organic electrochemistry is considered as one of the most developing areas in organic chemistry. Modern technological development has helped to simplify the setup, making it more convenient to handle.

The first report on organic electrochemistry is considered to be the anodic conversion of acetate anions to CO<sub>2</sub> and methane by M. Faraday in 1834.<sup>198</sup> This unexpected organic product (methane) in his reaction probably aroused the interest that electrochemistry could be applied for organic synthesis rather than just electrochemical decomposition of compounds. Few years later, H. Kolbe (1849)<sup>199</sup> discovered that electrolysis of organic acids (RCOOH) resulted in the formation of dimeric alkane (R-R), a reaction known today as Kolbe reaction and has remained the most renowned reference in organic electrochemistry. The pioneering studies by Faraday and Kolbe initiated interests in organic electrochemistry, prompting a diverse studies and discovery of many other electrochemical synthetic reactions.

## 2. Setup for organic electrochemistry

An electrochemical setup basically consists of two electrodes connected to a power source and in contact with a reaction solution (Figure 6.1). The anode (positively charged) is the oxidation electrode, while cathode (negatively charged) is the reduction electrode. Normally, electrons (charge) flow from the anode to the cathode, the electron deficient anode accepting electrons from the substrate, while the electron rich cathode giving out electrons to the substrate. This mimics oxidizing and reducing agents in traditional organic chemistry. Both anodic oxidation and cathodic reduction are coupled, which means that one cannot occur without the other.<sup>197</sup> Then movement of ions in reaction solution completes the electrical circuit.

*Undivided:* an undivided electrochemical cell has no physical separation between cathode and anode and is most widely used in organic electrochemistry due to some of its advantages including, lower internal resistance, long lifespan and low cost.<sup>200</sup>

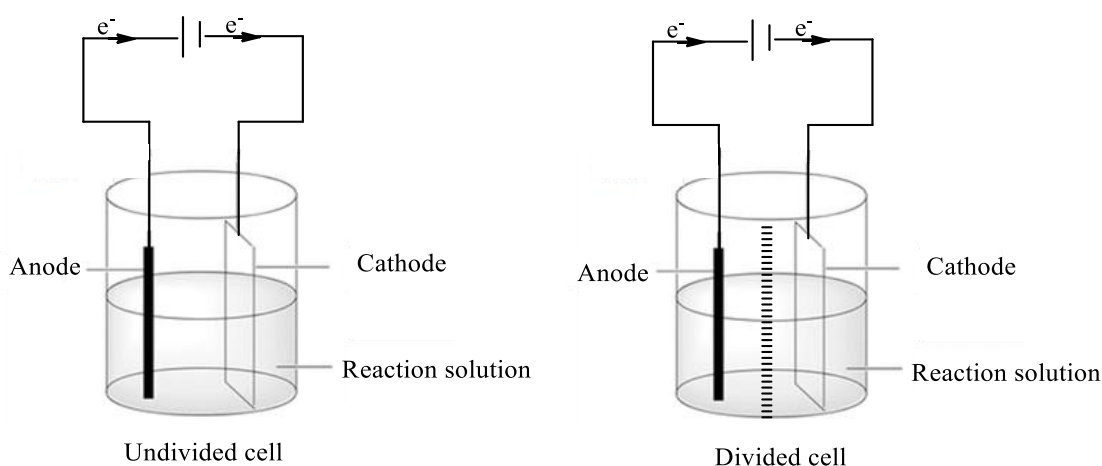


**Figure 6.1:** Simple electrochemical setups, divided and undivided cells

<sup>198</sup> M. Faraday, *Phil Trans R Soc.* **1834**, 124, 77-122.

<sup>199</sup> H. Kolbe, *Justus Liebigs Ann. Chem.* **1849**, 69, 257-372.

<sup>200</sup> D. S. P. Cardoso, B. Šljukić, D. M. F. Santos, C. A. C. Sequeira, *Org. Process Res. Dev.* **2017**, 21, 1213-1226.

*Divided cell:* in a divided cell, the anode is separated from the cathode by a diaphragm (ion-permeable barrier) which allows ion exchange between the cells but limits mixing of anolyte and catholyte. High cell resistance is common in divided cell due to high inter-electrode distance caused by the diaphragm. This however can be minimized by maintaining small distance between anode and cathode, by using low-resistance diaphragm, electrodes with large surface area and a compact cell.<sup>201</sup> Divided cell is suitable when reaction in one electrode interferes with that of the other electrode.

Electrochemical machines range from simple glassware beakers equipped with electrodes and bench-top power supply to more advanced commercially available machines including ElectraSyn (Figure 6.2). The latter has advantage of standardized parameters, which are vital for reproducibility of electrochemical reactions.<sup>202</sup>



**Figure 6.2:** Some common electrochemical reactors

### 3. Organic reactions at the electrodes

As mentioned earlier, the positive electrode (anode) of an electrochemical cell can accept electrons from organic molecules, thereby acting as oxidizing agent reminiscent of chemical oxidant in conventional organic reactions. In turn, negative electrode (cathode) can supply electrons to substrates acting as a reducing agent. Electrons exchange between electrodes and electroactive organic molecules primarily results in neutral or ionic radicals depending on whether the species is a molecule or an ion. These radicals are usually very unstable and would readily engage in a chemical reaction or undergo further transformations resulting in other organic intermediates such as carbocations, carbanions or carbenes that can engage in chemical reactions.<sup>201,197,203</sup> A single electron transfer between an electrode and an ion gives a neutral radical while electron transfer between an electrode and a neutral substrate results in a radical ion akin to photoredox catalysis (Figure 6.3).

<sup>201</sup> H. Lund, O. Hammerich, *Organic electrochemistry*, 4th Edn, Marcel Dekker Inc. New York, **2001**, pp 223-290

<sup>202</sup> D. Pollok, S. R. Waldvogel, *Chem. Sci.* **2020**, *11*, 12386-12400.

<sup>203</sup> R. H. Verschueren, W. M. De Borggraeve, *Molecules* **2019**, *24*, 2122.



**Figure 6.3:** Single electron transfer between substrates and electrodes

An electrochemical process is a heterogeneous process; electron transfer takes place at the surface of electrodes while the substrates are in solution. It is important to note that only electrode areas facing each other carry the current<sup>201</sup> and that is where electrochemical reactions predominantly occur.

The electrogenerated intermediates react through a thin reaction layer at the surface of electrodes, just a few thousand of micrometers from the surface of electrode (known as diffusion layer).<sup>197</sup> The concentration of the electrogenerated intermediate is higher near the surface of the electrode than in the bulk solution. Mass transfer from the surface of electrode to bulk solution plays an important role in electrochemical process.

Pure electron transfer is very rare in organic chemistry; electron transfer is often accompanied by atom or group transfer. In other words, electron transfer in organic chemistry often follows inner sphere involving bond formation between the reactants in transition state. However, electron transfer in organic electrochemistry follows outer sphere where pure electron is transferred directly between electrode and substrate without formation or breaking of bonds. This is because of inability of electrode to establish any bond with electroactive species. Electrode therefore acts as an electron source or sink.<sup>204</sup>

### 3.1. Working electrode and counter electrode

The electrode on which the desired transformation occurs is referred to as the working electrode while the other electrode is the counter electrode (or auxiliary electrode). For instance, in an electrochemical oxidation of a compound, the working electrode is the anode while cathode is the counter electrode. The reaction that occurs at counter electrode is known as counter reaction and it is equally important. For an efficient electrochemical process, counter reaction should be considered during process optimization because it could be a rate-determining factor.<sup>197a</sup> Usual counter reaction at the cathode includes solvent deprotonation resulting in hydrogen evolution while counter reaction at the anode could also be solvent degradation or oxidation of a sacrificial metal anode.<sup>205</sup>

### 3.2. Reference electrodes

A reference electrode is a stable electrode with a well-known electrode potential that can be used to precisely measure the potential of the working electrode in an electrochemical cell.<sup>206</sup> The standard hydrogen electrode (SHE) is the internationally accepted reference electrode. However, its use is not

<sup>204</sup> A. J. Fry, W. E. Britton, *Topics in Organic Electrochemistry*, Springer, New York, **1986**, p. 36.

<sup>205</sup> H. Wang, X. Gao, Z. Lv, T. Abdelilah, A. Lei, *Chem. Rev.* **2019**, *119*, 6769–6787.

<sup>206</sup> V. V. Pavlishchuk, A. W. Addison, *Inorg. Chim. Acta*, **2000**, *298*, 97–102.

convenient from experimental standpoint. Other reference electrodes which sometimes are referred to as secondary electrodes including saturated calomel electrode Hg/Hg<sub>2</sub>Cl<sub>2</sub> (SCE) and *silver-silver chloride* Ag/AgCl (SSCE) are more frequently used. The potential of SHE is conveniently fixed to be 0 V under standard conditions and is basically used as a reference electrode for standardizing other reference electrodes. The potential of other electrodes is often given relative to a reference electrode. For comparative purposes, conversion of voltage units to SHE reference is useful, and this can be achieved using the following relationships:<sup>207</sup>

$$\text{SHE} = \text{Ag/AgCl(saturated)} + 0.197\text{V} \quad (3)$$

$$\text{SHE} = \text{Ag/AgCl(3.5M)} + 0.205\text{V} \quad (4)$$

$$\text{SHE} = \text{SCE} + 0.241\text{V} \quad (5)$$

#### 4. Controlling organic reactions at the electrode

Electron transfer between electrode and organic molecules in an electrochemical cell is principally controlled by precise adjustment of the potential or current.<sup>197,201</sup> Electrode potential is the energy required to push electrons from the anode to cathode while current deals with the total amount of charge (electron) released into the reaction solution per unit of time. In principle, electrode potential must be above the redox potential of the substrate before reaction can occur.<sup>197</sup> On the other hand, too high potential may compromise reaction selectivity. Electrochemical reaction can be conducted under constant current (galvanostatic) or constant potential (potentiostatic) conditions.

*Constant current:* constant current setup is commonly used in organic electrochemistry because current density is easier to measure and kept constant.<sup>201</sup> In this system, potential is not controlled, it varies to maintain the set current; high potential means that there is high resistance between the two electrodes, which could be due to low conductivity of the solution or to the fact that the two electrodes are wide apart. This problem is usually solved by adding supporting electrolyte and/or reducing the distance between the two electrodes. The amount of current used in organic electrochemistry determines the rate of a reaction, the higher the current the higher the reaction kinetic. However, a low current density guarantees a milder reaction and is better for reaction selectivity.<sup>197</sup>

*Constant potential:* in this system, the potential also known as voltage across the electrodes is fix, the current then varies to maintain the set potential. Organic electrochemistry using constant potential appears interesting in the sense that the working potential can be controlled considering the redox potentials of the target molecules, which in principle holds more potential for high reaction selectivity. However, this technique requires a reference electrode in addition to the working and counter electrodes, which makes the setup, more complex compared to that of the constant current process, and the latter is therefore often preferred.<sup>208</sup>

<sup>207</sup> R. Cardeña, B. Cercado, G. Buitrón, *Microbial Electrolysis Cell for BI-OHydrogen Production*, Elsevier B.V, 2<sup>nd</sup> Edn, 2019, pp.159-181.

<sup>208</sup> Y. Kawamata, M. Yan, Z. Liu, D-H. Bao, J. Chen, J. T. Starr, P. S. Baran, *J. Am. Chem. Soc.* **2017**, *139*, 7448–7451.

## 5. Cyclic voltammetry

Cyclic voltammetry (CV) is a technique used to obtain information about the redox potential of electroactive species.<sup>209</sup> CV plays an important role in investigating reaction kinetics and mechanisms of electrochemical processes. Moreover, CV is very vital to ascertain the potential at which a certain redox transformation would be carried out to ensure good reaction selectivity. The setup for CV analysis consists of a special working electrode, counter electrode, and a reference electrode. During CV analysis, the potential at the working electrode is scanned at a fixed rate, (usually between 1 to 10 mV/s) and the electrical current produced during the scanning is measured and recorded by the potentiostat/galvanostat.<sup>207</sup> The presence of a species that can undergo redox reaction within the range of potential applied will cause a flow of current during its oxidation and reduction resulting in a peak known as voltammogram. A voltammogram is a plot of the current generated by the analyte versus the potential of the working electrode. This plot indicates the potential at which maximum current was observed during the oxidation ( $E^c$ ) and reduction ( $E^a$ ) of the species, then the mid-point of these peaks is taken as the redox potential ( $E^{1/2}$ ) of the species (Figure 6.4).

The voltage is swept between two values starting from  $V_1$  at a fixed rate, when the voltage reaches  $V_2$  the scan is reversed, and the voltage is swept back to  $V_1$ . In the forward sweep, current flows from electrode into the solution (cathodic current) while in the reverse sweep, current flow from the solution back to electrode (anodic current). Reduction of the analytes takes place in the first process and peak potentials  $E^a$  is the reduction potential of the analyte. In the reverse process, oxidation of the reduced analyte commenced and the peak potential  $E^c$  is the oxidation potential of the analyte, almost at equal magnitude. However, the CV for processes with irreversible electron transfer shows a different behavior. It is possible to estimate the electron transfer rate constants by analyzing the variation of peak position as a function of scan rate.

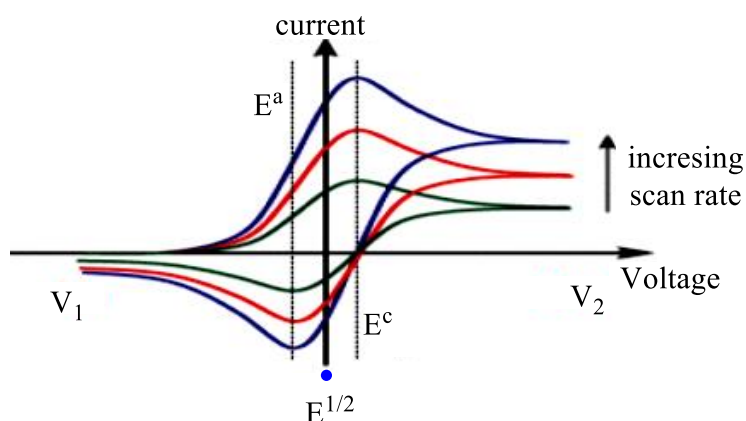


**Figure 6.4:** Voltammogram for a reversible single electrode transfer reaction

<sup>209</sup> H. Jurgen, *Angew. Chem. Int. Ed.* **1984**, *23*, 831–847.

## 6. Solvents for organic electrochemistry

Most early organic electrochemical reactions were performed in aqueous medium. However, the fact that the majority of organic substrates and reagents are not soluble in aqueous medium limits its application.<sup>200</sup> To breach this gap, researchers over the years have identified several organic solvents suitable for organic electrochemistry including aprotic solvents such as CH<sub>3</sub>CN, DMF, DMSO and THF, and protic solvents including hexafluoroisopropanol (HFIP), trifluoroethanol (TFE), MeOH and EtOH. In the choice of solvent for organic electrochemistry, the solvent window is vital; solvent window is the potential range in which the solvent is stable towards oxidation and reduction. The solvent windows of some common solvents used in organic electrochemistry are represented in Figure 6.5. CH<sub>3</sub>CN has a relatively high potential window and is most suitable for a reaction operating at high voltage. Also, CH<sub>3</sub>CN, DMF and DMSO have superior dissolving power for organic compounds and salts, but there is evidence that DMF could interfere with the electrogenerated intermediates through its nucleophilic or acido-basic properties or through hydrogen atom transfer to radical.<sup>201</sup> On the other hand, fluorinated solvents such as HFIP and TFE can help to stabilize generated radicals during electrochemistry, which is beneficial for the reaction.<sup>197,210</sup>

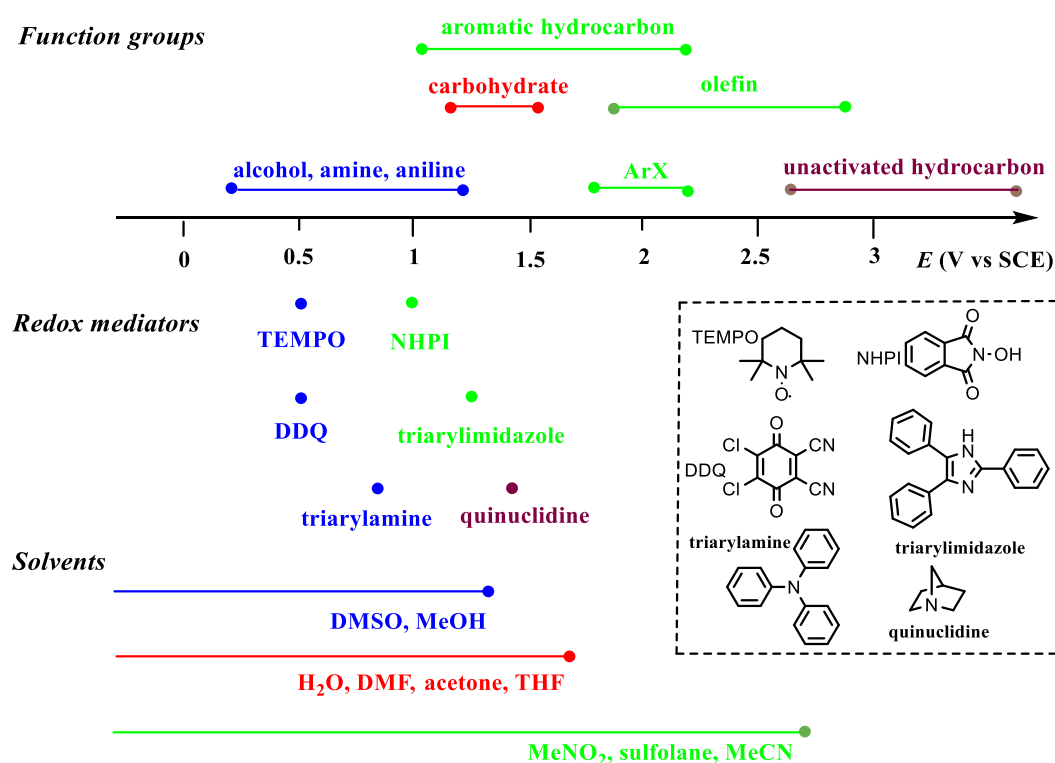


**Figure 6.5:** Redox potentials of some common organic functional group, solvents, and mediators.<sup>197,211</sup>

<sup>210</sup> R. Francke, D. Cericola, R. Kötzt, D. Weingarh, S. R. Waldvogel, *Electrochim. Acta*, **2012**, 62, 372–380.

<sup>211</sup> L. M. Reid, T. Li, Y. Cao, C. P. Berlinguette, *Sustain. Energy Fuels*, **2018**, 2, 1905–1927.

## 7. Supporting electrolytes for organic electrochemistry

Supporting electrolytes are often added in electrochemical solution to improve the electrical conductivity. Supporting electrolytes are usually compounds that are stable towards redox reactions and do not participate in the electrochemical reactions. These can be an acid, base or salt depending on the type of solvent used. Common supporting electrolytes for aprotic solvent includes tetraalkylammonium salts with  $\text{ClO}_4^-$ ,  $\text{PF}_6^-$  and  $\text{BF}_4^-$  as the counter ions. Other supporting electrolytes used in electrochemistry include alkali metal salts such as  $\text{Li}^+$  or  $\text{Na}^+$  with counter anions aforementioned. These inorganic salts supporting electrolytes have advantage of easy separation by aqueous workup and good stability under anodic oxidation. However, their poor solubility in many organic solvents, or deposit on the cathodes are among major limitations in their use.

## 8. Electrode materials for organic electrochemistry

Some common electrode materials used in organic electrochemistry are platinum, nickel foam, carbon-based electrodes (graphite, Reticulated Vitreous Carbon (RVC), or glassy carbon). Other include boron-doped diamond (BDD), mercury, lead, tin, iron, aluminum, cadmium, magnesium, silver, gold and composite electrodes.<sup>201,197</sup> While these electrodes can serve as cathode, the choice of anode is very limited because most metals are attacked under anodic conditions. Therefore, inert materials are preferred for anode, they include carbon-based electrodes, platinum and gold.

## 9. Kolbe reaction

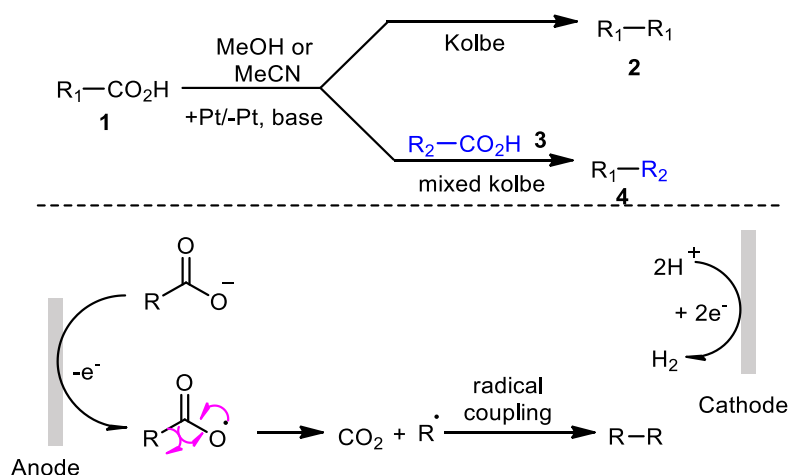
In 1849, Kolbe showed that anodic decarboxylation of carboxylate salts could generate alkyl radicals, which then underwent radical-radical coupling to furnish alkanes (Scheme 6.1).<sup>212</sup> This reaction is a powerful tool for the construction of C-C bond using carboxylic acids. Kolbe reaction is considered the pioneer of the modern organic electrochemical synthesis. Anodic one-electron oxidation of carboxylates would result in an unstable carboxyl radical, which decomposes rapidly by decarboxylation to give a carbon-centered radical. Homocoupling of this radical gives a symmetric alkane. When the reaction involves different kinds of carboxylic acids, unsymmetrical alkanes are formed and the reaction is termed mixed Kolbe reaction.<sup>213</sup> Kolbe coupling reaction works efficiently using water or methanol as the solvent, smooth platinum or iridium anodes and a very high current density, typically  $0.25 \text{ A/cm}^2$ , neutral or acidic medium and at temperature below  $50^\circ\text{C}$ .<sup>201,212</sup> Though Kolbe's reaction can also be conducted in an organic solvent such as DMF, however high current resistance is the major limitation in this case.<sup>214</sup>

---

<sup>212</sup> H. Kolbe, *Ann. Chem. Pharm.* **1849**, 69, 257-294.

<sup>213</sup> N. Chen, Z. Ye, F. Zhang, *Org. Biomol. Chem.* **2021**, 19, 5501-5513.

<sup>214</sup> L. Rand, A. F. Mohär, *J. Org. Chem.* **1965**, 30, 3156-3885.



**Scheme 6.1:** Kolbe reaction for the synthesis of dimeric alkanes from carboxylic acids

Reports on substrate scope for Kolbe reaction as summarized by Ross *et al.*,<sup>215</sup> indicated that longer straight chain carboxylic acids (> 5 carbon atoms) are more efficient in Kolbe dimerization reaction. Also, acids with  $\alpha$ -substitution, especially electron donating groups, favor a variant reaction known as Hofer-Moest reaction, where the generated radicals instead of coupling undergo a second oxidation to carbocation, which can engage in a reaction with a nucleophile to give a different product. Hofer-Moest reaction is discussed in more detail in the subsequent section. Furthermore,  $\alpha,\beta$ -unsaturated acids are not compatible with the coupling reaction, while  $\beta,\gamma$ -unsaturated acids gave mixture of products. Benzoic acid give benzene instead of expected biphenyl.

The choice of electrode is crucial in Kolbe reaction; platinum, rhodium, or glassy carbon electrodes favor dimerization products (R-R).<sup>216</sup> Radicals adsorb very weakly on platinum and rhodium surface,<sup>217</sup> which forces them to easily slip out of the electrode surface as soon as they are generated thereby limiting their further oxidation. On the other hand, graphite anode favors Hofer-Moest reaction because radicals can adsorb on carbon electrode, which encourages their second oxidation into carbocations.

Apart from being a powerful tool for preparation of long-chain alkanes from short-chain carboxylic acids, Kolbe anodic decarboxylation can be applied for synthesis of cyclic compound via radical cyclization.<sup>215,218,219</sup> Riant and co-workers recently described an environmentally friendly electrochemical synthesis of pyrrolidinones using Kolbe process (Scheme 6.2). From their proposed mechanism, anodic oxidation of the carboxylate would afford an unstable carboxylate radical **I** which undergoes decarboxylation to give radical intermediate **II**. Intramolecular cyclization of **II** would then afford **III**. Then, the radical coupling between **III** and ethyl radical issued from the decarboxylation of the co-acid (EtCOOH) furnishes the desired pyrrolidinone. Methanol or

<sup>215</sup> S. D. Ross, M. Finkelstein, E. J. Rudd, *Anodic Oxidation*, Academic Press, Inc., New York, **2013**, pp 134-152.

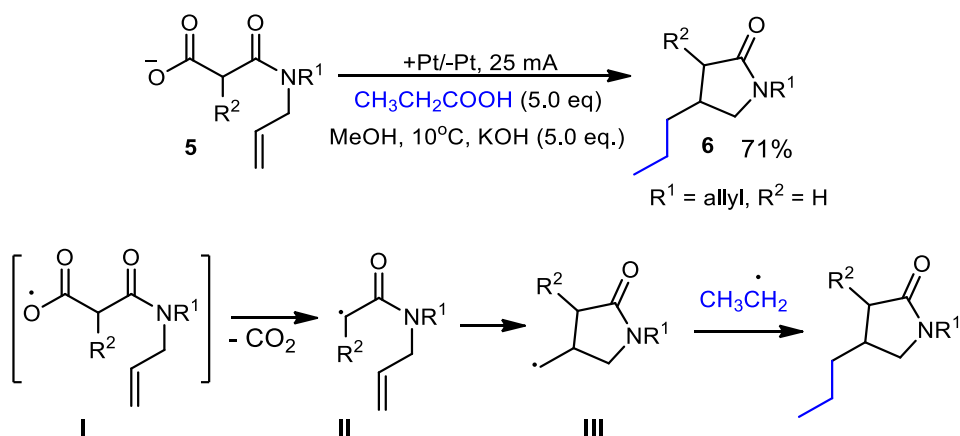
<sup>216</sup> K. Köster, H. Wendt, *Electro-organic syntheses*. In: J. O. Bockris, B.E. Conway, E. Yeager, R. E. White, *Comprehensive treatises of electrochemistry*, Plenum Press, New York, **1981**, pp 251 – 299.

<sup>217</sup> V. Plzak, H. Wendt, *Ber. Bunsenges Physik Chem.* **1979**, *83*, 481-486.

<sup>218</sup> J. Weiguny, H. J. Schäfer, *Liebigs Ann. Chem.* **1994**, *3*, 235-242.

<sup>219</sup> M. Huhtasaari, H. J. Schäfer, L. Becking, *Angew. Chem., Int. Ed. Engl.* **1984**, *23*, 980-981.

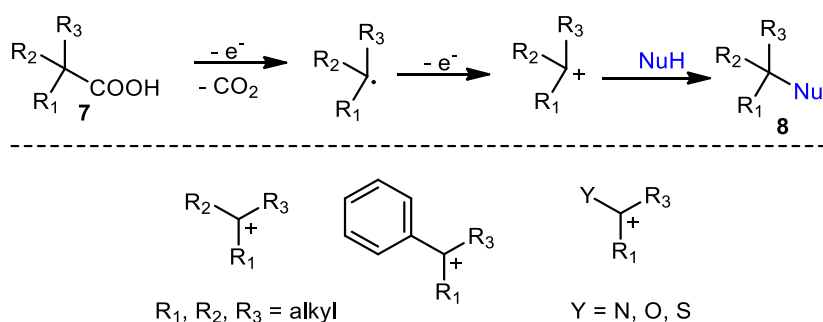
acetonitrile were shown to be competent solvents for the reaction. The authors observed that very dilute reaction solution (0.066 mol/L with respect to **I**) was important to limit homocoupling of **III**.



**Scheme 6.2:** Electrochemical synthesis of pyrrolidinones using mixed-Kolbe reaction

## 10. Hofer-Moest Reaction

Hofer-Moest reaction is a variant of the Kolbe reaction where the generated carbon-centered radical instead of coupling, undergoes a second oxidation to give the corresponding carbocation, which can then be trapped by a nucleophile present in the reaction medium (scheme 6.3).<sup>220</sup> The reaction is widely used for carbon–heteroatom bond formation in organic electrochemistry. Hofer-Moest reaction requires a stabilized carbon-centered radical such as tertiary alkyl radical or radical with  $\alpha$ -stabilization groups such as heteroatoms or  $\pi$ -systems.<sup>221</sup>



**Scheme 6.3:** Hofer-Moest reaction

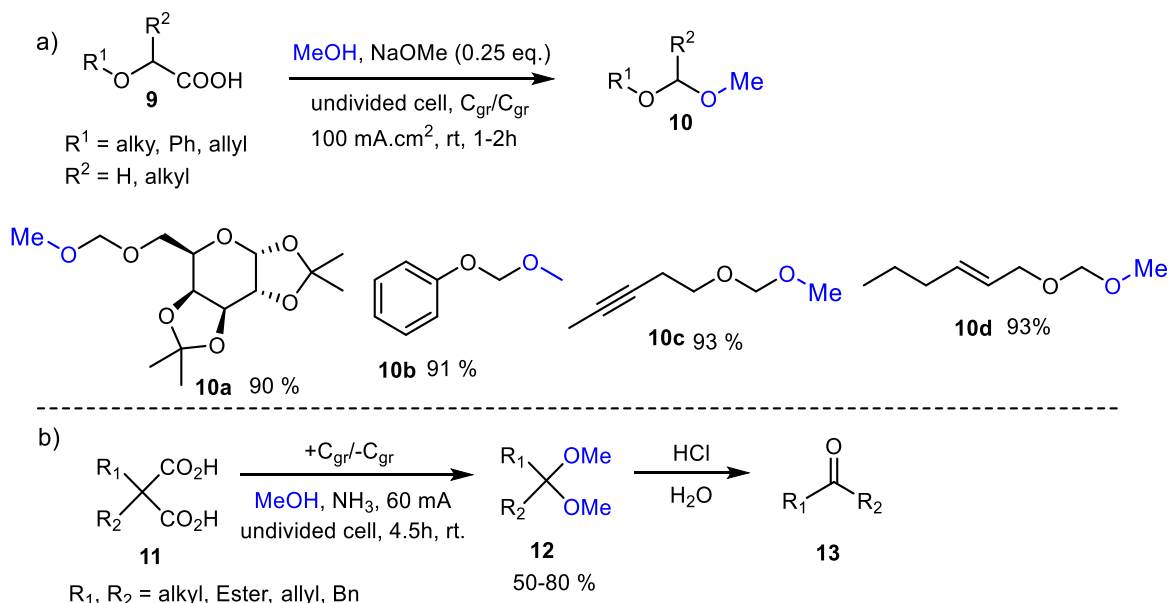
Besides the nature of substrates, some process conditions have been identified to favor Hofer-Moest reaction over Kolbe's; Hofer-Moest reaction operates more efficiently in low current density, carbon electrode and basic medium.<sup>222</sup> Temperature has no much influence on the reaction course.<sup>201</sup>

<sup>220</sup> H. Hofer, M. Moest, *Justus Liebigs Ann. Chem.* **1902**, 323, 284-323.

<sup>221</sup> Á. M. Martínez, D. Hayrapetyan, T. van Lingem, M. Dyga, L. J. Gooßen, *Nat. Commun.* **2020**, 11, 1-7.

<sup>222</sup> J. Xiang, M. Shang, Y. Kawamata, H. Lundberg, S. H. Reisberg, M. Chen, P. S. Baran *et al.*, *Nature* **2019**, 573, 398-402.

Over the years, lots of organic electrochemical procedures have been developed based on Hofer-Moest reaction including access to acetal from  $\alpha$ -alkoxy carboxylic acids as recently demonstrated by Lam and co-workers (Scheme 6.4).<sup>223</sup>



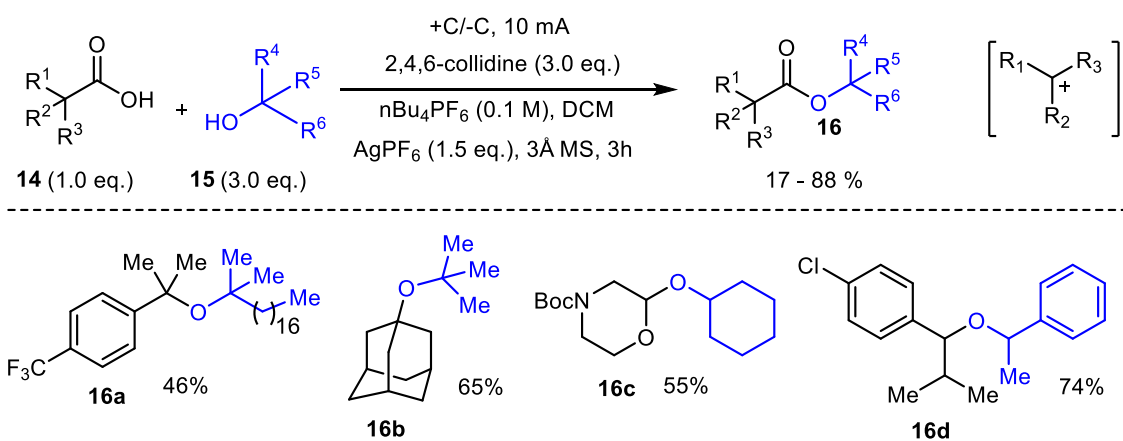
**Scheme 6.4:** Synthesis of acetal derivatives using Hofer-Moest reaction

In their reaction, methanol served as solvent and nucleophile. Graphite electrodes and constant current of 100 mA in an undivided cell were used. The desired acetal was obtained in an excellent yield, even in gram-scale. Markò *et al.*,<sup>224</sup> have shown that ketals could also be accessed efficiently using disubstituted malonic acid and that the subsequent treatment of this product with hydrochloric acid would afford ketone in moderate to excellent yields (Scheme 6.4b).

Since its invention, Hofer–Moest reaction for preparation of ether from carboxylic acid relies mainly on solvent-quantities of the alcoholic nucleophile, which however limits its scope. Alcoholic solvent is known to favor current conductivity as compared to most other organic solvents and it acts as electron sink in counter electrode reaction.<sup>222</sup> In an attempt to solve this problem, Baran group<sup>222</sup> recently unveiled a procedure, which allowed the uses of stoichiometric amount of alcohol and organic solvent to access varieties of hindered ethers (Scheme 6.5). However, the use of stoichiometric amount of  $\text{AgPF}_6$  in their system is a concern from a cost point of view.

<sup>223</sup> X. Luo, X. Ma, F. Lebreux, I. E. Marko, K. Lam, *Chem. Commun.* **2018**, 54, 9969-9972.

<sup>224</sup> X. Ma, X. Luo, S. Dochain, C. Mathot, I. E. Markò, *Org. Lett.* **2015**, 17, 4690-4693.



**Scheme 6.5:** Synthesis of hindered dialkyl ether with electrogenerated carbocations

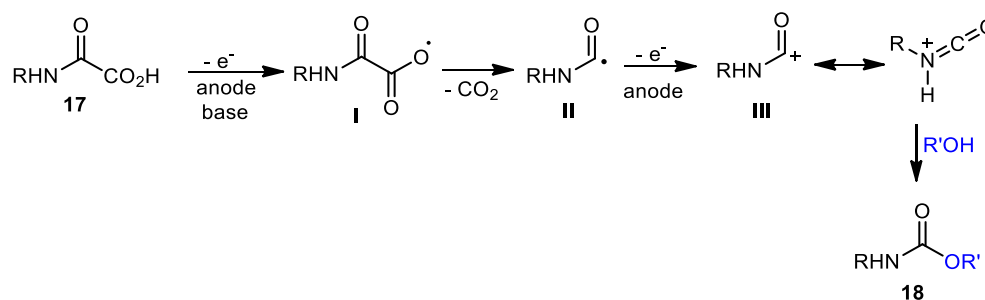
## Conclusion

There is increasing interest in the use of simple electrochemical set-up in organic synthesis due to its simplicity, promising environmental benefits and ability to limit the use of stoichiometric amount of expensive reagents and waste generation. Also, it has been shown that organic electrochemistry can facilitate some organic transformations that are rather difficult or impossible with conventional organic chemistry, which makes it an interesting complementary tool for traditional synthetic chemistry. Once more, modern technological development has helped to simplify the setup, leading that lots of interesting organic electrochemical reactions have been developed over the past two decades.

## PART 2: Design of a new non-phosgene route to urethane by electrochemical oxidation of oxamic acids

### 1. Introduction

Encouraged by our previous studies that urethanes can be accessed in a one-pot metal free photocatalyzed or PIDA-mediated oxidative decarboxylation of oxamic acids in the presence of alcohols, we sought to further simplify this greener route to urethane relying on organic electrochemistry. In our photocatalyzed or PIDA-mediated procedures, lipophilic hypervalent iodine was used as an oxidant. Our main goal in this present study was to replace this chemical oxidant with anodic oxidation, thereby leading to a metal-, photocatalyst-, light and chemical oxidant-free route procedure to urethane starting from oxamic acid as a green precursor. Based on our previous work using photocatalyzed procedure<sup>212,225</sup> and Hofer-Moest<sup>220</sup> reactions, we envisaged that electrochemistry could be used to mediate the single electron transfers during oxidation of oxamic acid; oxamic acid could lose one electron to anode to generate ketocarboxyl radical **I** which would rapidly undergo decarboxylation to release carbamoyl radical **II**. Then, a second oxidation of **II** at the anode would lead to carbamoyl cation **III**, which can also be written as a protonated isocyanate, alcohol would then trap this cationic species to furnish urethane (Scheme 6.6).



**Scheme 6.6:** Urethane synthesis from oxamic acid under electrochemical conditions

### 2. Reaction procedure and optimization

For this study, we chose IKA ElectraSyn 2.0 Package (Figure 6.6) as a standardized electrochemical reactor.<sup>222,197</sup> Oxamic acid **56a** was used as a model compound and MeOH served as both solvent and nucleophile to trap the *in-situ* generated isocyanate. Graphite electrodes were chosen as both anode and cathode based on antecedent literatures on Hofer-Moest type reactions.<sup>201,222</sup> A constant current mode was used in an undivided cell.

<sup>225</sup> G. G. Pawar, F. Robert, E. Grau, H. Cramail, Y. Landais, *Chem. Commun.* **2018**, 54, 9337-9340.

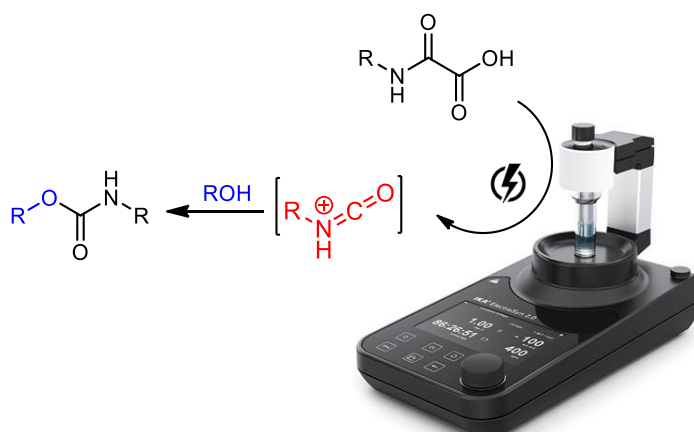
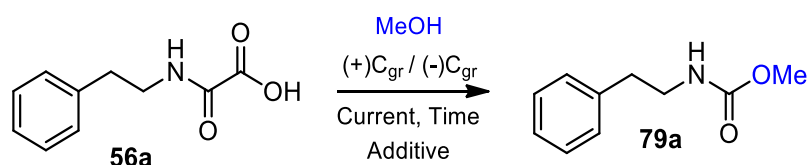


**Figure 6.6:** IKA ElectraSyn 2.0 Package used for electrochemical synthesis of urethanes from oxamic acids

The reaction was first performed using 1.0 eq. of triethylamine (TEA) as a base and a constant current of 60 mA.<sup>222,223,224</sup> Gratifyingly, we observed 72% of the corresponding methyl carbamate **79a** alongside 20% of 1,1-diethyl-3-phenethylurea **80** (*vide infra*) after 5h (Table 6.1, entry 1). The observed urea was due to triethylamine oxidation; previous studies<sup>226</sup> have shown that aliphatic tertiary amine can undergo a two-electron anodic oxidation in the presence of traces of water, resulting in a secondary amine and aldehyde. Secondary amine is equally a good nucleophile, which can trap the generated isocyanate to give urea. Then, the quantity of Et<sub>3</sub>N was reduced to 0.1 eq., which led to only a slight increase in the carbamate yield (entry 2), but urea formation was not observed. TEA was replaced with other bases including ammonia or guanidines (TBD or MTBD) but they did not improve the yield of **79a** (entries 3-5). Extending the reaction time to 8h did not show any significant effect on the yield neither (entry 6). The current was then lowered to 5 mA and reaction time extended up to 12h, resulting in an improved 80% yield (entry 7). Interestingly, the reaction worked also well without any additives including base resulting in 84% conversion with 77% isolated yield of **79a** (entry 8). The reaction time was extended to 18h under these conditions but it did not help to improve the yield of **79a** further (entry 9). The presence of tetrabutylammonium perchlorate (*n*-Bu<sub>4</sub>NClO<sub>4</sub>) as a supporting electrolyte<sup>222</sup> did not show any significant effect in the product yield (entry 10), while *n*-Bu<sub>4</sub>NI had a deleterious effect on the yield, possibly due to its competitive decomposition at the anode (entry 11).<sup>227</sup> Furthermore, the effect of electrodes was screened. Platinum anode drastically lowered the yield (entry 12). **79a** was not detected when stainless steel was used (entry 13), while Nickel foam exhibited a similar performance as graphite electrode (entry 14). These results are in agreement with literature that Hofer-Moest type reaction is favored by graphite or nickel anode compared to metallic electrodes.<sup>201,222</sup> Finally, the reaction was carried out without any precautions to exclude air and the yield remained the same (entry 15).

<sup>226</sup> M. Masui, H. Sayo, Y. Tsuda, *J. Chem. Soc. B*, **1968**, 973-976.

<sup>227</sup> K. Hu, Y. Zhang, Z. Zhou, Y. Yang, Z. Zha, Z. Wang, *Org. Lett.* **2020**, *22*, 5773-5777.



Entry <sup>a</sup>	Current (mA)	Additive (eq.)	Time (h)	Yield (%) <sup>b</sup>
1	60	TEA (1.0)	5	72
2	60	TEA (0.1)	5	78 (72)
3	60	NH <sub>3</sub> (0.1)	5	76
4	60	TBD (0.1)	5	70
5	60	MTBD (0.1)	5	68
6	60	TEA (0.1)	8	79
7	5	TEA (0.1)	12	80
8	5	-	12	84 (77)
9	5	-	18	84
10	5	<i>n</i> -Bu <sub>4</sub> NClO <sub>4</sub> (0.1)	12	83
11	5	<i>n</i> -Bu <sub>4</sub> NI (0.1)	12	26
12 <sup>c</sup>	5	-	12	40
13 <sup>d</sup>	5	-	12	ND
14 <sup>e</sup>	5	-	12	83
15 <sup>f</sup>	5	-	12	84

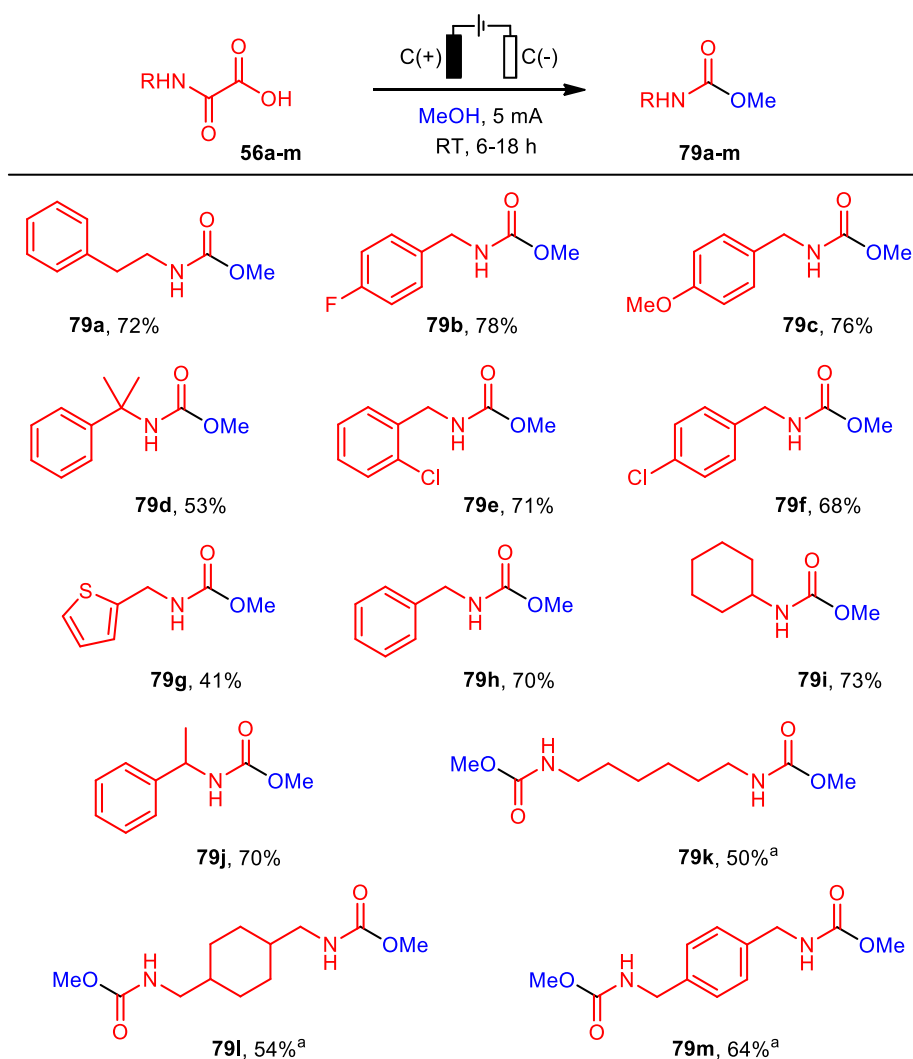
<sup>a</sup> Unless otherwise mentioned, all reactions were performed with **56a** (0.5 mmol), MeOH (3 mL), graphite anode and cathode, under argon atmosphere unless indicated, in an ElectraSyn vial, undivided cell at room temperature.

<sup>b</sup> Yields of **79a** determined by <sup>1</sup>H NMR with 1,3,5-trimethylbenzene as an external standard (Isolated yields of **18a** under brackets). <sup>c</sup> Platinum anode. <sup>d</sup> Stainless steel anode. <sup>e</sup> Nickel anode. <sup>f</sup> Reaction in air.

**Table 6.1:** Electrochemical conversion of oxamic acid **56a** into urethane **79a**.

### 3. Substrate scope

Next, the substrate scope was investigated using the optimal conditions (Table 6.1, entry 8); the nature of oxamic acids was varied in the presence of MeOH as a nucleophile and solvent (Scheme 6.7). A wide range of oxamic acids **56a-m** were shown to be compatible under these conditions, thus allowing access to various methyl carbamates **79a-m** in moderate to high yields, including both arenes bearing electron-withdrawing (**79b**, **79e-f**) and electron-donating (**79c**) substituents. Oxamic acids with benzylic substituents (**56b-c**, **56e-h**) which were shown to be unstable towards oxidation, using our previous photocatalytic conditions<sup>225</sup> furnished the corresponding urethanes in good yields under the electrochemical conditions. Furthermore, bis-oxamic acids were submitted to these electrochemical conditions, resulting in the corresponding bis(methyl carbamates) **79k-m** in good yields. Small quantity (0.1 eq.) of supporting electrolyte (*n*-Bu<sub>4</sub>NClO<sub>4</sub>) was however used in this case to improve conductivity and conversion.



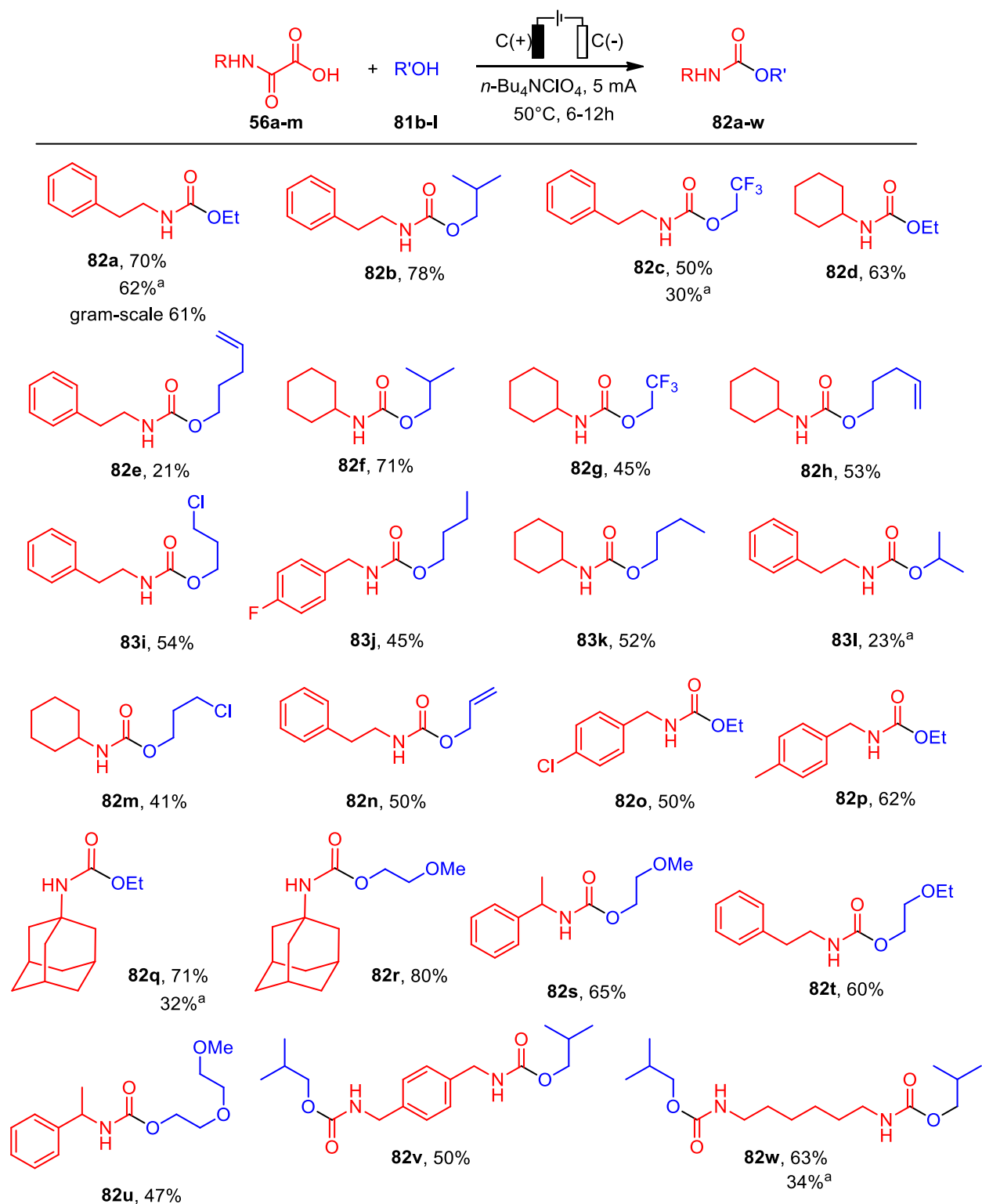
**Scheme 6.7:** Electrochemical decarboxylation of oxamic acids in the presence of MeOH. Oxamic acid scope. <sup>a</sup> (*n*-Bu<sub>4</sub>)NClO<sub>4</sub> (0.1 eq.) was added.

Furthermore, the electrochemical process was extended to other alcohols **81b-l** using the optimal conditions. Alcohols with higher molecular weight than methanol displayed relatively lower electrical conductivity.<sup>228</sup> However, using small quantities of *n*-Bu<sub>4</sub>NClO<sub>4</sub> as supporting electrolyte and a mild heating (50°C) during electrolysis, they were shown to be competent solvents and nucleophile for the reactions, affording the desired urethanes in moderate to good yields (Scheme 6.8). Besides enhancing the reactivity of the alcohols towards the generated isocyanates,<sup>229</sup> the mild heating improved the electrical conductivity,<sup>228</sup> solubility, and possibly the mass transport of ions to the electrodes.<sup>230</sup> Alcohols bearing a CF<sub>3</sub> group (**81c**, **81g**), Cl (**81i**, **81m**), ethers groups (**81r-u**) and a double bond (**81h**, **81n**) where all compatible with the electrochemical conditions, furnishing the desired products in satisfactory yields. The reaction was also reproduced on a one gram-scale with success, **81a** being obtained in 61% yield. With bis-oxamic acids, double addition was also observed resulting in the corresponding bis-urethanes **81v-w** in good yields.

<sup>228</sup> M. Prego, O. Cabeza, E. Carballo, C. F. Franjo, E. Jimenez, *J. Mol. Liq.* **2000**, *89*, 233-238.

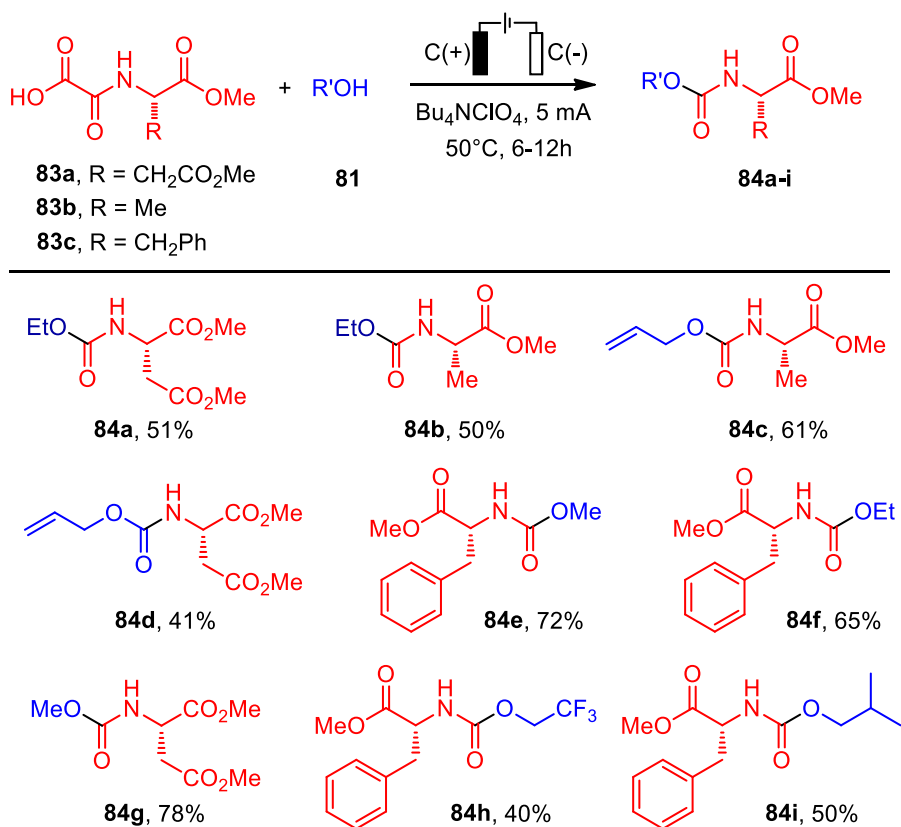
<sup>229</sup> S. Ozaki, *Chem. Rev.* **1972**, *72*, 457-496.

<sup>230</sup> C. Reichardt, *Solvents and Solvent Effects in Organic Chemistry*, Wiley-VCH, Weinheim, Germany, 3rd Ed., 2003, p. 578.



**Scheme 6.8:** Electrochemical decarboxylation of oxamic acids in the presence of alcohols **81b-l**. Alcohol scope. <sup>a</sup>Room temperature.

Using chiral oxamic acids **83a-c** derived from the corresponding (*L*)-amino acids, chiral urethanes **84a-i** were obtained in satisfying yields (Scheme 6.9) without racemization as shown by chiral HPLC on racemic and homochiral **83c** (Figure 6.7).



**Scheme 6.9:** Electrochemical decarboxylation of amino-acids derived oxamic acids in the presence of alcohols **81**.

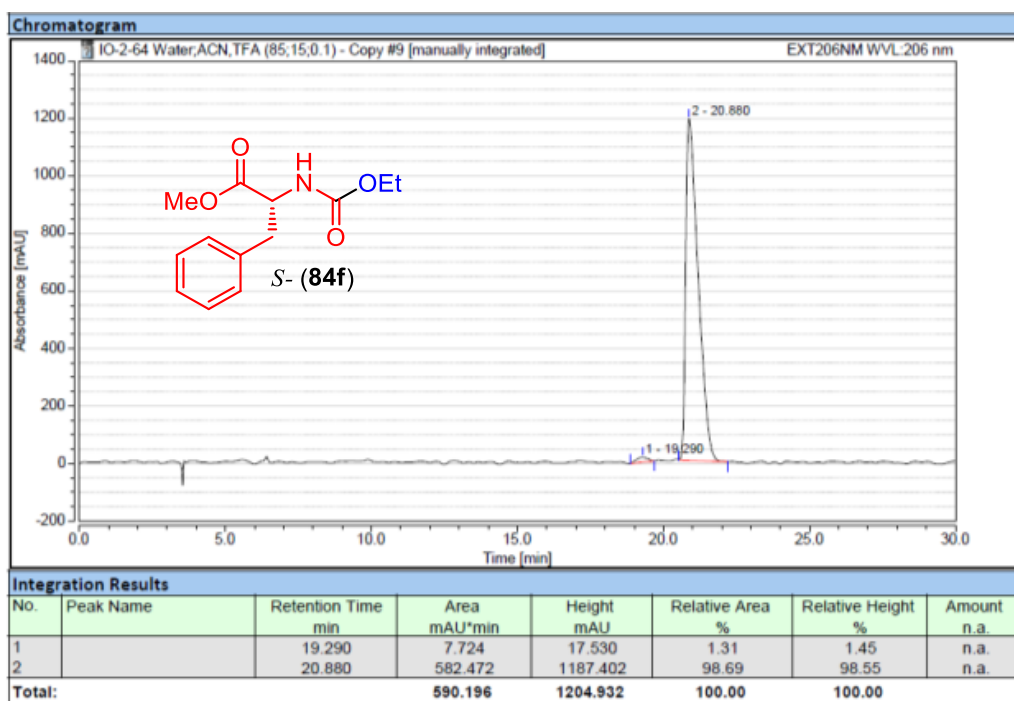


**Figure 6.7a:** HPLC Data for (*S*)-Methyl 2-((ethoxycarbonyl)amino)-3-phenylpropanoate (**84f**)

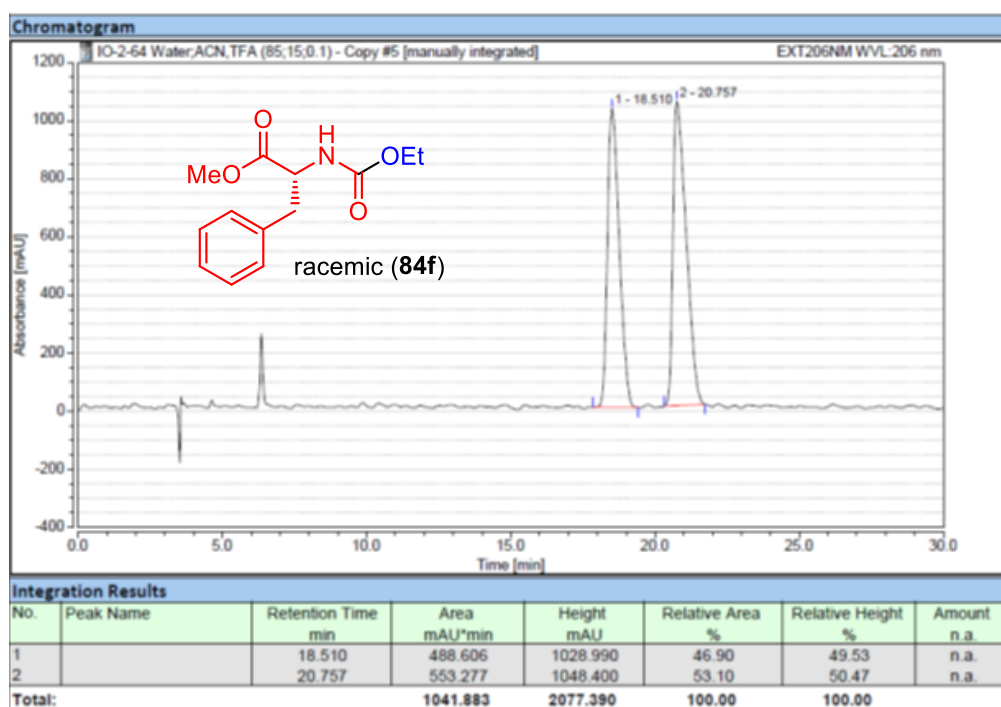


**Figure 6.7b:** HPLC Data for (*S*)-Methyl 2-((ethoxycarbonyl)amino)-3-phenylpropanoate (racemic-**84f**)

From a practical point of view, we could show that alcohol used as a solvent and nucleophile could be recovered after reaction. Simple vacuum distillation at the end of the process was thus successful, allowing about 90% alcohol recovery with satisfying purity ( $^1\text{H}$  NMR). Figure 6.8 shows the  $^1\text{H}$  NMR of recovered 3-chloro-1-propanol as an example.

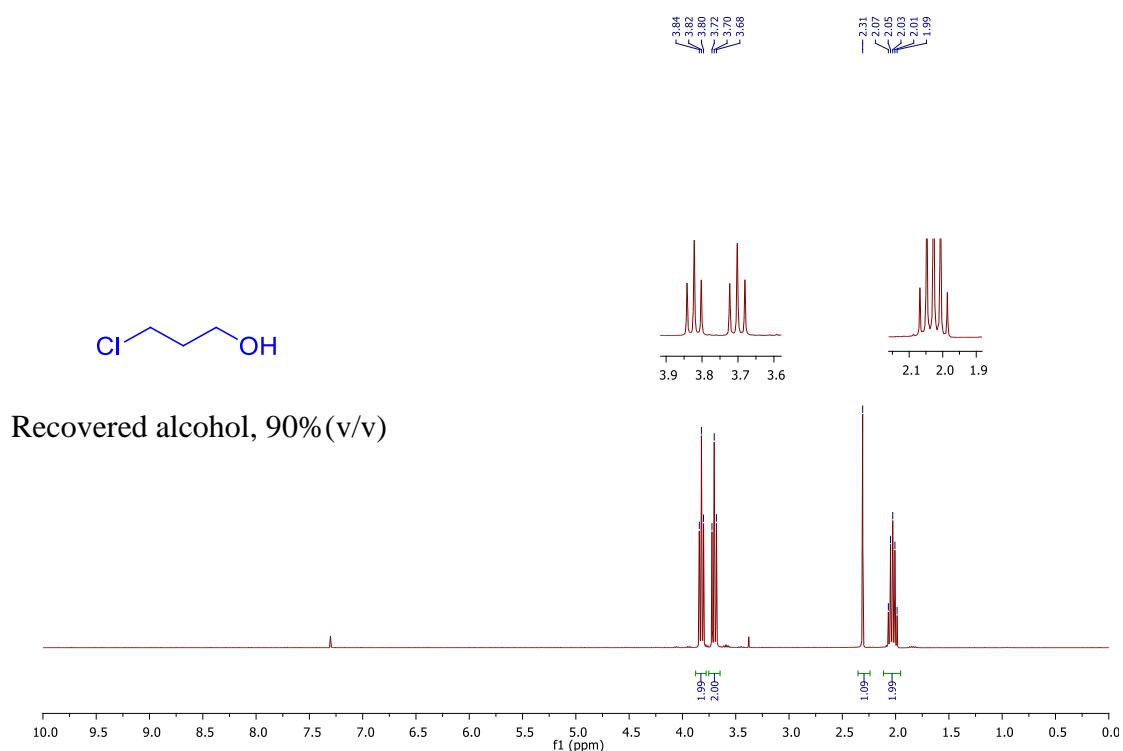


**Figure 6.8:**  $^1\text{H}$  NMR of recovered alcohol after electrochemical process

#### 4. Mechanistic studies

A tentative mechanism for the electrochemical synthesis of urethane is proposed as shown in Figure 6.9. Oxamic acid **A** undergoes a one electron oxidation at the anode to generate an unstable ketocarboxyl radical **I**, which would then suffer decarboxylation leading to the carbamoyl radical **II**.<sup>231</sup> A second oxidation of **II** would lead to a carbamoyl cation **III**, which may also be presented as a protonated isocyanate **IV**, then reaction of alcohol **B** with this intermediate would furnish the urethane **C**. Meanwhile,  $H^+$  is reduced in a counter reaction at the cathode, releasing hydrogen. During electrolysis of oxamic acid **17** in the presence of MeOH in  $CH_2Cl_2$ , a homocoupling product (diamide **24**) was observed confirming the formation of carbamoyl radical intermediate (Scheme 6.10). The formation of the coupling product **34** equally suggests that the oxidation of carbamoyl radical **II** to carbamoyl cation **III** is probably a slow process just as observed by Minisci.<sup>232</sup> Furthermore, formation of urea **80** when TEA was used as a base indicated a competing oxidation of the amine at the anode in agreement with the oxidative potential of  $NEt_3$  and oxamic acids which are around  $+0.95\text{ V}^{233}$  and  $+1.17\text{ V}^{234}$  (vs SCE) respectively. As mentioned earlier,  $Et_3N$  could, under two electron oxidation at the anode and in the presence of traces of water, produce dimethylamine **85** and acetaldehyde (Scheme 6.11),<sup>226</sup> the former then adding to the generated isocyanate **IV** resulting in **73** and thus supporting the formation of **IV** as an intermediate.

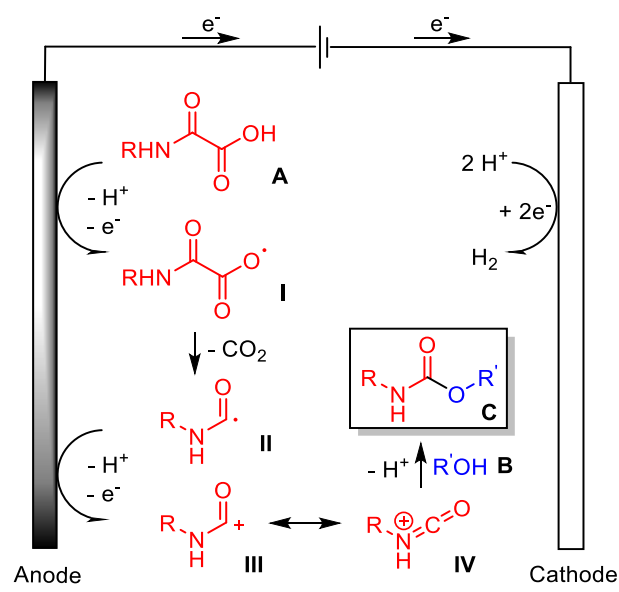


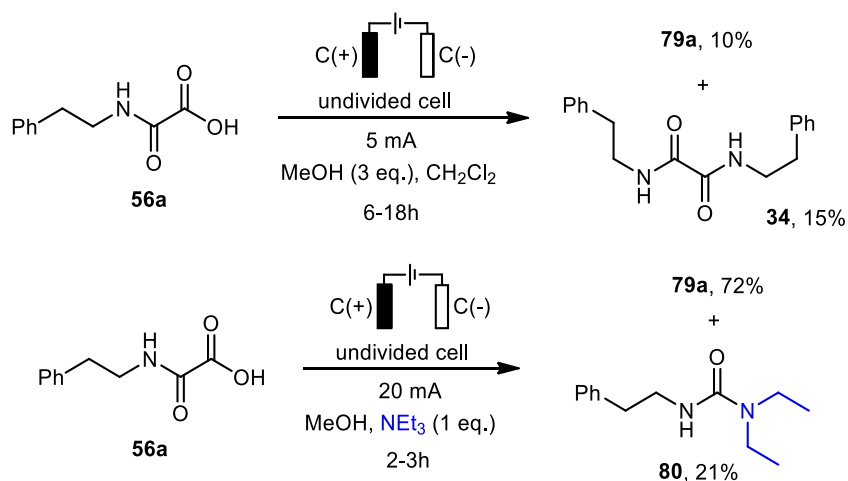
**Figure 6.9:** Mechanism of the electrochemical decarboxylation of oxamic acids.

<sup>231</sup> a) C. Chatgililoglu, D. Crich, M. Komatsu, I. Ryu, *Chem. Rev.* **1999**, *99*, 1991-2070. b) G. B. Gill, G. Pattenden, S. J. Reynolds, *J. Chem. Soc. Perkin Trans 1*, **1994**, 369-378.

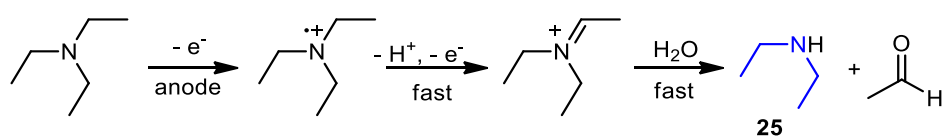
<sup>232</sup> a) F. Minisci, F. Coppa, F. Fontana, *J. Chem. Soc., Chem. Commun.* **1994**, 679. b) F. Minisci, F. Fontana, F. Coppa, Y. M. Yan, *J. Org. Chem.* **1995**, *60*, 5430-5433.

<sup>233</sup> F. Kanoufi, Y. Zu, A. J. Bard, *J. Phys. Chem. B*, **2001**, *105*, 210-216.

<sup>234</sup> X.-L. Lai, X.-M. Shu, J. Song, H.-C. Xu, *Angew. Chem. Int. Ed.* **2020**, *59*, 10626-10632.



**Scheme 6.10:** Mechanistic studies supporting the formation of carbamoyl radical **II** and cation **III-IV**



**Scheme 6.11:** Anodic oxidation of triethylamine<sup>226</sup>

From the cyclic voltammetry, while it was expected that two waves of oxidation ( $E_{ox1}$  and  $E_{ox2}$ ) would be seen in cyclic voltammetry (CV) of oxamic acid (Scheme 6.9 and 6.10), only one wave was observed. This may be rationalized by the small difference of voltage between  $E_{ox1}$  and  $E_{ox2}$  due to the stabilization of the carbamoyl cation **III** by resonance with the nitrogen center. Waldvogel *et al*<sup>235</sup> observed a similar event during electrochemical oxidation of arylamides.



**Scheme 6.12:** Anodic oxidation of oxamic acid

<sup>235</sup> T. Gieshoff, A. Kehl, D. Schollmeyer, K. D. Moeller, S. R. Waldvogel, *J. Am. Chem. Soc.* **2017**, *139*, 12317-12324.

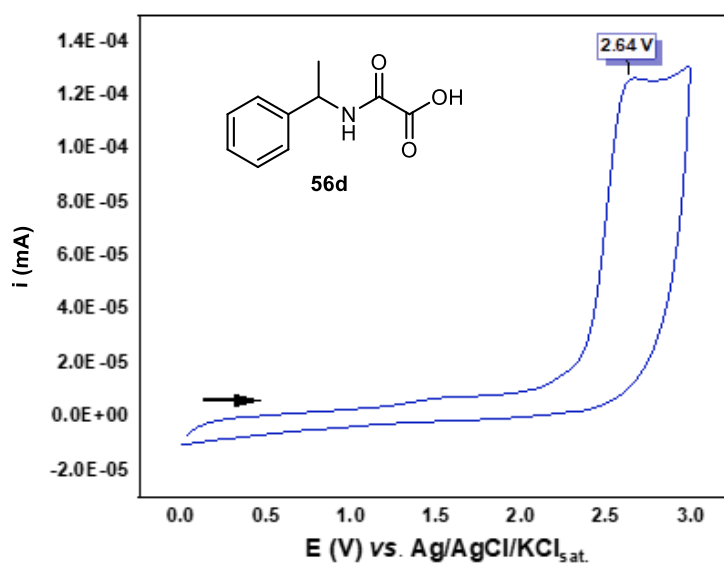


**Figure 6.10a.** Cyclic voltammogram for oxamic acid **56d** (5 mM) in  $\text{CH}_3\text{CN}/n\text{-Bu}_4\text{NPF}_6$  (0.1 M). Potential scan rate  $100 \text{ mV}\cdot\text{s}^{-1}$ . ( $E_{\text{ox}} = 2.595 \text{ V vs SCE}$ )

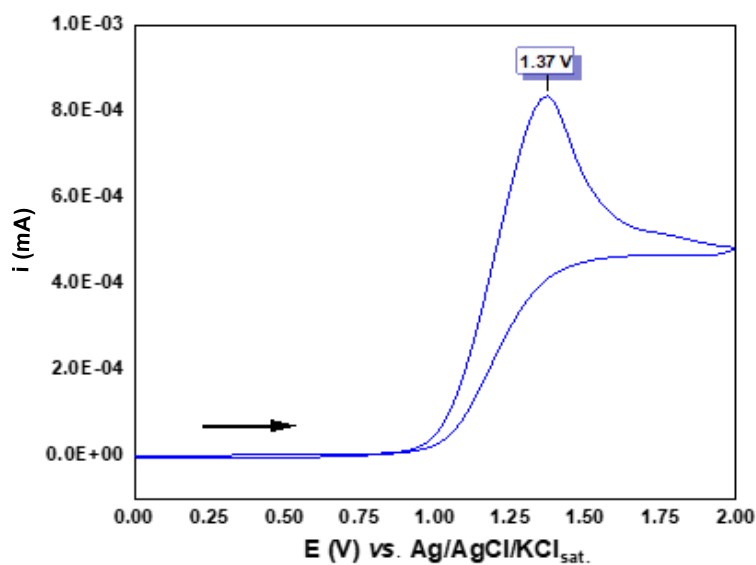


**Figure 6.10b.** Cyclic voltammogram for oxamic acid **56d** (5 mM) in the presence of  $\text{Et}_3\text{N}$  (5 mM), in  $\text{CH}_3\text{CN}/n\text{-Bu}_4\text{NPF}_6$  (0.1 M). Potential scan rate  $100 \text{ mV}\cdot\text{s}^{-1}$ . ( $E_{\text{ox}} = 1.32 \text{ V vs SCE}$ ).

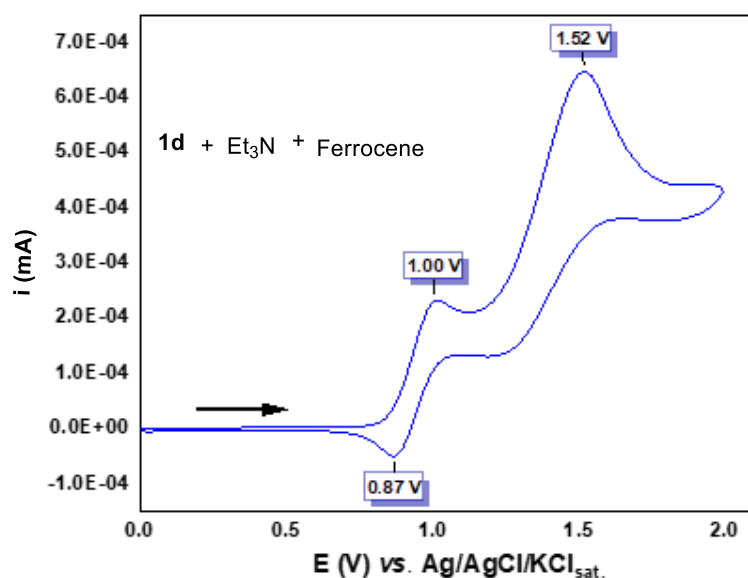


**Figure 6.10c.** Cyclic voltammogram for oxamic acid **56d** (5 mM), Et<sub>3</sub>N (5 mM) in CH<sub>3</sub>CN/*n*-Bu<sub>4</sub>NPF<sub>6</sub> (0.1 M) with ferrocene (5 mM) as internal reference. Potential scan rate 100 mV.s<sup>-1</sup>. ( $E_{\text{ox}} = 1.47$  V vs SCE)

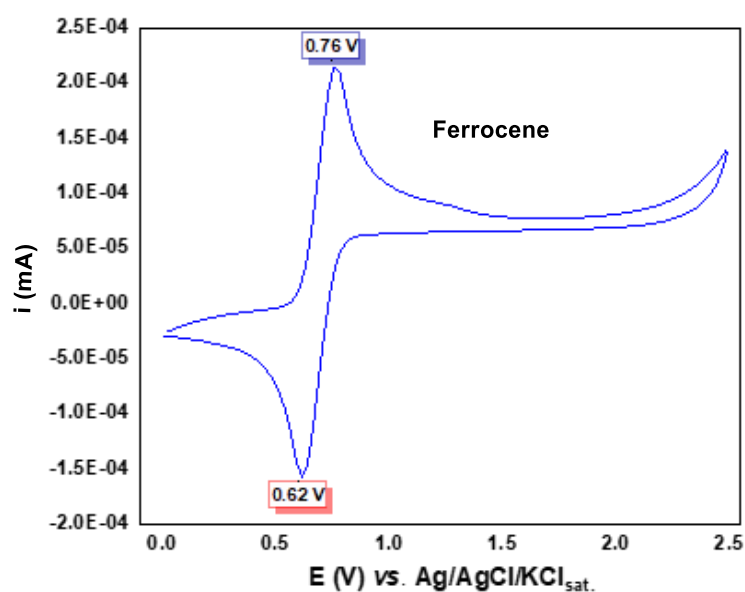
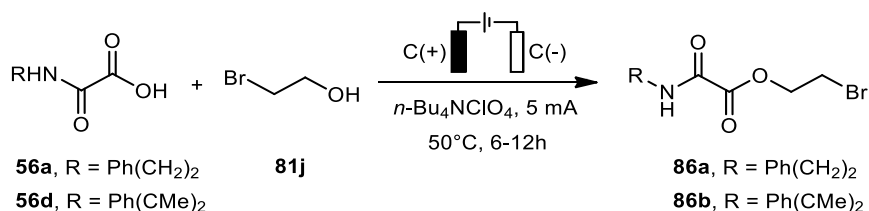


**Figure 6.10d.** Cyclic voltammogram for ferrocene (5 mM) in CH<sub>3</sub>CN/*n*-Bu<sub>4</sub>NPF<sub>6</sub> (0.1 M). Potential scan rate 100 mV.s<sup>-1</sup>.

## 5. Limitation of the electrochemical process

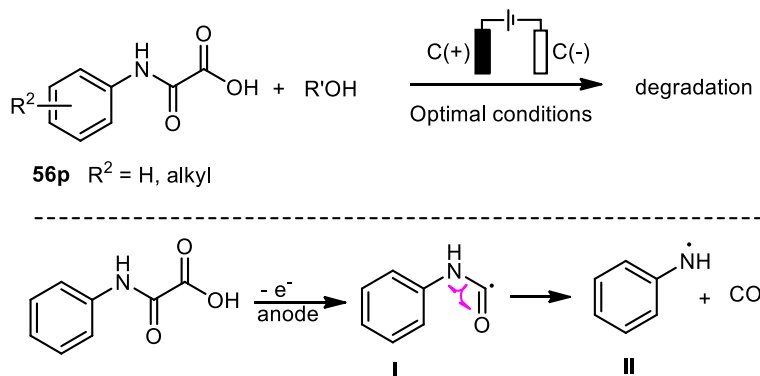
Some limitations were however observed during the electrochemical process, which include the following examples.

(1) When 2-bromoethanol **81j** (Scheme 6.11) was used as a solvent and nucleophile, esters of oxamic acids **86a-b** were obtained instead of the expected urethanes. We have currently no satisfying explanation to offer to rationalize this behavior.



**Scheme 6.11:** Electrolysis of oxamic acids and 2-bromoethanol gave esters of oxamic acids

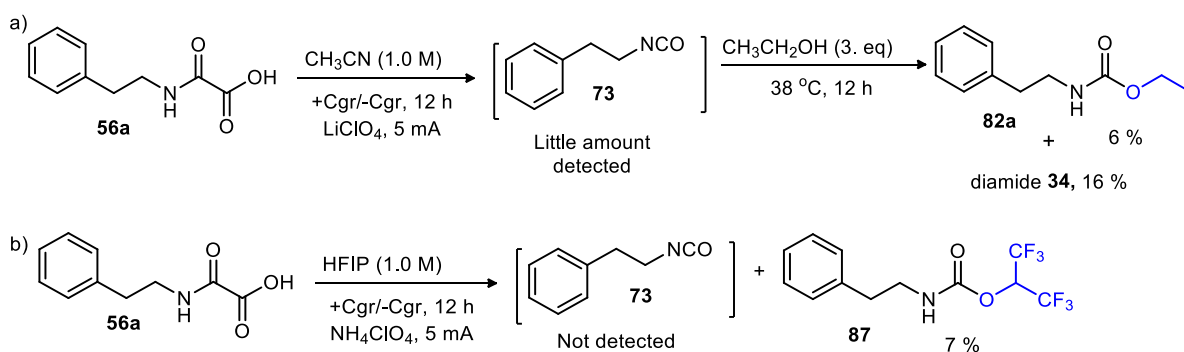
(2) Oxamic acids derived from anilines **56q** were not compatible with the electrochemical conditions. These substrates were equally not very stable for urethane synthesis using photocatalyzed procedure<sup>225</sup> probably due to the competitive decarbonylation of the carbamoyl radical intermediate leading to stabilized phenylaminy radical **II** (Scheme 6.12).<sup>232b</sup> They completely degraded during the electrochemical process.



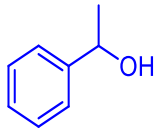
**Scheme. 6.12:** Unstable Aniline derived oxamic acids under the electrochemical conditions

(3) Attempt to perform the electrochemistry in other organic solvents such as CH<sub>3</sub>CN, CH<sub>2</sub>Cl<sub>2</sub> and HFIP, using only stoichiometric amount of alcohol was not successful, as less than 10% urethane was obtained alongside carbamoyl radical homocoupling product (diamide **34**). Table 6.2 shows more details of such trials. Urethane yields tend to increase with the increase in the alcohol concentration. Furthermore, a two-step process was equally tried where isocyanate would be electrochemically generated first followed by addition of alcohol in the second step to give urethane (Scheme 6.13a); only about 6% of urethane was equally observed in this case, alongside homocoupling product **34** when the reaction was carried out using CH<sub>3</sub>CN as solvent. Also, an attempt to use HFIP as solvent to generate the isocyanate led to formation of carbamate **87** in 7% yield (**b**). However, Lam and co-workers<sup>236</sup> recently showed that with collidine and 10 mol% of DBTDL catalyst, a moderate amount of urethane could be obtained by this method. Though, the use of high concentration of toxic tin in their method may limit its application as an environmentally friendly alternative to classical urethane route.

<sup>236</sup> A. Petti, C. Fagnan, C. G. W. van Melis, N. Tanbouza, A. D. Garcia, A. Mastrodonato, M. C. Leech, I. C. A. Goodall, A. P. Dobbs, T. Ollevier, K. Lam, *Org. Process Res. Dev.* **2021**, 25, 2614–2621.



**Scheme 6.13:** urethane synthesis from oxamic acids under electrochemical conditions using a two-steps approach

S/N	Solvent (0.1M)	ROH	Electrolyte (0.2 eq.)	Additive	Yield (%)	
					82	34
1	CH <sub>3</sub> CN	EtOH (3 eq.)	LiClO <sub>4</sub>	-	5	12
2	CH <sub>3</sub> CN	MeOH (3 eq.)	K <sub>2</sub> CO <sub>3</sub>	-	28	12
3	DCM	EtOH (3 eq.)	LiClO <sub>4</sub>	-	10	20
5	DCM	EtOH (3 eq.)	LiClO <sub>4</sub>	Et <sub>3</sub> N (1.0 eq.)	< 5	ND
6	DCM	EtOH (3 eq.)	LiClO <sub>4</sub>	Collidine (3.0 eq.), AgPF <sub>6</sub> (1.5 eq.), 3Å (150 mg)	17	ND
7	DCM/CH <sub>3</sub> CN (4:1)	EtOH (3 eq.)	LiClO <sub>4</sub>	-	9	10
8	CH <sub>3</sub> CN	 3.0 eq.	LiClO <sub>4</sub>	NH <sub>4</sub> I (0.15 eq.) HFIP (1.0 eq.)	12	ND
9	DCM/CH <sub>3</sub> CN (4:1)	EtOH (10 eq.)	LiClO <sub>4</sub>	-	19	12
10	DCM/CH <sub>3</sub> CN (4:1)	EtOH (20 eq.)	LiClO <sub>4</sub>	-	39	11
11	DCM	EtOH (20 eq.)	<i>n</i> -Bu <sub>4</sub> N <sub>4</sub> ClO <sub>4</sub>	-	40	12
12	HFIP	EtOH (20 eq.)	<i>n</i> -Bu <sub>4</sub> N <sub>4</sub> ClO <sub>4</sub>	-	12	trace
13	Acetone	EtOH (20 eq.)	<i>n</i> -Bu <sub>4</sub> N <sub>4</sub> ClO <sub>4</sub>	-	ND	ND

**Table 6.2:** Electrochemical synthesis of urethane from oxamic acids in organic solvent using stoichiometric amount of alcohol

## Conclusion

A practically simple electrochemical process for preparation of urethanes from oxamic acids and alcohols has been reported. This one-step procedure furnished urethanes in moderate to good yields through the *in-situ* generation of isocyanate by anodic oxidation of oxamic acids without any chemical oxidant required. The reaction operates at a very low current density of 5 mA making it mild. With methanol as alcoholic solvent, the corresponding carbamates were delivered in good yields without any additives or supporting electrolyte required. In addition, only simple purification exercise was required to obtain the product with high purity. This metal-, photocatalyst-, light- and oxidant-free reaction should serve as a useful tool to access important urethanes of pharmaceutical interest.

## General conclusion

In this project, new non-phosgene procedures for the synthesis of urethanes and polyurethanes through the *in-situ* generation of isocyanate from oxamic acids were developed. Processes that completely avoids the use toxic phosgene or the *in-situ* generation of carcinogenic isocyanates, using a safer precursor have continued to attract attentions in the research community.

Oxamic acids have been designated versatile greener precursors for the generation of isocyanates. They can easily be oxidized into isocyanates by radical mediated processes. Access to oxamic acids is straightforward, involving coupling of amines and oxalic acid derivatives, a process that is promising for accessing bio-sourced monomers for bio-sourced PU synthesis. Oxamic acids are bench stables and relatively non-toxic compounds, hence would be easier to handle and stored if chosen as raw material for urethane and polyurethane synthesis, compared to the current phosgene precursors. Oxamic acids have also been shown as potent carbamoyl radical sources for organic synthesis. A vast number of synthetic procedures developed in the two decades for the preparation of amides and heterocycles using oxamic acids are reviewed in this work.

A total of four new procedures for the synthesis of urethanes and polyurethanes from oxamic acids were developed in this project. First, a new visible-light mediated decarboxylation of oxamic acid for the synthesis of polyurethanes was unveiled.  $^1\text{H}$  NMR and FT-IR indicated that the obtained PUs have similar structures with one prepared using standard diisocyanate. Although relatively low to modest molecular weight PUs were obtained by this method as room temperature, it served as a foundation for the development of a more efficient synthetic route to PUs using oxamic acids as greener precursors.

Also, a new NIR light mediated procedure for the preparation of urethanes from oxamic acids was developed during this project. This new procedure uses very small amount of  $\text{Os}(\text{btpy})_2(\text{PF}_6)_2$  (0.3 mol%) as catalyst to furnish urethanes in excellent yield. Application of this procedure for carbamoylation of heteroarenes using oxamic acids was also successful. With mono-oxamic acid, the NIR light procedure demonstrated superior penetration depth into media compared to blue light counterpart. However, it was not suitable for polyurethane synthesis from bis-oxamic acid using bulk method, which was one of the main targets of this study. Nevertheless, this procedure can serve as a useful tool for the synthesis of carbamates and amides from oxamic acids with the advantage of relying on a very mild light source and low catalyst loading.

Furthermore, PIDA-mediated oxidative decarboxylation of oxamic acids under mild heating was also developed during this project. This practically simple procedure relies on the mild thermal activation of PIDA to trigger the decarboxylation of oxamic acids to generate urethanes in excellent yields in one-pot in the presence of alcohols, without isolation of the putative isocyanate intermediate. The method was shown to be competent for the synthesis of thermoplastic polyurethanes using a wide range of bis-oxamic acids and diols/polyols, furnishing polyurethanes with properties analogous to

PU samples made from commercial diisocyanates. Application of this procedure to the preparation of a self-blown PU foam using CO<sub>2</sub> released during the decarboxylation of oxamic acids as a blowing agent, was also demonstrated.

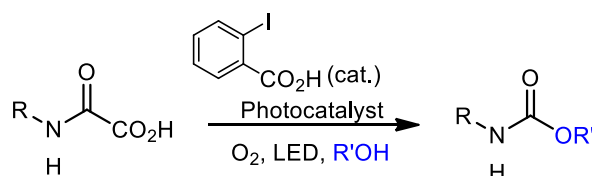
Lastly, a practically simple electrochemical process for preparation of urethanes from oxamic acids and alcohols was also developed during this project. This one-step procedure furnished urethanes in moderate to good yields through the *in-situ* generation of isocyanates by anodic oxidation of oxamic acids without any chemical oxidant required. The reaction operates at a very low current density of 5 mA making it mild. However, this electrochemical process was not suitable for polyurethane synthesis because it only worked efficiently using excess alcohol, which is not compatible for PUs synthesis.

## Perspectives

The new oxamic acid procedures for the synthesis of urethanes and polyurethanes developed in this project have prospects to serve as greener alternatives to the existing isocyanate route. Interestingly, the oxamic acid route may provide another platform for accessing bio-sourced PUs from the abundant bio-resources including amino-acid feedstock, fatty acids, terpenes, resinic acids, isosorbide as well as lignin derivatives or sugars.

Particularly, the PIDA-mediated procedure exhibited reasonable performance towards the synthesis thermoplastic PUs and well as PUs foams where the CO<sub>2</sub> released during the oxamic acid decarboxylation served as blowing agent. Procedure for accessing self-blown PU foams using safer precursors are interesting from industrial point of view. Also, high kinetics of this reaction during the foam formation is quite attractive as an alternative procedure for polyurethane synthesis.

However, further process optimizations are ongoing within the group to boost the viability of this promising alternative procedure. First, the chemical oxidant requirement for the reaction needs to be further optimized. Though an attempt was made during this project to address this issue by developing electrochemical process using anodic oxidation as a replacement for the stoichiometric amount of hypervalent iodine reagent, this method is not yet suitable for PUs synthesis. Another strategy that could address this problem is the use of a catalytic amount of hypervalent iodine precursor as proposed in the Scheme 6.14, where oxygen can serve as cheap terminal oxidant.



**Scheme 6.14:** Proposed catalytic amount of hypervalent iodine precursor for the oxidation of oxamic acids into isocyanates

Also, another limitation that is being addressed is the control of the foaming process. Though flexible foams were obtained during this project by dropping the pressure at some point during the foaming process, this strategy may not be suitable for industrial applications.

Lastly, more experimentation is still needed to gain more insight into the mechanism of the PIDA-mediated procedure for urethane and PUs synthesis from oxamic acids.



# Experimental Part

## 1. General Information:

### *Chemicals/reagents*

All reagent-grade chemicals were obtained from commercial suppliers and were used as received unless otherwise noted. CH<sub>2</sub>Cl<sub>2</sub> (DCM), MeOH, THF and diethyl ether were dried over activated alumina columns on MBraun Solvent Purification System (SPS-800). 1,2-dichloroethane and MeCN were distilled from CaH<sub>2</sub>, anhydrous dimethylformamide (DMF) (99.8%,) was purchased from Acros organics. Phenyliodine(III) diacetate (PIDA, 98%) was purchased from Fluorochem. Poly(ethylene glycol) at 1500 g.mol<sup>-1</sup> (PEG-1500) and 1,6-diaminohexane (>98%) were purchased from Alfa Aesar company. Poly(tetrahydrofuran) at 1000 g.mol<sup>-1</sup> (PTMO-1000) was sourced from Sigma Aldrich. Bis(trifluoromethanesulfonyl)imide (TFMI), *N,N*-Dimethylformamide, 1,5-pentandiol (98%) were the products of Acros Organics, 1,4-butandiol (> 99.0%) was obtained from TCI Chemicals. Some of the alcohols especially relatively older ones were purified by azeotropic distillation in toluene. Hemoglobin bovine (lyophilized powder, CAS Number: 9008-02-0) was procured from Sigma Aldrich company and the solution was made by dissolving the powder in water (17.0 g/L).

### 1.1. Instruments and Methods

*NMR Analysis:* <sup>1</sup>H NMR and <sup>13</sup>C-NMR were recorded on various spectrometers: a Bruker Avance 300 (<sup>1</sup>H: 300 MHz, <sup>13</sup>C: 75.46 MHz), and a Bruker DRX400 (<sup>1</sup>H: 400 MHz, <sup>13</sup>C: 100.6 MHz) using CDCl<sub>3</sub> as internal reference unless otherwise indicated. The chemical shifts ( $\delta$ ) and coupling constants ( $J$ ) are expressed in ppm and Hz respectively. The following abbreviations were used to explain the multiplicities: bs = broad singlet, s = singlet, d = doublet, t = triplet, q = quartet, dd = doublet of doublets, m = multiplets.

*High Resolution Mass Spectrometry (HRMS):* This was recorded with a Waters Q-TOF 2 spectrometer in the electrospray ionization (ESI) or atmospheric pressure chemical ionization (APCI) mode.

*High-Performance Liquid Chromatography (HPLC):* This was done using a Thermo Scientific Dionex Ultimate 3000 with a column Lux 5 $\mu$ m Cellulose-3, 250x4.6 mm. The eluent was a mixture of water: acetonitrile: trifluoroacetic acid (22:45:0.1).

*Optical rotations:* Optical rotation was determined using a Rudolph Research Analytical Autopol III Automatic Polarimeter.

*Size Exclusion Chromatography (SEC) Analysis:* SEC analysis was performed using Ultimate 3000 system from Thermoscientific equipped with diode array detector DAD. The system also include a multi-angles light scattering detector MALS and differential refractive index detector dRI from Wyatt technology. For the SEC in HFIP, HFIP + 0,05% KTFA was as the eluent. Polymers were separated on two PL HFIP gel columns (300 x 7.5 mm) (exclusion limits from 100 Da to 150 000 Da) at a flowrate of 0.8 mL/min. Columns temperature was held at 40°C. Easivial kit of PMMA from Agilent was used as the standard. All the PU samples were solubilized in the indicated solvent 24h, filtered using PTFE filter (0.45  $\mu$ m).

For SEC in DMF, DMF + lithium bromide LiBr 1g/L was used as the eluent. Polymers were separated on two Shodex Asahipack gel columns GF310 and GF510 (300 x 7.5 mm) (exclusion limits

from 500 Da to 300 000 Da) at a flowrate of 0.5 mL/min. Columns temperature was held at 50°C. Easivial kit of Polystyrene from Agilent was used as the standard (Mn from 162 to 364 000 Da).

**Column chromatography:** Flash chromatography was used with silica gel (0.043-0.063 mm).

**Thin Layer Chromatography (TLC):** TLC was done using silica gel 60 F254 pre-coated plates (Merck). Ultraviolet light, potassium permanganate or ceric ammonium molybdate were used for visualizing the spots.

**Fourier Transform Infrared Spectroscopy (FTIR) Analysis:** Bruker-Tensor 27 spectrometer, equipped with a diamond ATR cell was used to record infrared spectra from 400 to 4000  $\text{cm}^{-1}$ , using 64 scans at a resolution of 4  $\text{cm}^{-1}$ .

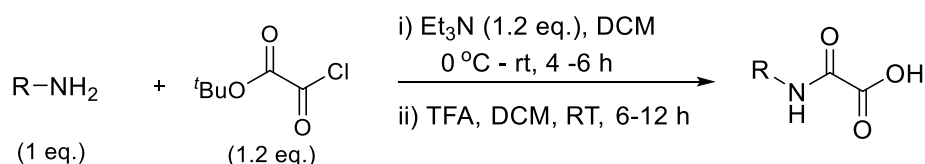
**ThermoGravimetric Analysis (TGA):** TGA was performed using TGA-Q50 and TGA-Q500 system, TA Instruments. The analyses were conducted under a nitrogen atmosphere at a heating rate of 10°C.min<sup>-1</sup> from room temperature to 600°C and then under air atmosphere from 600 to 700°C.

**Differential Scanning Calorimetry (DSC):** DSC was recorded using a DSC Q100 apparatus, TA Instruments. The analysis was done using two heating cycles from -80 to 180°C at 10°C.min<sup>-1</sup>. The melting point and glass transition temperatures were determined from the second curve.

**Melting points (m.p):** Stuart melting point apparatus was used to record melting points of molecular compounds while that of polymers was determined from DSC analysis.

## 2. General procedure for preparation of oxamic acids

### Method A: Preparation of mono-oxamic acids<sup>237,238,239,240,241,242.</sup>



To a two-neck round-bottom flask equipped with magnetic stirrer and containing anhydrous  $\text{CH}_2\text{Cl}_2$  (0.3 M), amine (1 eq.) and  $\text{Et}_3\text{N}$  (1.2 eq.) were added under argon atm. Note: for solid amine, it was first weighed into the flask, flushed with argon before solvent and  $\text{Et}_3\text{N}$  were added. The resulted solution was cooled to 0°C using ice. This was followed by the addition of *t*-butyl-2-chloro-2-oxoacetate (1.2 eq.) dropwise over 10 min. The mixture was warmed to room temperature and allowed to stir for 4–6 h, thereafter washed with 1M HCl (20 mL). The aqueous layer was further extracted with DCM (2 x 20 mL) and the combined organic layer was washed with brine, dried with anhydrous  $\text{Na}_2\text{SO}_4$  and concentrated under reduced pressure. The resulted ester was dissolved in DCM (0.3 M). TFA (5.0 eq.) was added to the solution which was stirred at room temperature for 6 to 12h. Completion of the *t*-butyl ester deprotection was monitored by TLC. The solution was concentrated

<sup>237</sup> I. M. Ogbu, J. Lusseau, G. Kurtay, F. Robert, Y. Landais, *Chem. Commun.*, **2020**, 56, 12226-12229.

<sup>238</sup> G. G. Pawar, F. Robert, E. Grau, H. Cramail, Y. Landais, *Chem. Commun.*, **2018**, 54, 9337-9340.

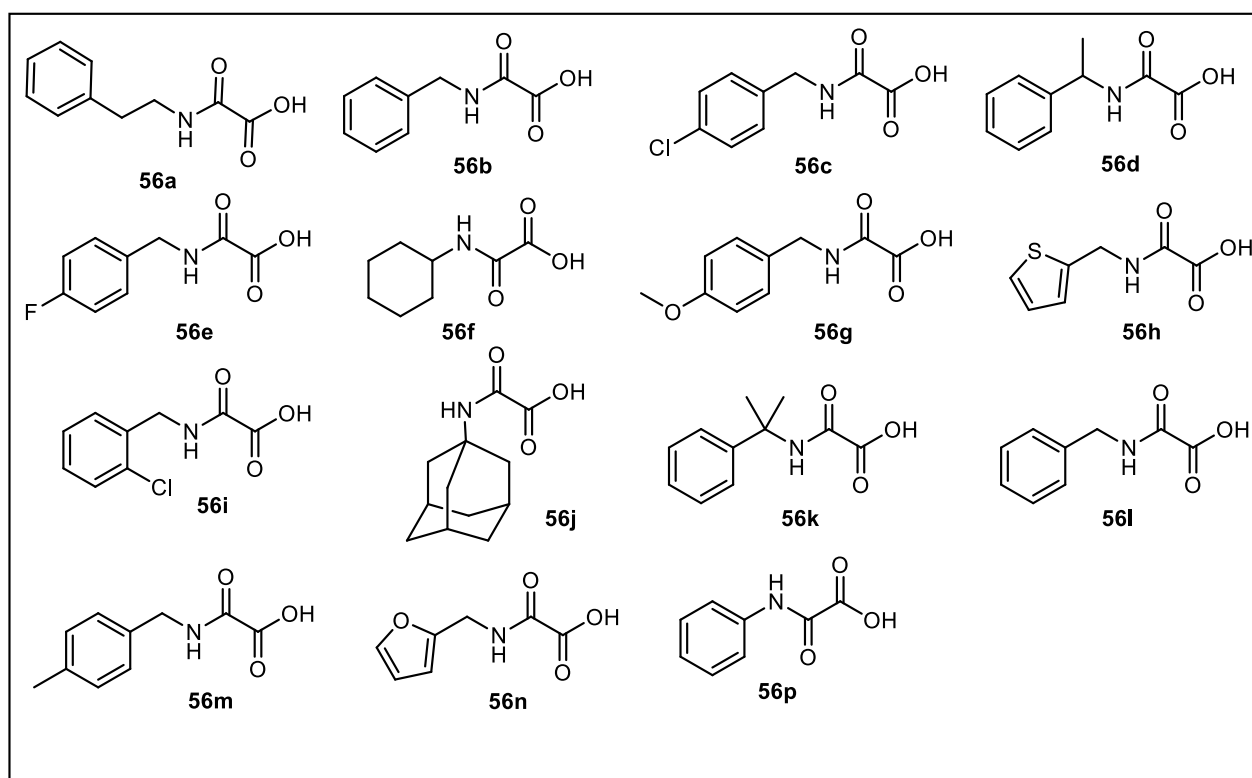
<sup>239</sup> A. H. Jatoi, G. G. Pawar, F. Robert, Y. Landais, *Chem. Commun.*, **2019**, 55, 466-469.

<sup>240</sup> a) S. D. Linton *et. al. J. Med. Chem.* **2005**, 48, 6779-6782. b) H. Hanchu, J. Kunfang, C. Yiyun, *Angew. Chem. Int. Ed.* **2015**, 54, 1881-1884.

<sup>241</sup> J. Bálint, G. Egri, M. Czugler, J. Schindler, V. Kiss, Z. Juvancz, E. Fogassy, *Tetrahedron: Asymmetry* **2001**, 12, 1511-1518.

<sup>242</sup> N. S. Vujicic, Z. Glasovac, N. Zweep, J. H. van Esch, M. Vinkovic, J. Popovic, M. Zinic, *Chem. Eur. J.* **2013**, 19, 8558-8572

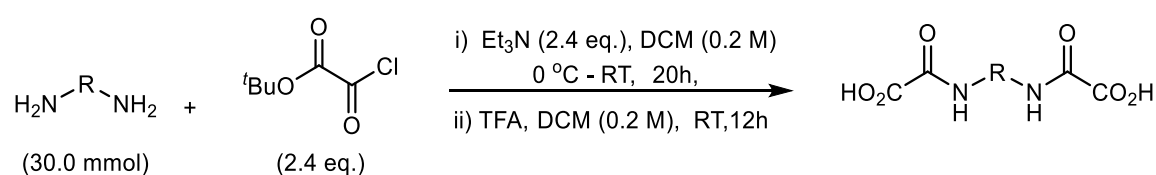
*in vacuo* to deliver the oxamic acids as milky to white solids. The spectroscopic data of the synthesized oxamic acids were in agreement with literature<sup>238,240,241,242</sup>.



Ref: **56a**<sup>240</sup>, **56b**<sup>240</sup>, **56c**<sup>238</sup>, **56d**<sup>241</sup>, **56e**<sup>238</sup>, **56f**<sup>240</sup>, **56g**, **56h**<sup>238</sup>, **56i**<sup>238</sup>, **56j**<sup>238</sup>, **56k**<sup>238</sup>, **56l**<sup>238</sup>, **56m**<sup>238</sup>, **56n**<sup>238</sup>, **56p**<sup>240</sup>, **56p**<sup>238</sup>

**Figure S1:** Oxamic acids substrates synthesized from method A

### Method B: Preparation of bis-oxamic acids<sup>237,238,239</sup>



**Scheme S2.** Preparation of oxamic acids

To a two-neck round-bottom flask equipped with magnetic stirrer, corresponding bis-amine (30.0 mmol) was added and flushed with argon. CH<sub>2</sub>Cl<sub>2</sub> (100 mL) and Et<sub>3</sub>N (72.0 mmol, 2.4 eq.) were added under argon atm. *t*-Butyl-2-chloro-2-oxoacetate (72.0 mmol, 2.4 eq.) was added dropwise at 0°C under argon atm for 15 min. The reaction was continued at room temperature for 20h at room temperature and thereafter was washed with water (100 mL). The aqueous layer was further extracted with CH<sub>2</sub>Cl<sub>2</sub> (2x30 mL), the combined organic layer was washed with brine, dried over sodium sulfate, and concentrated under reduced pressure to obtain crude solid compound. The crude product was then treated with TFA (10 eq.) in dichloromethane (0.3 M) for 12h at room temperature and then mixture was concentrated under reduced pressure to give desired bis-oxamic acid product as a white solid.

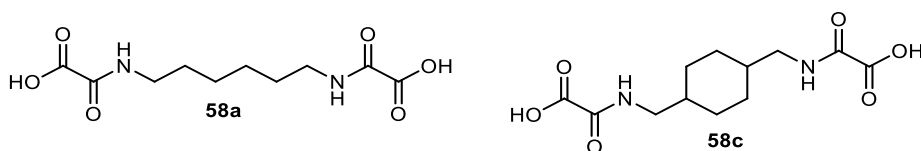
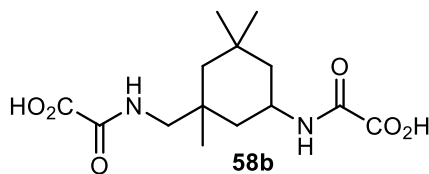


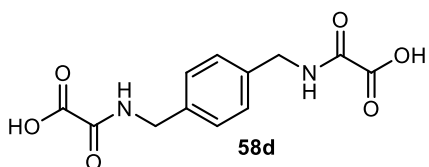
**Figure S2:** Bis-oxamic acids substrates synthesized from method B: **58a**<sup>242</sup> and **58c**<sup>238</sup>

**2-(((5-(Carboxyformamido)-1,3,3-trimethylcyclohexyl)methyl)amino)-2-oxoacetic acid**



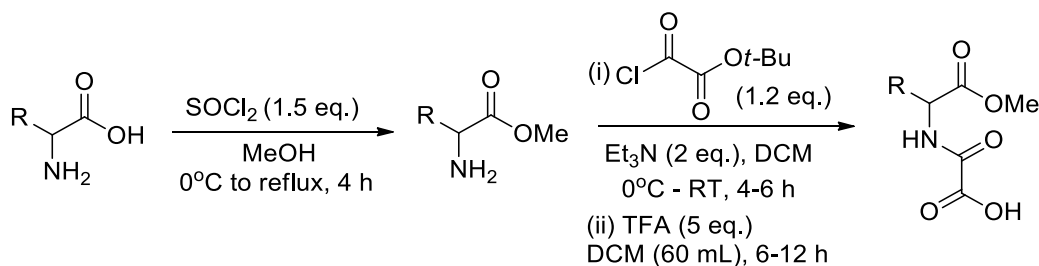
**58b** (8.15 g) was obtained through the general procedure in 86% yield as a white solid; m.p. : 127-130°C; <sup>1</sup>H NMR (300 MHz, DMSO-*d*<sub>6</sub>) δ : 13.78 (s, 2H), 8.83 - 8.47 (m, 2H), 4.15 - 3.68 (m, 1H), 3.04 - 2.74 (m, 2H), 1.41 (t, *J* = 10.8 Hz, 2H), 1.25 - 0.95 (m, 10H), 0.89 (s, 3H). <sup>13</sup>C NMR (75 MHz, DMSO-*d*<sub>6</sub>) δ : 162.9, 159.5, 158.1, 55.4, 52.8, 47.2, 44.8, 43.0, 40.8, 37.2, 35.4, 31.8, 27.9, 23.7.

**2,2'-((1,4-Phenylenebis(methylene))bis(azanediy))bis(2-oxoacetic acid) (1q)**



Following the general procedure 2A, using 7.3 mmol of the corresponding diamine, oxamic acid **58d** (2.29 g, 90%) was obtained as a white solid, m.p. : 204-205°C. <sup>1</sup>H NMR (300 MHz, MeOD) δ : 7.28 (s, 4H), 4.44 (s, *J* = 8.9 Hz, 4H). <sup>13</sup>C NMR (76 MHz, MeOD) δ : 161.4, 158.9, 137.0, 127.5, 42.6. IR (neat) ν<sub>max</sub> (cm<sup>-1</sup>) : 3347, 3168, 1757, 1677, 1554. HRMS (ESI): Calcd. for C<sub>12</sub>H<sub>11</sub>O<sub>6</sub>N<sub>2</sub> [M-H]<sup>-</sup> 279.0622, found 279.0620.

**Method C: Preparation of chiral oxamic acids**



**Scheme S3:** Preparation of amino acid derived oxamic acids

The corresponding amino acid (30.0 mmol) was added in a dry two-neck round-bottom flask equipped with a reflux condenser. The content was flushed with argon, methanol (25 mL) was added under argon. Thionyl chloride (45.11 mmol) was added to the resulted heterogeneous mixture dropwise at 0°C over 15 min and under constant stirring, after which a homogeneous solution was obtained. The mixture was warmed to room temperature and then reflux for 4 h. The reaction mixture was concentrated under reduced pressure to give a colorless oil. The product was washed with *n*-hexane by stirring it in the solvent for 10 min, then decanting the solvent. This was repeated twice to give a solid product. The latter was dissolved in DCM (60 mL) under argon atm, cooled to 0°C, Et<sub>3</sub>N (60.15 mmol) was added into the mixture and *t*-butyl-2-chloro-2-oxo acetate (36.08 mmol) added dropwise over 10 min under constant stirring. The reaction was continued at room temperature for 4-6h and thereafter washed successively with water (100 mL) and brine (100 mL), dried over sodium sulfate and concentrated under reduced pressure to give a solid product. The crude product was

dissolved in DCM (60 mL) and treated with TFA (11.5 mL, 150 mmol) at room temperature for 6 h. the resulted solution was concentrated *in vacuo* to give the desired chiral oxamic acid.

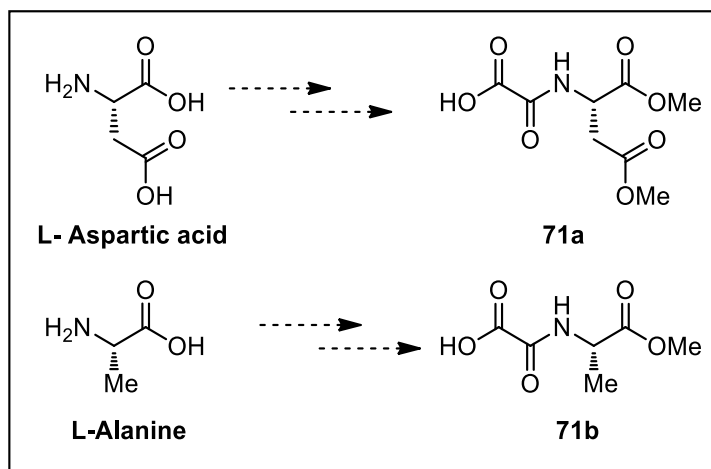
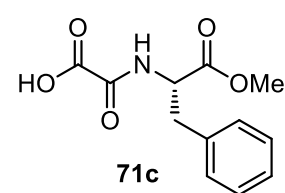


**Figure S3:** Amino acid-derived chiral oxamic acid substrates previously reported<sup>239</sup>

### (S)-2-((1-Methoxy-1-oxo-3-phenylpropan-2-yl)amino)-2-oxoacetic acid (71c)



Following the general procedure 2B, using 12 mmol of corresponding amino acid, the corresponding oxamic acid **71c** (1.22 g, 80%) was obtained as a light brown gel, which later solidified, m.p. : 101-102°C. <sup>1</sup>H NMR (300 MHz, CDCl<sub>3</sub>) δ : 7.63 (s, 1H), 7.44 – 7.20 (m, 3H), 7.13 (dd, J = 7.5, 1.7 Hz, 2H), 4.98 – 4.72 (m, 1H), 3.79 (s, 3H), 3.21 (m, J = 14.0, 6.1 Hz, 2H). <sup>13</sup>C NMR (76 MHz, CDCl<sub>3</sub>) δ : 170.2, 158.9, 156.9, 134.7, 129.1, 128.9, 127.6, 54.3, 52.8, 37.8. IR (neat) ν<sub>max</sub> (cm<sup>-1</sup>): 3327, 3023, 2943, 1742, 1692, 1535. HRMS (ESI): Calcd. for C<sub>12</sub>H<sub>13</sub>O<sub>5</sub>NNa [M+Na]<sup>+</sup> 274.0685, found 274.0679. [α]<sub>D</sub><sup>25</sup> : +43.04 (c = 0.5, CHCl<sub>3</sub>).

## Experimental Part: Chapter 3

### 3. Experimental setup visible-light photocatalyzed reactions

All the visible-light photocatalyzed polymerization were set up on bench-top in the open air and the reactions were carried out in Schlenk tube, degassed and backfilled with argon. Unless otherwise noted, all the reaction were carried out at room temperature. Unless otherwise noted, the solvents and the solutions of reagents/reactants were transferred *via* microsyringe or plastic syringe (fitted with metal needle) into the reaction test tubes under a positive argon pressure. Photochemical reactions were performed at 455 nm with Castorama blue LEDs (λ = 455 nm (± 15 nm), 12 V, 500 mA).

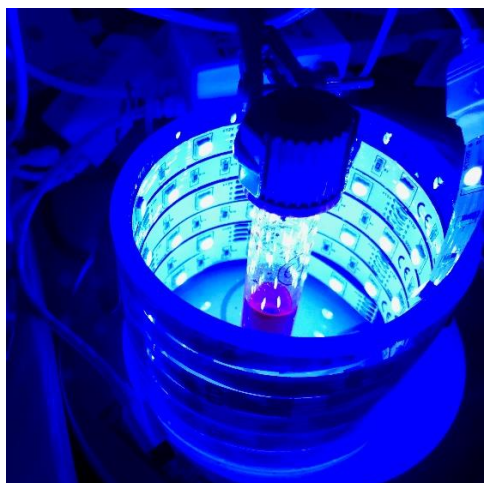
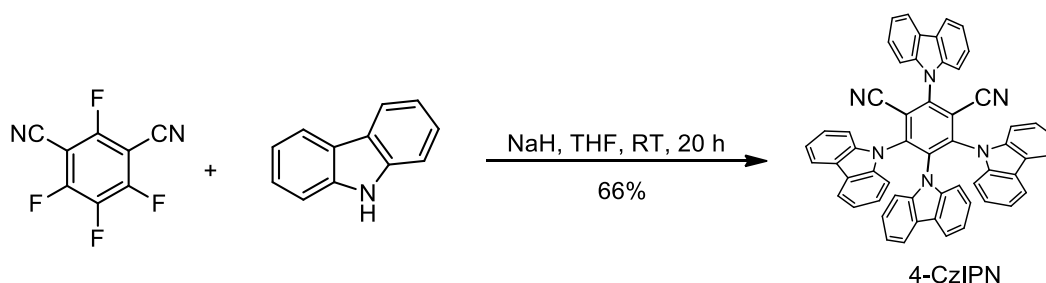


**Figure S4.** Experimental Setup

### 3.1. Synthesis of 1,2,3,5-tetrakis(carbazol-9-yl)-4,6-dicyanobenzene (4-CzIPN):



**Scheme S4.** Synthesis of 4-CzIPN

Carbazole (4.18 g, 25 mmol) was dissolved in dry THF (100 mL) in a two-neck round-bottom flask under an argon atm, at room temperature. NaH (60% in oil, 1.4 g, 60 mmol) was added slowly under stirring. The mixture was stirred for 30 min, thereafter tetrafluoroisophthalonitrile (1.0 g, 5 mmol) was added and the mixture was stirred for 12h. The reaction was quenched with water (5 mL) and concentrated *in vacuo*. The mixture was washed with water and EtOH successively to afford yellow solid product. The product was recrystallized by dissolving it in minimum quantity of CH<sub>2</sub>Cl<sub>2</sub> and adding pentane to give the pure 4-CzIPN (3.1 g, 79% ) as a yellow solid; <sup>1</sup>H NMR (300 MHz, CDCl<sub>3</sub>) δ : 8.25 (dt, *J* = 7.8, 1.0 Hz, 2H), 7.80 - 7.66 (m, 8H), 7.57 - 7.47 (m, 2H), 7.36 (d, *J* = 7.6 Hz, 1H), 7.32 - 7.21 (m, 5H), 7.19 - 7.05 (m, 8H), 6.91 - 6.79 (m, 4H), 6.73 - 6.60 (m, 2H). <sup>13</sup>C NMR (75 MHz, CDCl<sub>3</sub>) δ : 145.2, 144.6, 140.0, 138.2, 137.0, 134.8, 127.0, 125.79, 125.0, 124.8, 124.6, 123.9, 122.4, 122.0, 121.4, 121.0, 120.4, 119.7, 116.4, 111.6, 110.0, 109.5, 109.4. Spectroscopic data were in good agreement with literature.<sup>243</sup>

<sup>243</sup> H. Uoyama, K. Goushi, K. Shizu, H. Nomura, C. Adachi, *Nature* **2012**, 492, 234-238.

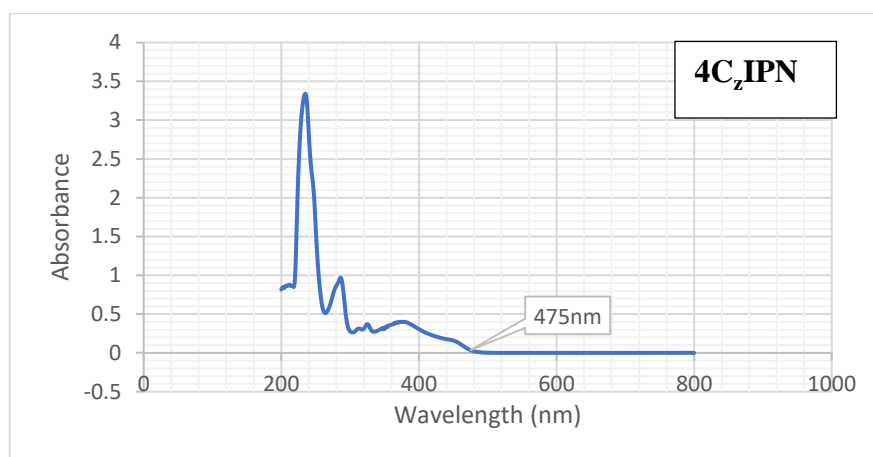


**Figure S5.** UV-visible absorption of 4CzIPN in DCE

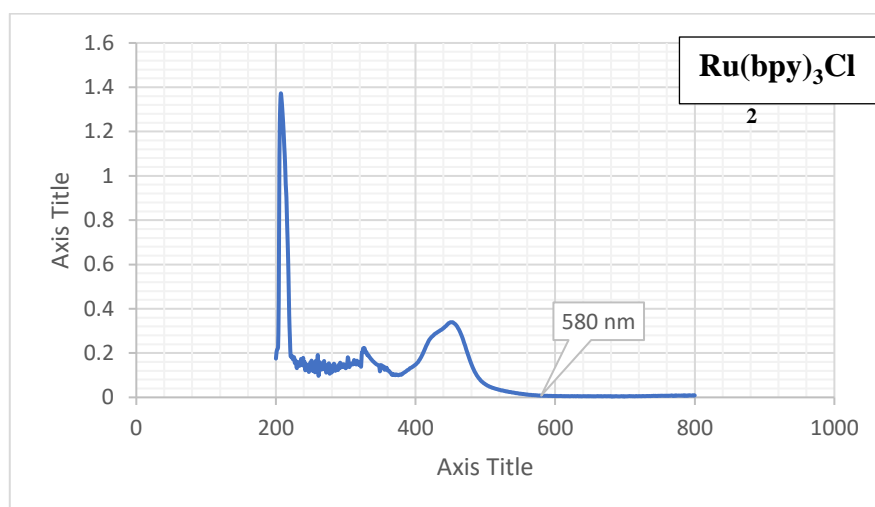
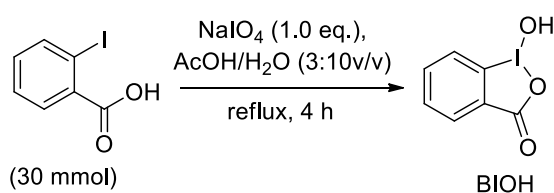


**Figure S6.** UV-visible absorption of  $\text{Ru}(\text{bpy})_3\text{Cl}_2$  in acetone

### 3.2. 1-Hydroxy-1,2-benziodoxol-3(1H)-one



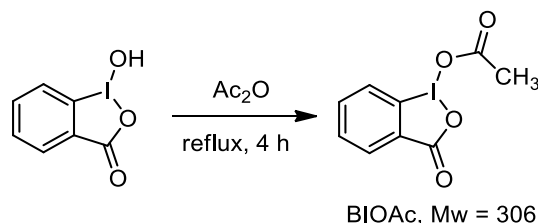
**Scheme S5:** Preparation of 2-iodobenzoic acid

2-iodobenzoic acid (BI-OH, CAS: 131-62-4), was prepared following a reported procedure.<sup>238,244</sup> 2-iodobenzoic acid (7.4 g, 30.0 mmol, 1.0 eq.) and sodium periodate (6.7 g, 31.0 mmol, 1.0 eq.) were weighed into a 100 mL round-bottom flask. A mixture of 13.5 mL acetic acid and 31.5 mL of water was added. The reaction mixture was refluxed for 4 h under constant stirring and protection from light using aluminum foil. Thereafter, 120 mL of cold water was added, and the mixture was allowed to cool to room temperature. The white solid product was obtained by filtration and was successively

<sup>244</sup> Fernández González, D.; Brand, J. P.; Waser, *J. Chem. Eur. J.* **2010**, *16*, 9457-9461.

washed with ice-cold water (3x30 mL), acetone (3x30 mL) and then, air dried in the dark overnight. 1-Hydroxy-1,2-benziodoxol-3(1H)-one (6.6 g, 84%) was obtained as a white solid compound. <sup>1</sup>H NMR (300 MHz, DMSO-d<sub>6</sub>) δ : 8.09 - 7.91 (m, 3H), 7.85 (dd, J = 8.2, 1.1 Hz, 1H), 7.70 (td, J = 7.3, 1.1 Hz, 1H). <sup>13</sup>C NMR (75 MHz, DMSO-d<sub>6</sub>) δ : 168.2, 134.9, 132.0, 131.6, 130.8, 126.7, 120.9. Spectroscopic data were in good agreement with literature.<sup>238,244</sup>

### 3.3. B. Preparation of 1-Acetoxy-1,2-benziodoxol-3-(1H)-one

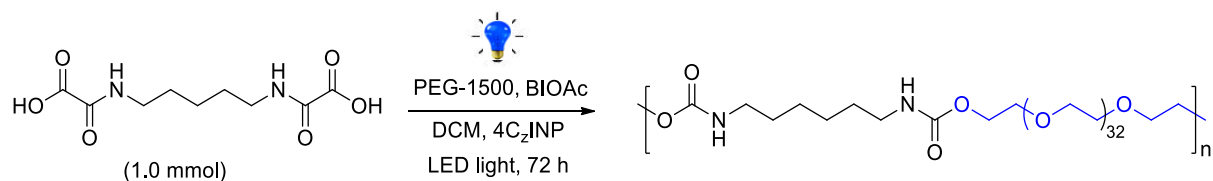


#### Scheme S6: Preparation of BI-OAc

1-Acetoxy-1,2-benziodoxol-3-(1H)-one (BI-OAc, CAS: 1829-25-0), was prepared following previously reported procedure<sup>Error! Bookmark not defined.</sup><sup>245</sup> BI-OH (6.0 g, 22.7 mmol) was mixed with acetic anhydride (20 mL) in a round-bottom flask equipped with reflux condenser. The solution was heated under reflux until BI-OH completely dissolved. The solution was allowed to cool to room temperature and thereafter was further cooled to -20°C using dry ice/acetone system. The product (white crystals) was obtained by filtration, dried under vacuum for 12 h.

BI-OAc (6.1 g, 88%, m.p. : 171-173°C. <sup>1</sup>H NMR (300 MHz, CDCl<sub>3</sub>) δ : 8.23 (dt, J = 7.6, 1.4 Hz, 1H), 7.99 (ddt, J = 8.3, 1.2, 0.5 Hz, 1H), 7.91 (ddd, J = 8.4, 7.0, 1.6 Hz, 1H), 7.70 (ddt, J = 7.6, 7.0, 0.9 Hz, 1H), 2.24 (s, 3H). <sup>13</sup>C NMR (75 MHz, CDCl<sub>3</sub>) δ : 176.4, 168.2, 136.1, 133.2, 131.3, 129.3, 129.0, 118.3, 20.3. Spectroscopic data were in good agreement with literature<sup>238,245</sup>

### 3.4. Procedure for photocatalyzed polymerization

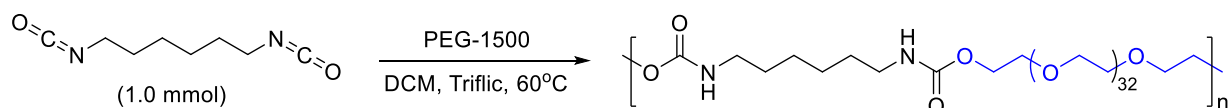


#### Scheme S7: Visible light photocatalyzed synthesis of polyurethane synthesis from bis-oxamic acids

Bis-oxamic acid (1.0 mmol, 1.0 eq.), PEG-1500 (1.0 mmol, 1.0 eq.), BI-OAc (2.5 eq.) and 4CzIPN (5 mol%) were charged into an oven-dried Schlenk tube equipped with a magnetic bar. The tube was degassed and back filled with argon. Dry CH<sub>2</sub>Cl<sub>2</sub> (0.2M) was added into the tube under argon atm. The tube was placed in blue LED light at room temperature and under constant stirring for 24-72 h. The polyurethane was precipitated from diethyl ether and dried at reduced pressure.

<sup>245</sup> P. Eisenberger, S. Gischig, A. Togni, *Chem. Eur. J.* **2006**, *12*, 2579-2586.

### 3.5. Procedure for synthesis of polyurethane from commercial diisocyanate

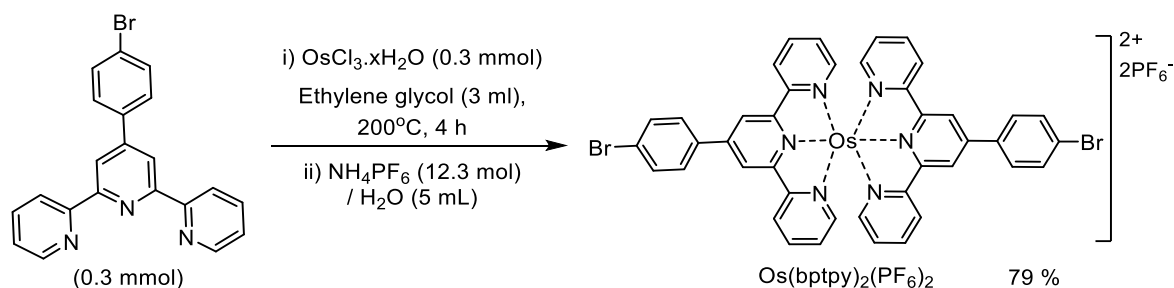


**Scheme S8:** Synthesis of polyurethane from commercial diisocyanate

PEG1500 (5.0 mmol, 1.0 eq.) was charged into an oven-dried re-sealable tube. The content of the tube was degassed and backfilled with argon. Dry DCE (0.5 mL), HDI (5.0 mmol, 1.0 eq.) and triflic acid (5.0 mol%) were added under argon atm. The reaction mixture was heated to 60°C for 24 h. The polyurethane was precipitated from diethyl ether and dried at reduced pressure.

## 4. Experimental Part: Chapter 4

### 4.1. Synthesis of Os(btpy)<sub>2</sub>(PF<sub>6</sub>)<sub>2</sub>



**Scheme S9:** Synthesis of Os(btpy)<sub>2</sub>(PF<sub>6</sub>)<sub>2</sub>

Os(btpy)<sub>2</sub>(PF<sub>6</sub>)<sub>2</sub> complex was synthesized according to reported literature<sup>246</sup> with some modifications. Osmium (III) chloride hydrate (89.4 mg, 0.30 mmol) and 4'-(4-bromophenyl)-2,2':6',2''-terpyridine (CAS: 89972-76-9, 234.6 mg, 0.60 mmol) were mixed in ethylene glycol (3 mL) in a round bottom flask equipped with magnetic stirrer and reflux condenser. The mixture was degassed, backfilled with argon then refluxed under continuous stirring at 200°C in a 200°C-preheated hotplate for 5 h. Thereafter, the dark mixture was directly transferred into 5 mL saturated solution of NH<sub>4</sub>PF<sub>6</sub> (2 g in 5 mL of deionized water). The resulted dark purple precipitates were collected by filtration, purified using column chromatography (alumina, toluene/CH<sub>3</sub>CN 1:1) to obtain the desired complex as a dark purple solid 298 mg, 79%. <sup>1</sup>H NMR (300 MHz, DMSO) δ : 9.53 (s, 4H), 9.11 (d, J = 8.1 Hz, 4H), 8.40 (d, J = 8.4 Hz, 4H), 8.10 - 7.86 (m, 8H), 7.44 (d, J = 5.4 Hz, 4H), 7.22 (t, J = 6.5 Hz, 4H). <sup>13</sup>C NMR (76 MHz, DMSO) δ : 160.1, 155.2, 152.7, 145.2, 138.3, 135.1, 132.6, 130.4, 128.5, 125.4, 124.6, 120.1. Spectroscopic data were in good agreement with literature.<sup>246,247</sup>

<sup>246</sup> Y. Sasaki, S. Amemori, H. Kouno, N. Yanai, N. Kimizuka, *J. Mater. Chem. C*, **2017**, *5*, 5063-5067.

<sup>247</sup> B.D. Ravetz, N.E.S. Tay, C.L. Joe, M. Sezen-Edmonds, M.A. Schmidt, Y. Tan, J.M. Janey, M.D. Eastgate, T. Rovis, *ACS Cent. Sci.* **2020**, *6*, 2053-2059.

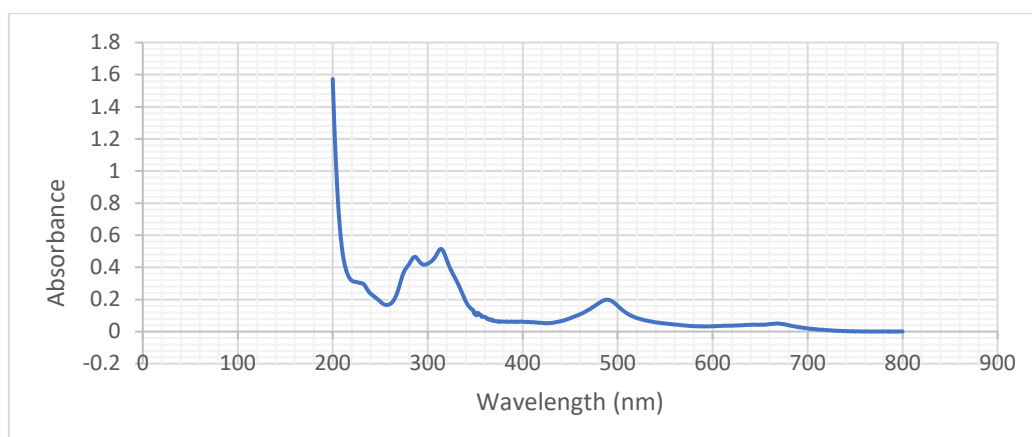
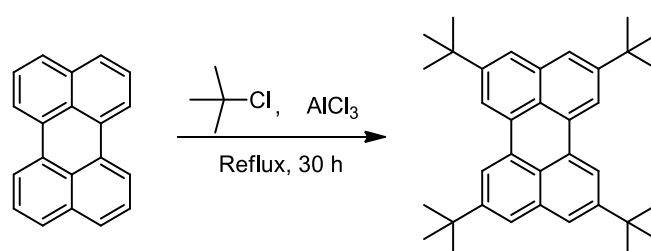


**Figure S7:** UV-visible absorption of Os(btpy)<sub>2</sub>(PF<sub>6</sub>)<sub>2</sub> complex in CH<sub>3</sub>CN

#### 4.2. Synthesis of 2,5,8,11-Tetra(*tert*-butyl)perylene (TTBP)



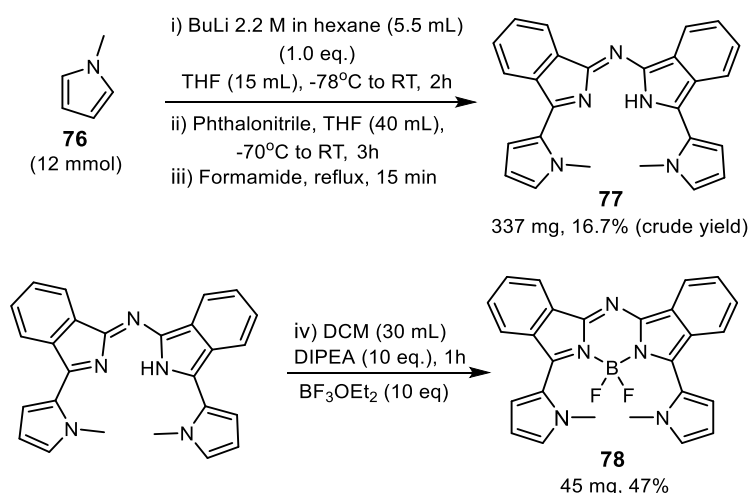
**Scheme S10:** Synthesis of TTBP

2,5,8,11-Tetra(*t*-butyl)perylene (TTBP) was synthesized following a reported literature.<sup>248</sup> In a two-necked round bottom flask equipped with reflux condenser and magnetic bar, perylene (0.5 g, 1.98 mmol) was added. The content was flushed with argon and dry *t*-butyl chloride (50 mL) was added into the flask under argon atm, followed by the addition of anhydrous aluminium trichloride (1.0 g). The mixture was then refluxed for 6 h. Additional *t*-Butyl chloride (30 mL) was added and the reaction mixture was allowed to reflux overnight. Thereafter, additional 20 mL of *t*-butyl chloride and 1.0 g anhydrous aluminium trichloride were added to the mixture and allowed to reflux for additional 24h. After cooling to room temperature, the mixture was extracted with 100 mL of brine in a separatory funnel. The aqueous layer was further extracted with DCM (3x50 mL). The combined organic layer including the *t*-butyl chloride portion was dried with anhydrous Na<sub>2</sub>SO<sub>4</sub> and concentrated *in vacuo* at 80°C. The product obtained (viscous liquid) was further baked in a petri-dish at 170°C for 30h using a hot plate until smoke evolution stopped. Dark brown solid obtained was dissolved in a mixture of petroleum ether and chloroform (2:1). The mixture was purified by column chromatography (silica, petroleum ether/chloroform). The product was obtained as a yellow crystal (0.75 g, 80%), R<sub>f</sub> : 9.2 (CHCl<sub>3</sub>/petroleum ether, 1:1). <sup>1</sup>H NMR (300 MHz, CDCl<sub>3</sub>) δ : 8.27 (d, J = 1.7 Hz, 4H), 7.65 (d, J = 1.6 Hz, 4H), 1.53 (s, 36H). <sup>13</sup>C NMR (76 MHz, CDCl<sub>3</sub>) δ : 148.7, 134.9, 130.8, 125.8, 123.3, 117.7, 34.9, 31.4. Spectroscopic data were in good agreement with literature.<sup>248,249</sup>

<sup>248</sup> S. H. C. Askes, W. Pomp, S. L. Hopkins, A. Kros, S. Wu, T. Schmidt, S. Bonnet, *small* **2016**, 12, 40, 5579–5590.

<sup>249</sup> R. O. Al-Kaysi, T. Sang Ahn, A. M. Muller, C. J. Bardeen, *Phys. Chem. Chem. Phys.* **2006**, 8, 3453.

### 4.3. Synthesis of aza-BODIPY



**Scheme S11:** Synthesis of aza-BODIPY

Aza-BODIPY was synthesized in four steps following a procedure reported in the literature (Scheme S11).<sup>250</sup>

**(i) *N*-methyl-pyrrolyllithium (76):** This was first prepared by adding 5.5 mL of *n*-butyl lithium (1.0 eq., 2.2M in hexane) dropwise into a solution of *N*-methylpyrrole (0.97 g) in dry THF (15 mL) at -78°C, under vigorous stirring and in an argon atm. Thereafter, the solution was allowed to stir at room temperature for 2h and was used in the second step directly without purification.

**(ii) synthesis of aza-diisoindolmethine (77):** A mixture of phthalonitrile (10.0 mmol) in diethyl ether (40 mL) was cooled to -70°C under argon atm. The crude *N*-methylpyrrolyllithium obtained from step (i) was added into the suspension dropwise under vigorous stirring and was allowed to stir for 3h at room temperature. The solution was concentrated *in vacuo*. Formamide (50 mL) was added into the dark resulted mixture, and rapidly heated to about 210°C using a heat gun to obtain a coppery precipitate with a release of ammonia gas. The precipitate was separated by filtration and washed (5x30 mL) with a mixture of methanol/water (2:1 v/v). The obtained precipitate was further purified by flash column (silica, acetone/petroleum ether 20/80). Metalescent solid (337 mg, 16.7%). <sup>1</sup>H NMR (300 MHz, CDCl<sub>3</sub>) δ : 12.60 (s, 1H), 8.17 – 8.11 (m, 1H), 7.77 (d, J = 8.0 Hz, 2H), 7.43 – 7.36 (m, 2H), 7.34 – 7.26 (m, 2H), 6.95 (s, 2H), 6.88 (d, J = 2.4 Hz, 2H), 6.41 – 6.33 (m, 2H).

**(iii) aza-BODIPY 78** was obtained by dissolving the aza-diisoindolmethine precursor 77 (85 mg, 0.21 mmol) in a dry DCM (30 mL), anhydrous DIPEA (*N,N*-diisopropylethylamine, 10 eq., 271 mg) was added dropwise at room temperature. The reaction mixture was stirred for 1h and thereafter, BF<sub>3</sub>.OEt<sub>2</sub> (10 eq., 296 mg) was added dropwise in the reaction mixture at room temperature. The reaction was allowed to stir overnight. The mixture was added into brine (20 mL) and was extracted with DCM (3x30 mL). The combined organic layer was concentrated *in vacuo* and the obtained solid was purified by column chromatography (silica, DCM/petroleum ether 60/40) to obtain the final product as a dark green solid (45 mg, 47%). R<sub>f</sub> : 0.31 (DCM/petroleum ether, 60/40). <sup>1</sup>H NMR (300 MHz, CDCl<sub>3</sub>) δ : 8.13 (d, J = 8.2 Hz, 2H), 7.58 – 7.42 (m, 4H), 7.34 (t, J = 7.2 Hz, 2H), 7.03 – 6.86 (m, 4H), 6.37 (dd, J = 3.8, 2.7 Hz, 2H), 3.67 (s, 6H). <sup>13</sup>C NMR (101 MHz, CDCl<sub>3</sub>) δ : 143.2, 139.8, 133.1, 131.5, 129.8, 128.5, 126.9, 124.5, 124.1, 117.8, 110.2, 36.0. Spectroscopic data were in good agreement with literature.<sup>250</sup>

<sup>250</sup> T.-Y. Li, T. Meyer, R. Meerheim, M. Hoppner, C. Korner, K. Vandewal, O. Zeika, K. Leo, *J. Mater. Chem. A*, **2017**, *5*, 10696.

#### 4.4. Synthesis of BODIPY B-7

BODIPY **B-7** was synthesized in five steps following procedure reported in literature (Scheme S12).<sup>251</sup>

(i) Benzoyl chloride **102** (1.4 g, 10 mmol) and 2,4-dimethylpyrrole (2 mL, 20 mmol) were added into a dry two-necked round bottom flask containing dry DCM (80 mL) under argon. The mixture was stirred overnight at room temperature. Triethylamine (10 mL) and BF<sub>3</sub>.Et<sub>2</sub>O (10 mL) were added under ice-cold condition. The reaction mixture was stirred for additional 1h at room temperature and thereafter was transferred into water (100 mL). The organic layer was collected, dried with MgSO<sub>4</sub> and concentrated *in vacuo*. The crude mixture was purified using column chromatography (silica, AcOEt/petroleum ether 20/80) to obtain the precursor BODIPY **103** as a greenish/brownish solid (665 mg, 21%). R<sub>f</sub> = 0.72 (DCM/hexane, 1:1). <sup>1</sup>H NMR (300 MHz, CDCl<sub>3</sub>) δ : 7.58 – 7.42 (m, 3H), 7.36 – 7.22 (m, 2H), 6.00 (s, 2H), 2.58 (s, 6H), 1.40 (s, 6H). <sup>13</sup>C NMR : (76 MHz, CDCl<sub>3</sub>) δ 155.4, 143.2, 141.7, 135.0, 131.4, 130.6, 129.4, 129.1, 128.9, 128.3, 127.9, 121.2, 14.6, 14.3.

(ii) **103** (1.24 mmol, 400 mg) was dissolve in dry DCM (100 ml) in a two-neck round bottom flask equipped with a magnetic stirrer under argon atm. *N*-iodo-succinimide (NIS, 1.24 mmol, 280 mg) was first dissolved in dry CH<sub>3</sub>CN (1 mL) under argon atm to obtain a homogeneous solution, dry DCM (9 mL) was added to make the solution up to 10 mL, The resulted succinimide solution was added dropwise to the BODIPY solution using a syringe pump over a period of 1h at 10-15°C and under continuous stirring. The reaction mixture was concentrated *in vacuo* and purified using chromatography (silica, petroleum ether/ DCM: 2/1 v/v) to obtain the iodinated product as a red solid **104** (430 mg, 77%), R<sub>f</sub> : 0.37 (petroleum ether/DCM: 2/1). <sup>1</sup>H NMR (300 MHz, CDCl<sub>3</sub>) δ : 7.66 – 7.39 (m, 3H), 7.28 (dd, J = 6.4, 3.1 Hz, 2H), 6.07 (s, 1H), 2.66 (s, 3H), 2.59 (s, 3H), 1.40 (d, J = 1.9 Hz, 6H).

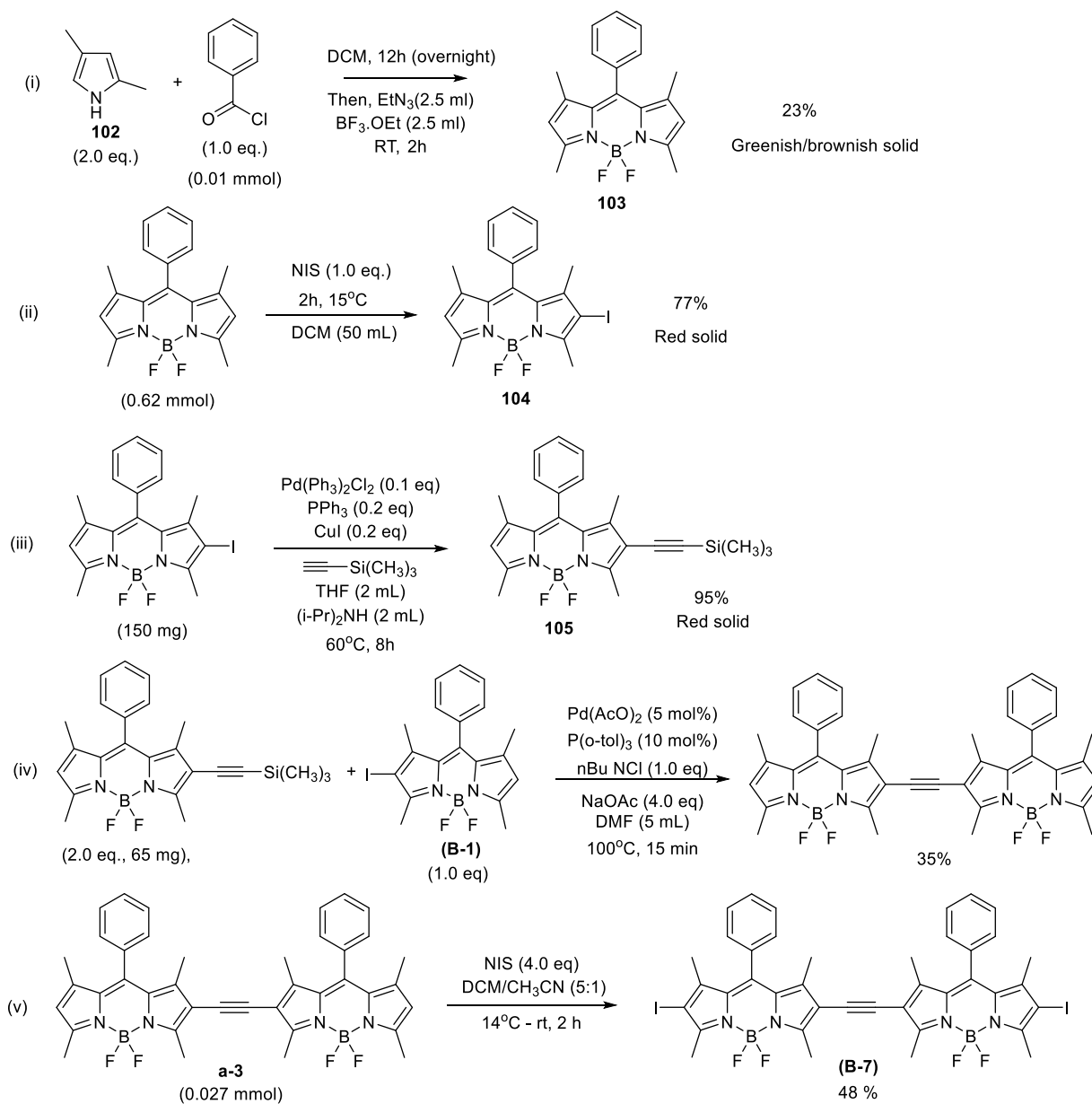
(iii) Iodinated BODIPY **104** (0.33 mmol, 1.0 eq., 150 mg), Pd(PPh<sub>3</sub>)<sub>2</sub>Cl<sub>2</sub> (0.1 eq., 13.5 mg), PPh<sub>3</sub> (17.4 mg, 0.2 eq.), and CuI (12.6 mg, 0.2 eq.) were weighed into a dry two-neck flask equipped with a magnetic bar and stirrer. The mixture was degassed using Schlenk line and backfilled with argon, the cycle was repeated three time. A mixture of (*i*-Pr)<sub>2</sub>NH (5 mL) and THF (10 mL) deaerated with argon was added into the mixture under argon using a syringe. Trimethylsilylacetylene (3.0 eq., 97.0 mg) was added. The mixture was reflux for 8h under argon atm. The solution was concentrated *in vacuo* and resulted solid purified by column chromatography (silica, DCM/petroleum ether 1:1) to obtain red solid **105** (133 mg, 95%). R<sub>f</sub> : 0.64 (DCM/petroleum ether 1:1). <sup>1</sup>H NMR (300 MHz, CDCl<sub>3</sub>) δ : 7.60 – 7.41 (m, 3H), 7.39 – 7.20 (m, 2H), 6.04 (s, 1H), 2.64 (d, J = 9.9 Hz, 3H), 2.60 (d, J = 9.9 Hz, 3H), 1.46 (s, 3H), 1.43 – 1.37 (m, 3H), 0.25 – 0.19 (m, 9H).

(iv) The BODIPY **104** (1.0 eq., 34.7 mg) and **105** (1.5 eq., 65 mg), palladium acetate (0.05 eq., 1.0 mg), Bu<sub>4</sub>NCl (1.0 eq., 21.4 mg), P(*o*-tol)<sub>3</sub> (0.1 eq., 2.3 mg), NaOAc (4.0 eq., 49.2 mg) were weighed into a dry two-neck round bottom flask. The mixture was flushed with argon. Deaerated DMF (2mL) was added to the mixture under argon and the solution was heated in a pre-heated oil bath at 100°C for 15 min., and then allowed to cool to room temperature. The mixture was added into saturated aqueous NaHCO<sub>3</sub> and extracted with ethyl acetate (3x20 mL). The combined organic layer was dried with MgSO<sub>4</sub> and concentrated *in vacuo*. The obtained crude mixture was purified by column (silica, DCM/petroleum ether 1:1) to give **106** as dark green solid (18 mg, 35%).

(v) **106** (18 mg, 1.0 eq.) was iodinated using NIS (24 mg, 4.0 eq.) by the same procedure described in step (ii). Flash column chromatography (silica, petroleum ether/DCM 2:1) furnished the final

<sup>251</sup> W. Wu, H. Guo, W. Wu, S. Ji, J. Zhao, *J. Org. Chem.* **2011**, *76*, 7056–7064.

product **B-7** (12 mg, 48%), Rf : 0.5 (DCM/petroleum ether 1:1).  $^1\text{H}$  NMR (300 MHz,  $\text{CDCl}_3$ )  $\delta$  : 7.58 – 7.47 (m, 6H), 7.28 (s, 4H), 2.67 (s, 12H), 1.46 (s, 6H), 1.42 (s, 6H).



**Scheme S12: Synthesis of BODIPY (B-7)**

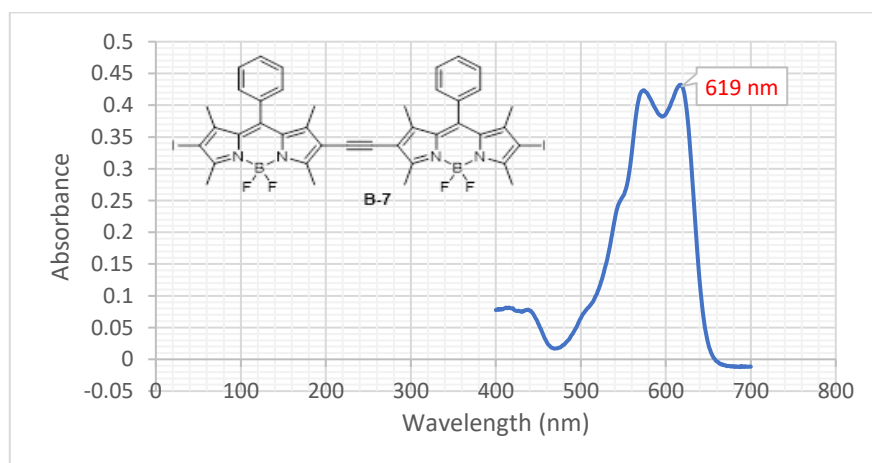
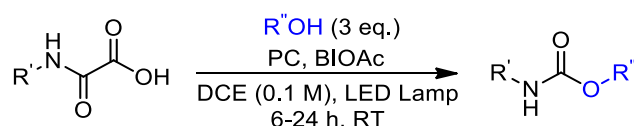


**Figure S8: UV-visible spectroscopy of B-7 in DCE.**

#### 4.5. General procedures for the photocatalyzed urethane synthesis using NIR light



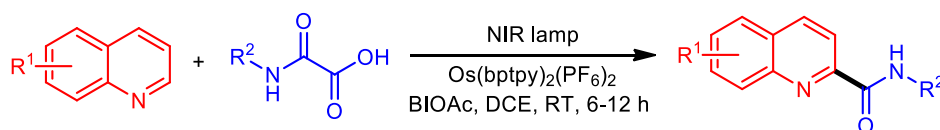
**Scheme S13:** General procedure for photocatalyzed urethane synthesis

All the reactions were carried out in a re-sealable test tube using red/NIR light LED: 630, 660, 780 or 850 nm lamp. The corresponding oxamic acid (0.5 mmol, 1.0 eq.), BI-OAc (0.75 mmol, 1.5 eq.) and NIR photocatalyst PC (0.1 to 10 mol%) were weighed into a dry re-sealable test-tube equipped with a magnetic bar. The tube was sealed with Teflon septum and degassed for 5 min using Schlenk line then back filled with argon. The cycle was repeated three times. Dry CH<sub>2</sub>Cl<sub>2</sub> (0.1 M) and the corresponding alcohol (1.5 mmol; 3.0 eq.) were added into the tube under argon atm. Note: For solid alcohol, it was added alongside oxamic acid before degassing. The tube was then placed in the NIR LED light at room temperature under constant stirring for 6-24h. The reaction mixture was diluted with DCM (10 mL), washed successively with NaHCO<sub>3</sub> and brine, dried with Na<sub>2</sub>SO<sub>4</sub> and concentrated using rotavap. The crude mixture was purified by flash column chromatography (silica gel, cyclohexane/ethyl acetate 5/95 to 20/80) to obtain the pure urethane.



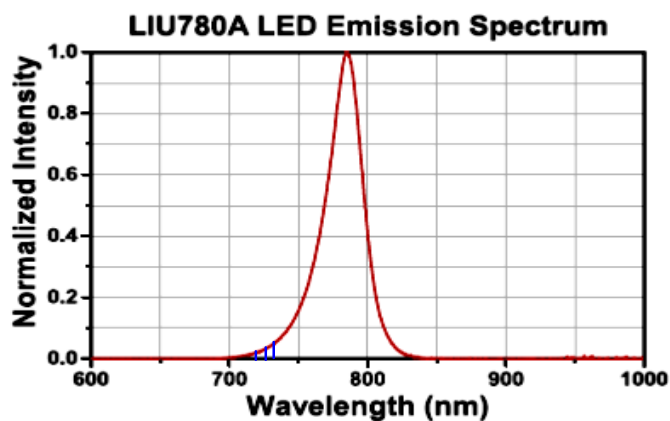
**Figure S9.** Experimental Setup NIR light reactions

#### 4.6. General procedures for carbamoyl radical addition to heteroarenes under NIR light

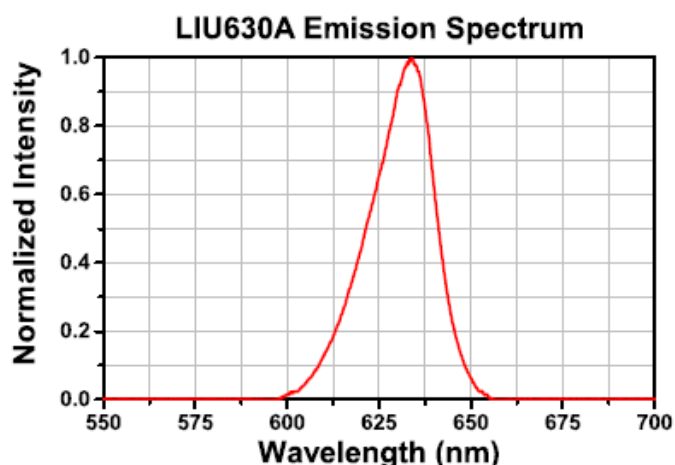


**Scheme S14:** General procedure for carbamoyl radical addition to heteroarenes using NIR light

The reaction was carried out in a re-sealable test tube and under a NIR light irradiation. The corresponding oxamic acid (0.25 mmol, 2.0 eq.), heteroarene (1.0 eq.), BI-OAc (2.0 eq.) and Os(btpy)<sub>2</sub>(PF<sub>6</sub>)<sub>2</sub> (0.3 mol%) were weighed into a dry re-sealable test-tube equipped with a magnetic bar. The tube was sealed with Teflon septum and was degassed and backfilled with argon. Dry DCE (2.5 mL) was added into the tube under argon atm. The tube was placed in the NIR light at room temperature (18-29°C) under constant stirring for 6-12h. The reaction mixture was directly washed successively with sodium bicarbonate (10 mL) and brine, dried using sodium sulfate and then concentrated using rotavap. The crude mixture was purified by flash column chromatography (silica gel, petroleum/ethyl acetate 90/10 to 70/30) to obtain the pure amide.



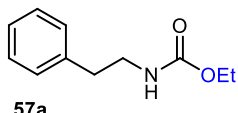
**Figure S10:** Emission spectrum of 780 nm LED lamp (NIR). Intensity = 3.7 mW/cm<sup>2</sup> (determined 100 mm from the LED along the emission axis)



**Figure S11:** Emission spectrum of 630 nm LED lamp. Intensity = 2.4 mW/cm<sup>2</sup> (determine 100 mm from the LED along the emission axis)

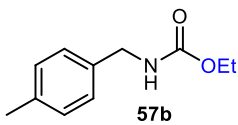
#### 4.7. Urethanes from NIR light photocatalysis

##### Ethyl phenethylcarbamate (**57a**)


  
**57a**

Following the general procedure and the corresponding oxamic acid (0.25 mmol), **57a** (84 mg, 88%) was obtained as a colorless gel. R<sub>f</sub> : 0.43 (EtOAc/petroleum ether 20/90). <sup>1</sup>H NMR (300 MHz, CDCl<sub>3</sub>) δ : 7.40 – 7.16 (m, 5H), 4.69 (s, 1H), 4.13 (q, *J* = 7.2 Hz, 2H), 3.46 (q, *J* = 6.8 Hz, 2H), 2.84 (t, *J* = 7.0 Hz, 2H), 1.25 (t, *J* = 7.2 Hz, 3H); <sup>13</sup>C NMR (75 MHz, CDCl<sub>3</sub>) δ : 156.6, 138.8, 130.0, 128.8, 128.7, 128.6, 126.5, 60.7, 42.1, 36.2, 14.6. Spectroscopic data were in good agreement with literature.<sup>238</sup>

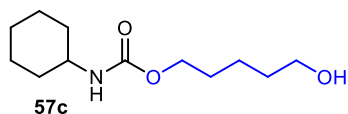
##### Ethyl 4-methylbenzylcarbamate (**57b**)


  
**57b**

Following the general procedure and the corresponding oxamic acid (0.25 mmol), **57b** (38 mg, 78%) was obtained as white solid, m.p. : 57-59°C. R<sub>f</sub> = 0.43 (AcOEt/petroleum ether 20/80). <sup>1</sup>H NMR (300 MHz, CDCl<sub>3</sub>) δ : 7.18 (q,

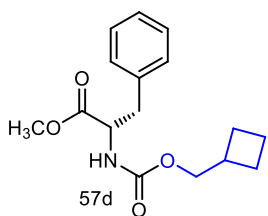
$J = 8.2$  Hz, 4H), 4.98 (s, 1H), 4.34 (d,  $J = 5.6$  Hz, 2H), 4.17 (q,  $J = 7.1$  Hz, 2H), 2.36 (s, 3H), 1.33 – 1.22 (t, 3H).  $^{13}\text{C}$  NMR (76 MHz,  $\text{CDCl}_3$ )  $\delta$  : 156.7, 137.1, 135.6, 129.3, 128.9, 127.5, 60.9, 44.8, 21.1, 14.7. Spectroscopic data were in good agreement with literature.

### 5-Hydroxypentyl cyclohexylcarbamate (**57c**)



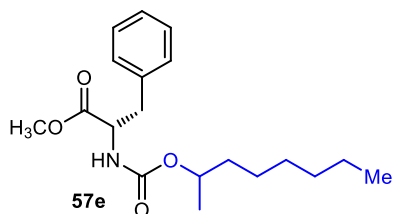
Following the general procedure and the corresponding oxamic acid (0.5 mmol), **57b** (100 mg, 87%) was obtained as white solid, m.p. : 78–79°C. Rf = 0.23 (AcOEt/petroleum ether 40/60).  $^1\text{H}$  NMR (300 MHz,  $\text{CDCl}_3$ )  $\delta$  4.63 (s, 1H), 4.05 (dd,  $J = 11.8, 5.8$  Hz, 2H), 3.64 (t,  $J = 6.4$  Hz, 2H), 3.44 (s, 1H), 1.98 – 1.83 (m, 2H), 1.78 – 1.53 (m, 8H), 1.49 – 1.28 (m, 4H), 1.22 – 1.02 (m, 4H).  $^{13}\text{C}$  NMR (76 MHz,  $\text{CDCl}_3$ )  $\delta$  : 155.9, 64.5, 62.6, 49.7, 33.4, 32.3, 28.9, 25.5, 24.8, 22.2. IR (neat)  $\nu_{\text{max}}$  ( $\text{cm}^{-1}$ ): 3319, 2939, 2862, 1693, 1533, 1449. HRMS (ESI): Calcd. for  $\text{C}_{19}\text{H}_{29}\text{O}_4\text{N}$   $[\text{M}+\text{H}]^+$  230.1751, found 230.1741.

### (S)-Methyl 2-(((cyclobutylmethoxy)carbonyl)amino)-3-phenylpropanoate (**57d**)



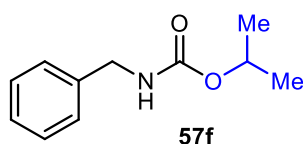
Following the general procedure and the corresponding oxamic acid (0.25 mmol), **57d** (54 mg, 73%) was obtained as colorless gel. Rf : 0.52 (AcOEt/petroleum ether 20/80).  $^1\text{H}$  NMR (300 MHz,  $\text{CDCl}_3$ )  $\delta$  : 7.39 – 7.21 (m, 3H), 7.15 (m, 2H), 5.15 (d,  $J = 7.3$  Hz, 1H), 4.67 (dd,  $J = 13.8, 6.0$  Hz, 1H), 4.05 (d,  $J = 6.8$  Hz, 2H), 3.74 (s, 1H), 3.23 – 3.01 (m, 2H), 2.70 – 2.47 (m, 1H), 2.15 – 1.67 (m, 6H).  $^{13}\text{C}$  NMR (76 MHz,  $\text{CDCl}_3$ )  $\delta$  : 172.1, 156.1, 135.8, 134.3, 129.3, 128.6, 127.1, 69.0, 54.7, 52.3, 38.3, 34.3, 24.6, 18.4. IR (neat)  $\nu_{\text{max}}$  ( $\text{cm}^{-1}$ ) = 3341, 3034, 2953, 2862, 1720, 1604, 1521. HRMS (ESI): Calcd. for  $\text{C}_{16}\text{H}_{22}\text{O}_4\text{N}$   $[\text{M}+\text{H}]^+$  292.1543, found 292.1543.  $[\alpha]_{\text{D}}^{25} +49.17$  (c 0.53,  $\text{CHCl}_3$ ).

### (2S)-Methyl 2-(((octan-2-yloxy)carbonyl)amino)-3-phenylpropanoate (**57e**)



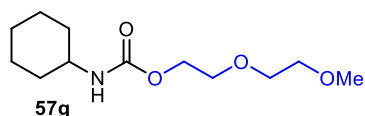
Following the general procedure and the corresponding oxamic acid (0.25 mmol), **57e** was obtained as a colorless gel (61 mg, 73%). Rf : 0.43 (AcOEt/petroleum ether 20/80).  $^1\text{H}$  NMR (300 MHz,  $\text{CDCl}_3$ )  $\delta$  : 7.29 (m, 3H), 7.18–7.06 (m, 2H), 5.08 (d,  $J = 7.7$  Hz, 1H), 4.79 (dq,  $J = 12.3, 6.2$  Hz, 1H), 4.67 (d,  $J = 6.2$  Hz, 1H), 3.74 (d,  $J = 0.8$  Hz, 3H), 3.13 (qd,  $J = 13.8, 5.9$  Hz, 2H), 1.69 – 1.39 (m, 2H), 1.30 (d,  $J = 3.7$  Hz, 8H), 1.20 (d,  $J = 6.2$  Hz, 3H), 0.90 (q,  $J = 6.6$  Hz, 3H).  $^{13}\text{C}$  NMR (75 MHz,  $\text{CDCl}_3$ )  $\delta$  : 172.1, 155.7, 135.9, 129.3, 128.5, 127.1, 72.0, 54.6, 52.2, 38.3, 36.2, 31.8, 29.2, 25.3, 22.6, 20.3, 14.1. IR (neat)  $\nu_{\text{max}}$  ( $\text{cm}^{-1}$ ): 3345, 3026, 2927, 2849, 1746, 1720, 1606, 1501. HRMS (ESI): Calcd. for  $\text{C}_{19}\text{H}_{29}\text{O}_4\text{NNa}$   $[\text{M}+\text{Na}]^+$  358.1988, found 358.1986.  $[\alpha]_{\text{D}}^{25} +43.41$  (c 0.49,  $\text{CHCl}_3$ ).

### Isopropyl benzylcarbamate (**57f**)



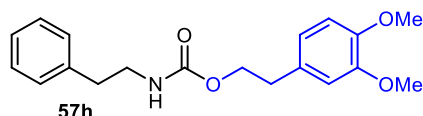
Following the general procedure and the corresponding oxamic acid (0.25 mmol), **57f** was obtained as a colorless gel (36 mg, 75%). Rf : 0.42 (AcOEt/petroleum ether 20/80).  $^1\text{H}$  NMR (300 MHz,  $\text{CDCl}_3$ )  $\delta$  : 7.46 – 7.16 (m, 5H), 4.97 (m, 2H), 4.38 (d,  $J = 5.2$  Hz, 2H), 1.26 (d,  $J = 6.3$  Hz, 6H).  $^{13}\text{C}$  NMR (76 MHz,  $\text{CDCl}_3$ )  $\delta$  : 156.3, 138.7, 128.6, 127.5, 127.4, 68.3, 45.0, 22.2. IR (neat)  $\nu_{\text{max}}$  ( $\text{cm}^{-1}$ ) : 3332, 3030, 2983, 2931, 1693, 1533, 1454. Spectroscopic data were in good agreement with literature.<sup>237,238</sup>

### 2-(2-Methoxyethoxy)ethyl cyclohexylcarbamate (**57g**)



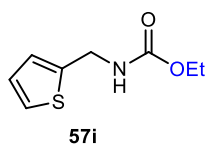
Following the general procedure and the corresponding oxamic acid (0.5 mmol), **57g** was obtained as a colorless gel (86 mg, 70%). Rf : 0.46 (AcOEt/petroleum ether 40/60).  $^1\text{H NMR}$  (300 MHz,  $\text{CDCl}_3$ )  $\delta$  : 4.65 (s, 1H), 4.24 – 4.15 (m, 2H), 3.70 – 3.60 (m, 4H), 3.55 (m, J = 6.8, 3.2 Hz, 2H), 3.44 (s, 1H), 3.37 (s, 3H), 1.96 – 1.83 (m, 2H), 1.73 – 1.51 (m, 3H), 1.40 – 1.00 (m, 5H).  $^{13}\text{C NMR}$  (76 MHz,  $\text{CDCl}_3$ )  $\delta$  : 155.5, 71.9, 70.4, 69.7, 63.6, 59.1, 49.8, 33.4, 25.5, 24.7. IR (neat)  $\nu_{\text{max}}$  ( $\text{cm}^{-1}$ ) : 3328, 2935, 2858, 1699, 1536, 1452. HRMS (ESI): Calcd. for  $\text{C}_{12}\text{H}_{24}\text{O}_4\text{N}$   $[\text{M}+\text{H}]^+$  246.1699, found 246.1700.

### 3,4-dimethoxyphenethyl phenethylcarbamate (**57h**)



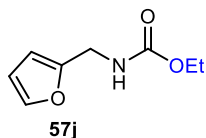
Following the general procedure and the corresponding oxamic acid (0.5 mmol), **57h** was obtained as white (65 mg, 40%) solid, m.p. : 87-89°C. Rf : 0.37 (AcOEt/cyclohexane 40/60).  $^1\text{H NMR}$  (300 MHz,  $\text{CDCl}_3$ )  $\delta$  : 7.35 – 7.12 (m, 5H), 6.84 – 6.68 (m, 3H), 4.67 (s, 1H), 4.25 (t, J = 7.1 Hz, 2H), 3.87 (s, Hz, 6H), 3.44 (d, J = 6.2 Hz, 2H), 2.83 (dt, J = 11.2, 6.9 Hz, 4H).  $^{13}\text{C NMR}$  (76 MHz,  $\text{CDCl}_3$ )  $\delta$  : 156.4, 148.9, 147.7, 130.5, 128.8, 128.6, 126.5, 120.8, 112.1, 111.3, 65.4, 55.9, 55.8, 42.1, 36.1, 35.1. IR (neat)  $\nu_{\text{max}}$  ( $\text{cm}^{-1}$ ) : 3323, 2935, 2836, 1688, 1591. HRMS (ESI): Calcd. for  $\text{C}_{19}\text{H}_{24}\text{O}_4\text{N}$   $[\text{M}+\text{H}]^+$  330.1699, found 330.1701.

### Ethyl (thiophen-2-ylmethyl)carbamate (**57i**)



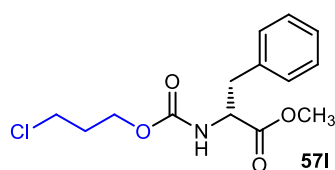
Following the general procedure and the corresponding oxamic acid (0.3 mmol), **57i** was obtained as light brown gel (30 mg, 54%). Rf : 0.43 (AcOEt/petroleum ether 20/80).  $^1\text{H NMR}$  (300 MHz,  $\text{CDCl}_3$ )  $\delta$  : 7.24 (dd, J = 4.8, 1.6 Hz, 1H), 6.96 (dd, J = 4.8, 3.5 Hz, 2H), 5.08 (s, 1H), 4.54 (d, J = 5.4 Hz, 2H), 4.17 (q, J = 7.0 Hz, 2H), 1.27 (t, J = 7.1 Hz, 3H).  $^{13}\text{C NMR}$  (76 MHz,  $\text{CDCl}_3$ )  $\delta$  : 156.3, 141.5, 126.9, 125.7, 125.1, 61.1, 39.8, 14.6. IR (neat)  $\nu_{\text{max}}$  ( $\text{cm}^{-1}$ ) : 3319, 3103, 3069, 2978, 2927, 1693, 1527.

### Ethyl (furan-2-ylmethyl)carbamate (**57j**)



Following the general procedure and the corresponding oxamic acid (0.3 mmol), **57j** was obtained as light brown gel (21 mg, 41%). Rf : 0.39 (AcOEt/petroleum ether 20/80).  $^1\text{H NMR}$  (300 MHz,  $\text{CDCl}_3$ )  $\delta$  : 7.37 (dd, J = 1.8, 0.8 Hz, 1H), 6.33 (dd, J = 3.2, 1.9 Hz, 1H), 6.24 (d, J = 2.9 Hz, 1H), 5.02 (s, 1H), 4.36 (d, J = 5.6 Hz, 2H), 4.16 (q, J = 7.1 Hz, 2H), 1.26 (t, J = 7.1 Hz, 3H).  $^{13}\text{C NMR}$  (76 MHz,  $\text{CDCl}_3$ )  $\delta$  : 156.4, 151.7, 142.1, 110.4, 107.1, 61.1, 38.0, 14.6. IR (neat)  $\nu_{\text{max}}$  ( $\text{cm}^{-1}$ ) : 3328, 3121, 2989, 2935, 1703, 1527. Spectroscopic data were in good agreement with literature.<sup>238</sup>

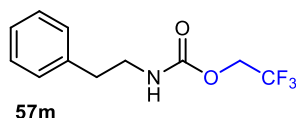
### (R)-methyl 2-(((3-chloropropoxy)carbonyl)amino)-3-phenylpropanoate (**57l**)



Following the general procedure and the corresponding oxamic acid (0.3 mmol), **57l** was obtained as light brown gel (60 mg, 80%). Rf : 0.36 (AcOEt/petroleum ether 20/80).  $^1\text{H NMR}$  (300 MHz,  $\text{CDCl}_3$ )  $\delta$  : 7.36 – 7.25 (m, 3H), 7.17 – 7.10 (m, 2H), 5.18 (s, 1H), 4.66 (dd, J = 14.1, 6.0 Hz, 1H), 4.22 (t, J = 6.0 Hz, 2H), 3.75 (s, 3H), 3.59 (t, J = 6.4 Hz, 2H), 3.13 (qd, J = 13.9, 6.0 Hz, 2H), 2.14 – 1.99 (m, 2H).  $^{13}\text{C NMR}$  (76 MHz,  $\text{CDCl}_3$ )  $\delta$  : 172.0, 155.5, 135.7, 129.2, 128.6, 127.2, 61.9, 54.7, 52.4, 41.2, 38.2, 31.9. IR (neat)  $\nu_{\text{max}}$  ( $\text{cm}^{-1}$ ) : 3336, 3025, 2956,

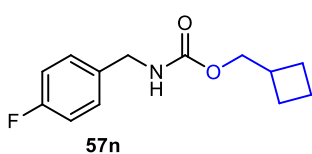
1722, 1604, 1520. HRMS (ESI): Calcd. for  $C_{14}H_{18}O_4NCINa$   $[M+Na]^+$  322.08167, found 322.0809.  $[\alpha]_D^{25} +47.22$  (c 0.73,  $CHCl_3$ ).

### 2,2,2-Trifluoroethyl phenethylcarbamate (**57m**)



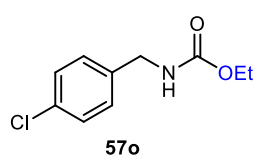
Following the general procedure and the corresponding oxamic acid (0.25 mmol), **57m** was obtained as light brown gel (38 mg, 61%). Rf : 0.74 (AcOEt/petroleum ether 20/80).  $^1H$  NMR (300 MHz,  $CDCl_3$ )  $\delta$  : 7.44 – 7.05 (m, 5H), 4.93 (s, 1H), 4.47 (q, J = 8.5 Hz, 2H), 3.51 (dd, J = 13.1, 6.8 Hz, 2H), 2.86 (t, J = 6.9 Hz, 2H).  $^{13}C$  NMR (75 MHz,  $CDCl_3$ )  $\delta$  : 154.5, 138.4, 123.3 (q,  $^1J_{CF} = 277.5$  Hz), 60.9 (q,  $^2J_{CF} = 36.4$  Hz), 42.6, 36.0. IR (neat)  $\nu_{max}$  ( $cm^{-1}$ ): 3345, 3064, 3030, 2945, 1730, 1604, 1604, 1526. Spectroscopic data were in good agreement with literature.<sup>238</sup>

### Cyclobutylmethyl 4-fluorobenzylcarbamate (**57n**)



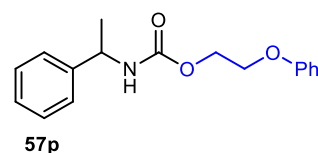
Following the general procedure and the corresponding oxamic acid (0.25 mmol), **57n** was obtained as white solid (30 mg, 50%), m.p. : 58–60°C. Rf : 0.48 (AcOEt/petroleum ether 20/80).  $^1H$  NMR (300 MHz,  $CDCl_3$ )  $\delta$  : 7.28 (dd, J = 8.7, 5.1 Hz, 2H), 7.13 – 6.94 (m, 2H), 5.01 (s, 1H), 4.35 (d, J = 5.4 Hz, 2H), 4.08 (d, J = 6.8 Hz, 2H), 2.71 – 2.44 (m, 1H), 2.06 (ddd, J = 13.7, 8.7, 4.8 Hz, 2H), 1.99 – 1.71 (m, 4H).  $^{13}C$  NMR (76 MHz,  $CDCl_3$ )  $\delta$  : 162.2 (d,  $^1J_{CF} = 245.6$  Hz), 156.8, 134.4 (d,  $^3J_{CF} = 3.2$  Hz), 129.2, 115.5 (d,  $^2J_{CF} = 21.5$  Hz), 68.9, 44.4, 34.4, 24.6, 18.4. IR (neat)  $\nu_{max}$  ( $cm^{-1}$ ): 3336, 3065, 2969, 2931, 1699, 1607, 1512. Spectroscopic data were in good agreement with literature.<sup>238</sup>

### Ethyl 4-chlorobenzylcarbamate (**57o**)



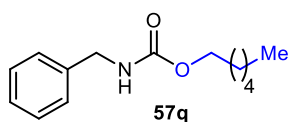
Following the general procedure and the corresponding oxamic acid (0.25 mmol), **57o** was obtained as white solid (38 mg, 72%), m.p. : 60–61°C. Rf : 0.31 (AcOEt/petroleum ether 20/80).  $^1H$  NMR (300 MHz,  $CDCl_3$ )  $\delta$  : 7.29 (ddd, J = 22.0, 12.3, 5.2 Hz, 4H), 5.04 (s, 1H), 4.34 (d, J = 6.0 Hz, 2H), 4.16 (q, J = 7.1 Hz, 2H), 1.27 (t, J = 7.1 Hz, 3H).  $^{13}C$  NMR (76 MHz,  $CDCl_3$ )  $\delta$  : 156.6, 137.2, 133.2, 128.8, 61.1, 44.3, 14.6. IR (neat)  $\nu_{max}$  ( $cm^{-1}$ ): 3310, 3051, 2982, 2870, 2784, 1696, 1544, 1407. Spectroscopic data were in good agreement with literature.<sup>237</sup>

### 2-Phenoxyethyl (1-phenylethyl)carbamate (**57p**)



Following the general procedure and the corresponding oxamic acid (0.5 mmol), **57p** was obtained as white solid (110 mg, 78%), m.p. : 88–90°C. Rf : 0.43 (AcOEt/petroleum ether 20/80).  $^1H$  NMR (300 MHz,  $CDCl_3$ )  $\delta$  : 7.31 (dd, J = 8.6, 7.5 Hz, 7H), 7.07 – 6.85 (m, 3H), 5.11 (s, 1H), 4.98 – 4.78 (m, 1H), 4.53 – 4.32 (m, 2H), 4.17 (d, J = 4.1 Hz, 2H), 1.53 (t, J = 10.9 Hz, 3H).  $^{13}C$  NMR (76 MHz,  $CDCl_3$ )  $\delta$  : 158.5, 155.4, 143.4, 129.5, 128.7, 127.4, 125.9, 121.1, 114.6, 66.4, 63.3, 50.8, 22.5. IR (neat)  $\nu_{max}$  ( $cm^{-1}$ ): 3332, 3060, 3030, 2978, 2922, 2871, 1690, 1583, 1596, 1533, 1497, 1452. HRMS (ESI): Calcd. for  $C_{17}H_{19}O_3NNa$   $[M+Na]^+$  308.1257, found 308.1249.

### Hexyl benzylcarbamate (**57q**)



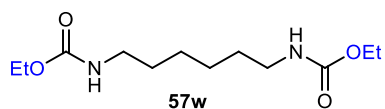
Following the general procedure and the corresponding oxamic acid (0.25 mmol), **57q** was obtained as colorless gel (41 mg, 71%). Rf : 0.7 (AcOEt/petroleum ether 20/80). <sup>1</sup>H NMR (300 MHz, CDCl<sub>3</sub>) δ : 7.42 – 7.20 (m, 5H), 5.05 (s, 1H), 4.38 (d, J = 5.5 Hz, 2H), 4.11 (t, J = 6.7 Hz, 2H), 1.70 – 1.54 (m, 2H), 1.28 (d, J = 28.6 Hz, 6H), 0.92 (dd, J = 8.8, 4.7 Hz, 3H). <sup>13</sup>C NMR (76 MHz, CDCl<sub>3</sub>) δ : 156.8, 138.7, 128.6, 127.5, 127.4, 65.2, 45.0, 31.5, 29.0, 25.5, 22.6, 14.0. IR (neat) ν<sub>max</sub> (cm<sup>-1</sup>): 3332, 3030, 2961, 2927, 2858, 1697, 1533. Spectroscopic data were in good agreement with literature.<sup>238</sup>

### Pent-4-en-1-yl phenethylcarbamate (**57r**)



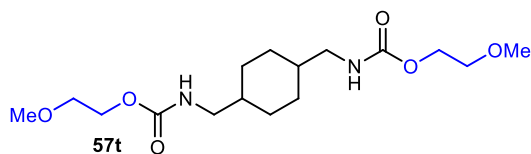
Following the general procedure and the corresponding oxamic acid (0.25 mmol), **57r** was obtained as colorless gel (33 mg, 30%). Rf : 0.46 (AcOEt/petroleum ether 20/80). <sup>1</sup>H NMR (300 MHz, CDCl<sub>3</sub>) δ : 7.49 – 6.99 (m, 5H), 5.83 (m, J = 16.9, 10.2, 6.6 Hz, 1H), 5.01 (d, J = 10.2 Hz, 2H), 4.68 (s, 1H), 4.09 (t, J = 6.6 Hz, 2H), 3.47 (dd, J = 13.0, 6.5 Hz, 2H), 2.84 (t, J = 7.0 Hz, 2H), 2.13 (dd, J = 13.9, 6.8 Hz, 2H), 1.81 – 1.62 (m, 2H). <sup>13</sup>C NMR (76 MHz, CDCl<sub>3</sub>) δ : 156.6, 138.8, 137.6, 128.8, 128.6, 126.5, 115.1, 64.3, 42.1, 36.2, 30.0, 28.3. IR (neat) ν<sub>max</sub> (cm<sup>-1</sup>) = 3335, 3065, 3028, 2940, 1703, 1641, 1531. Spectroscopic data were in good agreement with literature.<sup>237</sup>

### Diethyl hexane-1,6-diyl dicarbamate (**57w**)



Following the general procedure and the corresponding oxamic acid (0.25 mmol), **57w** was obtained as white solid (54 mg, 82%), m.p. : 71-73°C. Rf : 0.46 (AcOEt/petroleum ether 20/80). <sup>1</sup>H NMR (300 MHz, CDCl<sub>3</sub>) δ : 4.70 (bs, 2H), 4.12 (q, J = 7.2 Hz, 4H), 3.17 (q, J = 6.6 Hz, 4H), 1.67 – 1.43 (m, 4H), 1.40 – 1.31 (m, 4H), 1.09 (m, 6H). <sup>13</sup>C NMR (75 MHz, CDCl<sub>3</sub>) δ : 156.72, 60.64, 40.72, 29.93, 26.26, 14.66. IR (neat) ν<sub>max</sub> (cm<sup>-1</sup>): 3314, 2984, 2936, 1685. Spectroscopic data were in good agreement with literature.<sup>237,238</sup>

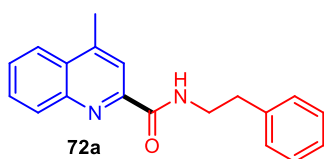
### Bis(2-methoxyethyl) (cyclohexane-1,4-diylbis(methylene))dicarbamate (**57t**)



Following the general procedure with the corresponding oxamic acid (0.25 mmol), **57t** was obtained as white solid (60.6 mg, 70%), m.p. : 114-117°C. Rf : 0.5 (AcOEt/petroleum ether 50/50). <sup>1</sup>H NMR (300 MHz, CDCl<sub>3</sub>) δ : 4.84 (s, 2H), 4.31 – 4.15 (m, 4H), 3.63 – 3.54 (m, 4H), 3.40 (s, 6H), 3.14 (dd, J = 13.2, 6.4 Hz, 1H), 3.04 (t, J = 6.4 Hz, 3H), 1.79 (d, J = 7.0 Hz, 3H), 1.57 – 1.27 (m, 4H), 1.03 – 0.82 (m, 3H). <sup>13</sup>C NMR (76 MHz, CDCl<sub>3</sub>) δ : 156.5, 71.0, 63.8, 58.9, 47.1, 38.2, 29.9, 26.1. IR (neat) ν<sub>max</sub> (cm<sup>-1</sup>): 3315, 2905, 2841, 1688, 1538, 1449. HRMS (ESI): Calcd. for C<sub>16</sub>H<sub>31</sub>O<sub>6</sub>N<sub>2</sub> [M+H]<sup>+</sup> 347.2177, found 347.2177.

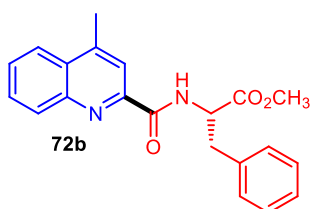
## 4.8. Amides from NIR photocatalysis

### 4-Methyl-*N*-phenethylquinoline-2-carboxamide (**72a**)



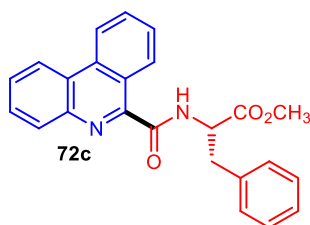
Following the general procedure and the corresponding heteroarene (0.125 mmol), **72a** was obtained as milky solid (27.0 mg, 75%), mp. : 98–101°C. Rf : 0.53 (AcOEt/petroleum ether 20/80). <sup>1</sup>H NMR (300 MHz, CDCl<sub>3</sub>) δ : 8.36 (d, J = 23.8 Hz, 1H), 8.18 (s, 1H), 8.06 (dd, J = 7.7, 4.4 Hz, 2H), 7.76 (t, J = 7.1 Hz, 1H), 7.64 (t, J = 7.1 Hz, 1H), 7.46 – 7.18 (m, 5H), 3.81 (dd, J = 13.8, 6.8 Hz, 2H), 3.02 (t, J = 7.2 Hz, 2H), 2.79 (s, 3H). <sup>13</sup>C NMR (76 MHz, CDCl<sub>3</sub>) δ : 164.8, 149.5, 146.5, 146.2, 139.2, 130.4, 129.8, 129.3, 129.0, 128.7, 127.7, 126.6, 124.0, 119.5, 41.0, 36.2, 19.0. Spectroscopic data were in good agreement with literature.<sup>239</sup>

### (*S*)-Methyl 2-(4-methylquinoline-2-carboxamido)-3-phenylpropanoate (**72b**)



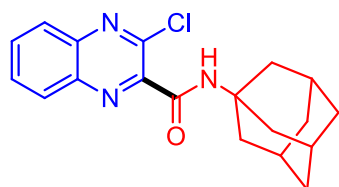
Following the general procedure and the corresponding heteroarene (0.125 mmol), **72b** was obtained as white solid (38mg, 86%), mp°C. 116-118 °C, Rf : 0.4 (AcOEt/petroleum ether 30/70). <sup>1</sup>H NMR (300 MHz, CDCl<sub>3</sub>) δ : 8.73 (d, J = 8.3 Hz, 1H), 8.16 – 8.02 (m, 3H), 7.77 (ddd, J = 8.4, 6.9, 1.4 Hz, 1H), 7.65 (ddd, J = 8.2, 6.9, 1.3 Hz, 1H), 7.37 – 7.21 (m, 5H), 5.14 (dt, J = 8.4, 6.1 Hz, 1H), 3.77 (s, 3H), 3.32 (d, J = 6.2 Hz, 2H), 2.79 (s, 3H). <sup>13</sup>C NMR (76 MHz, CDCl<sub>3</sub>) δ : 171.9, 164.4, 148.6, 146.4, 146.0, 136.1, 130.6, 129.7, 129.4, 129.3, 128.6, 127.7, 127.1, 123.8, 119.3, 53.5, 52.3, 38.4, 18.9. IR (neat) ν<sub>max</sub> (cm<sup>-1</sup>): 3379, 3064, 2952, 1744, 1675. HRMS (ESI): Calcd. for C<sub>21</sub>H<sub>21</sub>O<sub>3</sub>N<sub>2</sub> [M+H]<sup>+</sup> 349.1547, found 349.1538. [α]<sub>D</sub><sup>25</sup> +22.32 (c 0.48, CHCl<sub>3</sub>).

### (*S*)-Methyl 2-(phenanthridine-6-carboxamido)-3-phenylpropanoate (**72c**)



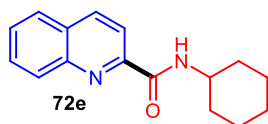
Following the general procedure and the corresponding heteroarene (0.25 mmol), **72c** was obtained as white solid (80 mg, 83%), mp. 107-110°C. Rf : 0.51 (AcOEt/petroleum ether 30/70). <sup>1</sup>H NMR (300 MHz, CDCl<sub>3</sub>) δ : 9.57 (d, J = 8.5, 0.7 Hz, 1H), 8.75 – 8.57 (m, 3H), 8.21 – 8.13 (m, 1H), 7.89 (ddd, J = 8.3, 7.0, 1.3 Hz, 1H), 7.83 – 7.71 (m, 3H), 7.41 – 7.24 (m, 5H), 5.19 (dt, J = 8.2, 6.0 Hz, 1H), 3.81 (s, 3H), 3.46 – 3.28 (m, 2H). <sup>13</sup>C NMR (76 MHz, CDCl<sub>3</sub>) δ : 172.0, 165.6, 148.5, 141.9, 136.1, 133.8, 130.9, 130.7, 129.5, 128.8, 128.8, 128.6, 128.6, 128.0, 127.2, 125.5, 124.3, 122.1, 121.8, 53.6, 53.4, 52.4, 38.3. IR (neat) ν<sub>max</sub> (cm<sup>-1</sup>): 3370, 3064, 3034, 2948, 1744, 1673. HRMS (ESI): Calcd. for C<sub>24</sub>H<sub>21</sub>O<sub>3</sub>N<sub>2</sub> [M+H]<sup>+</sup> 385.1547, found 385.1534. [α]<sub>D</sub><sup>25</sup> +41.52 (c 0.53, CHCl<sub>3</sub>).

### *N*-((1*s*,3*s*)-adamantan-1-yl)-3-chloroquinoxaline-2-carboxamide (**72d**)



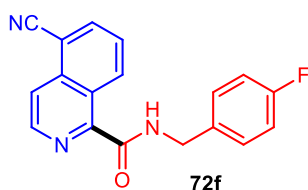
Following the general procedure and the corresponding heteroarene (0.25 mmol), **72d** was obtained as white solid (58 mg, 68%), mp. : 197-200°C. Rf : 0.4 (AcOEt/petroleum ether 30/70). <sup>1</sup>H NMR (300 MHz, CDCl<sub>3</sub>) δ : 8.16 – 8.04 (m, 2H), 7.94 – 7.79 (m, 2H), 7.17 (s, 1H), 2.22 (t, J = 7.9 Hz, 9H), 1.86 – 1.71 (m, 6H). <sup>13</sup>C NMR (76 MHz, CDCl<sub>3</sub>) δ : 161.7, 145.1, 144.1, 142.3, 138, 132.3, 130.8, 129.1, 128.2, 52.8, 41.4, 36.3, 29.7, 29.5. IR (neat) ν<sub>max</sub> (cm<sup>-1</sup>): 3288, 3064, 2909, 2849, 1662. Spectroscopic data were in good agreement with literature.<sup>239</sup>

### ***N*-cyclohexylquinoline-2-carboxamide (72e)**



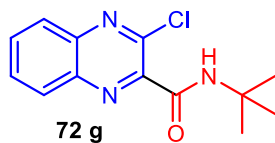
Following the general procedure and the corresponding heteroarene (0.25 mmol), **72e** was obtained as white solid (48 mg, 76%), mp. : 92-95°C. Rf : 0.38 (AcOEt/petroleum ether 20/80). <sup>1</sup>H NMR (300 MHz, CDCl<sub>3</sub>) δ : 8.38 – 8.28 (m, 2H), 8.17 (m, 2H), 7.89 (d, J = 8.2 Hz, 1H), 7.78 (ddd, J = 8.4, 6.9, 1.5 Hz, 1H), 7.63 (ddd, J = 8.1, 6.9, 1.1 Hz, 1H), 4.06 (qd, J = 10.2, 4.0 Hz, 1H), 2.15 – 2.03 (m, 2H), 1.89 – 1.59 (m, 3H), 1.59 – 1.21 (m, 5H). <sup>13</sup>C NMR (76 MHz, CDCl<sub>3</sub>) δ : 163.4, 150.1, 137.4, 130.0, 129.7, 129.2, 127.7, 118.9, 48.4, 33.1, 25.6, 25.0. IR (neat) ν<sub>max</sub> (cm<sup>-1</sup>): 3375, 3056, 2935, 2835, 2849, 1674. Spectroscopic data were in good agreement with literature.<sup>239</sup>

### **5-Cyano-N-(4-fluorobenzyl)isoquinoline-1-carboxamide (72f)**



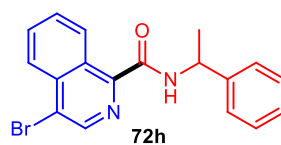
Following the general procedure and the corresponding heteroarene (0.125 mmol), **72f** was obtained as white solid (30.5 mg, 80%), mp. 159–162°C. Rf : 0.28 (AcOEt/petroleum ether 20/80). <sup>1</sup>H NMR (300 MHz, CDCl<sub>3</sub>) δ : 10.04 (dd, J = 8.8, 0.9 Hz, 1H), 8.67 (d, J = 5.7 Hz, 2H), 8.20 (ddd, J = 8.3, 6.4, 1.0 Hz, 2H), 7.78 (dd, J = 8.8, 7.2 Hz, 1H), 7.49 – 7.33 (m, 2H), 7.18 – 6.98 (m, 2H), 4.70 (d, J = 6.1 Hz, 2H). <sup>13</sup>C NMR (76 MHz, CDCl<sub>3</sub>) δ : 165.0, 162.3 (d, <sup>1</sup>J<sub>CF</sub> = 245.8 Hz), 148.5, 142.6, 136.8, 136.6, 133.8, 133.5, 129.5 (d, <sup>3</sup>J<sub>CF</sub> = 8.1 Hz), 127.8, 126.6, 121.4, 116.6, 115.6 (d, <sup>2</sup>J<sub>CF</sub> = 21.5 Hz), 109.8, 42.9. IR (neat) ν<sub>max</sub> (cm<sup>-1</sup>): 3362, 3051, 2922, 2225, 16668. Spectroscopic data were in good agreement with literature.<sup>239</sup>

### ***N*-(*tert*-butyl)-3-chloroquinoxaline-2-carboxamide (72g)**



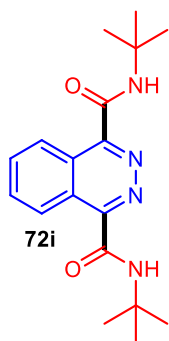
Following the general procedure and the corresponding heteroarene (0.125 mmol), **72g** was obtained as light-yellow solid (20.9mg, 61%), mp. : 145-149°C. Rf : 0.57 (AcOEt/petroleum ether 30/70). <sup>1</sup>H NMR (300 MHz, CDCl<sub>3</sub>) δ : 8.19 – 8.00 (m, 2H), 7.95 – 7.77 (m, 2H), 7.28 (s, 1H), 1.56 (s, 9H). <sup>13</sup>C NMR (76 MHz, CDCl<sub>3</sub>) δ 162.0, 145.0, 144.1, 142.4, 138.9, 132.4, 130.8, 129.1, 128.3, 52.0, 28.7. IR (neat) ν<sub>max</sub> (cm<sup>-1</sup>): 3267, 3077, 2969, 2926, 1647. HRMS (ESI): Calcd. for C<sub>17</sub>H<sub>19</sub>O<sub>3</sub>NNa [M+Na]<sup>+</sup> 286.0717, found 286.0714.

### **4-Bromo-N-(1-phenylethyl)-1-naphthamide (72h)**



Following the general procedure, **72h** was obtained as pale yellow gel (24 mg, 56%). Rf : 0.32 (AcOEt/petroleum ether 10/90). <sup>1</sup>H NMR (300 MHz, CDCl<sub>3</sub>) δ : 9.74 – 9.63 (m, 1H), 8.68 (s, 1H), 8.47 (d, J = 7.8 Hz, 1H), 8.29 – 8.19 (m, 1H), 7.80 (dddd, J = 30.9, 8.3, 6.9, 1.3 Hz, 2H), 7.52 – 7.25 (m, 5H), 5.46 – 5.27 (m, 1H), 1.69 (d, J = 6.9 Hz, 3H). <sup>13</sup>C NMR (76 MHz, CDCl<sub>3</sub>) δ : 164.3, 147.3, 143.3, 141.7, 136.0, 132.0, 129.5, 128.7, 128.5, 128.2, 127.4, 126.2, 126.1, 123.5, 49.2, 22.2. IR (neat) ν<sub>max</sub> (cm<sup>-1</sup>): 3379, 3064, 3064, 3021, 2974, 2926, 1664, 1559. Spectroscopic data were in good agreement with literature.<sup>239</sup>

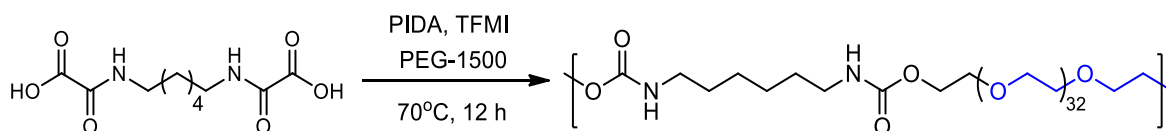
## N<sup>1</sup>,N<sup>4</sup>-Di-*tert*-butylphthalazine-1,4-dicarboxamide (72i)



Following the general procedure and the corresponding heteroarene (0.125 mmol), **72i** was obtained as pale yellow solid (31 mg, 76%), mp : 126-131°C. Rf : 0.6 (AcOEt/DCM 20/80). <sup>1</sup>H NMR (300 MHz, CDCl<sub>3</sub>) δ : 9.50 (dd, J = 6.5, 3.4 Hz, 2H), 8.10 – 7.88 (m, 4H), 1.58 (s, 18H). <sup>13</sup>C NMR (76 MHz, CDCl<sub>3</sub>) δ : 163.3, 151.3, 133.5, 127.0, 126.3, 51.9, 28.7. IR (neat) ν<sub>max</sub> (cm<sup>-1</sup>) : 3262, 3051, 2951, 2969, 1668. HRMS (ESI): Calcd. for C<sub>18</sub>H<sub>24</sub>O<sub>2</sub>N<sub>4</sub>Na [M+Na]<sup>+</sup> 351.1792, found 351.1787.

## 5. Experimental Part: Chapter 5

### 5.1. Standard procedure for polyurethane synthesis from bis-oxamic acid using PIDA-mediated thermal process



**Scheme 15.** Polyurethane synthesis from bis-oxamic acids by PIDA-mediated process

Bis-oxamic acid (1.0 mmol, 1.0 eq.), PEG-1500 (1.0 mmol, 1.0 eq.), PIDA (2.5 eq.) and TFMI (5 mol%) were charged into an oven-dried Schlenk tube equipped with a magnetic stirrer, the content was degassed and backfilled with argon. The tube was heated to 70°C (oil bath) during which the molten polyol helped to solubilize the solid bis-oxamic acids and PIDA. As the reaction progressed, iodobenzene and acetic acid (liquids) released by PIDA also helped more in homogenizing the reaction mixture. Thereafter, crude polymer, which was highly viscous, was diluted with DCM (2 mL) and precipitated using diethyl ether. In some cases, the ether was cooled using ice before the precipitation. The obtained PUs was dried *in vacuo*.

### 5.2. Standard procedure for kinetic investigation

The kinetics of the reaction were studied using mechanical stirring (Figure S12). Bis-oxamic acid (2.0 mmol, 1.0 eq.), PEG-1500 (1.8 mmol, 0.9 eq.) and TFMI (5 mol%) were charged into an oven-dried Schlenk tube, the paddle stirrer for mechanical stirring was inserted into the Schlenk tube and the steel mixing paddle was screwed to an IKA RW20 Digital instrument. The tube was purged with nitrogen and thereafter heated to desired temperature under slow (50 rpm) stirring and continuous nitrogen flow. During this process, the polyol melted resulting in a homogeneous paste. Then, PIDA (5 mmol, 2.5 eq.) was added, and the stirring ramped up to 200 rpm and still under continuous nitrogen flow. Samples were taken from the reaction mixture at different intervals of time using a syringe and were analyzed by NMR, FTIR and SEC.



**Figure S12:** Set up for kinetic studies on PUs synthesis from bis-oxamic acids using PIDA-mediated process

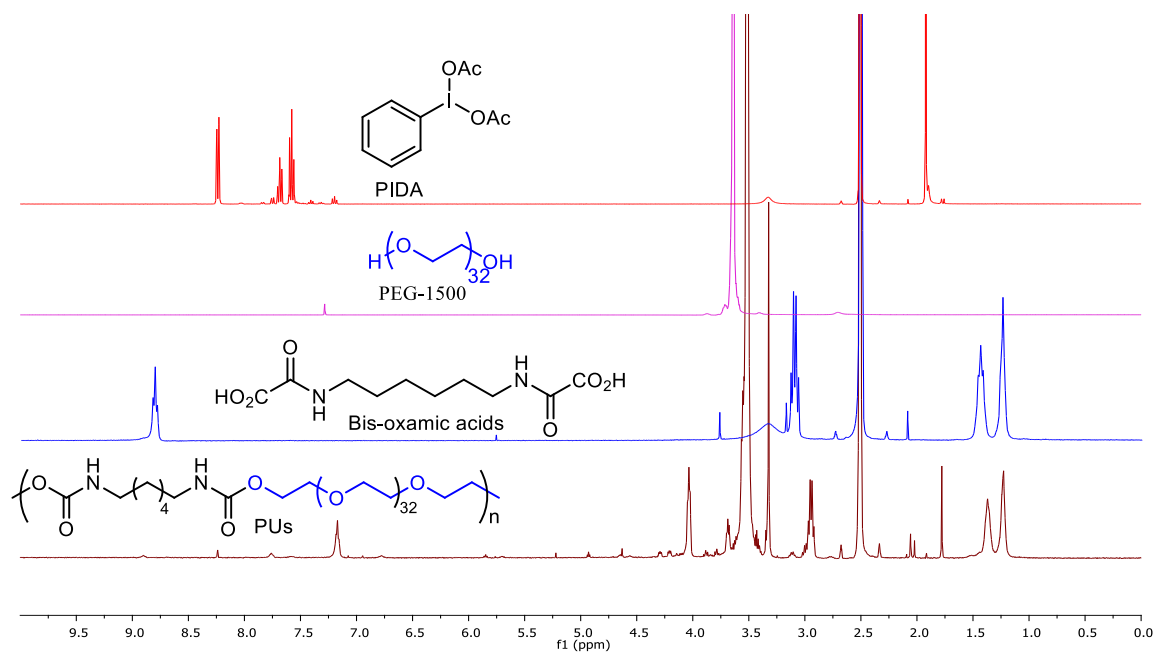


**Figure S13:** NMR comparison of starting material and synthesized PUs. This was useful during the polymerization, for determining structure of the prepared PUs formed and conversion of starting materials.

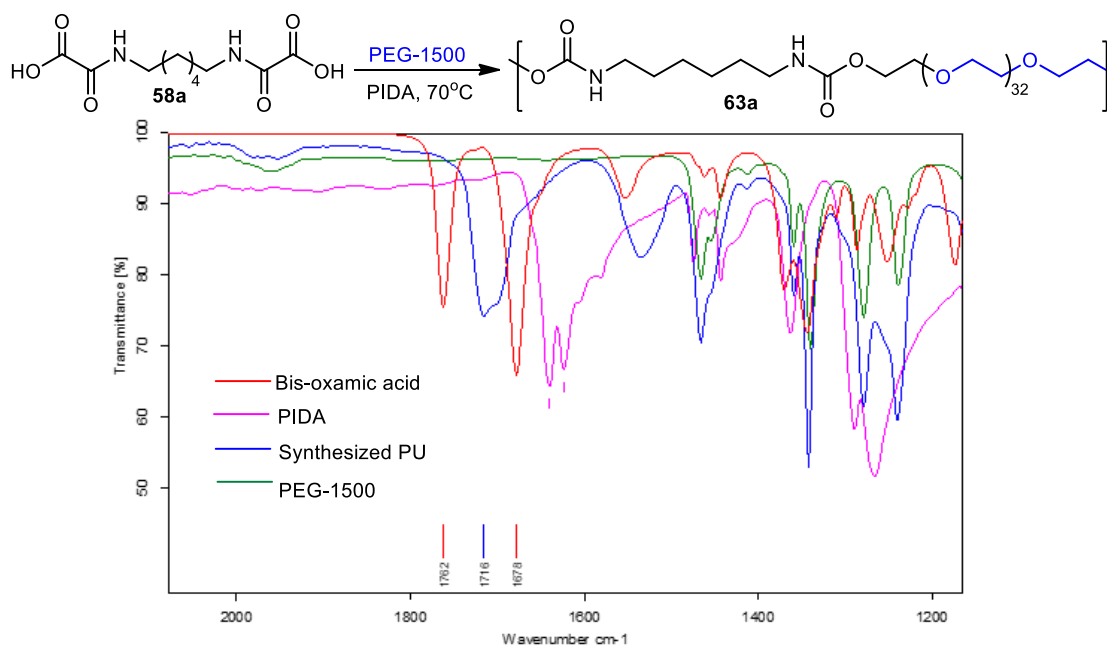


**Figure S14:** FTIR comparison of starting material and synthesized PUs. This also gave useful information on product formation and starting materials conversion.

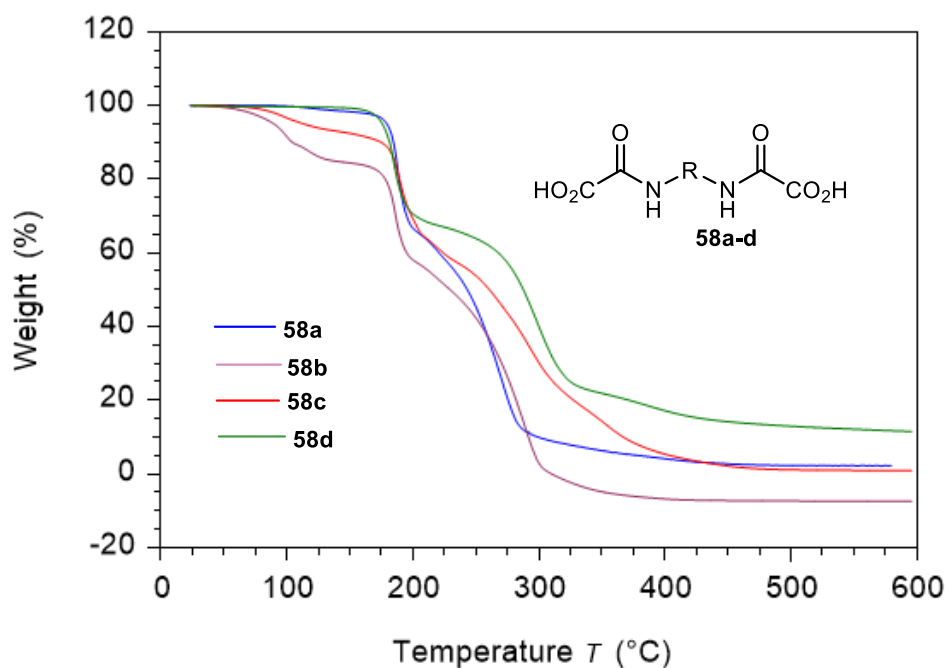
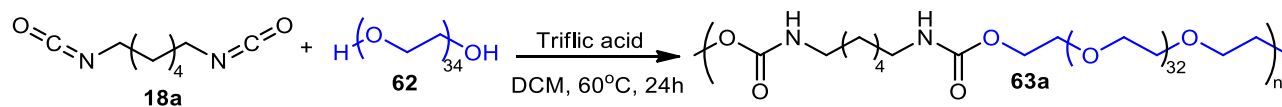


**Figure S15:** TGA analysis of different bis-oxamic acids

### 5.3. Comparing the SEC analysis of the thermoplastic PU in different solvents

HFIP was shown to be better solvent for the SEC analysis in terms of better molecular weight and polydispersity (Figure S16 a). Moreover, intense light scattering signal (LS, between the retention time 10 and 20 min) observed in SEC in DMF (Figure S16 b) and THF (Figure S16 c) could be an indication that probably more PU aggregates were in the solution due to incomplete solubility of the

polymer in the solvents. This signal however was very minimal for SEC in HFIP (Figure S16 a), signifying better solubility of the PU in HPLC. A similar observation was equally noted in most of the PU samples, though PUs from short chain diols still showed pronounced LS signal even in HFIP due to their poor solubility (Figure S17).



Sample	HFIP/Đ	THF/Đ	DMF/Đ
Classical route	66300/2.0	34900/2.1	50800/2.3

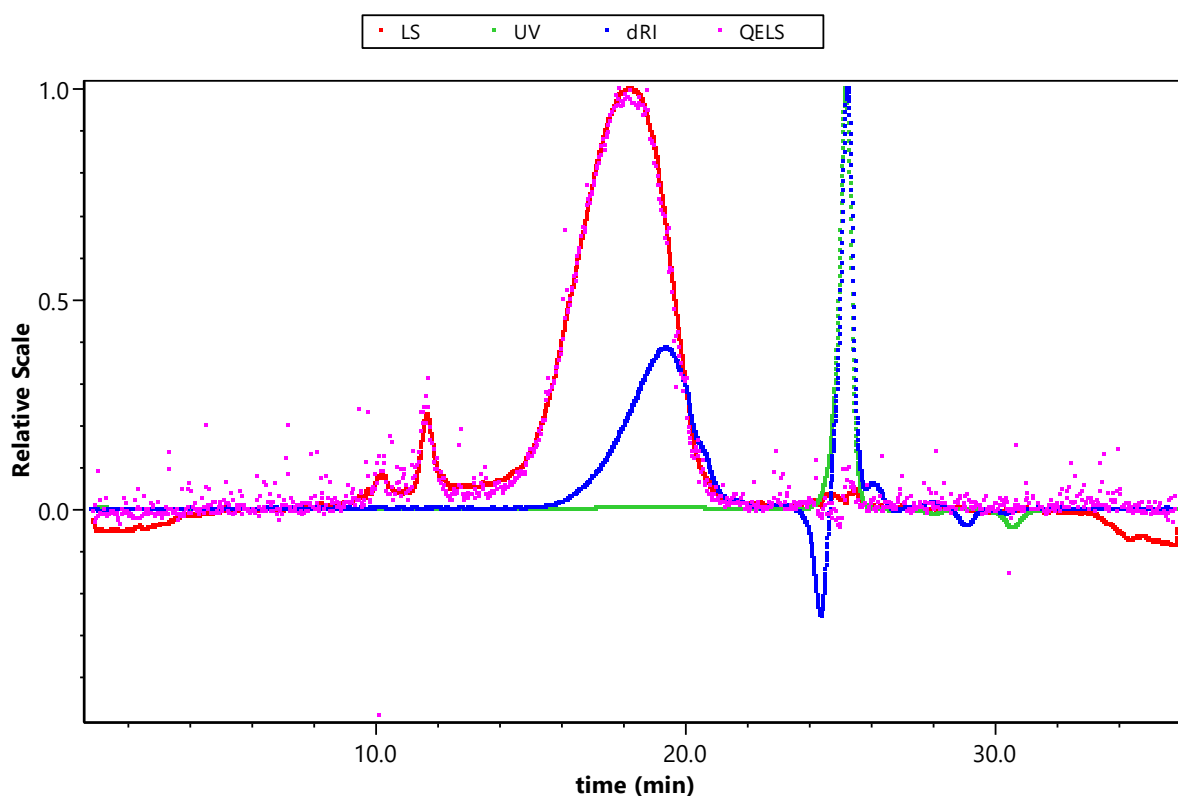


**Figure S16a:** SEC (HFIP) trace of PUs **63a** from commercial diisocyanate **18**, showing less light scattering signal (**LS**) probably due to better solubility of the PU. Note: **UV** = UV detector, **dRI** = differential refractive index, **QELS** = Quasi-Elastic Light Scattering.

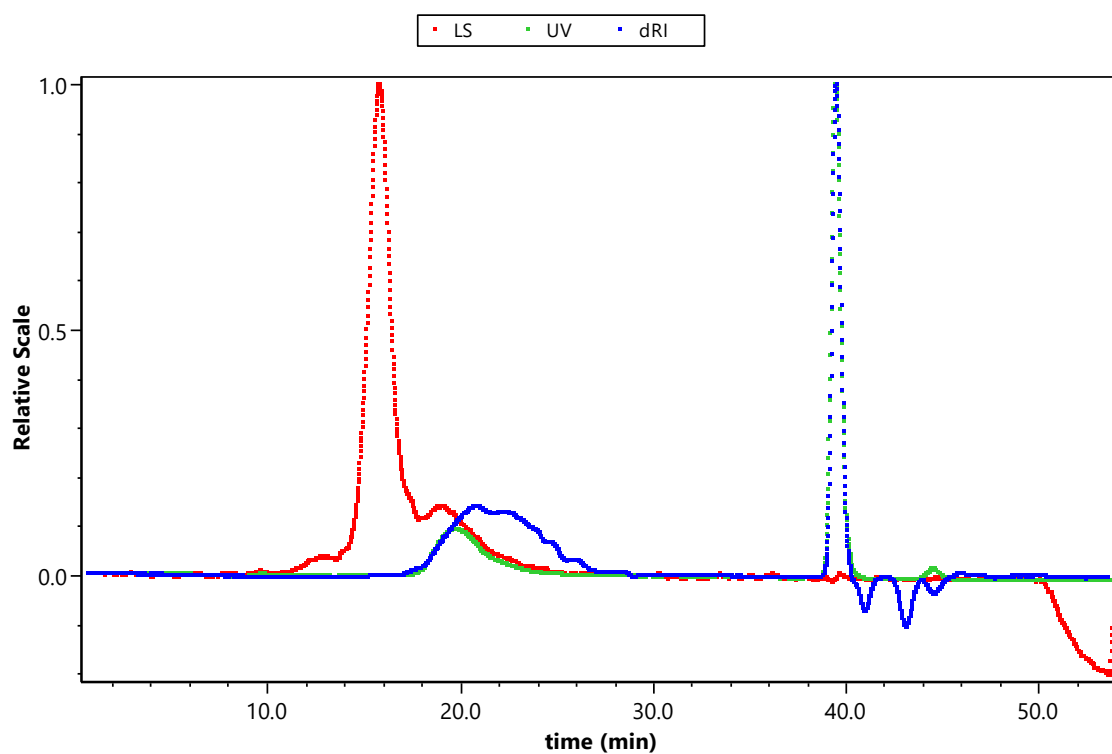


**Figure S16b:** SEC (DMF) trace of PUs **63a** from commercial diisocyanate **18**, showing intense light scattering signal (LS) probably due to PU aggregates as a result of poor solubility.

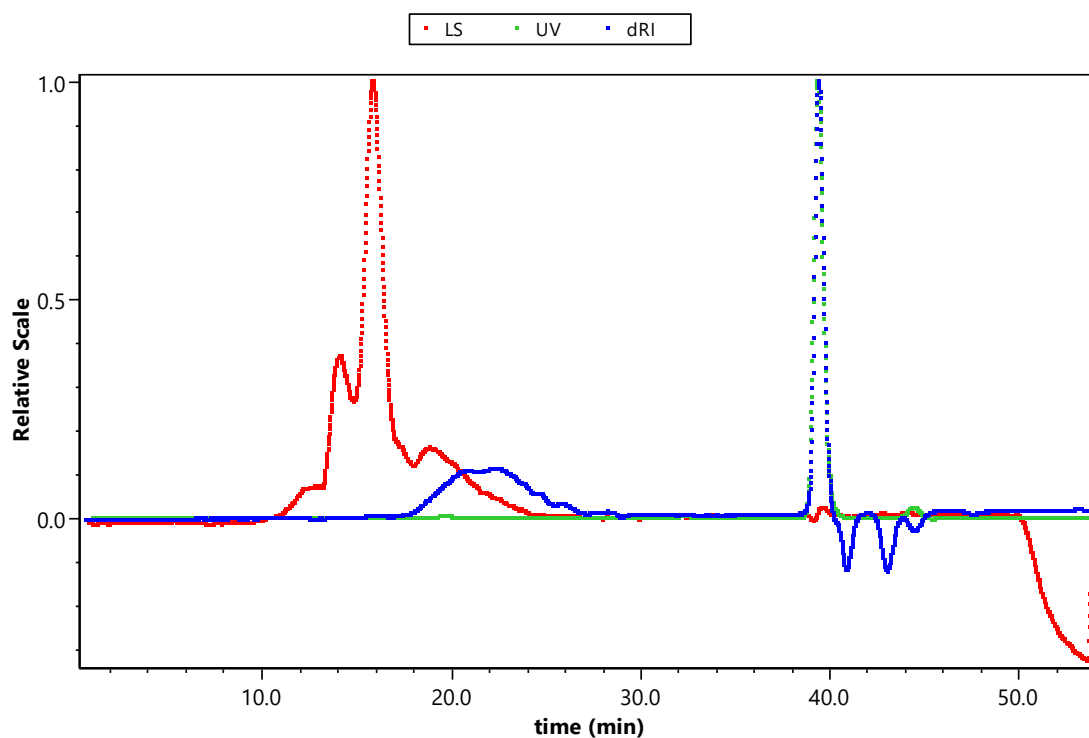


**Figure S16c:** SEC (THF) trace of PUs **63a** from commercial diisocyanate **18**, showing intense light scattering signal (LS) probably due to PU aggregates as a result of poor solubility.

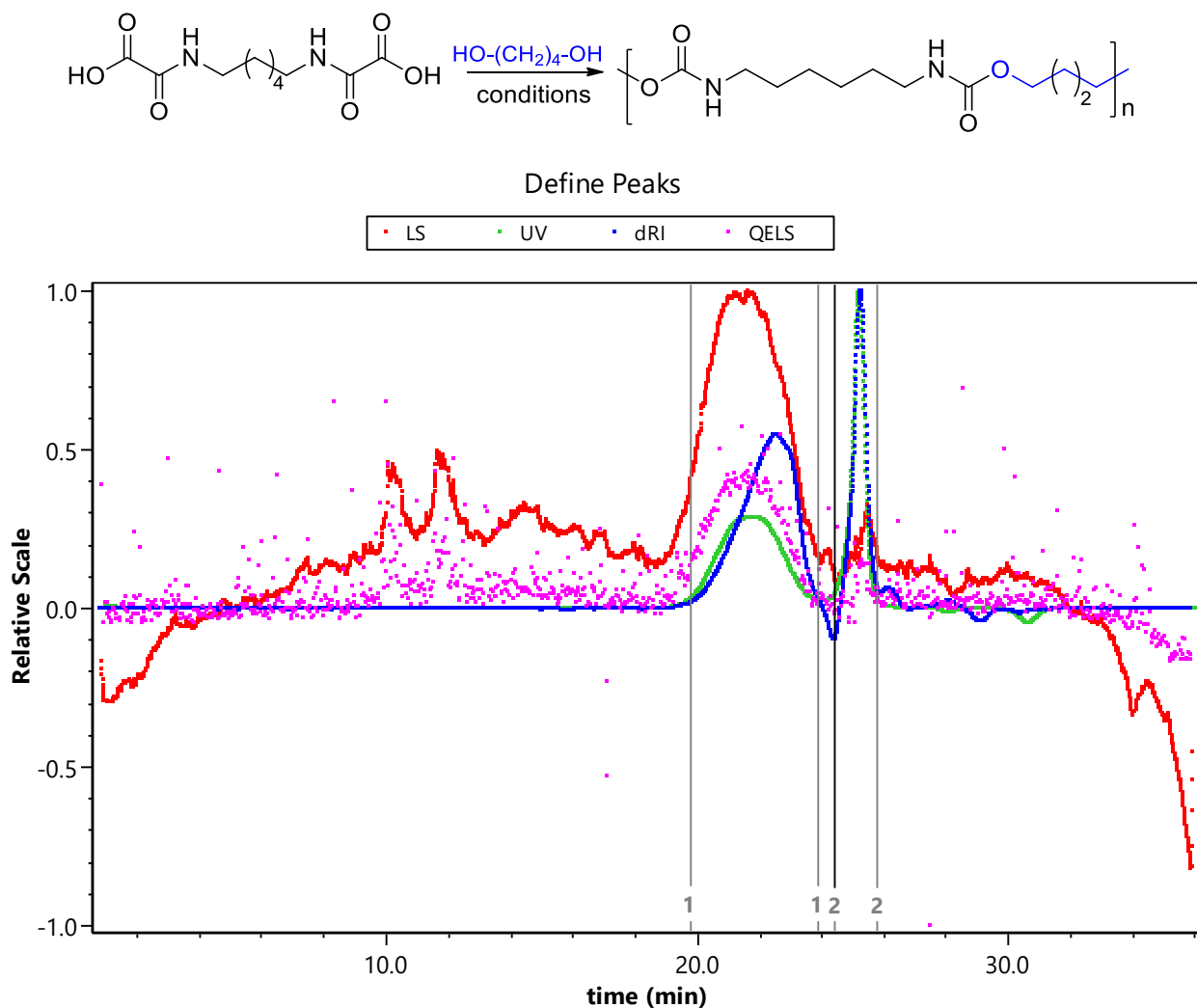


**Figure S17:** SEC (HFIP) trace of short chain-diol derived PU from bis-oxamic acid route, showing much light scattering signal (**LS**) due to its poor solubility in HFIP during SEC analysis. Note: **UV** = UV detector, **dRI** = differential refractive index, **QELS** = Quasi-Elastic Light Scattering.

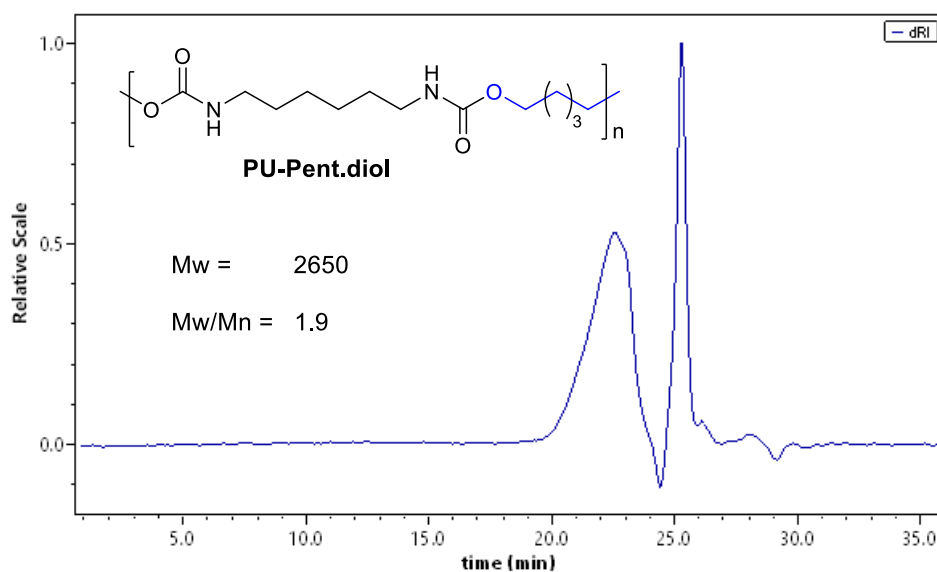


**Figure S18:** SEC (in HFIP) of 1,5-Pentandiol based PUs obtained from bis-oxamic acid **58a**

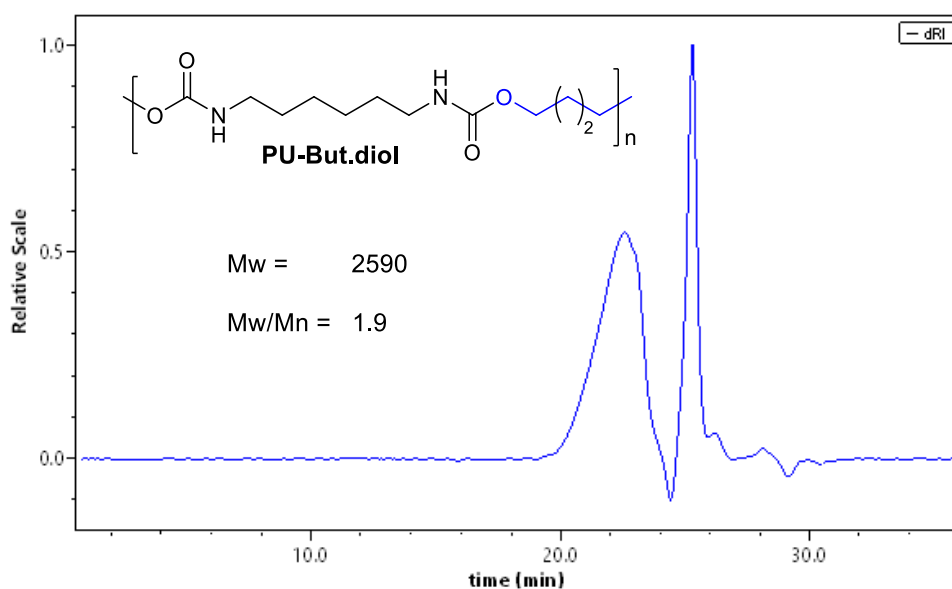
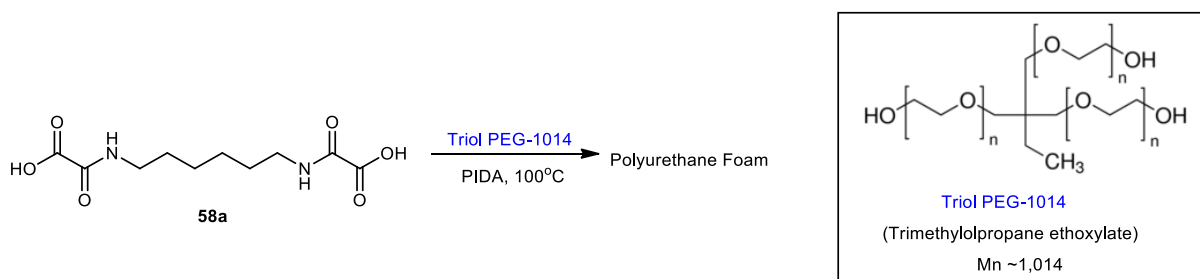


**Figure S19:** SEC (in HFIP) of 1,4-Butandiol based PUs obtained from bis-oxamic acid **58a**

#### 5.4. Standard procedure for PU foam synthesis from bis-oxamic acid

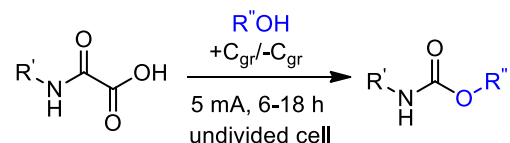


Bis-oxamic acid **58a** (1.0 mmol, 1.0 eq.), PIDA (2.2 mmol, 2.2 eq.), Triol PEG-1014 (0.67 mmol, 0.67 eq.) were charged into a dry 10 mL screw cap (Teflon sealed) vial containing a magnetic stirrer. The content was degassed and then heated to 100°C (oil bath) with constant stirring to form a homogeneous liquid (after about 5-10 min.) which eventually crosslinked to deliver the PU foam after about 10-20 min. Note: once a homogeneous solution was obtained, the stirring was reduced to 50 rpm. The CO<sub>2</sub> released during the decarboxylation of the oxamic acids served as the blowing agent to deliver the expected foam. During the process, CO<sub>2</sub> released built reasonable pressure in the vial. Without releasing the pressure, a rigid PU foam was obtained. However, for a more flexible foam, the pressure in the vial was slowly released (by a needle puncture on the Teflon cap) at the "maximum gelation", which was taken as the point when the magnetic stirrer stopped rotating. The obtained foam was allowed at 80°C for 1h, and thereafter, the curing was continued at reduced pressure to remove the liquid by-product (acetic acid and iodobenzene) from the PIDA.

## 6. Experimental Part: Chapter 6

### 6.1. General Procedure for Electrochemical Synthesis of Urethane

#### Method A:



Oxamic acid (0.5 mmol, 1.0 eq.) was charged into ElectraSyn vial (5 mL) equipped with a stir bar. The cap bearing graphite electrodes as both cathode and anode was fitted in the vial. A hole on the cap was securely covered with a septum, and through the septum the vial was degassed using Schlenk line for 10 min (Figure S20, **a**). With a syringe, dry alcohol (3 mL) was added into the vial under argon atm. The vial was then fastened to the ElectraSyn machine and electrolyzed at a constant current of 5 mA, stirring rate of 400 rpm and under argon atm. At the completion of the reaction, which was monitored by TLC, the reaction mixture was transferred to a round-bottom flask, the vial rinsed with DCM (3x3 mL). The combined solution was concentrated *in vacuo*. Column chromatography (AcOEt/petroleum ether) was then used to purify the resulted crude mixture.

Note: For bis-oxamic acid,  $\text{Bu}_4\text{NClO}_4$  (0.01 M) was necessary for more efficient electrical conductivity.

#### Method B:



Oxamic acid (0.5 mmol, 1.0 eq.) was charged into ElectraSyn vial (5 mL) equipped with a stir bar. The cap bearing graphite electrodes as both cathode and anode was fitted in the vial. A hole on the cap was securely covered with a septum, and through the septum the vial was degassed using Schlenk line for 10 min. With a syringe, dry alcohol (3 mL) was added into the vial under argon atm. The vial was then clamped in an oil bath at 50°C. The anode and cathode of the vial were connected to the ElectraSyn machine using external flexible wire with alligator clips (4 mm), (Figure S20, **b**). The mixture was electrolyzed at a constant current of 5 mA, stirring rate of 400 rpm and under argon atm. At the completion of the reaction, which was monitored by TLC, the reaction mixture was transferred to a round-bottom flask and the vial rinsed with DCM (3x3 mL). The combined solution was concentrated *in vacuo*. Column chromatography (AcOEt/petroleum ether) was then used to purify the resulted crude mixture.



(b) Setup for reaction at room temperature



(b) Setup for reaction at 50°C

**Figure S20:** Set-up for Urethane Synthesis by Electrochemical Decarboxylation of Oxamic

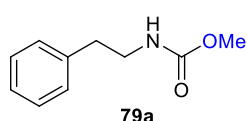
### Method C: General Procedure for Electrochemical Synthesis of Urethane on gram-scale



Oxamic acid (1.0 g, 5.18 mmol) and  $\text{Bu}_4\text{NClO}_4$  (0.03M) were charged into an ElectroSyn vial (10 mL) equipped with a stir bar. The cap bearing graphite electrodes as both cathode and anode was fitted in the vial. A hole on the cap was securely covered with a septum, and through the septum the vial was degassed using Schlenk line for 10 min. With a syringe, dry alcohol (10 mL) was added into the vial under argon atm. The vial was then clamped in an oil bath at 50°C. The anode and cathode of the vial were connected to the ElectroSyn machine using external flexible wire with alligator clips (4 mm), electrolyzed at a constant current of 5 mA with a stirring rate of 400 rpm and under argon atm. At the completion of the reaction, which was monitored by TLC, the reaction mixture was transferred to a round-bottom flask and the vial rinsed with DCM (5x3 mL). The combined solution was concentrated *in vacuo*. Column chromatography (AcOEt/petroleum ether) was then used to purify the resulted crude mixture.

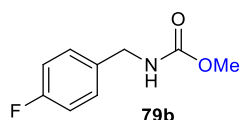
### 6.2. $^1\text{H}$ and $^{13}\text{C}$ NMR data of urethanes in the electrochemical process

#### Methyl phenethyl carbamate (79a)



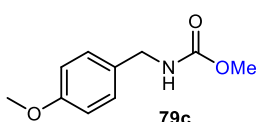
Following the general procedure A, the corresponding oxamic acid (0.5 mmol) was used. Purification by column chromatography (silica, petroleum ether/ethyl acetate 90/10) afforded **79a** (65 mg, 72%) as a colorless viscous liquid.  $R_f$  : 0.25 (EtOAc-petroleum ether 20/80).  $^1\text{H}$  NMR (300 MHz,  $\text{CDCl}_3$ )  $\delta$  : 7.40 – 7.11 (m, 5H), 4.78 (s, 1H), 3.68 (s, 3H), 3.46 (dd,  $J = 13.1, 6.6$  Hz, 2H), 2.83 (t,  $J = 7.0$  Hz, 2H).  $^{13}\text{C}$  NMR (76 MHz,  $\text{CDCl}_3$ )  $\delta$  : 157.0, 138.8, 128.8, 128.6, 126.5, 52.0, 42.2, 36.2. IR (neat)  $\nu_{\text{max}}$  ( $\text{cm}^{-1}$ ): 3336, 3027, 2946, 1709, 1603, 1532. HRMS (ESI): Calcd. for  $\text{C}_{10}\text{H}_{14}\text{O}_2\text{N}$   $[\text{M}+\text{H}]^+$  180.1019, found 180.1010.

### Methyl 4-fluorobenzylcarbamate (**79b**)



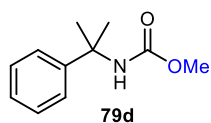
Following the general procedure A, the corresponding oxamic acid (0.5 mmol) was used. Purification by column chromatography (silica, petroleum ether/ethyl acetate 90/10) afforded **79b** (71.4 mg, 78%) as a white solid, m.p. : 68-70°C. Rf : 0.25 (EtOAc- petroleum ether, 20/80). <sup>1</sup>H NMR (300 MHz, CDCl<sub>3</sub>) δ : 7.37 – 7.12 (m, 2H), 7.01 (t, J = 8.7 Hz, 2H), 5.04 (s, 1H), 4.32 (d, J = 6.0 Hz, 2H), 3.69 (s, 3H). <sup>13</sup>C NMR (101 MHz, CDCl<sub>3</sub>) δ : 163.4, 161.0, 157.0, 134.4, 129.2, 129.1, 115.6, 115.4, 52.3, 44.4. IR (neat) ν<sub>max</sub> (cm<sup>-1</sup>): 3318, 3000, 2879, 1688, 1600, 1548. HRMS (ESI): Calcd. for C<sub>9</sub>H<sub>11</sub>O<sub>2</sub>NF [M+H]<sup>+</sup> 184.0768, found 184.0760.

### Methyl 4-methoxybenzylcarbamate (**79c**)



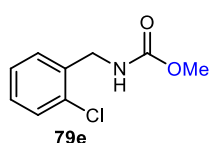
Following the general procedure A, the corresponding oxamic acid (0.5 mmol) was used. Purification by column chromatography (silica, petroleum ether/ethyl acetate 90/10) afforded **79c** (79 mg, 76%) as a light golden gel. Rf : 0.15 (EtOAc-petroleum ether, 20/80). <sup>1</sup>H NMR (300 MHz, CDCl<sub>3</sub>) δ : 7.34 – 7.18 (m, 1H), 6.95 – 6.75 (m, 3H), 5.09 (s, 1H), 4.36 (d, J = 5.9 Hz, 2H), 3.82 (s, 3H), 3.72 (s, 3H). <sup>13</sup>C NMR (101 MHz, CDCl<sub>3</sub>) δ : 159.9, 157.10, 140.2, 129.7, 112.9, 55.2, 52.2, 45.1. IR (neat) ν<sub>max</sub> (cm<sup>-1</sup>): 3340, 3008, 2943, 2831, 1705. HRMS (ESI): Calcd. for C<sub>10</sub>H<sub>13</sub>O<sub>3</sub>NNa [M+Na]<sup>+</sup> 218.0787, found 218.0788.

### Methyl (2-phenylpropan-2-yl) carbamate (**79d**)



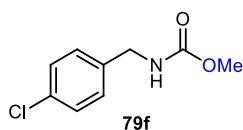
Following the general procedure A, the corresponding oxamic acid (0.5 mmol) was used. Purification by column chromatography (silica, petroleum ether/ethyl acetate 90/10) afforded **79d** (51 mg, 53%) as a colorless viscous liquid, Rf : 0.35 (EtOAc/petroleum ether 20/80). <sup>1</sup>H NMR (300 MHz, CDCl<sub>3</sub>) δ : 7.55 – 7.11 (m, 5H), 5.17 (s, 1H), 3.62 (s, 3H), 1.69 (s, 6H). <sup>13</sup>C NMR (76 MHz, CDCl<sub>3</sub>) δ : 156.7, 141.3, 126.9, 125.7, 125.1, 52.3, 39.9. IR (neat) ν<sub>max</sub> (cm<sup>-1</sup>): 3340, 3056, 2958, 2926, 1713. HRMS (ESI): Calcd. for C<sub>11</sub>H<sub>15</sub>O<sub>2</sub>NNa [M+Na]<sup>+</sup> 216.0995, found 216.0993.

### Methyl 2-chlorobenzyl carbamate (**79e**)



Following the general procedure A, the corresponding oxamic acid (0.3 mmol) was used. Purification by column chromatography (silica, petroleum ether/ethyl acetate 90/10) afforded **79e** (42.5 mg, 71%) as a colorless liquid that solidified into a white solid afterwards, m.p. : 61-63°C. Rf : 0.29 (EtOAc- petroleum ether 20/80). <sup>1</sup>H NMR (300 MHz, CDCl<sub>3</sub>) δ : 7.39 – 7.15 (m, 4H), 5.06 (s, 1H), 4.35 (d, J = 6.1 Hz, 2H), 3.72 (s, 3H). <sup>13</sup>C NMR (76 MHz, CDCl<sub>3</sub>) δ : 157.0, 135.9, 133.5, 129.5, 128.9, 127.0, 52.3, 43.0. IR (neat) ν<sub>max</sub> (cm<sup>-1</sup>): 3329, 3080, 2951, 1707, 1529. HRMS (ESI): Calcd. for C<sub>9</sub>H<sub>10</sub>O<sub>2</sub>N<sup>35</sup>ClNa [M+Na]<sup>+</sup> 222.0292, found 222.0292.

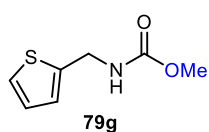
### Methyl 4-chlorobenzylcarbamate (**79f**)



Following the general procedure A, the corresponding oxamic acid (0.4 mmol) was used. Purification by column chromatography (silica, cyclohexane/ethyl acetate 85/15) afforded **79f** (54 mg, 68%) as white solid, m.p. : 83 – 86°C. Rf = 0.36 (EtOAc- petroleum ether 20/80). <sup>1</sup>H NMR (300 MHz, CDCl<sub>3</sub>) δ : 7.43 – 7.08 (m, 4H), 5.06 (s, 1H), 4.35 (d, J = 6.2 Hz, 2H), 3.72 (s, 3H). <sup>13</sup>C NMR (76 MHz, CDCl<sub>3</sub>) δ :

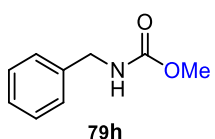
157.1, 137.1, 133.3, 128.8, 52.3, 44.4. IR (neat)  $\nu_{\max}$  (cm<sup>-1</sup>): 3312, 2995, 1689, 1545. HRMS (ESI): Calcd. for C<sub>9</sub>H<sub>9</sub>O<sub>2</sub>N<sup>35</sup>Cl [M-H]<sup>-</sup> 198.0327, found 198.0326.

### Methyl (thiophen-2-ylmethyl) carbamate (79g)



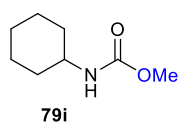
Following the general procedure A, the corresponding oxamic acid (0.5 mmol) and Bu<sub>4</sub>NClO<sub>4</sub> (0.01M) were used. Purification by column chromatography (silica, cyclohexane/ethyl acetate 85/15) afforded **79g** (45 mg, 41%) as a light brown gel. Rf : 0.23 (AcOEt/petroleum ether, 20/80). <sup>1</sup>H NMR (300 MHz, CDCl<sub>3</sub>)  $\delta$  : 7.26 – 7.20 (m, 1H), 7.00 – 6.93 (m, 2H), 5.20 (s, 1H), 4.54 (d, J = 5.8 Hz, 2H), 3.71 (s, 3H). <sup>13</sup>C NMR (76 MHz, CDCl<sub>3</sub>)  $\delta$  : 156.7, 141.3, 126.8, 125.7, 125.1, 52.3, 39.9. IR (neat)  $\nu_{\max}$  (cm<sup>-1</sup>): 3327, 3064, 2952, 1703, 1529. HRMS (ESI): Calcd. for C<sub>7</sub>H<sub>9</sub>O<sub>2</sub>NSNa [M+Na]<sup>+</sup> 194.0246, found 194.0246.

### Methyl benzyl carbamate (79h)



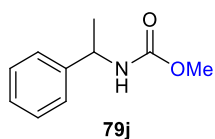
Following the general procedure A, the corresponding oxamic acid (0.5 mmol) was used. Purification by column chromatography (silica, 100% DCM) afforded **79h** (63 mg, 76%) as a white solid, m.p. : 50-52°C. Rf : 0.34 (DCM). <sup>1</sup>H NMR (300 MHz, CDCl<sub>3</sub>)  $\delta$  : 7.58 – 7.25 (m, 5H), 5.06 (s, 1H), 4.39 (d, J = 5.9 Hz, 2H), 3.72 (s, 3H). <sup>13</sup>C NMR (76 MHz, CDCl<sub>3</sub>)  $\delta$  : 157.1, 138.5, 128.7, 127.5, 52.2, 45.1. IR (neat)  $\nu_{\max}$  (cm<sup>-1</sup>): 3331, 3030, 2950, 1705, 1530. HRMS (ESI): Calcd. for C<sub>9</sub>H<sub>11</sub>O<sub>2</sub>NNa [M+Na]<sup>+</sup> 188.0682, found 188.0681.

### Methyl cyclohexyl carbamate (79i)



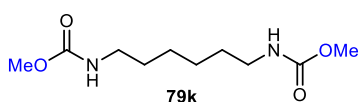
Following the general procedure A, the corresponding oxamic acid (0.5 mmol) was used. Purification by column chromatography (silica, petroleum ether/ethyl acetate 90/10) afforded **79i** (57 mg, 73%) as a white crystalline solid, m.p. : 75°C. Rf = 0.41 (AcOEt/petroleum ether, 20/80). <sup>1</sup>H NMR (300 MHz, CDCl<sub>3</sub>)  $\delta$  : 4.67 (s, 1H), 3.64 (s, 3H), 3.45 (s, 1H), 2.02 – 1.78 (m, 2H), 1.76 – 1.48 (m, 3H), 1.48 – 1.23 (m, 2H), 1.22 – 1.03 (m, 3H). <sup>13</sup>C NMR (101 MHz, CDCl<sub>3</sub>)  $\delta$  : 156.3, 51.7, 49.8, 33.4, 25.5, 24.8. IR (neat)  $\nu_{\max}$  (cm<sup>-1</sup>): 3344, 2941, 2841, 1691, 1536. HRMS (ESI): Calcd. for C<sub>8</sub>H<sub>16</sub>O<sub>2</sub>N [M+H]<sup>+</sup> 158.1175, found 158.1175.

### Methyl (1-phenylethyl)carbamate (79j)



Following the general procedure A, the corresponding oxamic acid (1.0 mmol) used. Purification by column chromatography (silica, 100% DCM) afforded **79j** (125 mg, 70%) as a white solid, m.p. : 59°C. Rf : 0.25 (AcOEt/petroleum ether, 20/80). <sup>1</sup>H NMR (300 MHz, CDCl<sub>3</sub>)  $\delta$  : 7.26 (m, 5H), 5.04 (s, 1H), 4.79 (s, 1H), 3.59 (s, 3H), 1.42 (d, J = 6.9 Hz, 3H). <sup>13</sup>C NMR (101 MHz, CDCl<sub>3</sub>)  $\delta$  : 156.3, 143.7, 128.6, 127.3, 125.9, 52.1, 50.7, 22.4. IR (neat)  $\nu_{\max}$  (cm<sup>-1</sup>) = 3318, 3038, 2982, 1703, 1530. HRMS (ESI): Calcd. for C<sub>10</sub>H<sub>13</sub>O<sub>2</sub>NNa [M+Na]<sup>+</sup> 202.0836, found 202.0838.

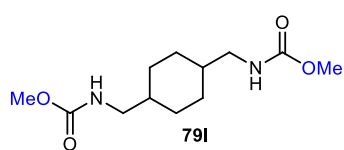
### Dimethyl hexane-1,6-diyl dicarbamate (79k)



Following the general procedure A, the corresponding oxamic acid (0.5 mmol) and Bu<sub>4</sub>NClO<sub>4</sub> (0.01M) were used. Purification by column chromatography (silica, DCM/MeOH 98/2) afforded **79k** (56 mg, 50%) as a white solid, m.p. : 117-119°C. Rf : 0.37 (MeOH/DCM, 4/96). <sup>1</sup>H NMR (300 MHz, CDCl<sub>3</sub>)  $\delta$  : 4.79 (s, 2H), 3.66 (s, 6H), 3.26 – 2.93 (m, 4H), 1.63 – 1.41 (m, 4H), 1.39 – 1.22 (m, 4H). <sup>13</sup>C NMR (76 MHz, CDCl<sub>3</sub>)  $\delta$  : 157.1, 52.0, 40.8, 29.9, 26.2. IR (neat)

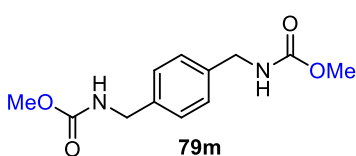
$\nu_{\max}$  ( $\text{cm}^{-1}$ ): 3337, 2942, 2855, 1689, 1535. HRMS (ESI): Calcd. for  $\text{C}_{10}\text{H}_{21}\text{O}_4\text{N}_2$   $[\text{M}+\text{H}]^+$  233.1495, found 233.1493.

### Dimethyl (cyclohexane-1,4-diylbis(methylene))dicarbamate (79l)



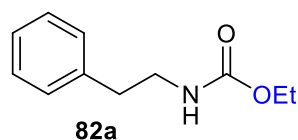
Following the general procedure A, the corresponding oxamic acid (0.5 mmol) and  $\text{Bu}_4\text{NClO}_4$  (0.01M) were used. Purification by column chromatography (silica, DCE/MeOH 98/2) afforded **79l** (70 mg, 54%) as white solid, m.p. : 119-123°C. Rf : 0.36 (MeOH-  $\text{CH}_2\text{Cl}_2$  4/96).  $^1\text{H}$  NMR (300 MHz,  $\text{CDCl}_3$ )  $\delta$  : 4.76 (s, 2H), 3.66 (s, 6H), 3.08 (dt,  $J = 27.2, 6.6$  Hz, 4H), 1.87 – 1.57 (m, 3H), 1.57 – 1.28 (m, 5H), 1.02 – 0.83 (m, 2H).  $^{13}\text{C}$  NMR (76 MHz,  $\text{CDCl}_3$ )  $\delta$  : 157.2, 52.0, 47.1, 44.6, 38.3, 35.8, 29.9, 26.1. IR (neat)  $\nu_{\max}$  ( $\text{cm}^{-1}$ ): 3330, 2923, 2854, 1704, 1539. HRMS (ESI): Calcd. for  $\text{C}_{12}\text{H}_{22}\text{O}_4\text{N}_2\text{Na}$   $[\text{M}+\text{Na}]^+$  281.1471, found 281.1468.

### Dimethyl (1,4-phenylenebis(methylene)) dicarbamate (79m)



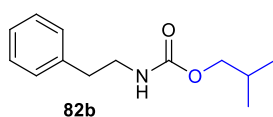
Following the general procedure A, the corresponding oxamic acid (0.5 mmol) and  $\text{Bu}_4\text{NClO}_4$  (0.01M) were used. Purification by column chromatography (silica, DCM/MeOH 98/2) afforded **79m** (80 mg, 64%) as a white solid, m.p. : 190-193°C. Rf : 0.14 MeOH/DCM, 4/96)  $^1\text{H}$  NMR (300 MHz,  $\text{CDCl}_3$ )  $\delta$  : 7.27 (s, 4H), 5.03 (s, 2H), 4.36 (d,  $J = 6.0$  Hz, 4H), 3.72 (s, 6H).  $^{13}\text{C}$  NMR (101 MHz, DMSO)  $\delta$  : 157.3, 138.8, 127.5, 51.8, 44.1, 43.9. IR (neat)  $\nu_{\max}$  ( $\text{cm}^{-1}$ ): 3313, 3047, 2939, 1688, 1535. HRMS (ESI): Calcd. for  $\text{C}_{12}\text{H}_{16}\text{O}_4\text{N}_2\text{Na}$   $[\text{M}+\text{Na}]^+$  275.1001, found 275.0997.

### Ethyl phenethylcarbamate (82a)



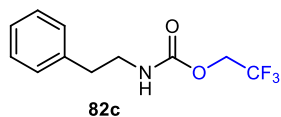
Following the general procedure A, the corresponding oxamic acid (0.5 mmol) and  $\text{Bu}_4\text{NClO}_4$  (0.03M) were used. Purification by column chromatography (silica, 100% DCM) afforded **82a** (59 mg, 62%) as a colorless gel. Rf : 0.40 (EtOAc/Hexane 10/90).  $^1\text{H}$  NMR (300 MHz,  $\text{CDCl}_3$ )  $\delta$  : 7.40 – 7.16 (m, 5H), 4.69 (s, 1H), 4.13 (q,  $J = 7.2$  Hz, 2H), 3.46 (q,  $J = 6.8$  Hz, 2H), 2.84 (t,  $J = 7.0$  Hz, 2H), 1.25 (t,  $J = 7.2$  Hz, 3H);  $^{13}\text{C}$  NMR (75 MHz,  $\text{CDCl}_3$ )  $\delta$  : 156.6, 138.8, 130.0, 128.8, 128.7, 128.6, 126.5, 60.7, 42.1, 36.2, 14.6. IR (neat)  $\nu_{\max}$  ( $\text{cm}^{-1}$ ): 3334, 2980, 2934, 1702, 1533. Spectroscopic data were in good agreement with literature<sup>1</sup>.

### Isobutyl phenethyl carbamate (82b)



Following the general procedure B, the corresponding oxamic acid (0.5 mmol) and  $\text{Bu}_4\text{NClO}_4$  (0.03M) were used. Purification by column chromatography (silica, 100% DCM) afforded **82b** (71 mg, 64%) as a light brown viscous liquid. Rf : 0.35 (AcOEt/petroleum ether, 20/80).  $^1\text{H}$  NMR (300 MHz,  $\text{CDCl}_3$ )  $\delta$  : 7.37 – 7.17 (m, 5H), 4.70 (s, 1H), 3.86 (d,  $J = 6.6$  Hz, 2H), 3.46 (dd,  $J = 13.1, 6.6$  Hz, 2H), 2.84 (t,  $J = 7.0$  Hz, 2H), 1.91 (dt,  $J = 13.0, 6.5$  Hz, 1H), 0.94 (d,  $J = 6.6$  Hz, 6H).  $^{13}\text{C}$  NMR (76 MHz,  $\text{CDCl}_3$ )  $\delta$  : 156.7, 138.8, 128.8, 128.6, 126.5, 71.0, 42.1, 36.2, 28.0, 19.0. IR (neat)  $\nu_{\max}$  ( $\text{cm}^{-1}$ ): 3331, 3021, 2965, 2866, 1703, 1529. HRMS (ESI): Calcd. for  $\text{C}_{13}\text{H}_{19}\text{O}_2\text{NNa}$   $[\text{M}+\text{Na}]^+$  244.1308, found 244.1308.

### 2,2,2-Trifluoroethyl phenethylcarbamate (**82c**)



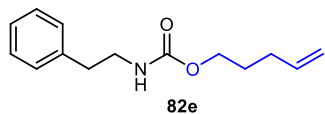
Following the general procedure B, the corresponding oxamic acid (0.5 mmol) and  $\text{Bu}_4\text{NClO}_4$  (0.05M) were used. Purification by column chromatography (silica, petroleum ether/ethyl acetate 90/10) afforded **82c** (61 mg, 50%) as a colorless liquid.  $R_f$  : 0.6 (EtOAc-Hexane 20/80).  $^1\text{H}$  NMR (300 MHz,  $\text{CDCl}_3$ )  $\delta$  : 7.44 – 7.05 (m, 5H), 4.93 (s, 1H), 4.47 (q,  $J$  = 8.5 Hz, 2H), 3.51 (dd,  $J$  = 13.1, 6.8 Hz, 2H), 2.86 (t,  $J$  = 6.9 Hz, 2H).  $^{13}\text{C}$  NMR (76 MHz,  $\text{CDCl}_3$ )  $\delta$  : 154.3, 138.3, 128.7, 128.7, 126.7, 61.1, 60.6, 42.4, 35.8. IR (neat)  $\nu_{\text{max}}$  ( $\text{cm}^{-1}$ ): 3345, 3064, 3030, 2945, 1730, 1604, 1604, 1526. HRMS (ESI): Calcd. for  $\text{C}_{11}\text{H}_{12}\text{O}_2\text{NF}_3$   $[\text{M}+\text{Na}]^+$  270.0712, found 270.0708. Spectroscopic data were in good agreement with literature<sup>1</sup>.

### Ethyl cyclohexylcarbamate (**82d**)



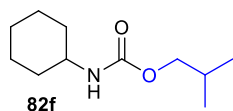
Following the general procedure B, the corresponding oxamic acid (0.5 mmol) and  $\text{Bu}_4\text{NClO}_4$  (0.03M) were used. Purification by column chromatography (silica, 100% DCM) afforded **82d** (54 mg, 63%) as a white crystalline solid. m.p. : 59°C.  $R_f$  : 0.40 (AcOEt/petroleum ether, 20/80).  $^1\text{H}$  NMR (300 MHz,  $\text{CDCl}_3$ )  $\delta$  : 4.52 (s, 1H), 4.12 (q,  $J$  = 7.1 Hz, 2H), 3.49 (s, 1H), 2.04 – 1.86 (m, 2H), 1.80 – 1.55 (m, 3H), 1.46 – 1.03 (m, 8H).  $^{13}\text{C}$  NMR (76 MHz,  $\text{CDCl}_3$ )  $\delta$  : 155.8, 60.4, 49.7, 33.4, 25.5, 24.8, 14.6. IR (neat)  $\nu_{\text{max}}$  ( $\text{cm}^{-1}$ ): 3314, 2978, 2922, 2853, 1688, 1542. HRMS (ESI): Calcd. for  $\text{C}_9\text{H}_{18}\text{O}_2\text{N}$   $[\text{M}+\text{H}]^+$  172.1332, found 172.1331.

### Pent-4-en-1-yl phenethylcarbamate (**82e**)



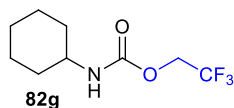
Following the general procedure B, the corresponding oxamic acid (0.5 mmol) and  $\text{Bu}_4\text{NClO}_4$  (0.08M) were used. Purification by column chromatography (silica, petroleum ether/ethyl acetate 90/10) afforded **82e** (24 mg, 21%) as a colorless gel.  $R_f$  : 0.56 (EtOAc/Hexane 20/80).  $^1\text{H}$  NMR (300 MHz,  $\text{CDCl}_3$ )  $\delta$  : 7.49 – 6.99 (m, 5H), 5.83 (m,  $J$  = 16.9, 10.2, 6.6 Hz, 1H), 5.01 (d,  $J$  = 10.2 Hz, 2H), 4.68 (s, 1H), 4.09 (t,  $J$  = 6.6 Hz, 2H), 3.47 (dd,  $J$  = 13.0, 6.5 Hz, 2H), 2.84 (t,  $J$  = 7.0 Hz, 2H), 2.13 (dd,  $J$  = 13.9, 6.8 Hz, 2H), 1.81 – 1.62 (m, 2H).  $^{13}\text{C}$  NMR (76 MHz,  $\text{CDCl}_3$ )  $\delta$  : 156.6, 138.8, 137.6, 128.8, 128.6, 126.5, 115.1, 64.3, 42.1, 36.2, 30.0, 28.3. IR (neat)  $\nu_{\text{max}}$  ( $\text{cm}^{-1}$ ): 3335, 3065, 3028, 2940, 1703, 1641, 1531. HRMS (ESI): Calcd. for  $\text{C}_{14}\text{H}_{20}\text{O}_2\text{N}$   $[\text{M}+\text{H}]^+$  234.1488, found 234.1482.

### Isobutyl cyclohexylcarbamate (**82f**)



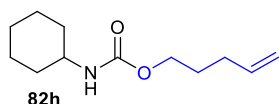
Following the general procedure B, the corresponding oxamic acid (0.7 mmol) and  $\text{Bu}_4\text{NClO}_4$  (0.05M) were used. Purification by column chromatography (silica, petroleum ether/ethyl acetate 95/5) afforded **82f** (99 mg, 71%) as a white solid. m.p. : 51-52°C.  $R_f$  : 0.71 (EtOAc/Hexane 20/80).  $^1\text{H}$  NMR (300 MHz,  $\text{CDCl}_3$ )  $\delta$  : 4.56 (s, 1H), 3.80 (d,  $J$  = 6.6 Hz, 2H), 3.52 – 3.34 (m, 1H), 1.90 (dt,  $J$  = 17.3, 6.5 Hz, 3H), 1.74 – 1.52 (m, 3H), 1.40 – 1.22 (m, 2H), 1.21 – 1.03 (m, 3H), 0.90 (d,  $J$  = 6.7 Hz, 6H).  $^{13}\text{C}$  NMR (76 MHz,  $\text{CDCl}_3$ )  $\delta$  : 156.0, 49.8, 33.5, 28.0, 25.5, 24.8, 19.1. IR (neat)  $\nu_{\text{max}}$  ( $\text{cm}^{-1}$ ): 3324, 2856, 2932, 1694. HRMS (ESI): Calcd. for  $\text{C}_{11}\text{H}_{21}\text{O}_2\text{NNa}$   $[\text{M}+\text{Na}]^+$  222.1464, found 222.1464.

### 2,2,2-Trifluoroethyl cyclohexylcarbamate (**82g**)



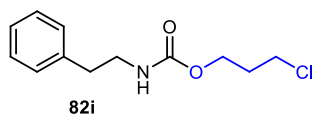
Following the general procedure B, the corresponding oxamic acid (0.7 mmol) and  $\text{Bu}_4\text{NClO}_4$  (0.05M) were used. Purification by column chromatography (silica, petroleum ether/ethyl acetate 95/5) afforded **82g** (71 mg, 45%) as a white solid. m.p. : 82-85°C. Rf : 0.76 (EtOAc/Hexane 20/80).  $^1\text{H}$  NMR (300 MHz,  $\text{CDCl}_3$ )  $\delta$  : 4.82 (s, 1H), 4.43 (q,  $J$  = 8.6 Hz, 2H), 3.55 – 3.39 (m, 1H), 1.93 (dd,  $J$  = 8.4, 4.0 Hz, 2H), 1.78 – 1.51 (m, 3H), 1.42 – 1.07 (m, 5H).  $^{13}\text{C}$  NMR (76 MHz,  $\text{CDCl}_3$ )  $\delta$  : 153.5, 125.0, 121.3, 61.4, 60.9, 60.4, 59.9, 50.3, 33.1, 25.4, 24.7. IR (neat)  $\nu_{\text{max}}$  ( $\text{cm}^{-1}$ ): 3325, 2925, 2859, 1703. HRMS (ESI): Calcd. for  $\text{C}_9\text{H}_{13}\text{O}_2\text{NF}_3$   $[\text{M}+\text{H}]^+$  224.0903, found 224.0898.

### Pent-4-en-1-yl cyclohexylcarbamate (**82h**)



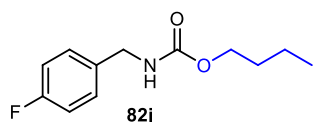
Following the general procedure B, the corresponding oxamic acid (0.5 mmol) and  $\text{Bu}_4\text{NClO}_4$  (0.08M) were used. Purification by column chromatography (petroleum ether/ethyl acetate 93/7) afforded **82h** (56 mg, 53%) as a white solid. m.p. : 40-41°C. Rf : 0.54 (EtOAc/Hexane 20/80).  $^1\text{H}$  NMR (300 MHz,  $\text{CDCl}_3$ )  $\delta$  : 5.83 (m,  $J$  = 16.9, 10.2, 6.6 Hz, 1H), 5.13 – 4.91 (m, 2H), 4.55 (s, 1H), 4.07 (t,  $J$  = 6.5 Hz, 2H), 3.47 (s, 1H), 2.22 – 2.02 (m, 2H), 2.05 – 1.83 (m, 2H), 1.77 – 1.53 (m, 5H), 1.47 – 1.00 (m, 5H).  $^{13}\text{C}$  NMR (76 MHz,  $\text{CDCl}_3$ )  $\delta$  : 155.8, 137.7, 115.0, 64.0, 49.7, 33.4, 30.0, 28.3, 25.5, 24.8. IR (neat)  $\nu_{\text{max}}$  ( $\text{cm}^{-1}$ ): 3325, 3077, 2932, 2855, 1697, 1533. HRMS (ESI): Calcd. for  $\text{C}_{12}\text{H}_{21}\text{O}_2\text{NNa}$   $[\text{M}+\text{Na}]^+$  234.1464, found 234.1459.

### 3-Chloropropyl phenethylcarbamate (**82i**)



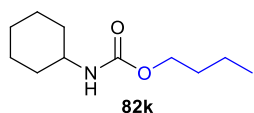
Following the general procedure B, the corresponding oxamic acid (0.5 mmol) and  $\text{Bu}_4\text{NClO}_4$  (0.08M) were used. Purification: vacuum distillation to remove excess alcohol, column chromatography (silica, petroleum ether/ethyl acetate 90/10) afforded **82i** (54%, NMR yield, 38 mg isolated, 31%) as a colorless liquid. Rf : 0.42 (EtOAc-Hexane 20/80).  $^1\text{H}$  NMR (300 MHz,  $\text{CDCl}_3$ )  $\delta$  : 7.43 – 7.16 (m, 5H), 4.71 (s, 1H), 4.23 (t,  $J$  = 6.0 Hz, 2H), 3.61 (t,  $J$  = 6.5 Hz, 2H), 3.47 (dd,  $J$  = 13.1, 6.6 Hz, 2H), 2.84 (t,  $J$  = 6.9 Hz, 2H), 2.09 (p,  $J$  = 6.2 Hz, 2H).  $^{13}\text{C}$  NMR (76 MHz,  $\text{CDCl}_3$ )  $\delta$  : 156.2, 138.7, 128.8, 128.6, 126.5, 61.5, 42.1, 41.3, 36.1, 32.0. IR (neat)  $\nu_{\text{max}}$  ( $\text{cm}^{-1}$ ): 3334, 3063, 3028, 2960, 1706, 1603, 1603, 1528. HRMS (ESI): Calcd. for  $\text{C}_{12}\text{H}_{16}\text{O}_2\text{NCl}^{35}\text{Na}$   $[\text{M}+\text{Na}]^+$  264.0761, found 264.0757.

### Butyl 4-fluorobenzylcarbamate (**82j**)



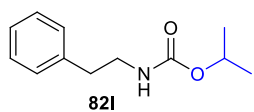
Following the general procedure B, the corresponding oxamic acid (0.5 mmol),  $\text{Bu}_4\text{NClO}_4$  (0.1M) and DCE (0.5 mL) and were used. Purification by column chromatography (silica, petroleum ether/ethyl acetate 95/5) afforded **82j** (50.6 mg, 45%) as a light brown gel. Rf : 0.58 (EtOAc/Hexane 20/80).  $^1\text{H}$  NMR (300 MHz,  $\text{CDCl}_3$ )  $\delta$  : 7.28 (dd,  $J$  = 8.9, 5.0 Hz, 2H), 7.03 (t,  $J$  = 8.7 Hz, 2H), 5.01 (s, 1H), 4.34 (d,  $J$  = 5.9 Hz, 2H), 4.11 (t,  $J$  = 6.7 Hz, 2H), 1.62 (tt,  $J$  = 8.2, 6.7 Hz, 2H), 1.38 (dt,  $J$  = 14.4, 7.4 Hz, 2H), 0.94 (dd,  $J$  = 9.6, 5.1 Hz, 3H).  $^{13}\text{C}$  NMR (76 MHz,  $\text{CDCl}_3$ )  $\delta$  : 163.8, 160.5, 156.7, 134.4, 129.1, 115.6, 115.3, 65.0, 44.3, 31.1, 19.1, 13.7. IR (neat)  $\nu_{\text{max}}$  ( $\text{cm}^{-1}$ ): 3332, 2958, 2928, 2883 1701, 1606, 1510. HRMS (ESI): Calcd. for  $\text{C}_{12}\text{H}_{16}\text{O}_2\text{NFNa}$   $[\text{M}+\text{Na}]^+$  248.1057, found 248.1055.

### Butyl cyclohexylcarbamate (**82k**)



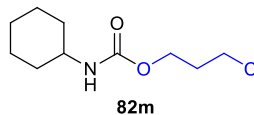
Following the general procedure B, the corresponding oxamic acid (0.5 mmol) and  $\text{Bu}_4\text{NCIO}_4$  (0.1M) were used. Purification by column chromatography (silica, petroleum ether/ethyl acetate 90/10) afforded **82k** (52 mg, 52%) as a white crystalline solid. m.p. : 52-53°C. Rf : 0.67 (AcOEt/petroleum ether, 20/80).  $^1\text{H}$  NMR (300 MHz,  $\text{CDCl}_3$ )  $\delta$  : 4.71 – 4.29 (s, 1H), 4.05 (t,  $J$  = 6.5 Hz, 2H), 3.64 – 3.23 (s, 1H), 2.03 – 1.85 (m, 2H), 1.78 – 1.49 (m, 5H), 1.49 – 1.24 (m, 4H), 1.25 – 1.03 (m, 3H), 0.94 (t,  $J$  = 7.3 Hz, 3H).  $^{13}\text{C}$  NMR (76MHz,  $\text{CDCl}_3$ )  $\delta$  : 156.0, 64.4, 49.7, 33.5, 31.1, 25.5, 24.8, 19.1, 13.7. IR (neat)  $\nu_{\text{max}}$  ( $\text{cm}^{-1}$ ): 3318, 2939, 2853, 1686, 1537. HRMS (ESI): Calcd. for  $\text{C}_{11}\text{H}_{21}\text{O}_2\text{NNa}$  [ $\text{M}+\text{Na}$ ] $^+$  222.1464, found 222.1459.

### Isopropyl phenethylcarbamate (**82l**)



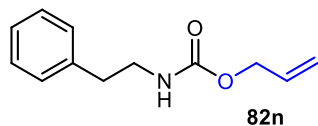
Following the general procedure B, the corresponding oxamic acid (0.5 mmol) and  $\text{Bu}_4\text{NCIO}_4$  (0.03M) were used. Purification by column chromatography (silica, petroleum ether/ethyl acetate 93/7) afforded **82l** (28 mg, 30%) as a colorless liquid, Rf : 0.054 (AcOEt/petroleum ether, 20/80).  $^1\text{H}$  NMR (300 MHz,  $\text{CDCl}_3$ )  $\delta$  : 7.40 – 7.07 (m, 5H), 4.91 (dt,  $J$  = 12.5, 6.2 Hz, 1H), 4.62 (s, 1H), 3.43 (d,  $J$  = 6.1 Hz, 2H), 2.81 (t,  $J$  = 7.0 Hz, 2H), 1.22 (d,  $J$  = 6.2 Hz, 6H).  $^{13}\text{C}$  NMR (76 MHz,  $\text{CDCl}_3$ )  $\delta$  : 156.2, 138.9, 128.8, 128.6, 126.4, 68.0, 42.0, 22.2. IR (neat)  $\nu_{\text{max}}$  ( $\text{cm}^{-1}$ ): 3340, 3034, 2978, 2935, 1694, 1532. HRMS (ESI): Calcd. for  $\text{C}_{12}\text{H}_{17}\text{O}_2\text{NNa}$  [ $\text{M}+\text{Na}$ ] $^+$  230.1151, found 230.1146.

### 3-chloropropyl cyclohexylcarbamate (**82m**)



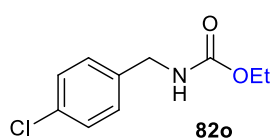
Following the general procedure B, the corresponding oxamic acid (0.7 mmol) and  $\text{Bu}_4\text{NCIO}_4$  (0.08M) were used. Purification by vacuum distillation to remove excess alcohol, then column chromatography (silica, petroleum ether/ethyl acetate 93/7) afforded **82m** (50% NMR yield, 63 mg isolated, 41%) as a white solid. m.p. : 59-60°C. Rf : 0.54 (EtOAc-Hexane 20/80).  $^1\text{H}$  NMR (300 MHz,  $\text{CDCl}_3$ )  $\delta$  : 4.55 (s, 1H), 4.19 (t,  $J$  = 5.8 Hz, 2H), 3.60 (t,  $J$  = 6.5 Hz, 2H), 3.46 (s, 1H), 2.12 – 2.00 (m, 2H), 1.97 – 1.85 (m, 2H), 1.75 – 1.55 (m, 3H), 1.41 – 1.04 (m, 5H).  $^{13}\text{C}$  NMR (101 MHz,  $\text{CDCl}_3$ )  $\delta$  : 155.5, 61.3, 49.8, 41.4, 33.4, 32.1, 25.5, 24.8. IR (neat)  $\nu_{\text{max}}$  ( $\text{cm}^{-1}$ ): 3328, 2932, 2856, 1706. HRMS (ESI): Calcd. for  $\text{C}_{10}\text{H}_{18}\text{O}_2\text{N}^{35}\text{ClNa}$  [ $\text{M}+\text{Na}$ ] $^+$  242.0918, found 242.0912.

### Allyl phenethylcarbamate (**82n**)



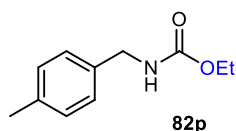
Following the general procedure B, the corresponding oxamic acid (0.5 mmol) and  $\text{Bu}_4\text{NCIO}_4$  (0.05M) were used. Purification by column chromatography (silica, petroleum ether/ethyl acetate 92/8) afforded **82n** (51 mg, 50%) as a colorless liquid. Rf : 0.57 (EtOAc-Hexane 20/80).  $^1\text{H}$  NMR (300 MHz,  $\text{CDCl}_3$ )  $\delta$  : 7.27 (m,  $J$  = 13.7, 7.8, 4.1 Hz, 5H), 5.94 (m,  $J$  = 22.7, 10.8, 5.6 Hz, 1H), 5.27 (m,  $J$  = 13.8, 11.5, 1.2 Hz, 2H), 4.81 (s, 1H), 4.58 (d,  $J$  = 5.5 Hz, 2H), 3.64 – 3.34 (dd, 2H), 2.84 (t,  $J$  = 7.0 Hz, 2H).  $^{13}\text{C}$  NMR (76 MHz,  $\text{CDCl}_3$ )  $\delta$  : 156.2, 138.7, 132.9, 128.7, 128.6, 126.5, 117.6, 65.5, 42.2, 36.1. IR (neat)  $\nu_{\text{max}}$  ( $\text{cm}^{-1}$ ): 3335, 3085, 3064, 3028, 2938, 2878, 1708, 1603, 1530. HRMS (ESI): Calcd. for  $\text{C}_{12}\text{H}_{15}\text{O}_2\text{NNa}$  [ $\text{M}+\text{Na}$ ] $^+$  228.0995, found 228.0992.

### Ethyl 4-chlorobenzylcarbamate (**82o**)



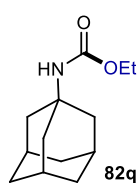
Following the general procedure B, the corresponding oxamic acid (0.3 mmol) and  $\text{Bu}_4\text{NCIO}_4$  (0.05M) were used. Purification by column chromatography (silica, petroleum ether/ethyl acetate 93/7) afforded **82o** (29 mg, 50%) as a gel. Rf : 0.46 (EtOAc/Hexane 20/80).  $^1\text{H}$  NMR (300 MHz,  $\text{CDCl}_3$ )  $\delta$  : 7.36 – 7.16 (m, 4H), 4.99 (s, 1H), 4.32 (d,  $J$  = 6.0 Hz, 2H), 4.14 (q,  $J$  = 7.1 Hz, 2H), 1.25 (t,  $J$  = 7.1 Hz, 3H).  $^{13}\text{C}$  NMR (76 MHz,  $\text{CDCl}_3$ )  $\delta$  : 156.6, 137.2, 133.2, 128.8, 61.1, 44.3, 14.6. HRMS (ESI): Calcd. for  $\text{C}_{10}\text{H}_{12}\text{O}_2\text{N}^{35}\text{ClNa}$   $[\text{M}+\text{Na}]^+$  236.0448, found 236.0447.

### Ethyl 4-methylbenzylcarbamate (**82p**)



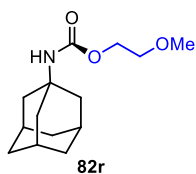
Following the general procedure B, the corresponding oxamic acid (0.5 mmol) and  $\text{Bu}_4\text{NCIO}_4$  (0.03M) were used. Purification by column chromatography (silica, petroleum ether/ethyl acetate 93/7) afforded **82p** (54 mg, 62%) as a colorless liquid. Rf : 0.46 (EtOAc/Hexane 20/80).  $^1\text{H}$  NMR (300 MHz,  $\text{CDCl}_3$ )  $\delta$  : 7.18 (q,  $J$  = 8.2 Hz, 4H), 4.92 (s, 1H), 4.35 (d,  $J$  = 5.7 Hz, 2H), 4.17 (q,  $J$  = 7.1 Hz, 2H), 2.36 (s, 3H), 1.27 (t,  $J$  = 7.1 Hz, 3H).  $^{13}\text{C}$  NMR (76 MHz,  $\text{CDCl}_3$ )  $\delta$  : 156.6, 137.1, 135.5, 129.3, 127.5, 60.9, 44.8, 21.1, 14.7. IR (neat)  $\nu_{\text{max}}$  ( $\text{cm}^{-1}$ ): 3317, 2980, 2860, 1689. HRMS (ESI): Calcd. for  $\text{C}_{11}\text{H}_{15}\text{O}_2\text{NNa}$   $[\text{M}+\text{Na}]^+$  216.0995, found 216.0993.

### Ethyl (3s,5s,7s)-adamantan-1-ylcarbamate (**82q**)



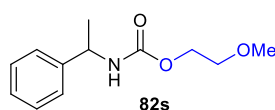
Following the general procedure B, the corresponding oxamic acid (0.5 mmol) and  $\text{Bu}_4\text{NCIO}_4$  (0.03M) were used. Purification by column chromatography (silica, petroleum ether) afforded **82q** (79 mg, 71%), as a white solid. m.p. : 94-96°C. Rf : 0.76 (EtOAc/Hexane 20/80).  $^1\text{H}$  NMR (300 MHz,  $\text{CDCl}_3$ )  $\delta$  : 4.53 (s, 1H), 4.05 (q,  $J$  = 7.1 Hz, 2H), 2.17 – 2.00 (m, 3H), 1.93 (d,  $J$  = 2.7 Hz, 6H), 1.66 (t,  $J$  = 3.0 Hz, 6H), 1.22 (t,  $J$  = 7.1 Hz, 3H).  $^{13}\text{C}$  NMR (76 MHz,  $\text{CDCl}_3$ )  $\delta$  : 154.6, 59.8, 50.5, 41.8, 36.5, 36.4, 36.3, 36.1, 29.6, 29.4, 29.2, 14.6. IR (neat)  $\nu_{\text{max}}$  ( $\text{cm}^{-1}$ ): 3339, 2908, 2851, 1706, 1527. HRMS (ESI): Calcd. for  $\text{C}_{13}\text{H}_{22}\text{O}_2\text{N}$   $[\text{M}+\text{H}]^+$  224.1645, found 224.1641.

### 2-Methoxyethyl (3s,5s,7s)-adamantan-1-ylcarbamate (**82r**)



Following the general procedure B, the corresponding oxamic acid (0.4 mmol) and  $\text{Bu}_4\text{NCIO}_4$  (0.08M) were used. Purification by column chromatography (silica, petroleum ether/ethyl acetate 90/10) afforded **82r** (81 mg, 80%) as a white gel. Rf : 0.64 (EtOAc/Hexane 30/70).  $^1\text{H}$  NMR (300 MHz,  $\text{CDCl}_3$ )  $\delta$  : 4.65 (s, 1H), 4.18 – 4.10 (t, 2H), 3.60 – 3.52 (m, 2H), 3.39 (s, 3H), 2.06 (s, 3H), 1.92 (d,  $J$  = 3.0 Hz, 6H), 1.66 (t,  $J$  = 3.1 Hz, 6H).  $^{13}\text{C}$  NMR (76 MHz,  $\text{CDCl}_3$ )  $\delta$  : 154.2, 71.0, 63.0, 58.9, 50.7, 41.8, 36.3, 29.4. IR (neat)  $\nu_{\text{max}}$  ( $\text{cm}^{-1}$ ): 3344, 2909, 2844, 1709, 1527. HRMS (ESI): Calcd. for  $\text{C}_{14}\text{H}_{24}\text{O}_3\text{N}$   $[\text{M}+\text{H}]^+$  254.1750, found 254.1749.

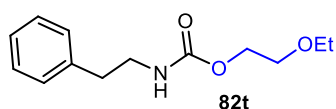
### 2-Methoxyethyl (1-phenylethyl)carbamate (**82s**)



Following the general procedure B, the corresponding oxamic acid (0.4 mmol) and  $\text{Bu}_4\text{NCIO}_4$  (0.05M) were used. Purification by column chromatography (silica, petroleum ether/ethyl acetate 90/10) afforded **82s** (58 mg, 65%) as a colorless gel. Rf : 0.32 (EtOAc/Hexane 30/70).  $^1\text{H}$  NMR (300 MHz,  $\text{CDCl}_3$ )  $\delta$  : 7.44 – 7.15 (5, 1H), 5.10 (s, 1H), 4.83 (p,  $J$  = 7.1 Hz, 1H), 4.34 – 4.09 (m, 2H), 3.56 (t,  $J$  = 4.7 Hz, 2H), 3.37 (s, 3H), 1.47 (s,  $J$  = 6.9 Hz, 3H).  $^{13}\text{C}$  NMR (76 MHz,  $\text{CDCl}_3$ )  $\delta$  :

155.5, 128.6, 127.3, 125.9, 63.8, 58.9, 50.7, 22.5. IR (neat)  $\nu_{\max}$  (cm<sup>-1</sup>): 3323, 3030, 2975, 2893, 1706, 1531. HRMS (ESI): Calcd. for C<sub>12</sub>H<sub>17</sub>O<sub>3</sub>NNa [M+Na]<sup>+</sup> 246.1100, found 246.1095.

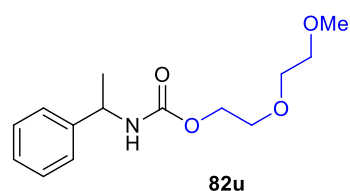
### 2-Ethoxyethyl phenethylcarbamate (**82t**)



Following the general procedure B, the corresponding oxamic acid (0.37 mmol) and Bu<sub>4</sub>NClO<sub>4</sub> (0.05M) were used. Purification by column chromatography (silica, petroleum ether/ethyl acetate 85/15) afforded **82t** (53 mg, 60%) as a colorless gel. R<sub>f</sub> : 0.40 (EtOAc/Hexane 30/70).

<sup>1</sup>H NMR (300 MHz, CDCl<sub>3</sub>)  $\delta$  : 7.37 – 7.12 (m, 5H), 4.77 (s, J = 5.3 Hz, 1H), 4.26 – 4.11 (t, 2H), 3.65 – 3.38 (m, 6H), 2.81 (t, J = 7.0 Hz, 2H), 1.21 (t, J = 7.0 Hz, 3H). <sup>13</sup>C NMR (76 MHz, CDCl<sub>3</sub>)  $\delta$  : 156.3, 138.7, 128.8, 128.6, 126.5, 68.8, 66.6, 64.0, 42.1, 36.1, 15.1. IR (neat)  $\nu_{\max}$  (cm<sup>-1</sup>): 3335, 3028, 2974, 2869, 1709, 1530. HRMS (ESI): Calcd. for C<sub>13</sub>H<sub>19</sub>O<sub>3</sub>NNa [M+Na]<sup>+</sup> 260.1275, found 260.1253.

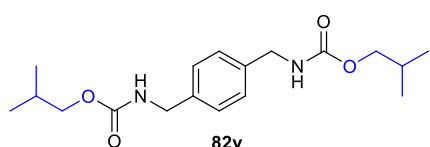
### 2-(2-Methoxyethoxy)ethyl (1-phenylethyl)carbamate (**82u**)



Following the general procedure B, the corresponding oxamic acid (0.4 mmol) and Bu<sub>4</sub>NClO<sub>4</sub> (0.05M) were used. Purification by column chromatography (silica, petroleum ether/ethyl acetate 75/25) afforded **82u** (50 mg, 47%) as a light brown gel. R<sub>f</sub> : 0.42 (EtOAc/Hexane 50/50).

<sup>1</sup>H NMR (300 MHz, CDCl<sub>3</sub>)  $\delta$  : 7.39 – 7.21 (m, 5H), 5.11 (s, 1H), 4.84 (p, J = 7.2 Hz, 1H), 4.23 (q, J = 4.4 Hz, 2H), 3.76 – 3.50 (m, 6H), 3.39 (s, 3H), 1.49 (d, J = 6.9 Hz, 3H). <sup>13</sup>C NMR (76 MHz, CDCl<sub>3</sub>)  $\delta$  : 155.5, 143.5, 128.6, 127.3, 125.9, 71.8, 70.4, 69.6, 63.9, 59.0, 50.7, 22.5. IR (neat)  $\nu_{\max}$  (cm<sup>-1</sup>): HRMS (ESI): Calcd. for C<sub>14</sub>H<sub>20</sub>O<sub>4</sub>N [M-H]<sup>-</sup> 266.1397, found 266.1396.

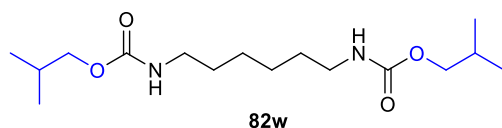
### Diisobutyl (1,4-phenylenebis(methylene))dicarbamate (**82v**)



Following the general procedure B, the corresponding oxamic acid (0.25 mmol) and Bu<sub>4</sub>NClO<sub>4</sub> (0.05M) were used. Purification by column chromatography (silica, DCM/MeOH 99/1) afforded **82v** (42 mg, 50%) as a white crystalline solid. m.p. : 161-163°C.

R<sub>f</sub> : 0.21 (EtOAc/Hexane 20/80). <sup>1</sup>H NMR (300 MHz, CDCl<sub>3</sub>)  $\delta$  : 7.28 (s, 4H), 4.98 (s, 2H), 4.37 (d, J = 5.8 Hz, 4H), 3.90 (d, J = 6.6 Hz, 4H), 1.93 (m, J = 13.4, 6.7 Hz, 2H), 0.94 (d, J = 6.7 Hz, 12H). <sup>13</sup>C NMR (75 MHz, DMSO)  $\delta$  : 156.7, 138.5, 129.8, 127.1, 70.9, 69.9, 43.5, 27.8, 23.2, 19.4, 19.1. IR (neat)  $\nu_{\max}$  (cm<sup>-1</sup>): 3313, 3064, 2957, 2865, 1683, 1540. HRMS (ESI): Calcd. for C<sub>18</sub>H<sub>29</sub>O<sub>4</sub>N<sub>2</sub> [M+H]<sup>+</sup> 337.2121, found 337.2116.

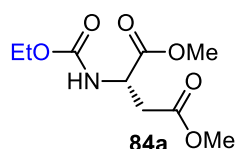
### Diisobutyl hexane-1,6-diyl dicarbamate (**82w**)



Following the general procedure B, the corresponding oxamic acid (0.25 mmol) and Bu<sub>4</sub>NClO<sub>4</sub> (0.05M) were used. Purification by column chromatography (silica, petroleum ether/ethyl acetate 85/15) afforded **82w** (50 mg,

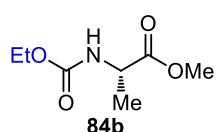
63%) as a white crystalline solid. m.p. : 116-118°C. R<sub>f</sub> : 0.43 (EtOAc/Hexane 30/70). <sup>1</sup>H NMR (300 MHz, CDCl<sub>3</sub>)  $\delta$  : 4.69 (s, 2H), 3.85 (d, J = 6.6 Hz, 4H), 3.18 (dd, J = 13.0, 6.5 Hz, 4H), 1.91 (m, J = 13.2, 6.6 Hz, 2H), 1.56 – 1.45 (m, 4H), 1.37 (dd, J = 4.1, 3.0 Hz, 4H), 0.94 (d, J = 6.7 Hz, 12H). <sup>13</sup>C NMR (76 MHz, CDCl<sub>3</sub>)  $\delta$  : 156.9, 70.9, 40.7, 30.0, 28.0, 26.3, 19.1. IR (neat)  $\nu_{\max}$  (cm<sup>-1</sup>): 3334, 2956, 2876, 1682, 1534. HRMS (ESI): Calcd. for C<sub>16</sub>H<sub>33</sub>O<sub>4</sub>N<sub>2</sub> [M+H]<sup>+</sup> 317.2434, found 317.24305.

### (S)-Dimethyl 2-((ethoxycarbonyl)amino)succinate (**84a**)



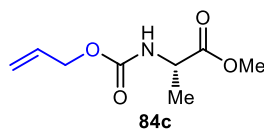
Following the general procedure B, the corresponding oxamic acid (0.5 mmol) and  $\text{Bu}_4\text{NClO}_4$  (0.05M) were used. Purification by column chromatography (silica, petroleum ether/ethyl acetate 88/12) afforded **84a** (59 mg, 51%) as a light brown gel.  $R_f$  : 0.31 (EtOAc/Hexane 20/80).  $^1\text{H NMR}$  (300 MHz,  $\text{CDCl}_3$ )  $\delta$  : 5.68 (d,  $J = 7.8$  Hz, 1H), 4.62 (dt,  $J = 8.7, 4.5$  Hz, 1H), 4.12 (dd,  $J = 9.5, 4.7$  Hz, 2H), 3.77 (s, 3H), 3.70 (s, 3H), 3.03 (dd,  $J = 17.1, 4.5$  Hz, 1H), 2.85 (dd,  $J = 17.1, 4.7$  Hz, 1H), 1.25 (t,  $J = 7.1$  Hz, 3H).  $^{13}\text{C NMR}$  (76 MHz,  $\text{CDCl}_3$ )  $\delta$  : 171.3, 156.1, 77.5, 77.0, 76.6, 61.3, 52.8, 52.0, 50.2, 36.5, 14.5. IR (neat)  $\nu_{\text{max}}$  ( $\text{cm}^{-1}$ ): 3366, 2993, 2956. 1733, 1524. HRMS (ESI): Calcd. for  $\text{C}_9\text{H}_{15}\text{O}_6\text{NNa}$   $[\text{M}+\text{Na}]^+$  256.0791, found 256.0787.  $[\alpha]_{\text{D}}^{25}$  : +32.47 (c 0.72,  $\text{CHCl}_3$ ).

### (S)-Methyl 2-((ethoxycarbonyl)amino)propanoate (**84b**)



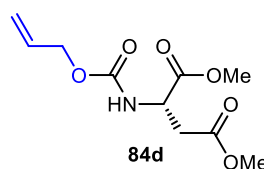
Following the general procedure B, the corresponding oxamic acid (0.5 mmol) and  $\text{Bu}_4\text{NClO}_4$  (0.05M) were used. Purification by column chromatography (silica, petroleum ether/ethyl acetate 93/7) afforded **84b** (54 mg, 50%) as a light brown liquid.  $R_f$  : 0.43 (EtOAc/Hexane 20/80).  $^1\text{H NMR}$  (300 MHz,  $\text{CDCl}_3$ )  $\delta$  : 5.26 (s, 1H), 4.40 – 4.24 (m, 1H), 4.09 (q,  $J = 7.1$  Hz, 2H), 3.72 (s, 3H), 1.38 (d,  $J = 7.2$  Hz, 3H), 1.25 – 1.15 (m, 3H).  $^{13}\text{C NMR}$  (76 MHz,  $\text{CDCl}_3$ )  $\delta$  : 173.6, 155.8, 61.0, 52.4, 49.4, 18.6, 14.5. IR (neat)  $\nu_{\text{max}}$  ( $\text{cm}^{-1}$ ): 3336, 2982, 1739, 1722, 1529. HRMS (ESI): Calcd. for  $\text{C}_7\text{H}_{13}\text{O}_4\text{NNa}$   $[\text{M}+\text{Na}]^+$  198.0736, found 198.0733.  $[\alpha]_{\text{D}}^{25}$  : -4.65 (c 0.51,  $\text{CHCl}_3$ ).

### (S)-Methyl 2-(((allyloxy)carbonyl)amino)propanoate (**84c**)



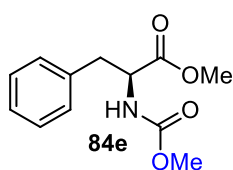
Following the general procedure B, the corresponding oxamic acid (0.5 mmol) and  $\text{Bu}_4\text{NClO}_4$  (0.05M) were used. Purification by column chromatography (silica, petroleum ether/ethyl acetate 93/7) afforded **84c** (56 mg, 61%) as a light brown liquid.  $R_f$  : 0.41 (EtOAc/Hexane 20/80).  $^1\text{H NMR}$  (300 MHz,  $\text{CDCl}_3$ )  $\delta$  : 5.93 (m,  $J = 17.2, 10.5, 5.6$  Hz, 1H), 5.38 – 5.13 (m, 2H), 4.59 (d,  $J = 5.6$  Hz, 2H), 4.47 – 4.28 (m, 1H), 3.77 (s, 3H), 1.43 (d,  $J = 7.2$  Hz, 3H).  $^{13}\text{C NMR}$  (76 MHz,  $\text{CDCl}_3$ )  $\delta$  : 173.5, 155.4, 132.6, 117.8, 65.8, 52.4, 49.5, 18.7. IR (neat)  $\nu_{\text{max}}$  ( $\text{cm}^{-1}$ ): 3344, 2991, 2952, 1722, 1528. HRMS (ESI): Calcd. for  $\text{C}_8\text{H}_{13}\text{O}_4\text{NNa}$   $[\text{M}+\text{Na}]^+$  210.0736, found 210.0734.  $[\alpha]_{\text{D}}^{25}$  : -3.72 (c 0.3,  $\text{CHCl}_3$ ).

### (S)-Dimethyl 2-(((allyloxy)carbonyl)amino)succinate (**84d**)



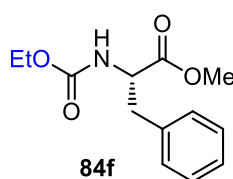
Following the general procedure B, the corresponding oxamic acid (0.5 mmol) and  $\text{Bu}_4\text{NClO}_4$  (0.05M) were used. Purification by column chromatography (silica, petroleum ether/ethyl acetate 85/15) afforded **84d** (44 mg, 41%) as a light brown gel.  $R_f$  : 0.28 (EtOAc/Hexane 20/80).  $^1\text{H NMR}$  (300 MHz,  $\text{CDCl}_3$ )  $\delta$  : 5.91 (m,  $J = 17.2, 10.5, 5.6$  Hz, 1H), 5.72 (d,  $J = 7.6$  Hz, 1H), 5.38 – 5.18 (m, 2H), 4.57 (d, 2H), 3.76 (s, 3H), 3.69 (s, 3H), 3.03 (dd,  $J = 17.1, 4.5$  Hz, 1H), 2.90 – 2.78 (dd, 1H).  $^{13}\text{C NMR}$  (76 MHz,  $\text{CDCl}_3$ )  $\delta$  : 171.3, 171.1, 155.8, 132.5, 117.9, 66.0, 52.8, 52.1, 50.3, 36.5. IR (neat)  $\nu_{\text{max}}$  ( $\text{cm}^{-1}$ ): 3340, 3025, 2956, 1729, 1650, 1520. HRMS (ESI): Calcd. for  $\text{C}_{10}\text{H}_{15}\text{O}_6\text{NNa}$   $[\text{M}+\text{Na}]^+$  268.0791, found 268.0783.  $[\alpha]_{\text{D}}^{25}$  : +21.32 (c 0.5,  $\text{CHCl}_3$ ).

### (S)-Methyl 2-((methoxycarbonyl)amino)-3-phenylpropanoate (**84e**)



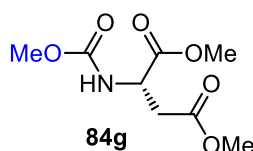
Following the general procedure B, the corresponding oxamic acid (0.5 mmol) and  $\text{Bu}_4\text{NClO}_4$  (0.08M) were used. Purification by column chromatography (silica, petroleum ether/ethyl acetate 90/10) afforded **84e** (85 mg, 70%) as a colorless gel. Rf : 0.4 (EtOAc/Hexane 20/80).  $^1\text{H}$  NMR (300 MHz,  $\text{CDCl}_3$ )  $\delta$  : 7.39 – 7.20 (m, 3H), 7.19 – 7.06 (m, 2H), 5.24 (s, 1H), 4.66 (dd,  $J = 13.7, 6.2$  Hz, 1H), 3.73 (s, 3H), 3.67 (s, 3H), 3.23 – 2.93 (m, 2H).  $^{13}\text{C}$  NMR (76 MHz,  $\text{CDCl}_3$ )  $\delta$  : 172.1, 156.3, 135.7, 129.2, 128.6, 127.1, 54.7, 52.3, 38.3. IR (neat)  $\nu_{\text{max}}$  ( $\text{cm}^{-1}$ ): 3340, 3025, 2956, 2844, 1729, 1526. HRMS (ESI): Calcd. for  $\text{C}_{12}\text{H}_{15}\text{O}_4\text{NNa}$   $[\text{M}+\text{Na}]^+$  260.0893, found 260.0892.  $[\alpha]_{\text{D}}^{25}$  : +58.92 (c 0.52,  $\text{CHCl}_3$ ).

### (S)-Methyl 2-((ethoxycarbonyl)amino)-3-phenylpropanoate (**84f**)



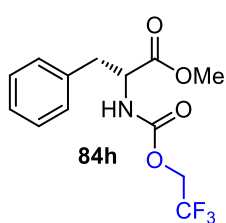
Following the general procedure B, the corresponding oxamic acid (0.5 mmol) and  $\text{Bu}_4\text{NClO}_4$  (0.08M) were used. Purification column by chromatography (silica, petroleum ether/ ethyl acetate 85/15) afforded **84f** (82 mg, 65%) as a colorless gel. Rf : 0.37 (EtOAc/Hexane 20/80).  $^1\text{H}$  NMR (300 MHz,  $\text{CDCl}_3$ )  $\delta$  : 7.35 – 7.19 (m, 3H), 7.16 – 7.04 (m, 2H), 5.07 (s, 1H), 4.63 (dd,  $J = 13.8, 6.0$  Hz, 1H), 4.09 (q,  $J = 7.1$  Hz, 2H), 3.70 (s, 3H), 3.15 – 2.95 (m, 2H), 1.21 (t,  $J = 7.1$  Hz, 3H).  $^{13}\text{C}$  NMR (76 MHz,  $\text{CDCl}_3$ )  $\delta$  : 172.1, 155.9, 135.8, 129.2, 128.6, 127.1, 61.2, 52.3, 38.3, 14.5. IR (neat)  $\nu_{\text{max}}$  ( $\text{cm}^{-1}$ ): 3340, 3030, 2987, 1746, 1722, 1524. HRMS (ESI): Calcd. for  $\text{C}_{13}\text{H}_{17}\text{O}_4\text{NNa}$   $[\text{M}+\text{Na}]^+$  274.1094, found 274.1044.  $[\alpha]_{\text{D}}^{25}$  : +56.74 (c 0.46,  $\text{CHCl}_3$ ).

### (S)-Dimethyl 2-((methoxycarbonyl)amino)succinate (**84g**)



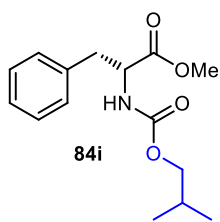
Following the general procedure B, the corresponding oxamic acid (0.5 mmol) and  $\text{Bu}_4\text{NClO}_4$  (0.01M) were used. Purification by column chromatography (silica, petroleum ether/ethyl acetate 85/15) afforded **84g** (85 mg, 78%) as a gel. Rf : 0.25 (EtOAc/Hexane 20/80).  $^1\text{H}$  NMR (300 MHz,  $\text{CDCl}_3$ )  $\delta$  : 5.72 (d,  $J = 7.6$  Hz, 1H), 4.62 (dt,  $J = 8.7, 4.5$  Hz, 1H), 3.77 (s, 3H), 3.69 (s, 6H), 3.03 (dd,  $J = 17.1, 4.5$  Hz, 1H), 2.85 (dd,  $J = 17.1, 4.6$  Hz, 1H).  $^{13}\text{C}$  NMR (76 MHz,  $\text{CDCl}_3$ )  $\delta$  : 171.3, 171.2, 156.5, 52.8, 52.0, 50.3, 36.5. IR (neat)  $\nu_{\text{max}}$  ( $\text{cm}^{-1}$ ): 3357, 3000, 2961, 2853, 1721, 1524. HRMS (ESI): Calcd. for  $\text{C}_8\text{H}_{13}\text{O}_6\text{NNa}$   $[\text{M}+\text{Na}]^+$  242.0635, found 242.0631.  $[\alpha]_{\text{D}}^{25}$  : +37.93 (c 0.64,  $\text{CHCl}_3$ ).

### (S)-Methyl 3-phenyl-2-(((2,2,2-trifluoroethoxy)carbonyl)amino)propanoate (**84h**)



Following the general procedure B, the corresponding oxamic acid (0.3 mmol) and  $\text{Bu}_4\text{NClO}_4$  (0.05M) were used. Purification column chromatography (silica, petroleum ether/ethyl acetate 92/8) afforded **84h** (39 mg, 40%) as a colorless gel. Rf : 0.45 (EtOAc/Hexane 20/80).  $^1\text{H}$  NMR (300 MHz,  $\text{CDCl}_3$ )  $\delta$  : 7.45 – 7.20 (m, 3H), 7.20 – 7.07 (m, 2H), 5.41 (d,  $J = 7.8$  Hz, 1H), 4.74 – 4.60 (m, 1H), 4.58 – 4.33 (m, 2H), 3.76 (s,  $J = 7.8$  Hz, 3H), 3.16 (m,  $J = 13.9, 5.8$  Hz, 2H).  $^{13}\text{C}$  NMR (76 MHz,  $\text{CDCl}_3$ )  $\delta$  : 171.4, 156.8, 153.7, 135.3, 129.2, 128.7, 127.3, 61.3, 60.8, 60.5, 55.0, 52.5, 38.1. IR (neat)  $\nu_{\text{max}}$  ( $\text{cm}^{-1}$ ): 3344, 3038, 2956, 1742, 1520. HRMS (ESI): Calcd. for  $\text{C}_{13}\text{H}_{14}\text{O}_4\text{NF}_3\text{Na}$   $[\text{M}+\text{Na}]^+$  328.0767, found 328.0760.  $[\alpha]_{\text{D}}^{25}$  : +49.86 (c 0.66,  $\text{CHCl}_3$ ).

### (S)-Methyl 2-((isobutoxycarbonyl)amino)-3-phenylpropanoate (**84i**)



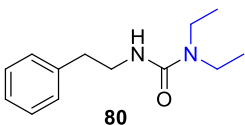
Following the general procedure B, the corresponding oxamic acid (0.4 mmol) and  $\text{Bu}_4\text{NClO}_4$  (0.08M) were used. Purification by column chromatography (silica, petroleum ether/ethyl acetate 92/8) afforded **84i** (69 mg, 50%) as a colorless gel. Rf : 0.45 (EtOAc/Hexane 20/80).  $^1\text{H}$  NMR (300 MHz,  $\text{CDCl}_3$ )  $\delta$  : 7.33 – 7.20 (m, 3H), 7.15 – 7.08 (m, 2H), 5.13 (d,  $J$  = 7.6 Hz, 1H), 4.64 (dd,  $J$  = 13.9, 6.0 Hz, 1H), 3.83 (dd,  $J$  = 6.7, 1.6 Hz, 2H), 3.71 (s, 3H), 3.10 (m,  $J$  = 6.1 Hz, 2H), 1.88 (m,  $J$  = 13.4, 6.7 Hz, 3H), 0.90 (d,  $J$  = 6.7 Hz, 6H).  $^{13}\text{C}$  NMR (76 MHz,  $\text{CDCl}_3$ )  $\delta$  : 172.1, 156.7, 156.0, 135.8, 129.3, 128.6, 127.1, 71.3, 54.7, 52.3, 38.3, 28.0, 19.0. IR (neat)  $\nu_{\text{max}}$  ( $\text{cm}^{-1}$ ): 3349, 3021, 2961, 2875, 1724, 1730, 1518. HRMS (ESI): Calcd. for  $\text{C}_{15}\text{H}_{21}\text{O}_4\text{NNa}$  [ $\text{M}+\text{Na}$ ] $^+$  302.1373, found 302.1357.  $[\alpha]_{\text{D}}^{25}$  : +46.32 (c 0.61,  $\text{CHCl}_3$ ).

### $\text{N}^1, \text{N}^2$ -Diphenethyloxalamide (**34**)



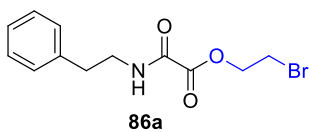
**34** (22 mg) was obtained in 15% as a white solid. m.p. : 164-167°C. Rf : 0.14 (EtOAc/Hexane 20/80).  $^1\text{H}$  NMR (300 MHz,  $\text{CDCl}_3$ )  $\delta$  : 7.51 (s, 2H), 7.41 – 7.16 (m, 10H), 3.59 (dd,  $J$  = 13.5, 7.1 Hz, 4H), 2.88 (t,  $J$  = 7.2 Hz, 4H).  $^{13}\text{C}$  NMR (76 MHz,  $\text{CDCl}_3$ )  $\delta$  : 159.7, 138.1, 128.7, 128.7, 126.7, 40.8, 35.4. IR (neat)  $\nu_{\text{max}}$  ( $\text{cm}^{-1}$ ): 3292, 3056, 2929, 2867, 1646. HRMS (ESI): Calcd. for  $\text{C}_{18}\text{H}_{20}\text{O}_2\text{N}_2\text{Na}$  [ $\text{M}+\text{Na}$ ] $^+$  319.1417, found 319.1414.

### 1,1-Diethyl-3-phenethylurea (**80**)



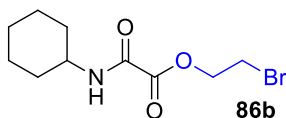
**80** (20% ( $^1\text{H}$ -NMR), 17 mg, 15%) was obtained as a light brown gel. Rf : 0.20 (AcOEt/DCM 10/90)  $^1\text{H}$  NMR (300 MHz,  $\text{CDCl}_3$ )  $\delta$  : 7.46 – 7.06 (m, 5H), 4.30 (s, 1H), 3.59 – 3.36 (m, 2H), 3.21 (q,  $J$  = 7.1 Hz, 4H), 2.91 – 2.77 (m, 2H), 1.12 – 1.01 (m, 6H).  $^{13}\text{C}$  NMR (76 MHz,  $\text{CDCl}_3$ )  $\delta$  : 157.2, 139.5, 128.9, 128.8, 128.5, 126.3, 42.0, 41.1, 36.4, 13.8. IR (neat)  $\nu_{\text{max}}$  ( $\text{cm}^{-1}$ ): 3345, 3027, 2972, 2929, 2871, 1625. HRMS (ESI): Calcd. for  $\text{C}_{13}\text{H}_{21}\text{ON}_2$  [ $\text{M}+\text{H}$ ] $^+$  221.1684, found 221.1638.

### 2-Bromoethyl 2-oxo-2-(phenethylamino)acetate (**86a**)



Following the general procedure B, the corresponding oxamic acid (0.5 mmol) and  $\text{Bu}_4\text{NClO}_4$  (0.08M) were used. Purification by column chromatography (silica, petroleum ether/ethyl acetate 90/10) afforded **86a** (78.6 mg, 53%) as a white solid. m.p. : 69-71°C. Rf : 0.2 (EtOAc/Hexane 20/80).  $^1\text{H}$  NMR (300 MHz,  $\text{CDCl}_3$ )  $\delta$  : 7.37 – 7.17 (m, 5H), 7.11 (s, 1H), 4.56 (t,  $J$  = 6.5 Hz, 2H), 3.69 – 3.53 (m, 4H), 2.89 (t,  $J$  = 7.1 Hz, 2H).  $^{13}\text{C}$  NMR (76 MHz,  $\text{CDCl}_3$ )  $\delta$  : 160.0, 155.8, 138.0, 126.8, 65.7, 41.1, 35.2, 27.1. IR (neat)  $\nu_{\text{max}}$  ( $\text{cm}^{-1}$ ): 3331, 2924, 1738, 1693. HRMS (ESI): Calcd. for  $\text{C}_{12}\text{H}_{14}\text{O}_3\text{N}^{79}\text{BrNa}$  [ $\text{M}+\text{Na}$ ] $^+$  322.0049, found 322.0049.

### 2-Bromoethyl 2-(cyclohexylamino)-2-oxoacetate (**86b**)

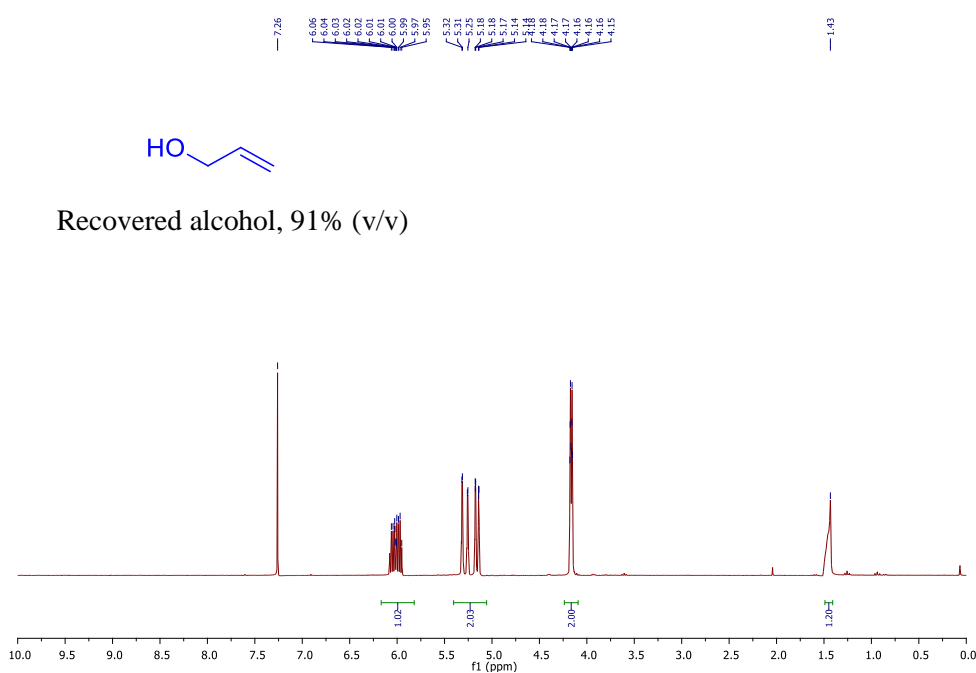
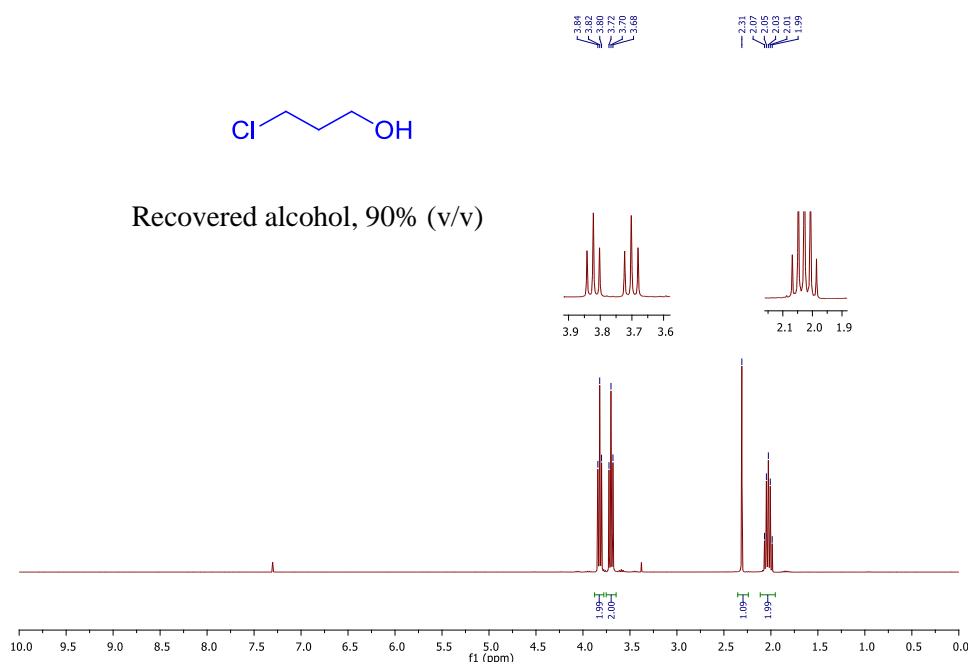


Following the general procedure B, the corresponding oxamic acid (0.7 mmol) and  $\text{Bu}_4\text{NClO}_4$  (0.08M) were used. Purification by column chromatography (silica, petroleum ether/ethyl acetate 90/10) afforded **86b** (138 mg, 79%) as a white solid. m.p. : 74-77°C. Rf : 0.2 (EtOAc/Hexane 20/80).  $^1\text{H}$  NMR (300 MHz,  $\text{CDCl}_3$ )  $\delta$  : 6.97 (s, 1H), 4.57 (t,  $J$  = 6.6 Hz, 2H), 3.92 – 3.71 (m, 1H),

3.60 (t,  $J = 6.6$  Hz, 2H), 1.96 (dd,  $J = 12.1, 2.9$  Hz, 2H), 1.82 – 1.56 (m, 3H), 1.50 – 1.08 (m, 5H).  $^{13}\text{C}$  NMR (76 MHz,  $\text{CDCl}_3$ )  $\delta$ : 160.4, 154.8, 65.7, 49.0, 32.5, 27.2, 25.3, 24.6. IR (neat)  $\nu_{\text{max}}$  ( $\text{cm}^{-1}$ ): 3289, 2933, 2856, 1740, 1683. HRMS (ESI): Calcd. for  $\text{C}_{10}\text{H}_{16}\text{O}_3\text{N}^{79}\text{BrNa}$   $[\text{M}+\text{Na}]^+$  300.0192, found 300.0198.

### 6.3. Alcohol Recovery after Electrochemical Reaction

After the electrochemical reaction, residual alcohol was recovered by vacuum distillation at low temperature ( $\leq 50^\circ\text{C}$ ), that allowed about 90% alcohol recovery with satisfying purity. Some spectra of the recovered alcohol are shown below.



#### 6.4. Cyclic voltammetry studies

Cyclic voltammetry was performed using a  $\mu$ AUTOLAB TYPE II potentiostat/galvanostat coupled to the electrochemical Systems (GPES, v.4.9 software; Serial No: AUT72173) (Eco Chemie BV, Utrecht, The Netherlands) and equipped with a cell containing three-electrodes, i.e. a silver wire as the pseudo-reference electrode (pseudo-RE), a glassy carbon electrode ( $\varnothing$ : 3 mm) as a working electrode and finally a Pt-wire counter-electrode.

The glassy carbon electrode (GCE) was polished prior to each measurement. 5 mM solutions of oxamic acid **56d** and 0.1M of n-Bu<sub>4</sub>NPF<sub>6</sub> in CH<sub>3</sub>CN were used. Reaction set-up was degassed using highly pure Argon gas bubbling for at least 5 min. This was done before each measurement, and the argon atmosphere was kept over the solution during the process. Cyclic voltammetry were recorded at 100 mV/s scan rate, at a temperature of 25 $\pm$ 0.5 $^{\circ}$ C. Generally, we also used the ferrocene as an external reference from which we measured the redox potential according to the same experimental conditions. For some specific cases, we used ferrocene as an internal standard (in 0.1M of n-Bu<sub>4</sub>NPF<sub>6</sub> in MeCN as supporting electrolyte solution).